STOCHASTIC FINITE-DIFFERENCE TIME-DOMAIN

by

Steven Michael Smith

A dissertation submitted to the faculty of
The University of Utah
in partial fulfillment of the requirements for the degree of

Doctor of Philosophy

Department of Electrical and Computer Engineering

The University of Utah

May 2011

The University of Utah Graduate School

STATEMENT OF DISSERTATION APPROVAL

The dissertation of **Steven Michael Smith**

has been approved by the following supervisory committee members:

Cynthia Furse	, Chair	**3/14/2011** Date Approved
J. Mark Baird	, Member	**3/22/2011** Date Approved
Behrouz Farhang-Boroujeny	, Member	**3/29/2011** Date Approved
Om P. Gandhi	, Member	**3/28/2011** Date Approved
Thomas R. Giallorenzi	, Member	**12/15/2010** Date Approved

and by **Gianluca Lazzi** , Chair of

the Department of **Electrical and Computer Engineering**

and by Charles A. Wight, Dean of The Graduate School.

ABSTRACT

This dissertation presents the derivation of an approximate method to determine the mean and the variance of electromagnetic fields in the body using the Finite-Difference Time-Domain (FDTD) method. Unlike Monte Carlo analysis, which requires repeated FDTD simulations, this method directly computes the variance of the fields at every point in space at every sample of time in the simulation. This Stochastic FDTD simulation (S-FDTD) has at its root a new wave called the Variance wave, which is computed in the time domain along with the mean properties of the model space in the FDTD simulation. The Variance wave depends on the electromagnetic fields, the reflections and transmission though the different dielectrics, and the variances of the electrical properties of the surrounding materials. Like the electromagnetic fields, the Variance wave begins at zero (there is no variance before the source is turned on) and is computed in the time domain until all fields reach steady state. This process is performed in a fraction of the time of a Monte Carlo simulation and yields the first two statistical parameters (mean and variance). The mean of the field is computed using the traditional FDTD equations. Variance is computed by approximating the correlation coefficients between the constituitive properties and the use of the S-FDTD equations.

The impetus for this work was the simulation time it takes to perform 3D Specific Absorption Rate (SAR) FDTD analysis of the human head model for cell phone power absorption in the human head due to the proximity of a cell phone being

used. In many instances, Monte Carlo analysis is not performed due to the lengthy simulation times required. With the development of S-FDTD, these statistical analyses could be performed providing valuable statistical information with this information being provided in a small fraction of the time it would take to perform a Monte Carlo analysis.

TABLE OF CONTENTS

LIST OF TABLES

Table

SYMBOLS

E	Electric Field Intensity
E_x^n	Electric Field Intensity x Component at Time Step n
H	Magnetic Field Intensity
H_y	Magnetic Field Intensity y Component
B	Magnetic Flux Density
$B_y^{n+1/2}$	Magnetic Flux Density
D	Electric Flux Density
$\underline{\sigma}$	Electrical Conductivity
ε_r	Relative Electrical Permittivity
ε_o	Free Space Electrical Permittivity
$\hat{x}$	Unit Vector in the x Direction
$\hat{y}$	Unit Vector in the y Direction
∂z	z Directed Cell Size
Δt	Time Step
$f(x)$	Function of x
$\underset{\sim}{E}\{\bullet\}$	Expectation
μ_x	Mean of x

Σ	Summation
$\sigma^2\{\bullet\}$	Variance
$\sigma\{\bullet\}$	Standard Deviation
$Cov\{X,Y\}$	Covariance
$g(\varepsilon_r,\underline{\sigma})$	Function g of $\varepsilon_r,\underline{\sigma}$
S-FDTD	Stochastic Finite-Difference Time-Domain
$\rho_{X,Y}$	Correlation Coefficient between X,Y
$\rho_{density}$	Specific Weight kg/m^3
μ	Magnetic Permeability

ACKNOWLEDGMENTS

I would like to take this opportunity to thank Dr. Cynthia Furse for her untiring help in the research and the writing of this dissertation and thanks go to my PhD Committee for their help in the directing of this work.

To my sweetheart Lethia, a big hug and kiss for the patience and support over the years that it took to complete this effort. The sacrifice was great and the support was very much needed and is very much appreciated and thanks to our children Greg and Veronica for their encouragement.

In loving memory of a brother that showed his courage, born of faith in Jesus Christ, at the end of a good life here on earth, see you later Doug.

CHAPTER 1

INTRODUCTION

1.1 The Problem

The analysis of radio wave absorption is a continuing concern for the cell phone industry due to health effects (and associated regulations) for the person using the cell phone [1, 2]. The amount of allowable power absorbed has a strong impact on the design of the phone (antenna, electromagnetic interference, shielding, etc.). Cost and size are typically also conflicting tradeoffs. The analysis of these designs prior to the building of prototypes and the actual testing of the radio is critical to contain cost and design cycle time, so numerical simulations are routinely used in this industry. One of the unanswered questions with these simulations is how variation between individuals or uncertainty in measured tissue properties may impact the absorbed power. Studies of adults and children have shown that size of the head and thickness of the ear have a significant effect on absorbed power [3-5]. Other studies [6, 7] have shown the nonnegligible effect of head shape. Variability in tissue properties (from person to person or just because of uncertainty in the measurements) has also been shown to have a significant effect on absorbed power [8].

This dissertation will develop a new Stochastic Finite-Difference Time-Domain (S- FDTD) method of directly calculating the range of expected absorbed power for

statistically varying tissue properties. This method directly carries this variability through the simulation, unlike others that use multiple simulations (such as Monte Carlo) to determine this variability. This new method also takes a small fraction of the time required for a traditional Monte Carlo analysis which is often prohibitively time consuming. S-FDTD can provide good approximations or bounds for these statistical analyses with only a moderate increase in simulation time over the traditional FDTD simulation. This new S-FDTD method is developed in this dissertation. It is validated using a one-dimensional layered body model and compared to Monte Carlo statistical analysis. Its application to bioelectromagnetic simulations is demonstrated on a 3D cell phone / human head interaction.

1.2 Methods

FDTD analysis is well established as a simulation method for determining the reflection and absorption of electromagnetic radiation. FDTD uses the average (mean) values of the constituitive properties of the materials in the model (such as human tissues in bioelectromagnetic models) and returns the expected (mean) electric and magnetic fields at every point in the model. These mean fields are then used to determine currents, voltages, power absorbed, specific absorption rate (SAR), etc. But biological tissues have significant variability. If this variability is to be taken into account, we can determine not only the mean values of the fields but the expected variance. This can be used to answer questions such as how much detuning an antenna may experience in various biological applications, [9, 10] what is the 90% confidence level that a cellular telephone will behave as expected, and what is the variance of SAR that can be expected for a measured range of tissue values. This latter question is the one we will demonstrate

in Chapter 6 of this dissertation.

Monte Carlo analysis is a multisimulation method where thousands of simulations are performed, each using a different parameter value selected according to its statistical variation. Often, as in [9, 10] and the Monte Carlo simulations done in Chapter 3 of this dissertation, the properties are assumed to have a Gaussian distribution, although other distributions could be used as well. The data from these individual simulations are tabulated and postprocessed to determine the first moment (mean) and the first central moment (variance). This method is extremely time consuming in terms of both computer time and man hours, and is therefore only rarely used. Still, the Monte Carlo method is the 'gold standard' for calculation of mean and variance and will be used to verify the validity of the new method developed in this dissertation.

Other types of simulation methods currently in use today for models with statistically varying properties include the Stochastic Finite Element Method (SFEM), which uses a combination of deterministic FEM plus uncertainties in the input parameters. SFEM uses various methods for simulating the statistical variations of the environment including Monte Carlo, perturbation, Neumann expansion, polynomial chaos expansion, and others [9]. Another group of methods called the Perturbation methods are based on Taylor series approximations, and are low in computational cost. They are accurate for small perturbations of the various input parameters [9]. Another stochastic evaluation method is the Delta method which could be considered to be a subset of the Perturbation methods, because it also uses a truncated Taylor series expansion to determine the mean and the variance of functions of random variables [11]. The Delta method is used to derive the S-FDTD approach in this dissertation.

1.3 Objective

A method for determining the mean and variance of the electromagnetic waves without the extremely long run times associated with Monte Carlo would be a welcome change in applied statistical analysis. Finite-Difference Time-Domain (FDTD) analysis is used extensively in electromagnetic simulation. This form of analysis takes Maxwell's equations and converts them to finite-difference equations in the time domain. These are then solved iteratively in space and time to provide a 'movie' of the fields at each location in the model. FDTD has been used extensively to simulate cell phones near the human head [4, 12]. This method is efficient and effective for simulating heterogeneous environments with various complex sources. It still requires substantial computational time for large and complicated models, and therefore is difficult to integrate with Monte Carlo, which requires extensive repetition of these costly simulations. The method developed in this dissertation speeds up stochastic analysis by extending the FDTD method to stochastic variables. This method provides a good approximation or bound for the variance of the fields with only a minor increase in computer simulation time and memory.

This is done using the Finite-Difference Time-Domain (FDTD) equations directly in approximating the mean and variance. Using a Taylor's series expansion of the stochastic FDTD equations, we determine an approximation to the mean of a function with numerous random variables and then perform the same operation to approximate the variance in the Stochastic FDTD (S-FDTD) equations.

In the following chapter, we will review the FDTD equations for the one-dimensional case. These are taken from Maxwell's equations (Faraday's and Ampere's laws). Sources of error are also discussed. This information provides the necessary

background for the S-FDTD method. Various methods of performing stochastic analysis are also discussed. The Delta method Taylor series expansion is discussed in detail in Chapter 2 and is used in Chapter 4 to derive S-FDTD equations. Chapter 3 uses the Monte Carlo method to evaluate the mean and variance for 1D layered tissue models, which will later provide a comparison with the new S-FDTD method results. This comparison is shown in Chapter 5.

The major contribution of this dissertation is the development of a new stochastic FDTD (S-FDTD) method that can directly provide an approximation or bound for the variance of the fields and related values in a numerical simulation. This is used to determine the variance of the SAR in the human head from a cell phone model originally published in [3].

CHAPTER 2

BACKGROUND

This chapter provides the background material necessary for the development of the (S-FDTD) method. One-dimensional FDTD equations using Faraday's and Ampere's law are derived in this chapter, and sources of error are discussed. Monte Carlo analysis and various other methods of stochastic analysis are discussed in more detail. The Delta method is discussed in detail, because it provides some of the necessary equations for the derivation of the Stochastic FDTD method.

2.1 Finite-Difference Time-Domain (FDTD)

The Finite-Difference Time-Domain method was first conceived by Kane Yee [13] in 1966. This method replaces Maxwell's differential equations with difference equations. Taflove developed the method further starting with his first paper written in 1975 [14]. The method is ideal for complicated heterogeneous models and has been used extensively in many applications. The algorithm proved to be robust in that it has no upper bound on the size of the problems it can solve numerically [15]. FDTD does not require the use of linear algebra for its solution and instead solves Maxwell's time domain equations in difference form iteratively in time. This produces a robust and efficient method. FDTD models have been run with as many as 10^9 field unknowns.

Frequency domain methods such as the Finite Element Method (FEM) require more computational memory and power and therefore are normally used on smaller problems. The largest FEM simulation is about 10^6 unknowns [15].

There are volumes written on the FDTD method. In searching the current state of the art, there were 5221 papers listed on Science Web as well as numerous books from 1996 to the present. Within this body of literature, the only use of FDTD for statistical analysis uses Monte Carlo (multiple) simulations [8].

The FDTD method has many properties that give it advantages over other methods. It is ideal for complex heterogeneous models, such as cell phone / human head interactions [16-20], radar cross-section of entire aircraft, missiles, circuit boards, waveguides, device packaging, passive and active circuit components, and more. This makes it an ideal method for bioelectromagnetic simulations such as the ones we are interested in for this dissertation.

2.1.1 FDTD Derivation

FDTD is considered a space grid time-domain technique that is a direct solution of Maxwell's differential curl equations. The region of the simulation is defined, and sources are modeled in the time domain. Antennas can be simulated in or near objects, and both near and far field reactions can be analyzed.

The unknown E and H fields are found from Maxwell's coupled equations, i.e. Faraday's (with Maxwell's correction) and Ampere's Laws:

$$\nabla x\mathbf{E} = -\frac{\partial \mathbf{B}}{\partial t} \quad \text{and} \quad \nabla x\mathbf{H} = \frac{\partial \mathbf{D}}{\partial t} + \underline{\sigma}\mathbf{E} \tag{2.1}$$

2.2 Maxwell's Equations

2.2.1 Faraday's Equation

Assuming one-dimensional TEM propagation in the z-direction:

$$\nabla x\mathbf{E} = -\frac{\partial \mathbf{B}}{\partial t} \qquad \nabla x\mathbf{E} = \begin{vmatrix} \hat{x} & \hat{y} & \hat{z} \\ \partial/\partial x & 0 & \partial/\partial z \\ E_x & 0 & 0 \end{vmatrix} = \frac{\partial E_x}{\partial z}\hat{y}$$

$$\frac{\partial \mathbf{B}}{\partial t} = \frac{\partial B_x}{\partial t}\hat{x} + \frac{\partial B_y}{\partial t}\hat{y} + \frac{\partial B_z}{\partial t}\hat{z} \tag{2.2}$$

$$\frac{\partial E_x}{\partial z} = -\frac{\partial B_y}{\partial t}$$

To convert this equation to its finite-difference form, we need a grid system that defines time and space. Figure 2-1 shows such a grid system with k indicating the special multiplier and n indicating the time multiplier.

There are a number of things that we need to understand about equation (2.3). The first is that it uses finite-difference approximations for the derivatives that are central difference in nature, also indicated in Figure 2-1. It can be seen that the left-hand side spatial derivative occurring at time n and the difference equation indicates the location to be at $k+1/2$ (central difference). The right-hand side is a time difference with the central difference yielding the time to be at n and the spatial location is also at $k+1/2$. It is seen that both the left- and right-hand side of the equation occur at the same time and same location. This will be a governing principle used throughout the derivation of the stochastic wave equations. Carried throughout this derivation will be the time superscript:

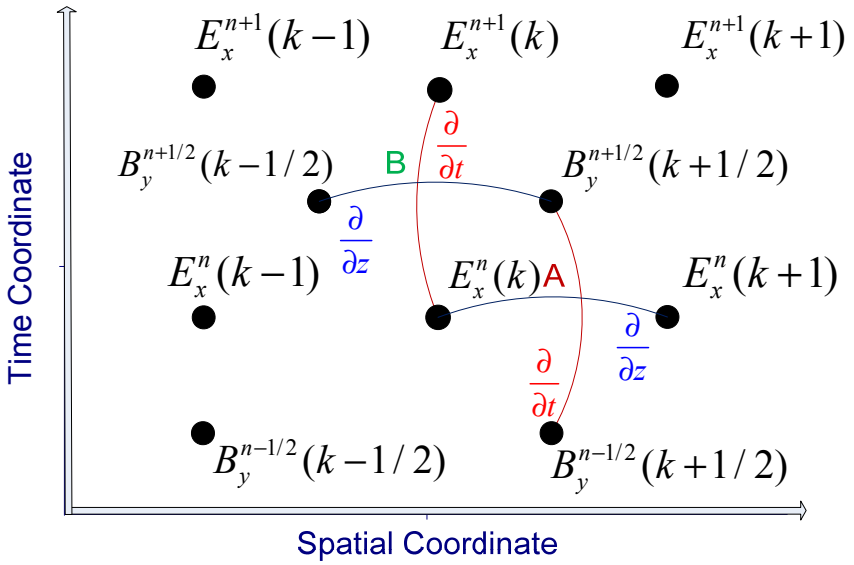

Figure 2-1 Time and space grid system

$$\frac{B_y^{n+1/2}(k+1/2)-B_y^{n-1/2}(k+1/2)}{\Delta t}=-\frac{\left(E_x^n(k+1)-E_x^n(k)\right)}{\Delta z} \tag{2.3}$$

n and the spatial counter k - so that we can see at what time and place the mean and the variance equations occur. The following equation illustrates the forgoing information in that the timing and spatial position are the same on the left side of the equation as on the right side of the equation. Equation (2.4) is a standard FDTD for one dimension:

$$B_y^{n+1/2}(k+1/2)=B_y^{n-1/2}(k+1/2)-\frac{\Delta t}{\Delta z}\left(E_x^n(k+1)-E_x^n(k)\right) \tag{2.4}$$

2.2.2 Ampere's Law

This next equation is a statement of Ampere's Law for the one-dimensional case and will be used to derive the one-dimensional Ampere's difference equation:

$$\nabla x\mathbf{H} = \frac{\partial \mathbf{D}}{\partial t} + \underline{\sigma}\mathbf{E} \qquad \begin{vmatrix} \hat{x} & \hat{y} & \hat{z} \\ 0 & 0 & \partial/\partial z \\ 0 & H_y & 0 \end{vmatrix} = -\hat{x}\frac{\partial H_y}{\partial z}$$

$$\frac{\partial \mathbf{D}}{\partial t} = \varepsilon_r \varepsilon_o \left(\frac{\partial E_x}{\partial t}\hat{x} + \frac{\partial E_y}{\partial t}\hat{y} + \frac{\partial E_z}{\partial t}\hat{z} \right) \tag{2.5}$$

$$\underline{\sigma}\mathbf{E} = \underline{\sigma}\left(E_x\hat{x} + E_y\hat{y} + E_z\hat{z} \right)$$

Notice that in this 1D derivation, we only have the $\hat{x}$ direction. Equating the $\hat{x}$ vectors yields the following equation:

$$\begin{gathered} -\hat{x}\frac{\partial Hy}{\partial z} = \varepsilon_r \varepsilon_o \frac{\partial E_x}{\partial t}\hat{x} + \underline{\sigma}E_x\hat{x} \\ \therefore \\ -\frac{\partial H_y}{\partial z} = \varepsilon_r \varepsilon_o \frac{\partial E_x}{\partial t} + \underline{\sigma}E_x \end{gathered} \tag{2.6}$$

Converting the above equation to a finite-difference equation yields the next equation:

$$-\left(\frac{H_y^{n+1/2}\left(k+1/2\right) - H_y^{n+1/2}\left(k-1/2\right)}{\Delta z} \right) = \varepsilon_r \varepsilon_o \left(\frac{E_x^{n+1}\left(k\right) - E_x^{n}\left(k\right)}{\Delta t} \right) + \underline{\sigma}\left(\frac{E_x^{n+1}\left(k\right) + E_x^{n}\left(k\right)}{2} \right)$$

(2.7)

Again observe that equation (2.7) is at the same location and time, i.e. k, $n+1/2$, on both sides of the equation. Collecting terms yields, considering only the E field terms for now we arrive at the next equation:

$$\varepsilon_r\varepsilon_o\left(\frac{E_x^{n+1}(k)-E_x^n(k)}{\Delta t}\right)+\underline{\sigma}\left(\frac{E_x^{n+1}(k)+E_x^n(k)}{2}\right)$$
$$=\left(\frac{\varepsilon_r\varepsilon_o}{\Delta t}+\frac{\underline{\sigma}}{2}\right)E_x^{n+1}(k)+\left(\frac{\underline{\sigma}}{2}-\frac{\varepsilon_r\varepsilon_o}{\Delta t}\right)E_x^n(k) \tag{2.8}$$

Solving for the future E field ($n+1$) term from equation (2.8) yields the next equation where the coefficient of the $E_x^{n+1}(k)$ is divided out on both sides of the equation:

$$E_x^{n+1}(k)=\frac{\frac{\varepsilon_r\varepsilon_o}{\Delta t}-\frac{\underline{\sigma}}{2}}{\frac{\varepsilon_r\varepsilon_o}{\Delta t}+\frac{\underline{\sigma}}{2}}E_x^n(k)-\frac{1}{\left(\frac{\varepsilon_r\varepsilon_o}{\Delta t}+\frac{\underline{\sigma}}{2}\right)\Delta z}\left(H_y^{n+1/2}(k)-H_y^{n+1/2}(k-1)\right) \tag{2.9}$$

2.2.3 Sources of Error

The sources of numerical error are well understood for FDTD simulations [15, 21]. These errors are modeling errors, truncation errors, and round off errors. The modeling errors are those that would be caused by the assumptions used in coming up with a mathematical model. Truncation errors have to do with the conversion from differential to difference equations where the Taylor series is truncated and the model space is discretized in both space and time. One can use longer Taylor series expansions and divide the space into finer and finer increments, but this would lead to more round off errors. Round off errors are due to the way numbers are represented in computers with finite precision. Knowing about these types of errors, one can modify the size of steps, increasing the precision of the computer simulation to use double precision and use more terms of the Taylor series expansion. With the exception of reducing the step size, these

methods are rarely done in practice for FDTD simulations.

This dissertation addresses one aspect of the modeling error – error, uncertainty, or variability in the electrical properties of the tissues. These types of errors have traditionally been ignored, either because they were assumed/hoped to be low or because there was no good way to address them. FDTD simulations use average electrical properties and produce average electric and magnetic fields. But if there is significant variability in the electrical properties of the tissues, we can expect this to produce significant variability in the electromagnetic fields. This is the crux of what this dissertation is about – determining the expected variability in the electromagnetic fields caused by variability or uncertainty in the electrical properties of the tissues.

2.3 Specific Absorption Rate (SAR)

Specific Absorption Rate is the parameter often used to calculate the localized power absorbed by the tissue:

$$SAR = \frac{\underline{\sigma} E_p^2}{2\rho} \text{ (W/kg)} \tag{2.10}$$

Equation (2.10) shows that the SAR is a function of the peak E field (E_p) and the conductivity ($\underline{\sigma}$) of the material the wave travels through divided by the specific weight (ρ) of the material. The units used for Specific Absorption Rate are W/kg.

This type of function is used extensively in 3D analysis of cell phone design.

2.4 Methods of Simulating Variability

What are we talking about when we refer to the mean, variance, or covariance? In this dissertation, we are addressing materials that have electrical properties that vary from one measurement to another for various reasons. In other words, samples of a particular material, including human tissue such as blood, fat, muscle, brain tissue, etc., vary when measured from person to person or from point to point in a given organ. This variability can be due to the age of the person, how soon after death these measurements are made, size of the individual, etc. So in order to take into account the variability of the material's electrical properties, many measurements from various samples of the same type of material are taken. These samples are averaged to give us the mean of the electrical parameter being measured, i.e. the permittivity or the conductivity. Additional data analysis gives the variance, which tells how much the material parameter varies from the mean. When talking about the covariance, we are referring to how two electrical properties vary together. Each of these statistical properties have mathematical definitions [22].

The mean, which is often referred to as the expectation (defined using $\underset{\sim}{E}$) is defined as:

$$\underset{\sim}{E}\{x\} = \mu_x = \sum_i x_i f(x_i)$$

This is the discrete version with $f(x)$ equal to the probability density. The continuous version is:

$$\underset{\sim}{E}\{X\} = \mu_X = \int_{-\infty}^{\infty} xf(x)\,dx \tag{2.11}$$

Of particular interest is the fact that the expectation operator is linear. This property will be used often within this dissertation. We shall use μ to indicate the mean value or expected value.

The variance is often referred to as the mean of the squared difference of each data point from the mean of the data. The discrete rendition is:

$$\sigma^2\{x\} = \underset{\sim}{E}\left\{(x-\mu_X)^2\right\} = \sum_x (x-\mu_X)^2 f(x)$$

and the continuous version is:

$$\sigma^2\{x\} = \underset{\sim}{E}\left\{(x-\mu_X)^2\right\} = \int_{-\infty}^{\infty} (x-\mu_X)^2 f(x) \tag{2.12}$$

Expanding the expectation operator for the variance yields the following form:

$$\underset{\sim}{E}\left\{(x-\mu_X)^2\right\} = \underset{\sim}{E}\left\{x^2\right\} - \mu_X^2$$

The derivation of this form can be found in Appendix C.2. The square-root of the variance gives the standard deviation $\sigma\{x\}$.

The covariance between two random variables is a measure of how these two variables are related to each other and is defined as:

$$Cov\{X,Y\} = \underset{\sim}{E}\left\{\left(X - \underset{\sim}{E}\{X\}\right)\left(Y - \underset{\sim}{E}\{Y\}\right)\right\}$$

where X and Y are random variables. With some manipulation this is reduced to:

$$Cov\{X,Y\} = E\{XY\} - E\{X\}E\{Y\}$$

A more complete derivation of these and other statistical properties are found in Appendix C of the dissertation.

These definitions and other statistical properties will be used throughout this dissertation to develop the S-FDTD equations.

2.4.1 Monte Carlo Analysis

The Monte Carlo method is really a class of various techniques for the simulation of stochastic properties and their responses. Monte Carlo methods have been extensively used in the physical sciences, engineering, the financial industry, risk analysis, etc. They have been used for the evaluation of unusually difficult to evaluate integrals. There are modified methods of Monte Carlo analysis such as "importance sampling" which is a way of restricting the sampling to speed up the evaluation, particularly in the simulation of rare events [23].

2.4.1.1 Basics of Monte Carlo analysis. Monte Carlo analysis takes this basic form:

1) Define the possible inputs and their statistical properties
2) Generate these inputs in a random manner according to their statistical properties

3) Perform a deterministic calculation using the randomly generated inputs
4) Collect all simulation responses
5) Analyze the collected data for their statistical properties

From this we can see the framework that is used most often in Monte Carlo analysis. It allows one to use the deterministic model for the simulation, varying only the parameters that are random in nature, and with the aid of computers, perform these calculations and analyze the data for the mean, variance, and any other statistical parameters. Drawbacks include time to simulate and the necessity of storing data for each simulation.

2.4.1.2 Application of Monte Carlo method. A very good example of the use of the Monte Carlo method is found in [8] which evaluated microstrip antenna detuning when implanted in the human body. The analysis of how the implantable antenna is detuned due to the tissue variations, which includes the various tissue thicknesses and their electrical properties, show that some antenna designs have a higher detuning over the range of expected variance in the tissues than others.

Following the outline given previously, [8] randomly generated the input parameters according to their statistical properties using a random number generator. These particular parameters were then used as inputs to the analytical model.

A variational method was used to develop a deterministic mathematical model of a multilayer system. From this, [8] determined the complex permittivity of the system and quantified the detuning of the antenna. Shifts in resonant frequency and changes in usable bandwidth were evaluated and used to define the detuning.

The calculated results from each simulation using randomly generated input

parameters were collected and stored. Finally, these data were analyzed to determine the statistical properties of the detuning of the implantable antenna.

This illustrates very well the use of the Monte Carlo analysis method and the steps needed to perform the analysis.

2.4.2 Stochastic Finite Element Method (SFEM)

The finite element method originated mainly in the field of structural analysis, and it has also been used in electromagnetics and other fields. It can handle complex geometries and is used in many software programs because of the generality of its method. The finite element method is comprised mainly of four steps: (1) discretizing the model space into a finite number of elements, (2) deriving the governing equations for the model space, (3) assembling all the elements into a solution region, and finally (4) solving the system of equations [21]. The SFEM process is akin to the standard FEM with stochastic equations that take into account the properties that are allowed to vary, i.e. material properties.

The stochastic equations can be so complex that they cannot be solved analytically and so are approximated using various methods such as truncated Taylor series expansions to linearize the problem and reduce the complexity of the analysis. Similar to the FDTD method, Monte Carlo could also be used with the FEM [24].

2.4.3 Perturbation Method

Perturbation theory [25] is used to find an approximate solution to a problem when it is very difficult to find an exact solution. In the classical sense, it assumes that the solution has a Taylor (or other) series expansion that is truncated using only the first

few terms. This truncated series is substituted into the equation, providing an approximation, and the equation is expanded. The coefficients of the Taylor series are then determined via linear algebra. This method has been used in a number of problems throughout history, including finding the stochastic properties of mechanical systems using FEM [24].

In the sense that it is being used here, the stochastic function $g(\varepsilon_R, \underline{\sigma})$ is expanded in a Taylor series about the mean of the random tissue property variables, ε_R (permittivity) and $\underline{\sigma}$ (conductivity), and the other random variables within the equation. The truncated series is substituted back into the equation for the expectation $\underset{\sim}{E}\{g(\varepsilon_R, \underline{\sigma})\}$ and that of the variance $\sigma^2\{g(\varepsilon_R, \underline{\sigma})\}$ which is equal to $\underset{\sim}{E}\left\{g(\varepsilon_R, \underline{\sigma})^2\right\} - \underset{\sim}{E}\{g(\varepsilon_R, \underline{\sigma})\}^2$ [22]. These equations are expanded using a Taylor series expansion, and higher order terms are discarded. This method is called the Delta method and will be elaborated on in great detail in Section 4.1.

2.5 Summary

A general background has been given within this chapter so as to set the stage for understanding the rest of this dissertation. Maxwell's equations, i.e. Faraday's and Ampere's Laws, are converted to the one-dimensional Finite-Difference Time-Domain (FDTD) equations. Methods of simulating variability were discussed. Perturbation methods were brought out to show how they can reduce a complex problem into a more manageable problem to develop an approximation of the function being analyzed.

In the coming chapters, we will discuss Monte Carlo analysis (Chapter 3) as the gold standard to determine how good the S-FDTD approximations are. In addition, it is

used to develop and evaluate additional approximations that are needed to develop the S-FDTD analysis method - such as the approximations to correlation coefficients between field components and the constituitive parameters. Monte Carlo analysis will give an opportunity to evaluate these approximations.

Chapter 4 goes into detail on the Delta method, deriving all the needed equations that comprise the method, then deriving the S-FDTD equations themselves, i.e. mean and variance. More detail about Taylor's series approximations will be discussed. Chapter 5 will be used to validate S-FDTD analysis and discuss what has been accomplished and what still needs to be addressed. Appendices have been added to add additional content useful for brief reviews of probability and a repository of tissue data used within this work.

CHAPTER 3

MONTE CARLO ANALYSIS

Monte Carlo analysis is a method for determining the variability effect due to random variations in material properties and any other type of random variable. It is used in science, engineering, and financial disciplines, as well as any field that needs to compute the variability of something. This method is discussed in Section 2.4.1, and we will refer to this type of analysis throughout this dissertation as M-FDTD when Monte Carlo is applied using FDTD analysis.

Monte Carlo analysis will be used here for a number of different purposes. First, it will be used (in Section 3.3) to help determine which approximations are best for the correlation coefficients used in the Stochastic-FDTD equations for E and H, which are derived in Chapter 4. Second, the same Monte Carlo analysis will be used to calculate the variance for different FDTD models, which are used as comparisons (in Chapter 5) to determine how closely the Stochastic-FDTD method is able to predict these same variances.

M-FDTD analysis requires repeated FDTD simulations using different parameters for the permittivity (ε_r) and conductivity ($\underline{\sigma}$), which are randomly generated according to their statistical distribution. These values are input to the model at the start of each simulation. Simple layered models (air-skin and air-skin-fat-muscle and permutations

thereof) are used to validate the S-FDTD method. For this dissertation, the thicknesses of the dielectric layers are held constant, but the electrical properties of the tissues are randomly determined (Gaussian distributed) at the beginning of each run of the FDTD analysis. The results of each simulation were then stored for postprocessing statistical analysis. This provided the variance of the fields as well as a way to check approximations such as the correlation coefficients used in the S-FDTD method and the final variances of the fields within the model.

3.1 Material Properties

Human tissue has significant variability. Tissue samples from many different types of animals as well as human tissues have been studied for decades for their electrical properties [26]. In a few such studies, systematic variations in these electrical parameters were seen with the age of the animal which were thought to extend to human tissue [27]. Gabriel explained that "biological material is a mixture of water, ion, and organic molecules" [27]. These electrical properties are frequency dependent and have three regions of dispersion that vary according to frequency. These regions are affected by the cell structure and the environment in which they find themselves. The same type of tissue varies in structure from person to person. Biological tissues are inhomogeneous. Their significant variability in structure and composition from person to person results in potentially significant differences in dielectric properties [27].

Gabriel looked at tissues from a strain of Wistar rats that were at various ages from 10 to 70 days old. All of her measurements were made from 3 to 5 hours after death of the rat. The tissue was maintained at 37℃ by placing the tissue in water at that temperature. The probe was also maintained at that temperature. The water bath also

helped maintain the hydration of the tissue. Her frequency range was 300 kHz to 1 GHz using a 10mm open-ended coaxial probe and computer controlled network analyzer. She took great care to minimize known sources of error, and her sample sizes were chosen to be appropriate for the frequency range she was using.

Measurements have been made through the years and some of these data have been listed in the following tables. The data in Table 3-1 and Table 3-2 list the mean and the variance of the electrical properties used in this analysis.

The electrical properties of tissues ($\underline{\sigma}$ (conductivity) and ε_r (relative permittivity)) will be modeled with a normal distribution and as independent random variables in this dissertation. With only limited data on the statistical variation of tissues, it is not certain that the tissue properties vary normally, so if this is determined by the measurement community to be different in the future, then the assumptions in this dissertation will need to be adapted to fit the new assumption of variation of tissues.

Let us look further into what it means to have normally distributed and independent random variables. The normal or Gaussian probability density function is:

$$f(x) = \frac{1}{\sqrt{2\pi\underline{\sigma}^2}} e^{\frac{-(x-\mu_x)^2}{2\underline{\sigma}^2}} \tag{3.1}$$

This equation is used to define a set of tissue properties (used to run the multiple FDTD simulations) that meet the mean and the variance of a specific normal distribution.

At the beginning of each of the FDTD simulations used in the Monte Carlo verification analysis, the random variable is selected per equation (3.1). Figure 3-1 shows the permittivity of 10,000 tissue samples used in the Monte Carlo analysis. The

Table 3-1 Nominal dielectric constants and conductivities and their standard deviations [SD] for human tissue [8]

Dielectric	ε_r Mean	ε_r [SD]	$\underline{\sigma}$ Mean (S/m)	$\underline{\sigma}$ [SD]	Nominal (mm) thickness
Muscle	55.0	4.6	0.87	0.10	42
Fat (infiltrated)	16.2	2.7	0.214	0.06	54
Skin	39.0	3.4	0.43	0.10	5.4

Table 3-2 Dielectric constants and conductivities for human tissues at 100MHz and 350MHz[28]

Organ	Dielectric Constant 100MHz	Conductivity (S/m) 100MHz	Dielectric Constant 350MHz	Conductivity (S/m) 350MHz
Muscle	73.5	1.1	53.0	1.33
Fat/bone	7.5	0.067	5.7	0.072
Blood	74.0	1.1	65.0	1.2
Intestine	36.2	0.55	26.5	0.66
Cartilage	7.5	0.067	5.7	0.072
Liver	77.0	0.62	50.0	0.82
Kidney	90.0	1.01	53.0	1.16
Pancreas	90.0	1.01	53.0	1.16
Spleen	100.0	0.82	90.0	0.9
Lung	75.0	1.03	35.0	1.1
Heart	76.0	0.75	56.0	1.0
Nerve	82.0	0.53	60.0	0.65
Skin	24.5	0.55	17.6	0.44
Eye	85.0	1.9	80.0	1.9

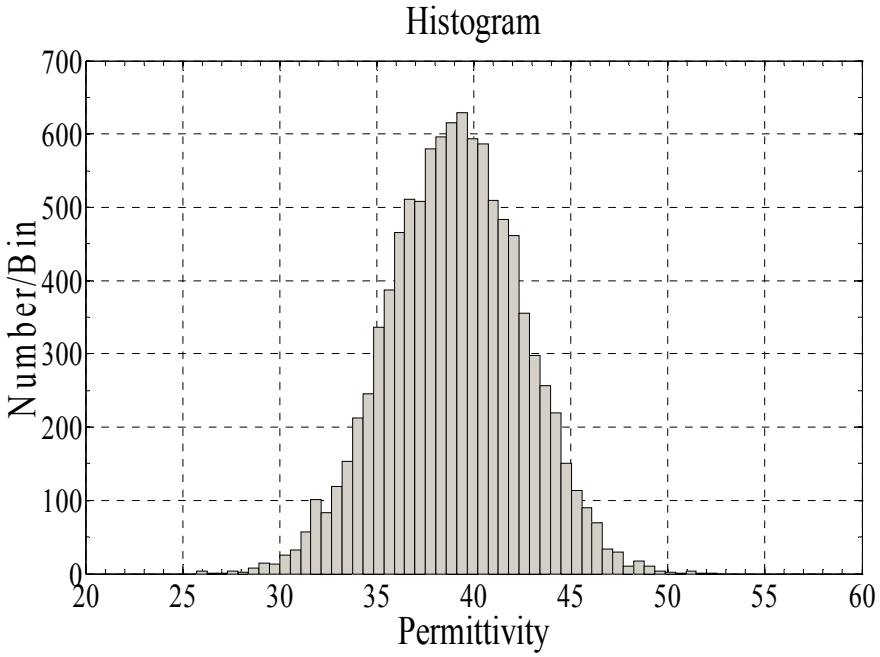

Figure 3-1 Relative permittivity of skin with a mean of 39 and standard deviation of 3.4[8]

histogram shows a normally distributed permittivity for skin with a mean of 39 and a standard deviation of 3.4 taken from Table 3-1. Independence in random variables means that each of the tissue properties were determined without regard to any other parameter. Furthermore, the permittivity and conductivity of any given tissue were varied independently as well. Complete independence is unlikely in realistic situations. For instance, if a person is well hydrated, it is likely their tissues will be more conductive than if they are dehydrated. But the data on statistical variability of tissues are insufficient to provide a more advanced model than normal distributed independent random variables. Future measurements could be used to refine this model and adapt the specifics of the method accordingly.

These random properties of the dielectric materials cause the amplitude and phase of the E and H fields to randomly vary. These fields will therefore also be random in

nature and will be treated as random variables throughout this dissertation. The goal of this work is to predict the variability (variance or standard deviation) of these fields and other properties associated with them (such as Specific Absorption Rate or SAR). The results of the Monte Carlo analysis will be used for comparison with the results of the S-FDTD method developed in this dissertation.

3.2 Monte Carlo Analysis (Using Randomized Electrical Properties)

3.2.1 Single-layer Analysis

A Monte Carlo analysis using a one-dimensional FDTD simulation with a model composed of a single layer interface is shown in Figure 3-2. The E field source (frequency of either 915MHz or 2GHz) is to the left of the interface in the air dielectric one wavelength away. The field propagates to the right through the dielectric interface where the thickness of the dielectric is infinite in extent. The grid was set so that we would have 40 steps (dx) per wavelength in the dielectric portion of the model. This same spatial step was also used in the air, which has a longer wavelength than the material, and thus a finer sampling per wavelength. The time step dt was chosen to be equal to $dx/(2c_o)$ where c_o is the speed of light in a vacuum. The total number of time steps per simulation is 10,000. The number of simulations per Monte Carlo analysis was 10,000. Each electrical parameter, i.e. $\varepsilon_r, \underline{\sigma}$ for skin, were determined using equation (3.1) with the mean and standard deviations taken from Table 3-1.

The electrical parameters were determined at the beginning of each simulation. The results were stored before another simulation would commence. Figure 3-3 shows postprocessing information for the E field mean peak amplitude[29], yielding the field

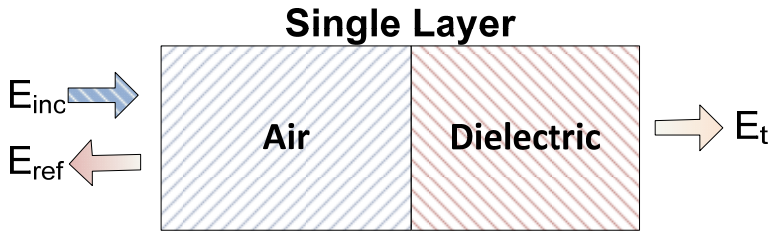

Figure 3-2 Single layer used for Monte Carlo analysis. Both layers are modeled as being infinite in extent using absorbing boundary conditions on the front and back of the model.

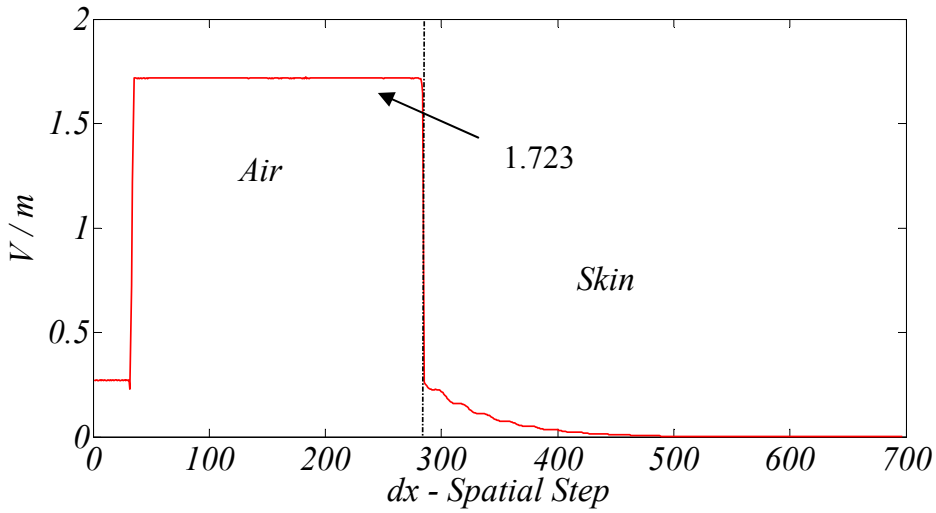

Figure 3-3 Monte Carlo analysis - Peak E field at 915MHz

amplitude at 915MH.

FDTD with the data in Figure 3-3 can be used to determine the reflection coefficient. The dielectric constant of skin is 39, and the conductivity is 0.43. We can determine the wave impedance by using the next equation:

$$\eta = \frac{j\omega\mu}{j\omega\sqrt{\mu\varepsilon'}\sqrt{1 - j\frac{\sigma}{\omega\varepsilon'}}}$$

which gives $\eta_{skin} = 59.677\angle -1.98^{\circ}$ ohms. The wave impedance of air is $120\pi\ \Omega$. For this simple two-layer system, the magnitude of the reflection coefficient is:

$$|\Gamma| = \left| \frac{\eta_{skin} - \eta_{air}}{\eta_{skin} + \eta_{air}} \right|$$

From Figure 3-3, the peak amplitude is 1.723 V/m for an incident wave of 1V/m. We can find the reflected field by subtracting the incident field from the total field and dividing by the incident field, giving the magnitude of the reflected wave to be 0.723 V/m. The reflection coefficients determined from FDTD analysis and by analytical means are close to each other.

The variance is determined by using the following equation:

$$\sigma^2 \left\{ E_{field\ data} \right\} = \frac{1}{N-1} \sum_{i=1}^{N} \left(E_{field\ data} - \mu_{E_{field\ data}} \right)^2$$

and is plotted in Figure 3-4 for the two-layer air-skin system shown in Figure 3-2.

Figure 3-4 is the instantaneous variance determined at the 10,000th time step, so it is a snap shot in time. In later sections of this dissertation, the peak values of variance were used, rather than the instantaneous values. These peak values were found using the 2E2U method [29] similar to how the peaks of the fields were found. For this example, the instantaneous value was used to verify the S-FDTD calculation of variance. One might wonder why there is variance in the E field in the air portion of the wave where there is no variance in the electrical properties of air. This variance comes from variation

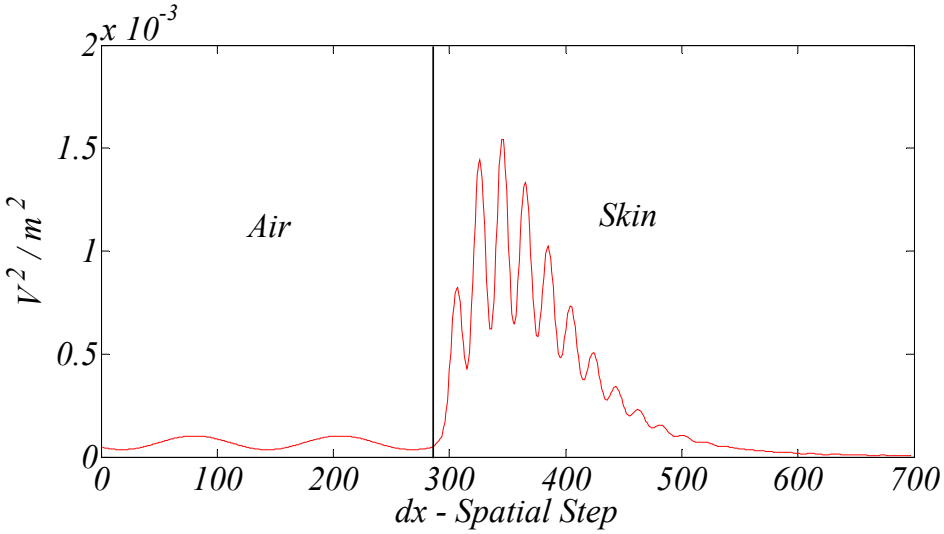

Figure 3-4 Monte Carlo analysis – Variance of the two-layer air-skin system shown in Figure 3-2 at 915MHz

in the skin properties, which affect the reflected fields from the skin interface and thus cause variance in the fields in air.

Performing the same analysis at 2GHz the reflection coefficient determined analytically (seen in Figure 3-5) was $|\Gamma| = 0.725$ and the Monte Carlo analysis yielded a reflection magnitude of 0.713.

The variance of the E field for the air-skin model at 2GHz is shown in Figure 3-6 to be used to verify the S-FDTD method found in Chapter 5.

Again we see a variance in the air portion of the model due to reflections off of the air/dielectric interface. This plot also shows a wave like structure to the variance which will be addressed more in Chapter 5 specifically the propagation of the variance within the model space.

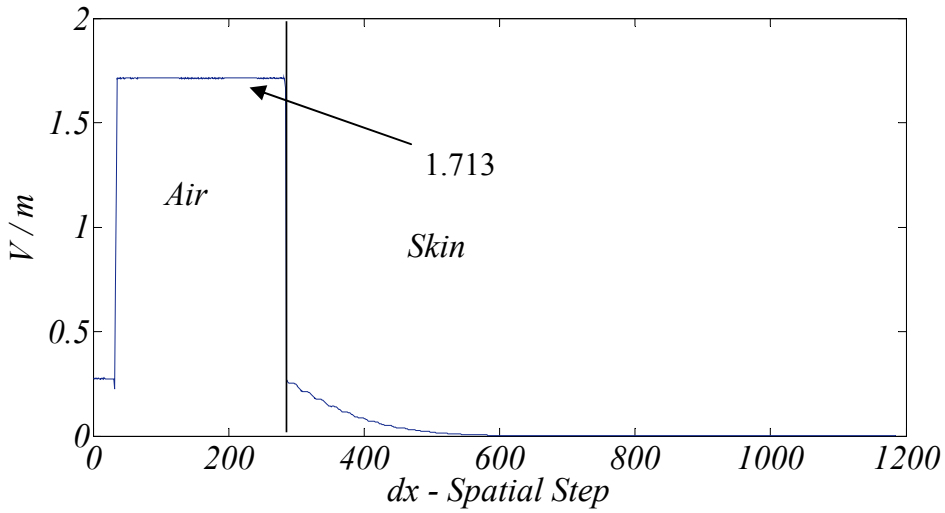

Figure 3-5 Monte Carlo analysis - Peak E field at 2GHz

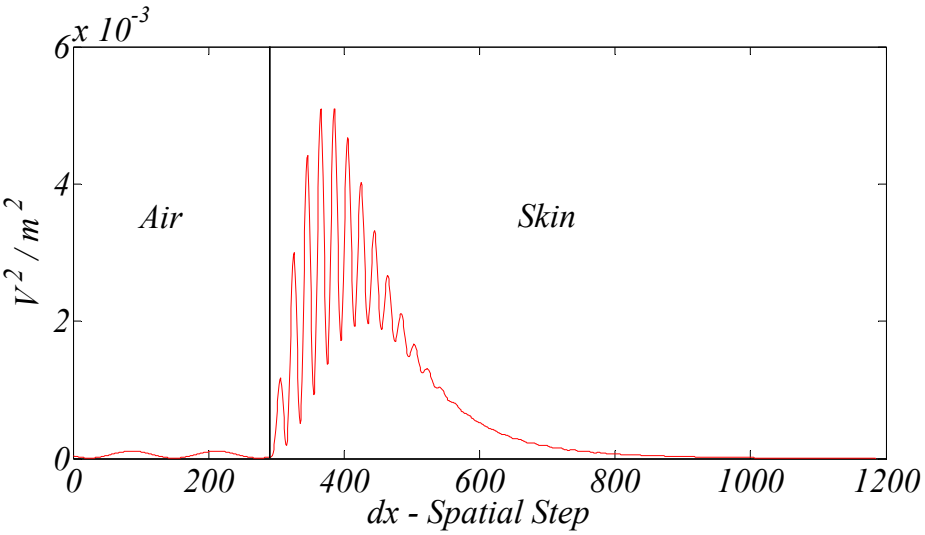

Figure 3-6 Monte Carlo analysis - Variance at 2GHz

3.2.2 Three-layer Analysis

The verification of the S-FDTD code was then extended to the three-layer model shown in Figure 3-7. The materials' electrical parameters as follows:

Layer 1: Skin with $\varepsilon_r = 39$ and a standard deviation = 3.4, $\underline{\sigma} = 0.43$ S/m standard deviation = 0.1, $thickness = 5.4mm$.

Layer 2: Fat with $\varepsilon_r = 16.2$ and a standard deviation of 2.7, $\underline{\sigma} = 0.214$ with a standard deviation of 0.06, and a $thickness = 54mm$.

Layer 3: Muscle with $\varepsilon_r = 55$ and a standard deviation of 4.6 and a $\underline{\sigma} = 0.87$ with a standard deviation of 0.1 and with a $thickness = 42mm$.

The 1V/m E field source (frequency = 2GHz) is to the left of the model in the air one wavelength away from the air-dielectric interface. The field propagates to the right through the various layers, first seeing the skin, then the fat, then the muscle, and finally the air in this case. The thicknesses of the three layers were based on the nominal thickness of human tissue, i.e. skin = 5.4mm, fat = 54mm, and the muscle 42mm [8]. The grid was set so that we would have 40 steps "dx" per wavelength in the material considering the smallest wavelength in the model. This would be in the highest dielectric permittivity material (skin in this case). This spatial step was 0.5 mm and was held constant in all dielectric regions. The time step was chosen to be equal to ($dt = dx/(2c_o)$) = $8.4275x10^{-13}$ sec for stability. The total number of time steps per simulation was 10,000. The number of simulations per Monte Carlo analysis was 10,000. Each electrical parameter, i.e. $\varepsilon_r, \underline{\sigma}$, was selected using equation (3.1) and with the mean and the variance selected from Table 3-1. Again each parameter was chosen independently (layer to layer).

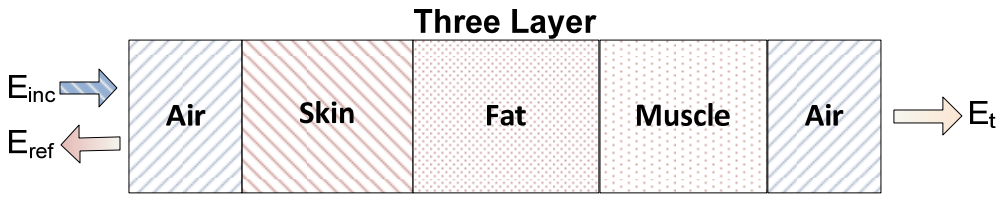

Figure 3-7 Three-layer structure used for the Monte Carlo analysis

This analysis took about 2.8 hours to run one full Monte Carlo analysis using an Intel Core™2 CPU 2.13GHz, with 2.00 GB of RAM. The thicknesses were held constant in all of these simulations.

To verify that each Gaussian variable was determined independently of the others from layer to layer, the correlation coefficient matrixes for both the conductance $\underline{\sigma}$ and the relative dielectric constant ε_r were determined:

$$\underline{\sigma},\ \text{correlation matrix} = \begin{bmatrix} 1.0000 & 0.0208 & 0.0126 \\ 0.0208 & 1.0000 & 0.0069 \\ 0.0126 & 0.0069 & 1.0000 \end{bmatrix}$$

and for the permittivity

$$\varepsilon_r,\ \text{correlation matrix} = \begin{bmatrix} 1.0000 & -0.0075 & -0.0224 \\ -0.0075 & 1.0000 & -0.0088 \\ -0.0224 & -0.0088 & 1.0000 \end{bmatrix}$$

The different matrices are determined by using the electrical parameter from each layer and to determine the correlation coefficients $\rho_{X,Y}$:

$$\rho_{X,Y} = \frac{Cov\{X,Y\}}{\sigma\{X\}\sigma\{Y\}}$$

Off diagonal elements of these matrices are the cross correlation coefficients of the different materials, whereas the diagonal elements are the variances. The range of the correlation coefficient $\rho_{X,Y}$ is $-1 \le \rho_{X,Y} \le 1$. The closer this coefficient is to zero, the more independent the terms are from each other. The matrices show the off diagonal elements to be close to zero, verifying that the electrical parameters are nearly independent of each other.

To illustrate how the fields move within the layers, a sample of the fields was taken from the 3rd layer at the beginning of the dielectric, with another sample taken from the end of the dielectric layer (see Figure 3-8). It can be seen that the *E* field varies from one simulation to another because of the various permittivities and conductivities of each dielectric layer. The more separation there is between each subsequent test (line) in Figure 3-8, the larger the variation. Figure 3-8 demonstrates how the Monte Carlo analysis performs each separate FDTD simulation using Gaussian distributed tissue properties, such as those shown in the histogram in Figure 3-1. The electric field is computed in the time domain as shown in Figure 3-8. The magnitude and phase of the electric field for each simulation are then stored for later analysis. Values of interest such as the mean or the variance of the fields are calculated by postprocessing these stored data. The following figures show the resultant average electric fields and variance of these fields. Figure 3-9 shows the peak E field at 915MHz with the model space arranged with 3 layers with the following order: skin, fat, and muscle. Next, Figure 3-10 shows the variance calculated at 915MHz for the same Monte Carlo data used to find the

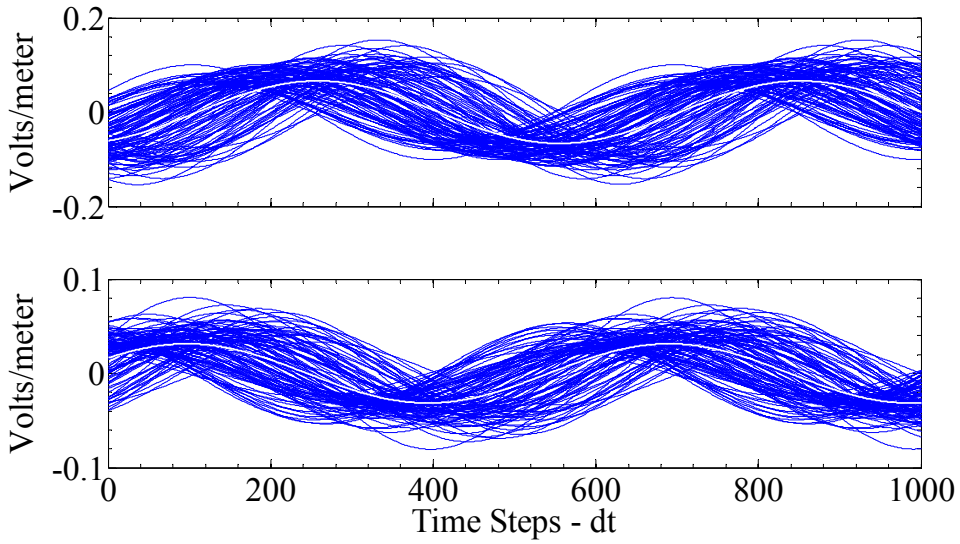

Figure 3-8 E Field variation at 2GHz taken at two different points within 3rd layer

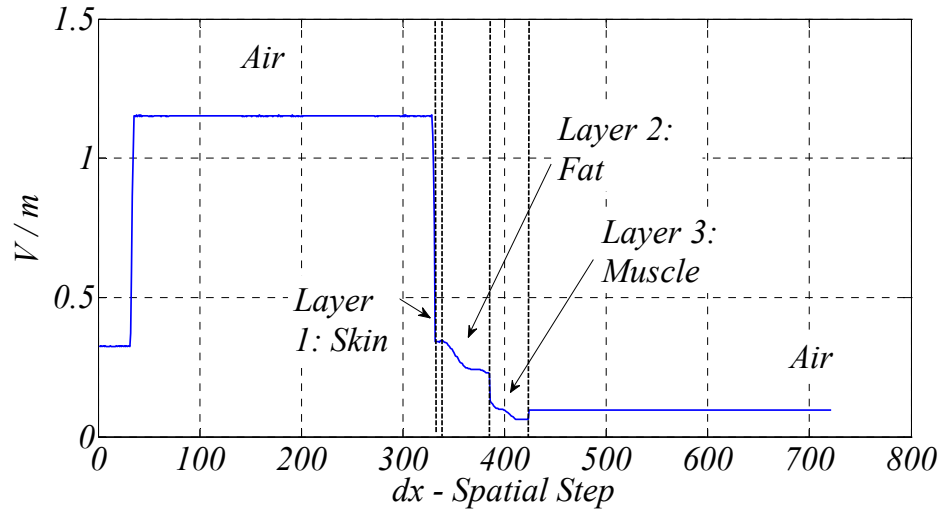

Figure 3-9 Mean peak E field at 915MHz for the three-layer model shown in Figure 3-7 calculated from the data gathered in the Monte Carlo analysis

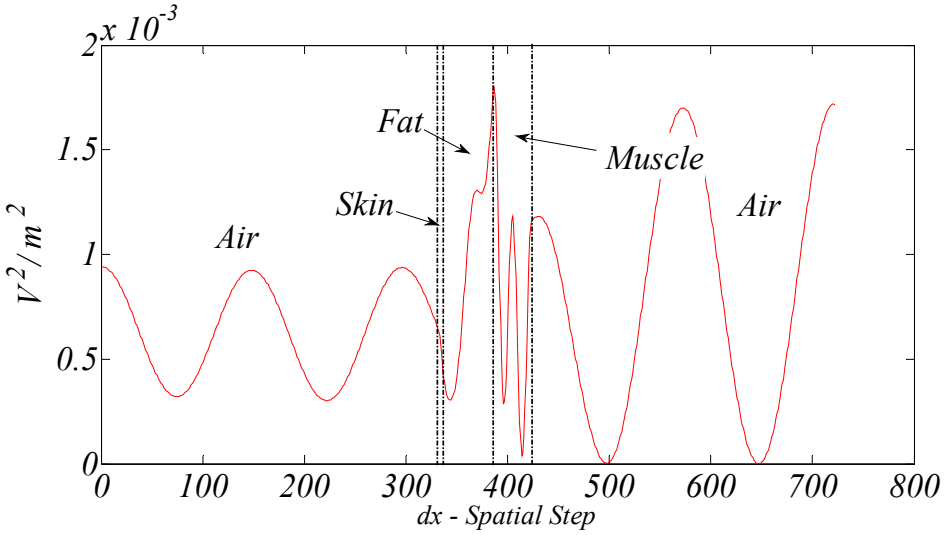

Figure 3-10 E field variance at 915MHz calculated from the data gathered in the Monte Carlo analysis

mean peak E field of the previous plot.

The next plots illustrate the same arrangement and simulated at 2GHz. The distance of the source from the first dielectric interface has been kept one wavelength away. Figure 3-11 is a plot of the peak mean E field.

Figure 3-12 uses the same data produced from the Mont Carlo analysis previously used to generate the peak mean E field data in Figure 3-11 to determine the variance of the wave data gathered. The different dielectrics have been labeled in each figure so that the changes in the mean and the variance can more readily be seen.

The objective of this dissertation research is to develop a Stochastic FDTD method that can compute the mean and variance of the fields from a single FDTD run. In the following discussions and figures, this method is called the S-FDTD method. The Monte Carlo method that runs the FDTD simulation multiple times using statistically varying tissue properties is called the M-FDTD method. It is not as efficient as the S-

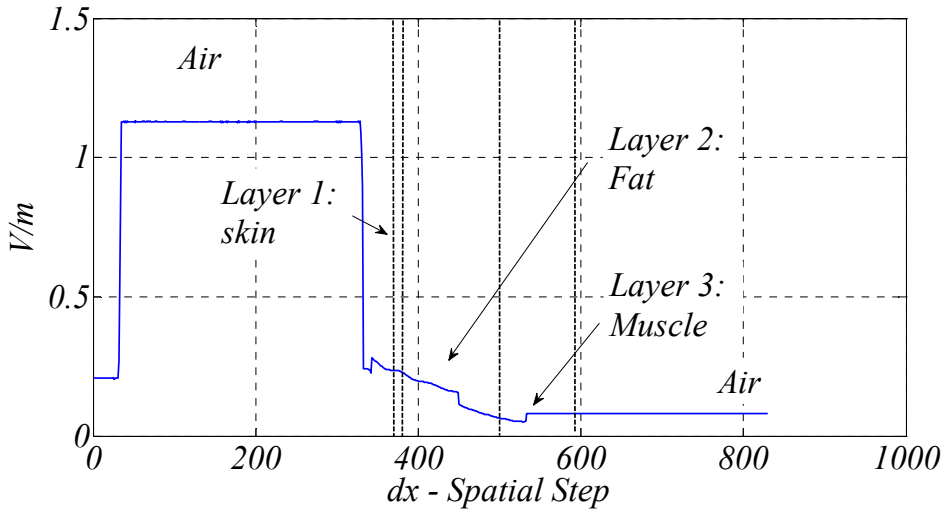

Figure 3-11 Mean peak E field at 2GHz for the same model space in Figure 3-7 calculated from the data gathered in the Monte Carlo Analysis

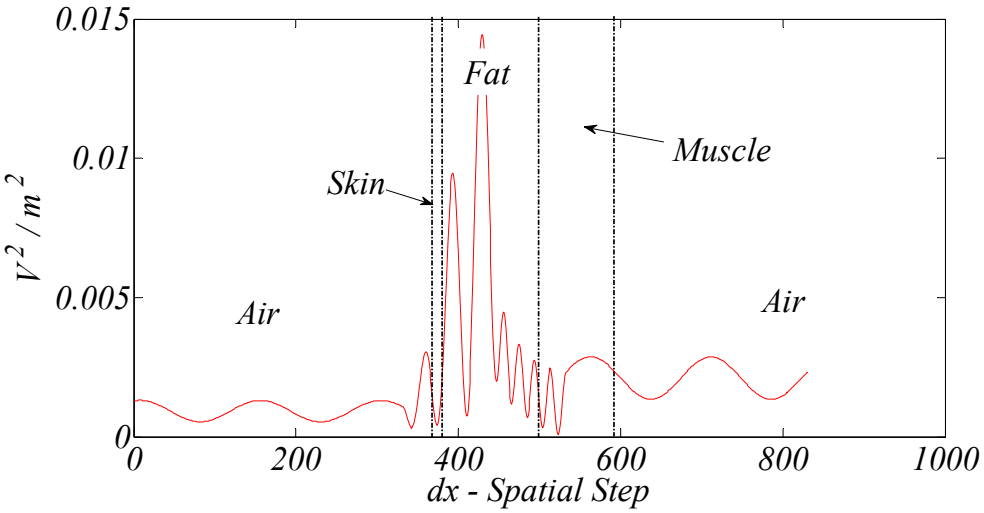

Figure 3-12 E field variance at 2GHz calculated from the data gathered in the Monte Carlo analysis

FDTD method but is used as the 'gold standard' for calculating variance. The mean and variance at each location obtained with the M-FDTD method are to be compared with the same values computed using the Stochastic FDTD (S-FDTD) method. These comparisons are found in Chapter 5.

In the analyses that follow, the dielectric layer thicknesses have been widened to 54mm, and the order of the layers (skin-fat-muscle) is changed. This is obviously not biologically realistic, but is a test of the numerical responsiveness of the model to changes. Overlaying the plots will allow the differences in mean and variance between the M-FDTD and the S-FDTD analyses to be more easily seen.

Figure 3-13 depicts the type of data that was taken, which is postprocessed in the M-FDTD method to determine the mean and the variance of the fields collected. The variability of the E field is shown in the figure. The amplitude and phase of the E field are modified for each run of the Monte Carlo analysis. The effect is the spreading of the various fields.

These data are then postprocessed in the M-FDTD method to determine the mean and variance, which are shown in the following figures (Figure 3-14 and Figure 3-15). We have chosen again to look at the mean in terms of the peak E field. Dielectric layers have been labled, and interfaces are indicated in the various plots. The plots show that the mean dimishes with distance through the dielectric model space which is due to the nonzero conductivity of each dieletric material. We see that the air portions of the plot show constant amplitude of the mean and the variance due to the lossless nature of the medium through which the wave propagates. Figure 3-15 shows the variance within each dielectric layer as the field propagates through the dielectric layers.

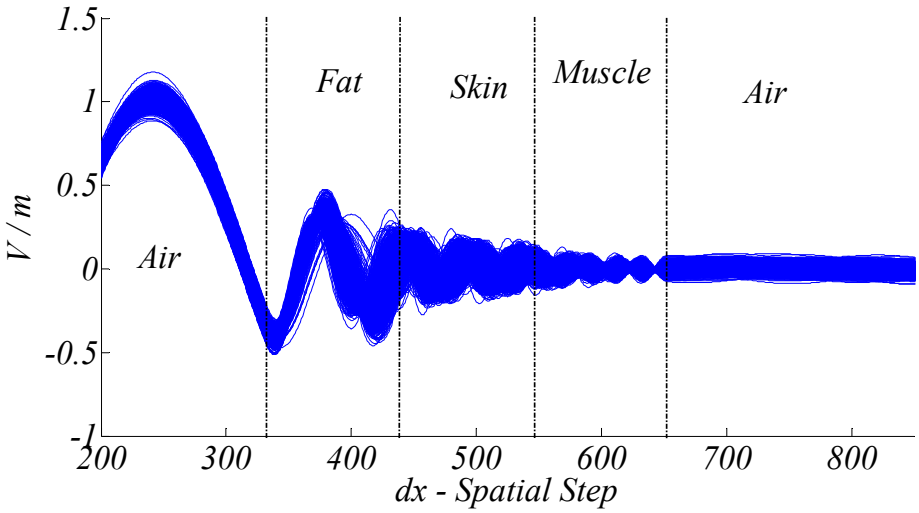

Figure 3-13 E field data gathered from M-FDTD analysis at 2GHz (Fat, Skin, Muscle)

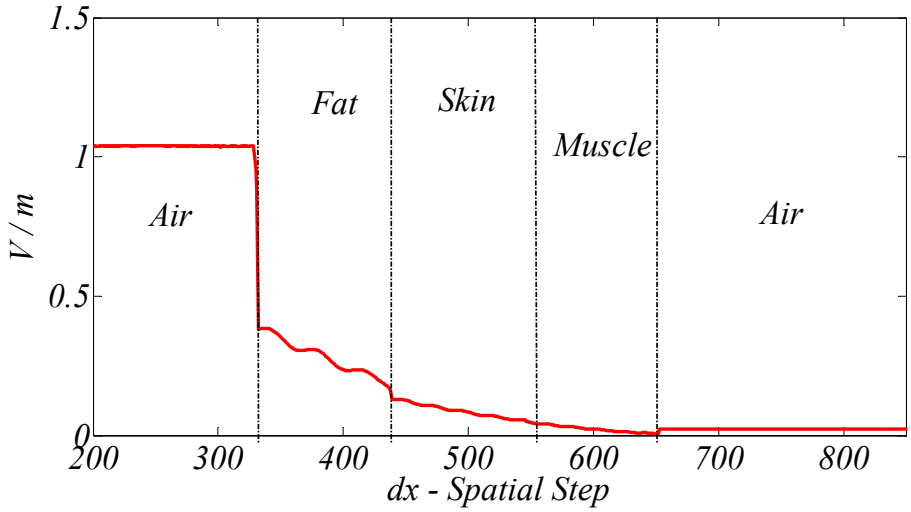

Figure 3-14 E field mean calculated from the data shown in Figure 3-13 (Fat, Skin, Muscle)

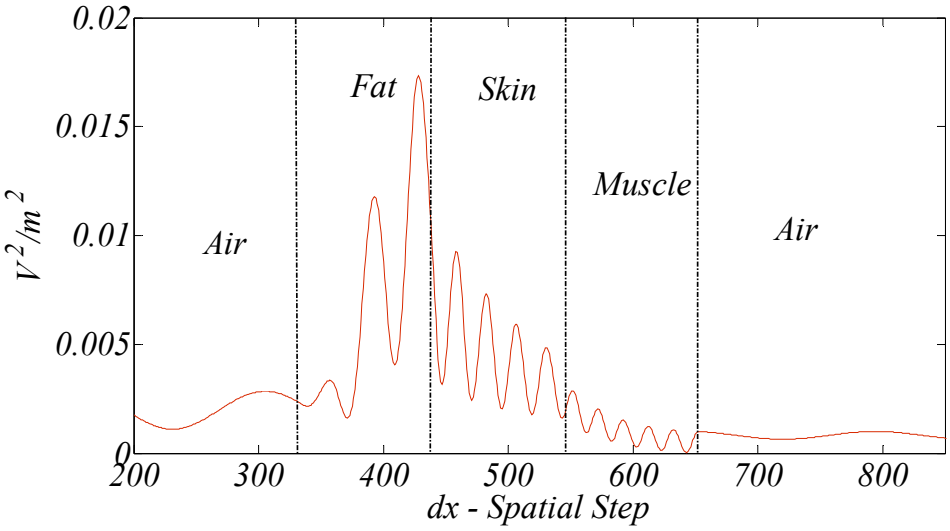

Figure 3-15 E field variance calculated from the fields shown in Figure 3-13. (Fat, Skin, Muscle)

Figure 3-16 shows that the variance increases as the wave propagates through the various dielectric layers using percent variation from the mean of the E field. 10,000 FDTD simulations were performed in the Monte Carlo simulation to gather this information.

The same type of analysis was performed with the order of the dielectric layers changed to muscle, fat, and skin. This was done to see how the order affects the variance of the fields propagating through the different layers. From Figure 3-17 we see that the E field gets more random as the wave propagates through the various dielectric layers, making it difficult to see the sinusoidal nature of the propagating wave. The same type of analysis is performed again for the model contained in Figure 3-17, and its results are found in the next few figures. In Figure 3-18 is shown the absolute variance and then in Figure 3-19 the variance is compared to the peak mean E field.

In Figure 3-20 the dielectric order is changed to muscle, skin, and fat. We see

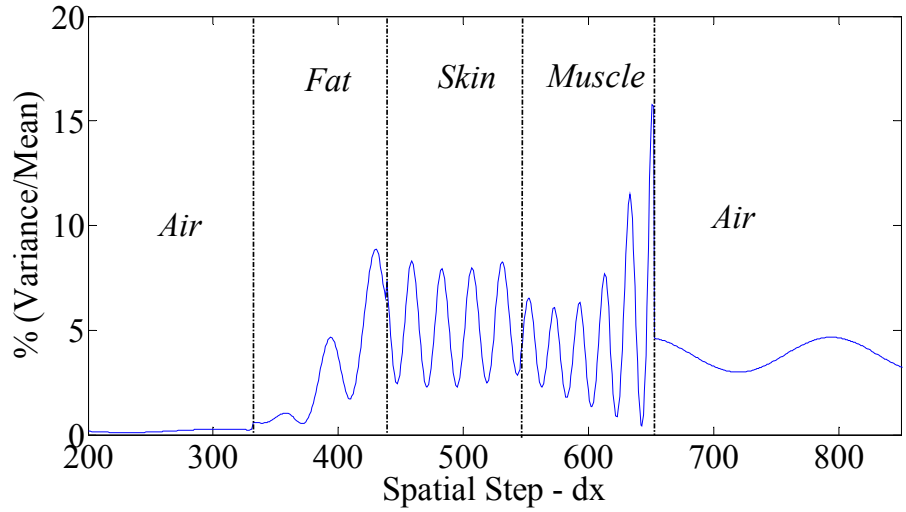

Figure 3-16 2GHz normalized percent comparison of the variance to mean peak E field (Fat, Skin, Muscle)

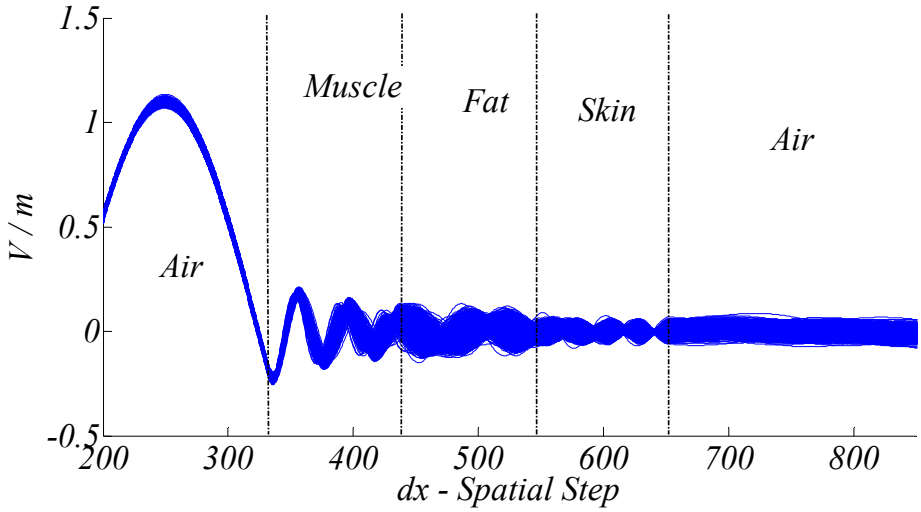

Figure 3-17 Electrical field as a functon of location for several different Monte Carlo simulations at 2GHz (Muscle, Fat, Skin)

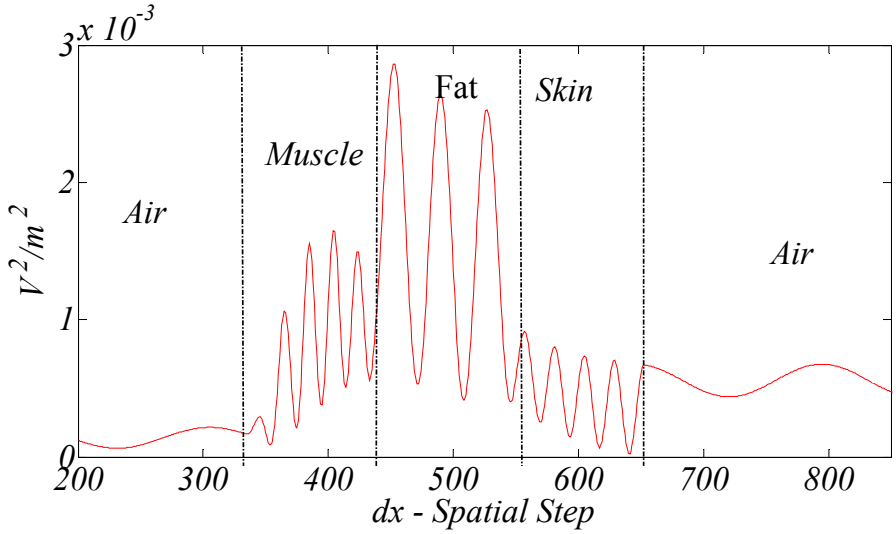

Figure 3-18 E field variance of the data shown in Figure 3-17 (Muscle, Fat, Skin)

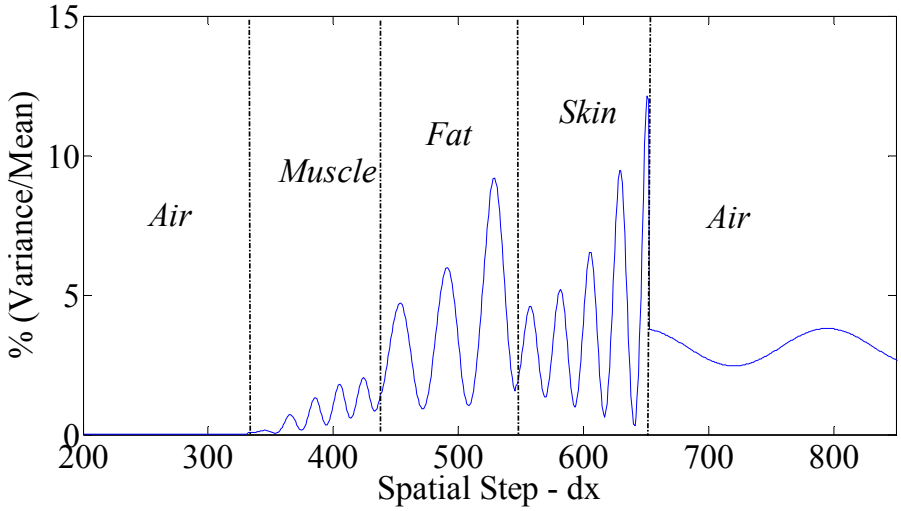

Figure 3-19 2GHz normalized percent comparison of the variance to mean peak E field for data shown in Figure 3-17 (Muscle, Fat, Skin)

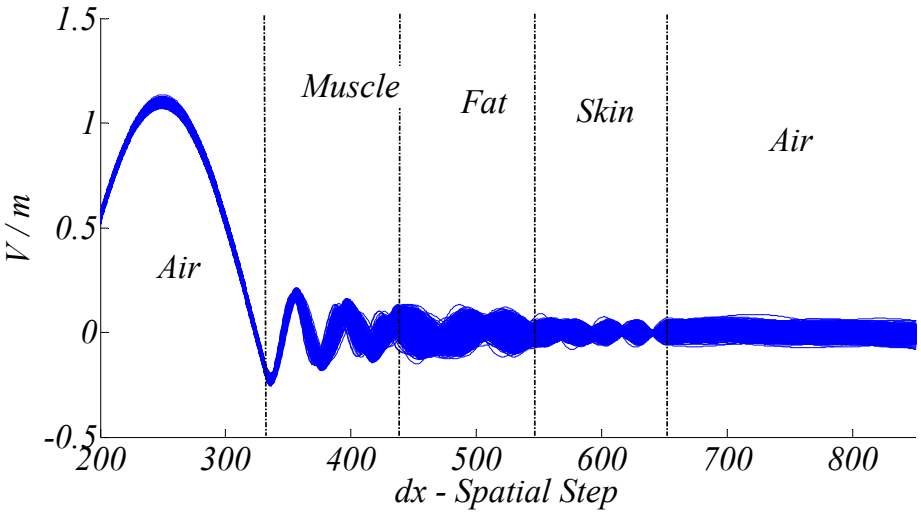

Figure 3-20 2GHz Monte Carlo analysis - E field variation (Muscle, Skin, Fat)

that the order affects the variablity of the E field through the various dielectrics.

Figure 3-21 shows the variance of the data collected from the Monte Carlo analysis. The variance increases as the wave propagates through the various layers of dielectric, as expected. This is shown in a number of the plots, i.e. Figure 3-16, Figure 3-19, and Figure 3-22. Figure 3-22 plots the percent of the variance relative to the mean.

3.2.3 Specific Absorption Rate (SAR) Analysis

Determination of the power absorbed in the human head is used in the evaluation of cell phone design, which we will study in detail in Chapter 6. The equation for peak E field.

Specific Absorption Rate [30] is:

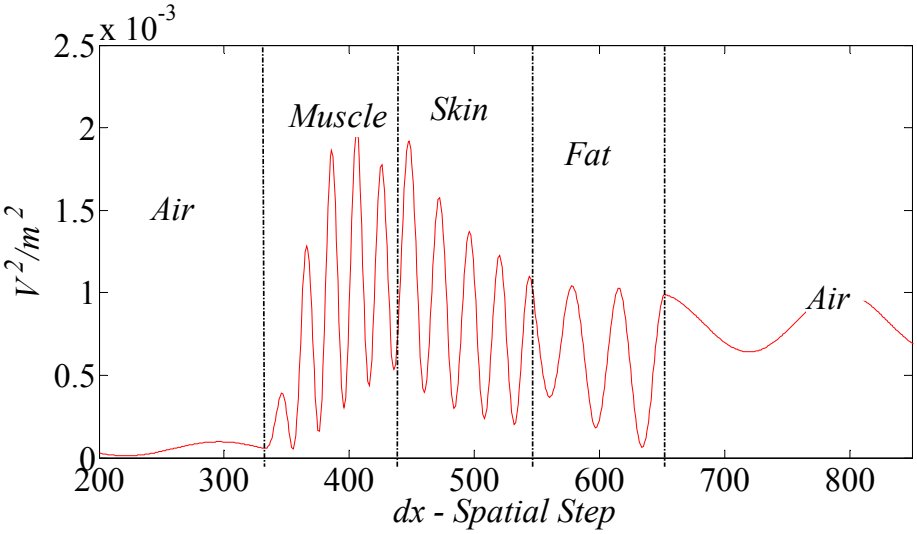

Figure 3-21 2GHz E field variance (Muscle, Skin, Fat)

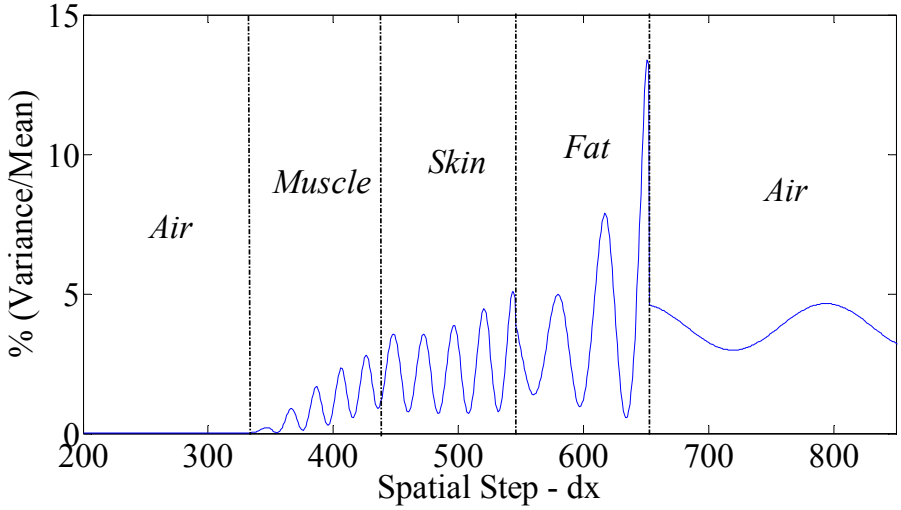

Figure 3-22 2GHz normalized percent error

$$SAR = \frac{\underline{\sigma} E_p^2}{2\rho_{density}} \tag{3.2}$$

The quantities used in the SAR are the conductivity ($\underline{\sigma}$), the peak E field (E_p), and the material density ($\rho_{density}$). Standards have been developed that regulate the amount of permissible power deposited in human tissue [1]. The mean SAR is routinely found using FDTD analysis, but the variance of this absorbed power is rarely found due to the amount of computation tie required for a 3D Monte Carlo analysis. In the analysis here, we will look at the results of a 1D analysis using Monte Carlo analysis. The Monte Carlo analysis determines the SAR at the completion of each simulation and stores this information. 10,000 simulations were performed, and the SAR data were analyzed for their statistical properties. Figure 3-23 shows the results of a Monte Carlo analysis of their variance of the SAR for a three-layer model with the order of the tissue being skin, fat, and muscle, with each of the layers having a thickness of 54mm.

There are some interesting findings about the SAR equation (3.2) that need to be mentioned at this point. At the end of each of the Monte Carlo simulations, the SAR is determined. The SAR equation calls for the peak value of the E field. The peak E field has less variation than the total E field, which includes phase variation. This is illustrated in Figure 3-24 where it can be seen that the variance of E_p is much less than the variance of the overall E field. The difference in the amplitude of the two different field descriptions is approximately 7 times greater for the full (time domain) E field as opposed to its magnitude only E_p.

In the next section, we will look at the assumptions that will be needed to simplify

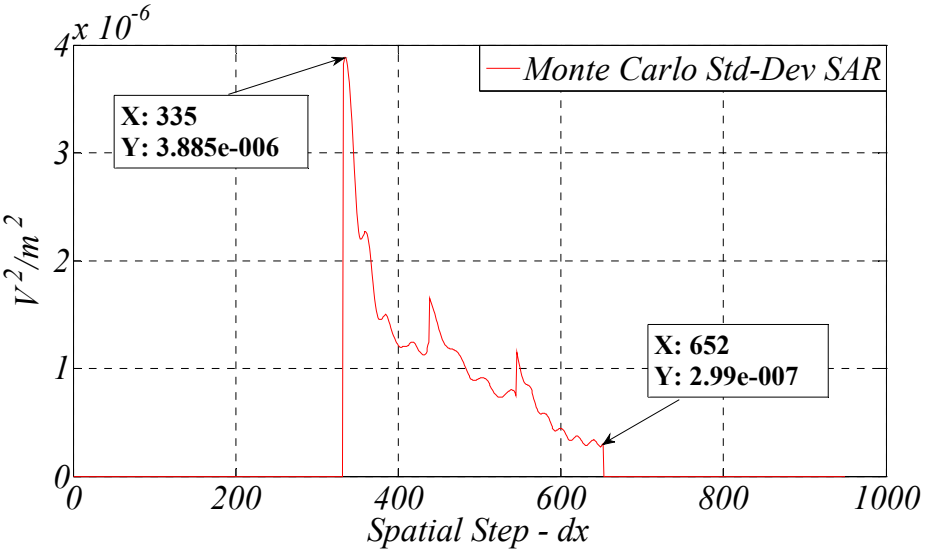

Figure 3-23 SAR standard deviation at 2GHz calculated using Monte Carlo

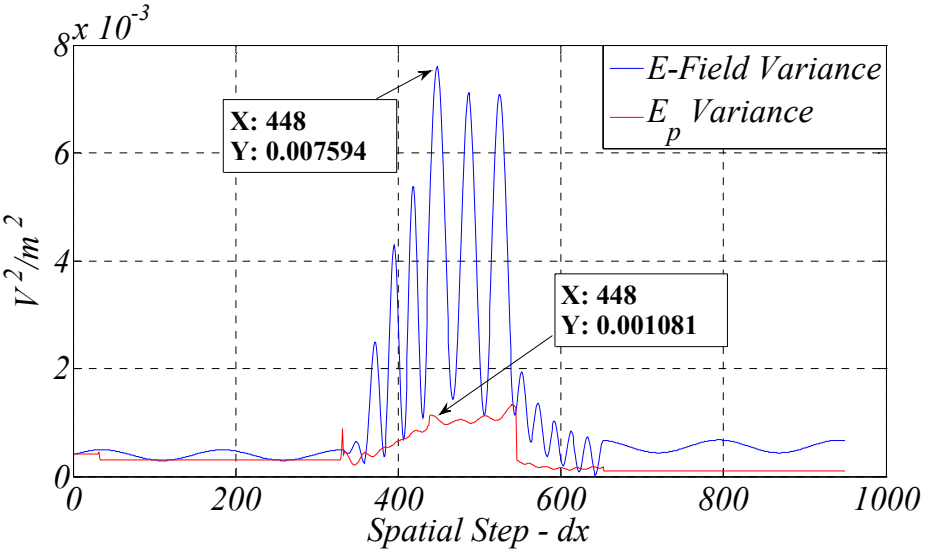

Figure 3-24 Comparison of the variation of the peak E field and the E field variance

the S-FDTD equations as they are derived. When we take the variance of two of Maxwell's equations, we will end up with equations that are the sum of random variables or random functions. We will apply a well-known identity:

$$\sigma^2\{aX \pm bY\} = a^2\sigma^2\{X\} + b^2\sigma^2\{Y\} \pm abCov\{X,Y\}$$

where a, b are constants.

The variance of the variables will be directly carried as a time-domain variable throughout the S-FDTD simulation, but the covariance must be estimated. There are several possible assumptions for the covariance that will be covered in the next section. The accuracy of these assumptions strongly impacts the accuracy of the S-FDTD variance.

3.3 Stochastic Approximations

In the traditional FDTD analysis, the electric and magnetic field at every point in space is carried through the simulation as a function of time. These time domain values are the expected (or mean) values of the fields for the average electrical properties of the materials in the model. In the development of the S-FDTD method, we will directly carry both the mean and variance as a function of time for the electric and magnetic field variables. The mean and variance of the tissue properties are predefined from measurements and are given in Table 3-1. In order to calculate the variance functions in the S-FDTD method, we need a value for the covariances between the various variables. This section discusses several possible choices for estimates for these covariances and ways in which they can be used in the S-FDTD method. These estimates are key factors

in the accuracy of this method. The estimates presented here should be considered preliminary, and more work in improving these estimates is justified.

One way to estimate the covariance is to bound it. A property of the covariance function is [31] $\left|Cov\{A,B\}\right|^2 \le \sigma^2(A)\sigma^2(B)$ which means that $\left|Cov\{A,B\}\right| \le \sqrt{\sigma^2(A)\sigma^2(B)}$. This equation would be an upper bound on the *Covariance* function. Therefore we can achieve a bounded approximation of the covariance function by assuming a correlation coefficient equal to one. This occurs when the two individual terms in the covariance are identical. This approximation has been used in Chapter 4 of this dissertation.

Another definition of the covariance is that it is equal to the product of the standard deviation of each of the factors multiplied by the correlation coefficient ρ_{AB}, i.e. $Cov\{A,B\} = \rho_{A,B}\sigma(A)\sigma(B)$. Thus, if we estimate this correlation coefficient, we can estimate the covariance. This also has been done in Chapter 4 of this dissertation.

3.3.1 Field Covariance Term Approximations

When we derive the FDTD equations from the time domain Maxwell's equations, we have E and H field terms as well as their derivatives in both time and space. Thus, when we calculate the variance equation, we will end up with the covariance of the E and H fields in both time and space. In Faraday's Law, we have the time derivative of the B field and the spatial derivative of the E field terms. In Ampere's Law, we have the time derivative of the E field terms and the spatial derivative of the H field terms. The equations also relate the fields and electrical properties of the materials, resulting in additional covariance terms between these variables and the fields.

The resultant covariance terms are:

$$Cov\left(H_y^{n+1/2}\left(k+1/2\right),H_y^{n-1/2}\left(k+1/2\right)\right) \tag{3.3}$$

$$Cov\left(E_x^n\left(k+1\right),E_x^n\left(k\right)\right) \tag{3.4}$$

$$Cov\left(E_x^{n+1}\left(k\right),\frac{\frac{\varepsilon_r\varepsilon_o}{\Delta t}-\frac{\sigma}{2}}{\frac{\varepsilon_r\varepsilon_o}{\Delta t}+\frac{\sigma}{2}}E_x^n\left(k\right)\right) \tag{3.5}$$

$$Cov\left(H_y^{n+1/2}\left(k+1/2\right),H_y^{n+1/2}\left(k-1/2\right)\right) \tag{3.6}$$

We will convert the covariance terms (equation (3.3) through equation (3.6)) to multiplication of the respective standard deviations and the correlation coefficients and then use an approximation for the various correlation coefficients so as to yield a close approximation to the covariances of the various terms.

We have used the Monte Carlo simulations to help guide the choice of approximations for the correlation coefficients. The correlation coefficients can be calculated directly from the Monte Carlo simulations. This would not be an efficient process for production simulations, because by the time the Monte Carlo multiple simulations are completed and the correlation coefficient is found, the variance can also be found directly, and there would be no need to run the S-FDTD method. But the Monte Carlo simulations are good for studying and developing the correlation coefficients, as we will do here. One of the correlated terms is *cc* shown below:

$$cc = \frac{\frac{\varepsilon_r \varepsilon_o}{\Delta t} - \frac{\sigma}{2}}{\frac{\varepsilon_r \varepsilon_o}{\Delta t} + \frac{\sigma}{2}}$$

In order to develop an approximation for the first correlation term above, the covariance term is compared with the product of the standard deviations of the individual terms in the covariance. For example, the following two terms are compared in Figure 3-25:

$$Cov\left(E_x^{n+1}(k), \frac{\frac{\varepsilon_r \varepsilon_o}{\Delta t} - \frac{\sigma}{2}}{\frac{\varepsilon_r \varepsilon_o}{\Delta t} + \frac{\sigma}{2}} E_x^n(k) \right) \text{ compared to } \sigma\left\{E_x^{n+1}(k)\right\} \sigma\left\{ \frac{\frac{\varepsilon_r \varepsilon_o}{\Delta t} - \frac{\sigma}{2}}{\frac{\varepsilon_r \varepsilon_o}{\Delta t} + \frac{\sigma}{2}} E_x^n(k) \right\} \tag{3.7}$$

In Figure 3-25, the two plots overlap so closely, they can barely be distinguished. This indicates a very high level of correlation, which tells us that the correlation coefficient ρ_{Corr} can be approximated as one. Figure 3-26 shows the normalized error ratio (difference of the two divided by the covariance term) of the covariance of the E field terms in the time derivative portion of Ampere's difference equation. The maximum error ratio shown in Figure 3-26 is approximately $1.06x10^{-4}$.

This same approximation was performed for each of the different model spaces, i.e. variations of order of the tissue. These comparisons are shown in Figure 3-25 through Figure 3-36. We first look at the fat, skin, and muscle model shown in Figure 3-27. Both plots again overlap. They are so similar that we can see no difference between them. Next, Figure 3-28 shows the difference between the two plots normalized

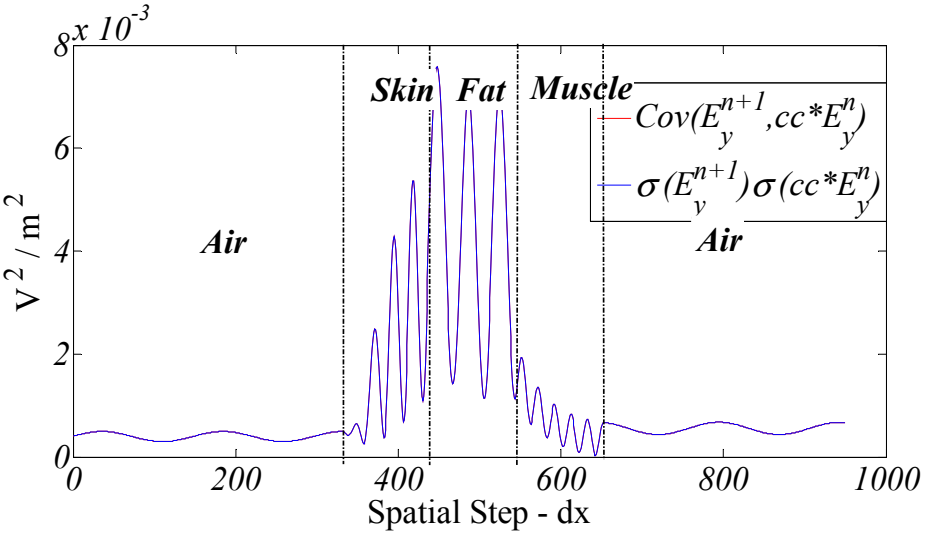

Figure 3-25 Covariance compared: *E* field time derivative (Skin, Fat, and Muscle)

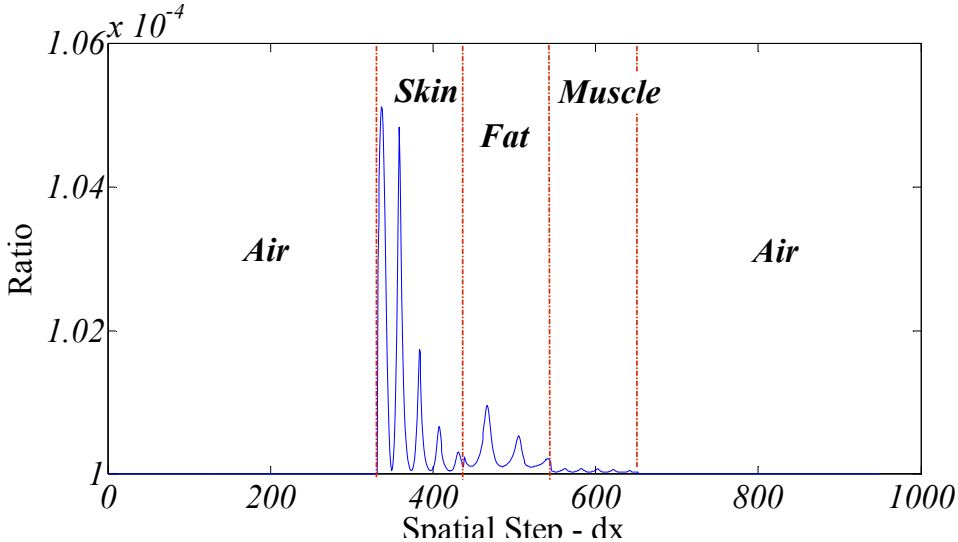

Figure 3-26 Normalized error covariance compared: *E* field time derivative (Skin, Fat, and Muscle)

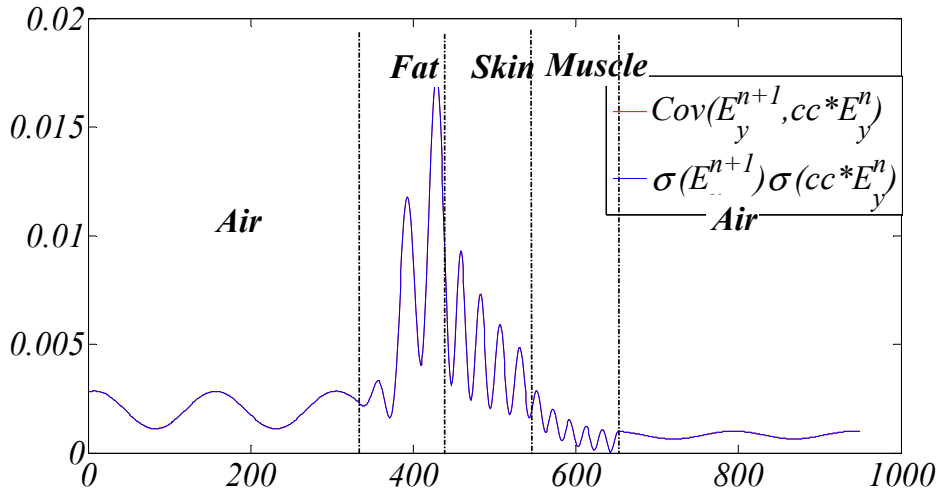

Figure 3-27 Covariance compared: *E* field time derivative
(Fat, Skin, Muscle)

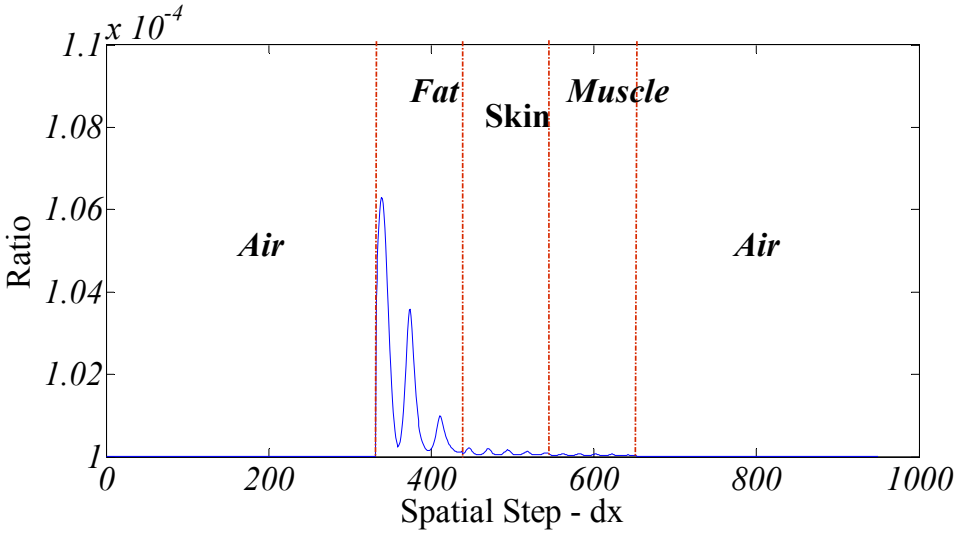

Figure 3-28 Normalized error covariance compared: *E* field time derivative
(Fat, Skin, and Muscle)

to the magnitude of the covariance term. Again using a correlation coefficient equal to one gives a very small error. Again changing the order of the tissues (this time to muscle-skin-fat) as shown in Figure 3-29, the differences are again very small as illustrated in Figure 3-30. Figure 3-30 shows the normalized error between the covariance of the two E field equation (3.5) terms at different time steps and the multiplication of their standard deviations. The smallness of the time step makes these compare very well.

Figure 3-31 and Figure 3-32 demonstrate the time derivative covariance with respect to the H field terms seen in equation (3.3). These plots demonstrate that the correlation coefficient ρ_{corr} for the time derivative is approximately equal to one for all time derivatives involving both Ampere's and Faraday's Laws. This result is used in Chapter 4; that is, correlation coefficients between time dependent derivatives of E and H field can be approximated by one with little error.

We next look at the derivative of the electric fields with respect to the spatial step dx. Figure 3-33 shows the covariance of the spatial derivative of the E terms (equation (3.4)) overlapped in the figure.

Figure 3-34 shows the difference or error between the two covariance terms with the correlation coefficient ρ_{corr} equal to 1. Figure 3-34 shows this error (graphically) to be larger than that seen with the time derivative terms but the correlation coefficient does not appear to be the governing variable for this difference; rather, the spatial step size seems to be the deciding difference.

Changing the correlation coefficient to something other than one does not seem to fix the error in it being more of a spatial difference problem; i.e. a smaller step size would improve the error seen in this covariance compared to the correlation coefficient times

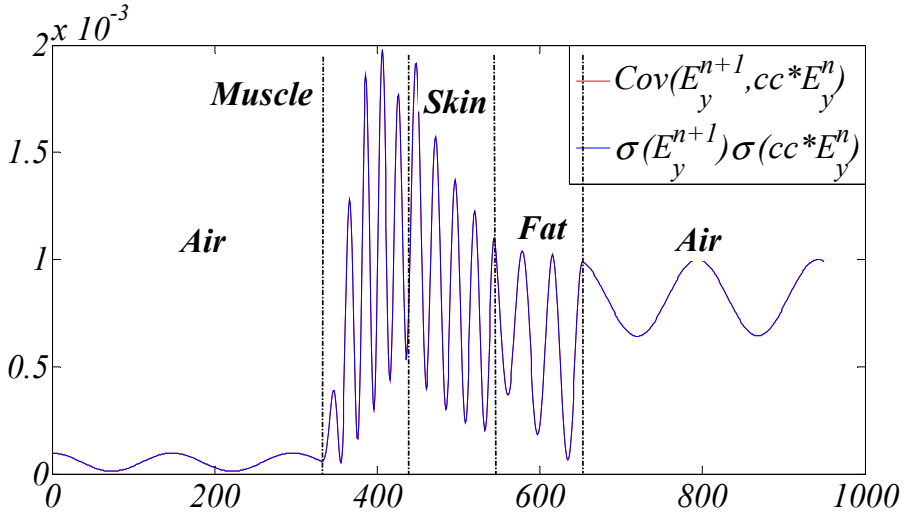

Figure 3-29 Covariance compared: *E* field time derivative
(Muscle, Skin, Fat)

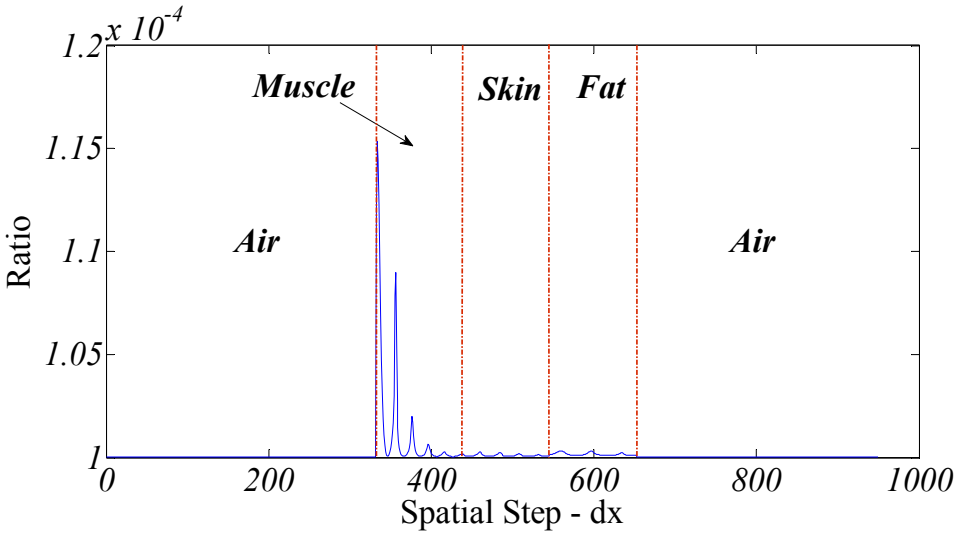

Figure 3-30 Normalized error covariance compared: *E* field time derivative
(Muscle, Skin, Fat)

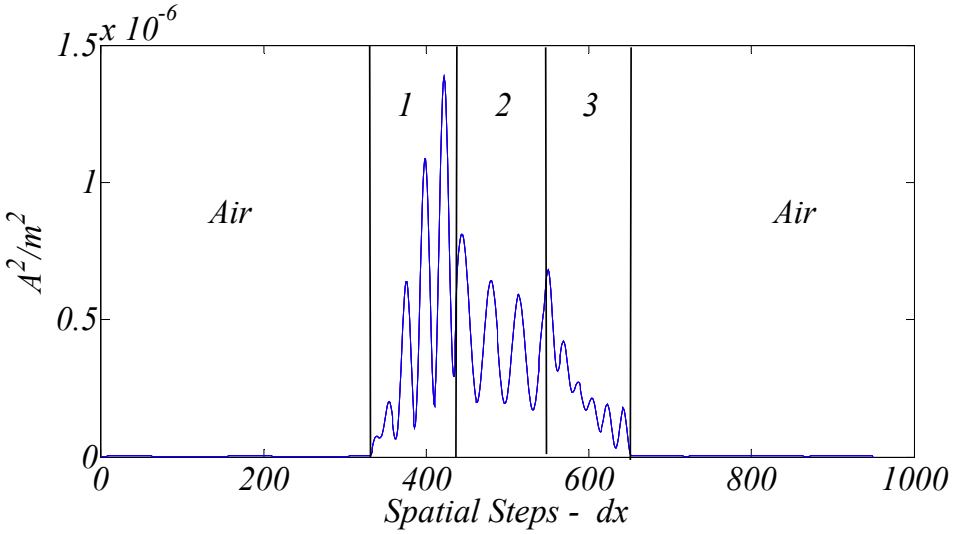

Figure 3-31 Covariance compared: *H* field time derivative covariance compared to the square-root of the variance of the H-fields

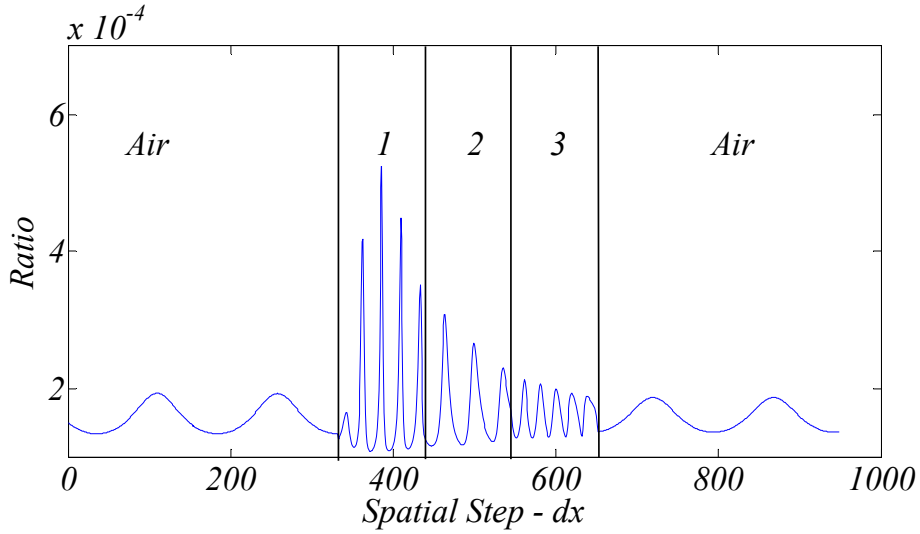

Figure 3-32 Normalized error covariance compared: *H* field time derivative

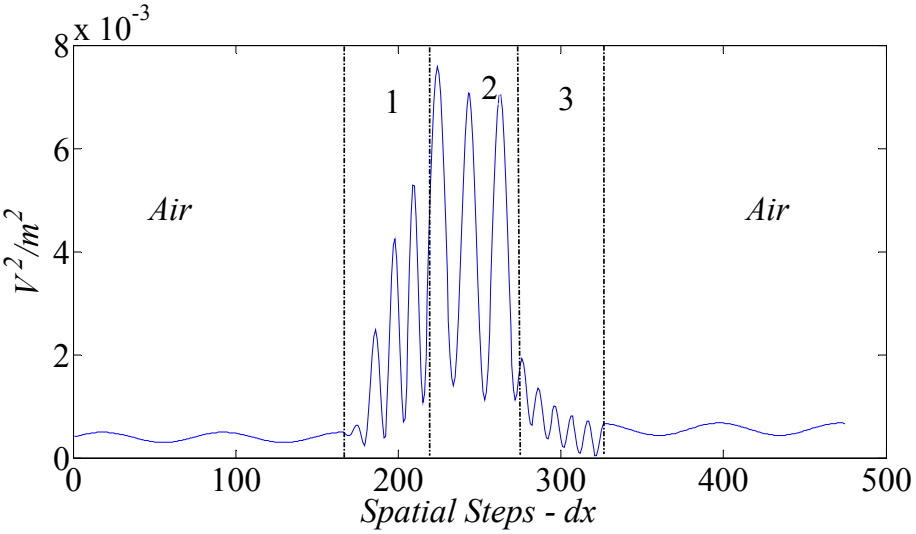

Figure 3-33 Covariance compared: *E* field spatial derivative

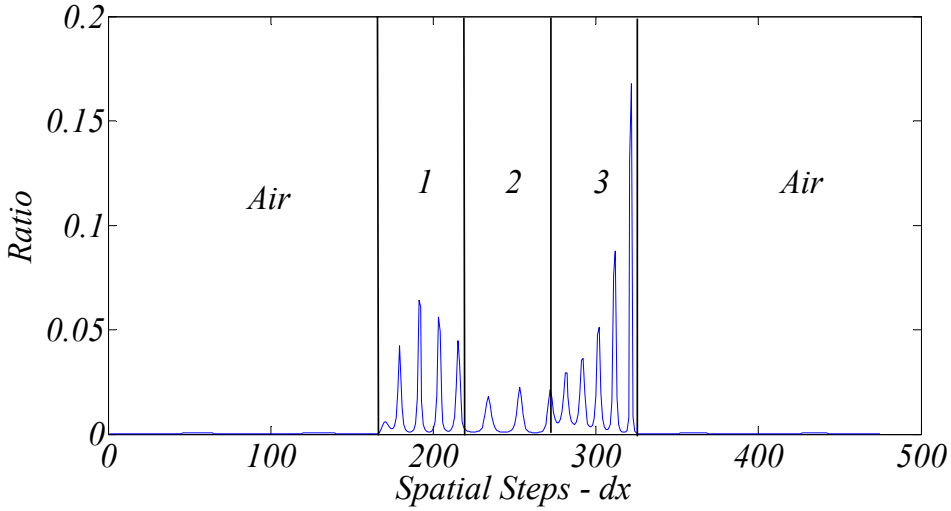

Figure 3-34 Normalized error covariance compared: *E* field spatial derivative

the standard deviation of the two E filed terms (equation (3.4)). Again the spatial step affects the closeness of the approximation of covariance of the spatial derivative terms. Figure 3-35 and Figure 3-36 show the same spatial dependency for the H field terms (equation (3.6)) as those of the previous E field covariance terms. Namely the difference between the covariance of the H field terms separate only in dx from the correlation coefficient multiplied by the standard deviation of the terms involved in the covariance. The error is due to the spatial difference between terms and not the correlation coefficient used. The result of this last analyses demonstrated that we can use as the correlation coefficients, approximating the covariance, of the time and spatial field terms (equations (3.3) through (3.6)) to be equal to one.

3.3.2 Electrical Parameters and Field Covariance Terms

In this section, we will evaluate how the correlation coefficients between the electrical properties of the dielectric layers, i.e. $\underline{\sigma}, \varepsilon$ and the E and H fields relate to each other.

The first is the correlation coefficient between the E field at two different spatial steps (offset from each other by one step) and the relative ε. The two terms are approximately equal, because the permittivity is generally within the same material and the field terms are approximately at the same location in space:

$$\rho_{\varepsilon_r, E_y^{n+1}(k+1)} \approx \rho_{\varepsilon_r, E_y^{n+1}(k)} \tag{3.8}$$

This next set of correlation coefficients is between the two field terms at the same time but offset by one spatial step and the material properties. The above argument also

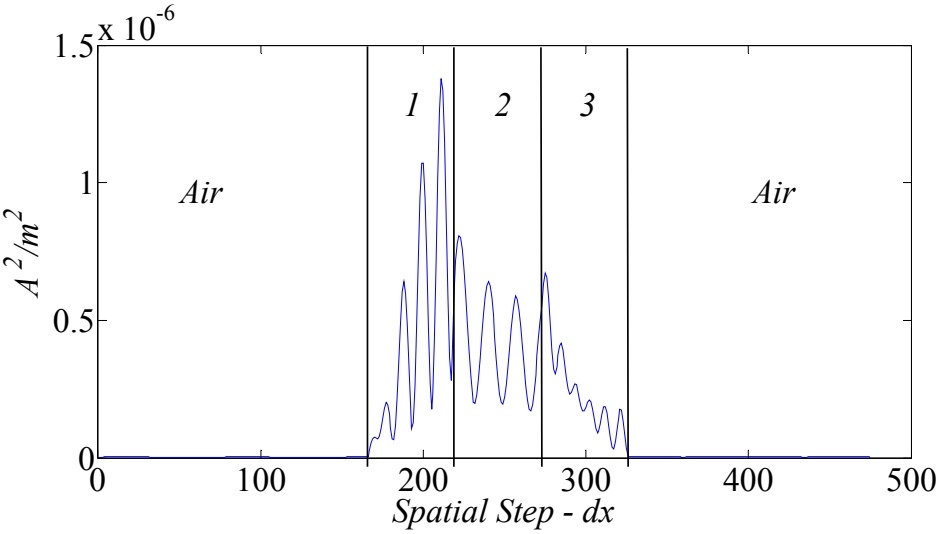

Figure 3-35 Covariance compared: *H* field spatial derivative

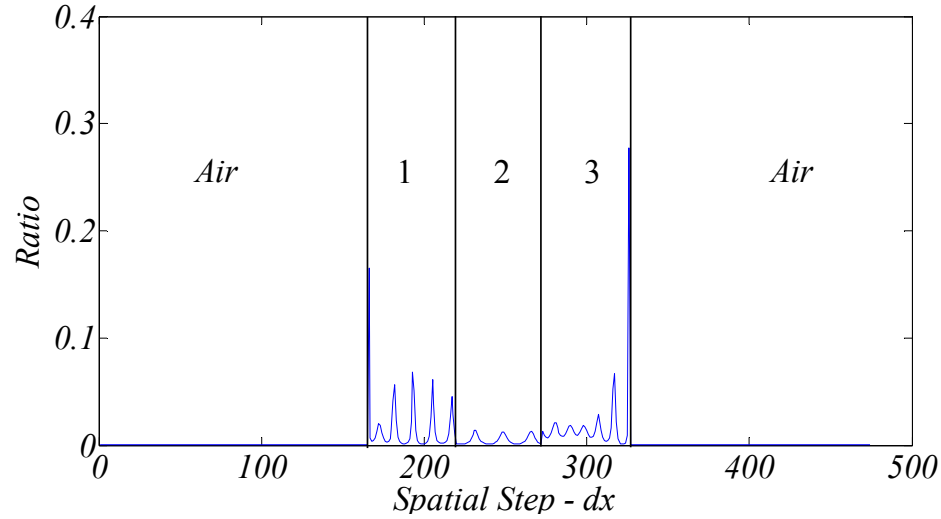

Figure 3-36 Normalized error covariance compared: *H* field spatial derivative

applies in the next three relations:

$$\rho_{\underline{\sigma},E_y^{n+1}(k+1)} \approx \rho_{\underline{\sigma},E_y^{n+1}(k)}$$

$$\rho_{\varepsilon_r,H_z^{n+1/2}(k+1/2)} \approx \rho_{\varepsilon_r,H_z^{n+1/2}(k-1/2)} \tag{3.9}$$

$$\rho_{\underline{\sigma},H_z^{n+1/2}(k+1/2)} \approx \rho_{\underline{\sigma},H_z^{n+1/2}(k-1/2)}$$

The error in the approximation would be larger at the boundaries of different dielectric layers, and the smaller the spatial step, dx, the more accurate the approximations will be.

3.3.3 Observations

These covariance terms (permittivity vs. E or H field and conductivity vs. E or H field, equation (3.9)) are an indication of how closely these parameters are correlated with each other.

Broader dielectric layer thickness could tend to isolate one layer from the next, and we would see that the electrical parameters correlate well with the field levels within the dielectric material. If the layers are thinner, it would allow the next layer to perturb the fields in the current layer more, reducing the strong correlation between the electrical properties and the field term at that point.

In future approximations, we should also be able to get some clue about the magnitude of the correlation coefficients from an analysis of the model space. This could be done looking at the reflection and transmission coefficients at dielectric boundaries.

In the next chapter, the Stochastic FDTD equations will be derived. The

approximations of correlation coefficients from this chapter will be used to simplify the S-FDTD equations. Mean and variance equations will be derived for both Faraday's and Ampere's laws. The method to do this derivation is rooted in using a few simple identities in stochastic analysis. The Delta method is used for approximating stochastic functions of random variables that would be hard to separate into simple standalone functions of each random variable without assuming that the random variables are independent. These items will be discussed and derived in Chapter 4.

CHAPTER 4

STOCHASTIC FDTD EQUATIONS

This dissertation focuses on the problem of how to determine the variability in the electric and magnetic fields caused by variation or ambiguity in the measured or assumed electrical properties of dielectric materials [27, 32] . Statistical analysis can provide us with a better understanding of how the variability of these electrical properties affects the scattering and absorption of electromagnetic energy and its range of possible effects.

Stochastic FDTD (S-FDTD) provides a computationally efficient method of finding the mean and also the variance of the EM fields in a complex, heterogeneous model. The current chapter will provide an explanation of the S-FDTD method and the derivation of the equations that are involved in its analysis.

The S-FDTD equations are derived using the Delta method [11] which uses Taylor series expansion to estimate the mean and the variance of multivariable stochastic equations. Additional approximations are used to determine the correlation coefficients that are needed to compute the covariance estimates.

4.1 Taylor Series Approximation Method (Delta Method)

The derivation of the stochastic FDTD equations begins by finding the mean of the electric and magnetic fields using Maxwell's time domain differential equations. The resultant difference equations for the mean fields end up being the same (identical to) the traditional FDTD equations for calculating the fields. In addition to the mean, the S-FDTD method also calculates the variance of the fields in the time domain at every location in the model. These variance equations end up behaving like an additional set of waves that are carried along in the simulation, reflect and refract and get absorbed within the model, require their own boundary condition, and otherwise behave like waves. This chapter derives the S-FDTD equations for both the mean fields as well as their variances.

4.1.1 Mean Approximation

We will next describe the S-FDTD derivation of the mean of the E and H fields. In the end, we will find that the traditional FDTD equations using the mean constituitive properties are the same as the S-FDTD equations for the means of the fields.

The FDTD time domain difference form of Faraday's Law derived in Section 2.2.1, equation (2.3) is used to determine the mean of the electric field. Each term is separable due to the linearity of the expectation operator $\underset{\sim}{E}\{\bullet\}$. The time step Δt, spatial resolution step Δz, and the permeability μ_o are constant within the FDTD simulation for nonmagnetic human tissues. The relative permittivity ε_r varies stochastically but is easily incorporated into the equation. This makes the equation for the expected (mean) value of the magnetic field exactly the same as the traditional FDTD equation for the magnetic field:

$$\underset{\sim}{E}\left\{B_y^{n+1/2}\left(k+1/2\right)\right\}=\underset{\sim}{E}\left\{B_y^{n-1/2}\left(k+1/2\right)\right\}\ -\ \frac{\Delta t}{\Delta z}\left[\underset{\sim}{E}\left\{E_x^n\left(k+1\right)\right\}-\underset{\sim}{E}\left\{E_x^n\left(k\right)\right\}\right]$$

The location in space is defined by the variable k (distance $z = k\Delta z$), and the time is defined by n (where time in seconds $= n\Delta t$). This equation is simple to derive for stochastic variables, because they are multiplied only by deterministic constants, not by other stochastic variables.

Ampere's Law, on the other hand, is not as easily derived if the variables are stochastic. The difference form of Ampere's equation (shown below) includes the multiplication of stochastic field and stochastic permittivity and conductivity terms:

$$E_x^{n+1}\left(k\right)-\frac{\frac{\varepsilon_r\varepsilon_o}{\Delta t}-\frac{\underline{\sigma}}{2}}{\frac{\varepsilon_r\varepsilon_o}{\Delta t}+\frac{\underline{\sigma}}{2}}E_x^n\left(k\right)=\frac{-1}{\left(\frac{\varepsilon_r\varepsilon_o}{\Delta t}+\frac{\underline{\sigma}}{2}\right)\Delta z}\left(H_y^{n+1/2}\left(k\right)-H_y^{n+1/2}\left(k-1\right)\right)$$

These would be separable if they were independent or constant, but they are not. Using a Taylor series expansion, we can expand this equation about the mean of the stochastic variables $\varepsilon_r, \underline{\sigma}, E_x^{n+1}, E_x^n, H_y^{n+1/2}, H_y^{n-1/2}$ and get a reasonable approximation to the function.

For the rest of this section, we will keep this derivation more general by defining the function $g\left[X_i\right]$. g is a function of multiple random variables, X_i random variables, which for this dissertation are the E, H fields and the conductivity and relative permittivity. We can then expand g about the mean of the random variables to find the overall mean.

We start with the Taylor's series expansion of a generic function g of random variables $x_1, x_2, x_3, \cdots, x_n$. The mean of these variables is indicated by using the symbols $\mu_{x_1}, \mu_{x_2}, \mu_{x_3}, \cdots, \mu_{x_n}$. This is not to be confused with the magnetic permeability μ without a subscript or μ_0, the magnetic permeability of free space. Then:

$$g\left(x_1, x_2, x_3, ..., x_n\right) = \tag{4.1}$$

$$g\left(\mu_{x_1}, \mu_{x_2}, \mu_{x_3}, ..., \mu_{x_n}\right) + \sum_{i=1}^{n} \frac{\partial g}{\partial x_i}\bigg|_{\mu_{x_1}, \mu_{x_2}, ..., \mu_{x_n}} (x_i - \mu_{x_i}) + \frac{1}{2!}\sum_{i=1}^{n}\sum_{j=1}^{n} \frac{\partial^2 g}{\partial x_i \partial x_j}\bigg|_{\mu_{x_1}, \mu_{x_2}, ..., \mu_{x_n}} (x_i - \mu_{x_i})(x_j - \mu_{x_j}) + ...$$

Taking the expectation $\underset{\sim}{E}\{\bullet\}$ of (4.1), we have:

$$\underset{\sim}{E}\left\{g\left(\mu_{x_1}, \mu_{x_2}, \mu_{x_3}, ..., \mu_{x_n}\right)\right\} =$$

$$\underset{\sim}{E}\left\{ g\left(\mu_{x_1}, \mu_{x_2}, \mu_{x_3}, ..., \mu_{x_n}\right) + \sum_{i=1}^{n} \frac{\partial g}{\partial x_i}\bigg|_{\mu_{x_1}, \mu_{x_2}, ..., \mu_{x_n}} (x_i - \mu_{x_i}) + \frac{1}{2!}\sum_{i=1}^{n}\sum_{j=1}^{n} \frac{\partial^2 g}{\partial x_i \partial x_j}\bigg|_{\mu_{x_1}, \mu_{x_2}, ..., \mu_{x_n}} (x_i - \mu_{x_i})(x_j - \mu_{x_j}) + ... \right\}$$

(4.2)

Because the expectation is a linear operator, we can open the brackets of (4.2) and apply the expectation operator to each term individually, yielding the following equation:

$$\underset{\sim}{E}\left\{g\left(\mu_{x_1}, \mu_{x_2}, \mu_{x_3}, ..., \mu_{x_n}\right)\right\} =$$

$$\underset{\sim}{E}\left\{g\left(\mu_{x_1},\mu_{x_2},\mu_{x_3},...,\mu_{x_n}\right)\right\}+\underset{\sim}{E}\left\{\sum_{i=1}^{n}\frac{\partial g}{\partial x_i}\bigg|_{\mu_{x_1},\mu_{x_2},...,\mu_{x_n}}(x_i-\mu_{x_i})\right\}$$

$$+\underset{\sim}{E}\left\{\frac{1}{2!}\sum_{i=1}^{n}\sum_{j=1}^{n}\frac{\partial^2 g}{\partial x_i\partial x_j}\bigg|_{\mu_{x_1},\mu_{x_2},...,\mu_{x_n}}(x_i-\mu_{x_i})(x_j-\mu_{x_j})\right\}+...$$

(4.3)

There are a number of terms in (4.3) that go to zero, such as any terms containing $\underset{\sim}{E}\left\{x_i-\mu_{x_i}\right\},\underset{\sim}{E}\left\{x_j-\mu_{x_j}\right\}$. Since the expectation operator is linear, these brackets can also be opened, yielding $\underset{\sim}{E}\left\{x_i\right\}-\underset{\sim}{E}\left\{\mu_{x_i}\right\},\underset{\sim}{E}\left\{x_j\right\}-\underset{\sim}{E}\left\{\mu_{x_j}\right\}$. The expectation of $\underset{\sim}{E}\left\{x_i\right\}=\mu_{x_i}$, $\underset{\sim}{E}\left\{x_j\right\}=\mu_{x_j}$, and the expectation of a constant equal to the same constant, so we have $\mu_{x_i}-\mu_{x_i}=0,\mu_{x_j}-\mu_{x_j}=0$ which cancels that term in (4.3). We can simplify (4.3) using the property $\underset{\sim}{E}\left\{aX\right\}=a\underset{\sim}{E}\left\{X\right\}$ [11, 22], where a is a constant. This allows the constant term to be brought outside the expectation operator:

$$\underset{\sim}{E}\left\{g\left(x_1,x_2,x_3,...,x_n\right)\right\}=g\left(\mu_{x_1},\mu_{x_2},\mu_{x_3},...,\mu_{x_n}\right)$$

$$+\overbrace{\sum_{i=1}^{n}\frac{\partial g}{\partial x_i}\bigg|_{\mu_{x_1},\mu_{x_2},...,\mu_{x_n}}\underset{\sim}{E}\left\{x_i-\mu_{x_i}\right\}}^{0}+\frac{1}{2!}\sum_{i=1}^{n}\sum_{j=1}^{n}\frac{\partial^2 g}{\partial x_i\partial x_j}\bigg|_{\mu_{x_1},\mu_{x_2},...,\mu_{x_n}}\underset{\sim}{E}\left\{(x_i-\mu_{x_i})(x_j-\mu_{x_j})\right\}+...$$

(4.4)

Neglecting high order terms reduces the equation even further, thus:

$$\underset{\sim}{E}\left\{g\left(x_1,x_2,x_3,...,x_n\right)\right\} \approx g\left(\mu_{x_1},\mu_{x_2},\mu_{x_3},...,\mu_{x_n}\right) \tag{4.5}$$

This is the approximation that will be used for the mean of our stochastic FDTD equations. This is also the approximation that makes these equations the same as the original FDTD equations. Higher order methods could be developed in the future including the higher order terms from the Taylor's series, but our tests later in this chapter will demonstrate that this is indeed a very good approximation. We now turn our attention to the variance equations.

4.1.2 Variance Approximation

In order to approximate the variance of the fields, we need to recall that we are dealing with stochastic equations that contain six random variables. These are the E fields terms, H fields terms, relative permittivity (ε_r), and conductivity ($\underline{\sigma}$). The symbol for conductivity is sigma (σ), and it has been changed to ($\underline{\sigma}$) to distinguish it from the symbol used for the standard deviation (σ). The variance sigma squared is the square of the standard deviation.

We now use a Taylor series expansion to approximate the variance of our function, i.e. find an approximation to $\sigma^2\left\{g\left(x_1,x_2,x_3,...,x_n\right)\right\}$ expanded about the mean of each random variable. The variance of a function is defined by [11]:

$$\sigma^2\left\{g\left(x_1,x_2,x_3,...,x_n\right)\right\} = \underset{\sim}{E}\left\{g\left(x_1,x_2,x_3,...,x_n\right)^2\right\} - \underset{\sim}{E}\left\{g\left(x_1,x_2,x_3,...,x_n\right)\right\}^2 \tag{4.6}$$

If a Taylor series expansion is used for both terms, i.e. $\underset{\sim}{E}\left\{g\left(x_1,x_2,x_3,...,x_n\right)^2\right\}$ and $\underset{\sim}{E}\left\{g\left(x_1,x_2,x_3,...,x_n\right)\right\}$, then we can square the second term and take the difference of the two to get an approximation for the variance ($\sigma^2\left\{g\left(x_1,x_2,x_3,...,x_n\right)\right\}$).

4.1.2.1 Variance - Taylor's series expansion. Next, we use a Taylor series expansion to expand about the mean of the constituitive properties ($\varepsilon_r,\underline{\sigma}$) and the *E* and *H* field terms. We will continue to use the generic function $g\left(x_1,x_2,x_3,...,x_n\right)$, where g is the electric or magnetic field, and the variables are fields and the electrical properties of the tissues:

$$g\left(x_1,x_2,x_3,...,x_n\right)=g\left(\mu_{x_1},\mu_{x_2},\mu_{x_3},...,\mu_{x_n}\right)$$

$$+\sum_{i=1}^{n}\frac{\partial g}{\partial x_i}\bigg|_{\mu_{x_1},\mu_{x_2},...,\mu_{x_n}}(x_i-\mu_{x_i})+\frac{1}{2!}\sum_{i=1}^{n}\sum_{j=1}^{n}\frac{\partial^2 g}{\partial x_i\partial x_j}\bigg|_{\mu_{x_1},\mu_{x_2},...,\mu_{x_n}}(x_i-\mu_{x_i})(x_j-\mu_{x_j})+...$$

Looking at the first term of the variance, namely $\underset{\sim}{E}\left\{g\left(x_1,x_2,x_3,...,x_n\right)^2\right\}$ (equation(4.6)), we first find $g\left(x_1,x_2,x_3,...,x_n\right)^2$ by squaring the above Taylor's series expansion of $g\left(x_1,x_2,x_3,...,x_n\right)$ yielding:

$$g\left(x_1,x_2,x_3,...,x_n\right)^2=g\left(\mu_{x_1},\mu_{x_2},\mu_{x_3},...,\mu_{x_n}\right)^2$$

$$+g\left(\mu_{x_1},\mu_{x_2},\mu_{x_3},...,\mu_{x_n}\right)\sum_{i=1}^{n}\frac{\partial g}{\partial x_i}\bigg|_{\mu_{x1},\mu_{x2},...,\mu_{xn}}(x_i-\mu_{x_i})+\sum_{i=1}^{n}\sum_{j=1}^{n}\frac{\partial g}{\partial x_i}\frac{\partial g}{\partial x_j}\bigg|_{\mu_{x1},\mu_{x2},...,\mu_{xn}}(x_i-\mu_{x_i})(x_j-\mu_{x_j})+$$

$$+\frac{1}{2!}g\left(\mu_{x_1},\mu_{x_2},\mu_{x_3},...,\mu_{x_n}\right)\sum_{i=1}^{n}\sum_{j=1}^{n}\frac{\partial^2 g}{\partial x_i\partial x_j}\bigg|_{\mu_{x1},\mu_{x2},...,\mu_{xn}}(x_i-\mu_{x_i})(x_j-\mu_{x_j})+...$$

Taking the mean of this equation yields:

$$\underset{\sim}{E}\left\{g\left(x_1,x_2,x_3,...,x_n\right)^2\right\}=g\left(\mu_{x_1},\mu_{x_2},\mu_{x_3},...,\mu_{x_n}\right)^2$$

$$+g\left(\mu_{x_1},\mu_{x_2},\mu_{x_3},...,\mu_{x_n}\right)\sum_{i=1}^{n}\frac{\partial g}{\partial x_i}\bigg|_{\mu_{x1},\mu_{x2},...,\mu_{xn}}\underset{\sim}{E}\left\{(x_i-\mu_{x_i})\right\}+\sum_{i=1}^{n}\sum_{j=1}^{n}\frac{\partial g}{\partial x_i}\frac{\partial g}{\partial x_j}\bigg|_{\mu_{x1},\mu_{x2},...,\mu_{xn}}\underset{\sim}{E}\left\{(x_i-\mu_{x_i})(x_j-\mu_{x_j})\right\}$$

$$+\frac{1}{2!}g\left(\mu_{x_1},\mu_{x_2},\mu_{x_3},...,\mu_{x_n}\right)\sum_{i=1}^{n}\sum_{j=1}^{n}\frac{\partial^2 g}{\partial x_i\partial x_j}\bigg|_{\mu_{x1},\mu_{x2},...,\mu_{xn}}\underset{\sim}{E}\left\{(x_i-\mu_{x_i})(x_j-\mu_{x_j})\right\}+.....$$

(4.7)

Terms containing expressions such as $\underset{\sim}{E}\left\{(x_i-\mu_{x_i})\right\}$ go to zero as discussed previously, leaving the following equation:

$$\underset{\sim}{E}\left\{g\left(x_1,x_2,x_3,...,x_n\right)^2\right\}=g\left(\mu_{x_1},\mu_{x_2},\mu_{x_3},...,\mu_{x_n}\right)^2$$

$$+\sum_{i=1}^{n}\sum_{j=1}^{n}\frac{\partial g}{\partial x_i}\frac{\partial g}{\partial x_j}\bigg|_{\mu_{x1},\mu_{x2},...,\mu_{xn}}\underset{\sim}{E}\left\{(x_i-\mu_{x_i})(x_j-\mu_{x_j})\right\}+...$$

Next, we find the second term in the variance equation (4.6) i.e. $\underset{\sim}{E}\left\{g\left(x_i\right)\right\}$ which will be squared:

$$\underset{\sim}{E}\left\{g\left(x_1,x_2,x_3,...,x_n\right)\right\}=g\left(\mu_{x_1},\mu_{x_2},\mu_{x_3},...,\mu_{x_n}\right)$$

$$+\sum_{i=1}^{n}\frac{\partial g}{\partial x_i}\bigg|_{\mu_{x_1},\mu_{x_2},...,\mu_{x_n}}\underset{\sim}{E}\left\{(x_i-\mu_{x_i})\right\}+\frac{1}{2!}\sum_{i=1}^{n}\sum_{j=1}^{n}\frac{\partial^2 g}{\partial x_i\partial x_j}\bigg|_{\mu_{x_1},\mu_{x_2},...,\mu_{x_n}}\underset{\sim}{E}\left\{(x_i-\mu_{x_i})(x_j-\mu_{x_j})\right\}+... \tag{4.8}$$

Again all terms such as $E\left\{(x_i-\mu_{x_i})\right\}$ go to zero, giving us:

$$\underset{\sim}{E}\left\{g\left(x_1,x_2,x_3,...,x_n\right)\right\}=g\left(\mu_{x_1},\mu_{x_2},\mu_{x_3},...,\mu_{x_n}\right)$$

$$+\frac{1}{2!}\sum_{i=1}^{n}\sum_{j=1}^{n}\frac{\partial^2 g}{\partial x_i\partial x_j}\bigg|_{\mu_{x_1},\mu_{x_2},...,\mu_{x_n}}\underset{\sim}{E}\left\{(x_i-\mu_{x_i})(x_j-\mu_{x_j})\right\}+...$$

Squaring the above equation, we obtain:

$$\underset{\sim}{E}\left\{g\left(x_1,x_2,x_3,...,x_n\right)\right\}^2=g\left(\mu_{x_1},\mu_{x_2},\mu_{x_3},...,\mu_{x_n}\right)^2$$

$$+\frac{1}{2!}g\left(\mu_{x_1},\mu_{x_2},\mu_{x_3},...,\mu_{x_n}\right)\sum_{i=1}^{n}\sum_{j=1}^{n}\frac{\partial^2 g}{\partial x_i\partial x_j}\bigg|_{\mu_{x_1},\mu_{x_2},...,\mu_{x_n}}\underset{\sim}{E}\left\{(x_i-\mu_{x_i})(x_j-\mu_{x_j})\right\}$$

$$+\left\{\frac{1}{2!}\sum_{i=1}^{n}\sum_{j=1}^{n}\frac{\partial^2 g}{\partial x_i\partial x_j}\bigg|_{\mu_{x_1},\mu_{x_2},...,\mu_{x_n}}\underset{\sim}{E}\left\{(x_i-\mu_{x_i})(x_j-\mu_{x_j})\right\}\right\}^2+...$$

Performing the subtraction $\underset{\sim}{E}\left\{g\left(x_1,x_2,x_3,...,x_n\right)^2\right\}-\underset{\sim}{E}\left\{g\left(x_1,x_2,x_3,...,x_n\right)\right\}^2$ from equation (4.6) we can find the variance of the variable (E or H field, in this case):

$$\sigma^2\left\{g\left(x_1,x_2,x_3,...,x_n\right)\right\}=\sum_{i=1}^{n}\sum_{j=1}^{n}\frac{\partial g}{\partial x_i}\frac{\partial g}{\partial x_j}\bigg|_{\mu_{x_1},\mu_{x_2},...,\mu_{x_n}}\underset{\sim}{E}\left\{(x_i-\mu_{x_i})(x_j-\mu_{x_j})\right\}+.....$$

By removing higher order terms, it is found that the variance of $g\left(x_1,x_2,x_3,...,x_n\right)$, expanded about the mean of the random variables, is approximately equal to:

$$\sigma^2\left\{g\left(x_1,x_2,x_3,...,x_n\right)\right\}\approx$$
$$\sum_{i=1}^{n}\sum_{j=1}^{n}\frac{\partial g}{\partial x_i}\frac{\partial g}{\partial x_j}\bigg|_{\mu_{x_1},\mu_{x_2},...,\mu_{x_n}}\underset{\sim}{E}\left\{(x_i-\mu_{x_i})(x_j-\mu_{x_j})\right\} \tag{4.9}$$

Putting this equation in terms of the covariance equation, we get the following:

$$\sigma^2\left\{g\left(x_1,x_2,x_3,...,x_n\right)\right\}\approx\sum_{i=1}^{n}\sum_{j=1}^{n}\frac{\partial g}{\partial x_i}\frac{\partial g}{\partial x_j}\bigg|_{\mu_{x_1},\mu_{x_2},...,\mu_{x_n}}Cov\left\{x_i,x_j\right\} \tag{4.10}$$

We have now derived two approximations, one for the mean (4.5) and the other for the variance (4.9), of a generic function of random variables, all based on a truncated Taylor series approximation. These are the approximations that will be used throughout the rest of this paper. They are repeated here for completeness:

The mean is (equation (4.5))

$$\underset{\sim}{E}\left\{g\left(x_1,x_2,x_3,...,x_n\right)\right\}\approx g\left(\mu_{x_1},\mu_{x_2},\mu_{x_3},...,\mu_{x_n}\right)$$

The variance is (equation (4.10))

$$\sigma^2\left\{g\left(x_1,x_2,x_3,...,x_n\right)\right\}\approx\sum_{i=1}^{n}\sum_{j=1}^{n}\frac{\partial g}{\partial x_i}\frac{\partial g}{\partial x_j}\bigg|_{\mu_{x_1},\mu_{x_2},...,\mu_{x_n}}Cov\left\{x_i,x_j\right\}$$

These equations constitute what is called the Delta method [11] of approximating a function of random variables, and this will be used in the following sections. The Delta method has been derived in the preceding pages with the intention of applying it to the multivariate Maxwell's equations. Previous derivations of the Delta method have been limited to equations involving a single stochastic variable, but this extension is necessary for our analysis. The following sections will use this method to derive the specific equations for the mean and variance of the fields in Faraday's and Ampere's Law. This will be done in a time domain difference form that can be programmed into an adapted FDTD method that we call the stochastic FDTD (S-FDTD) method.

4.2 Faraday's Law

The time domain difference form of Faraday's Law is:

$$B_y^{n+1/2}\left(k+1/2\right)-B_y^{n-1/2}\left(k+1/2\right)=-\frac{\Delta t}{\Delta z}\left(E_x^n\left(k+1\right)-E_x^n\left(k\right)\right)\qquad(4.11)$$

We will derive its mean and variance in this section using the Delta method

described in Section 4.1.2.

4.2.1 Mean Approximation

The expectation of Faraday's Law (4.10) is:

$$\underset{\sim}{E}\left\{B_y^{n+1/2}(k+1/2)-B_y^{n-1/2}(k+1/2)\right\}=\underset{\sim}{E}\left\{-\frac{\Delta t}{\Delta z}\left(E_x^n(k+1)-E_x^n(k)\right)\right\} \qquad (4.12)$$

Remember that Δt and Δz and the magnetic permeability μ are constants, and the electric and magnetic field variables are stochastic. The expectation is a linear operator, and recalling that $\underset{\sim}{E}\{aX+bY\} = a\underset{\sim}{E}\{X\} + b\underset{\sim}{E}\{Y\}$ with a, b constant, the brackets in (4.12) can be opened. Opening the brackets on the right and left side of the equation yields:

$$\underset{\sim}{E}\left\{B_y^{n+1/2}(k+1/2)\right\}-\underset{\sim}{E}\left\{B_y^{n-1/2}(k+1/2)\right\}=-\frac{\Delta t}{\Delta z}\left[\underset{\sim}{E}\left\{E_x^n(k+1)-E_x^n(k)\right\}\right] \qquad (4.13)$$

$$\underset{\sim}{E}\left\{B_y^{n+1/2}(k+1/2)\right\}-\underset{\sim}{E}\left\{B_y^{n-1/2}(k+1/2)\right\}=-\frac{\Delta t}{\Delta z}\left[\underset{\sim}{E}\left\{E_x^n(k+1)\right\}-\underset{\sim}{E}\left\{E_x^n(k)\right\}\right]$$

Solving for the expected magnetic field at the future time step $(n+1/2)$ $\underset{\sim}{E}\left\{B_y^{n+1/2}(k+1/2)\right\}$ yields:

$$\underset{\sim}{E}\left\{B_y^{n+1/2}(k+1/2)\right\}=\underset{\sim}{E}\left\{B_y^{n-1/2}(k+1/2)\right\}-\frac{\Delta t}{\Delta z}\left[\underset{\sim}{E}\left\{E_x^n(k+1)\right\}-\underset{\sim}{E}\left\{E_x^n(k)\right\}\right] \qquad (4.14)$$

Equation (4.14) which calculates the mean of the magnetic field is exactly the same as the original FDTD equation for Faraday's Law. It uses the mean value for all the field terms and the mean value for all of the variables, as is routinely done in practice.

4.2.2 Variance Approximation

Now we need to find the variance of Faraday's Law (2.4). Using the following identities:

$$\sigma^2\left[X \pm Y\right] = \sigma_X^2 + \sigma_Y^2 \pm 2Cov(X,Y)$$
$$\sigma^2\left\{aX\right\} = a^2\sigma^2\left\{X\right\} \tag{4.15}$$

The specific location and time where the FDTD fields and electrical properties are defined is an important consideration that controls the specifics of the final equations. Traditional FDTD requires two equations, one to solve for the electric field, and the other to solve for the magnetic field. Each individual equation must occur at the same time and at the same spatial location (the left and right side of the equation must be self-consistent in time and space). The two equations will be offset by half a step in both space and time in order to make this happen. This is often referred to as 'leap frogging' the equations. The 'Yee cell' is often referenced to define the leap frogged locations of the three vector field components of the E and H fields (a total of six vector components)[33]. In one dimension, there is only one vector component for the E and one for the H field. A diagram of the FDTD fields for one-dimensional equations is plotted in Figure 4-1.

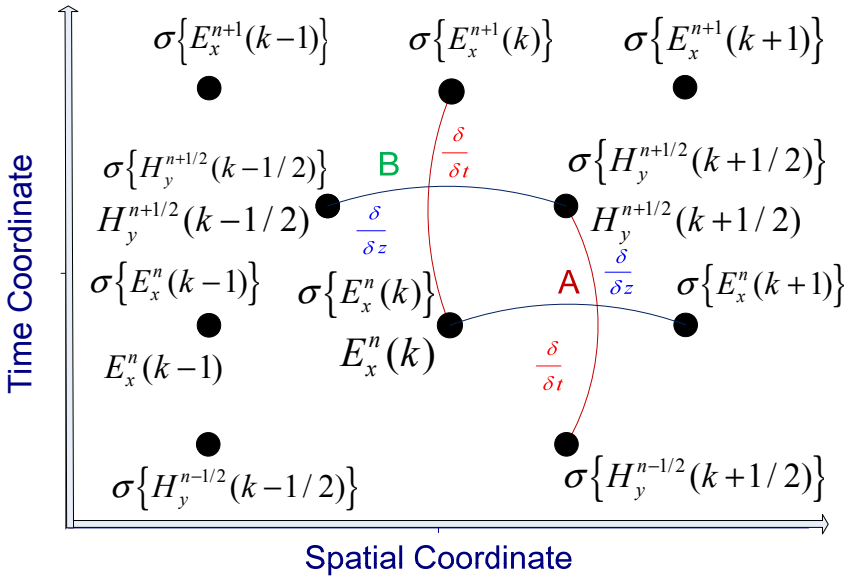

Figure 4-1 Spatial and time coordinate system

Figure 4-1 shows the locations of the variables in space and time and also the locations (A for Faraday's law and B for Ampere's law) where the equations themselves are defined. Notice that for Faraday's law (defined at point A) the E field terms are a central difference at $k+1/2$ and time n, while the H field terms are of the time derivative (central difference) at $k+1/2$ and occur at n. A similar set of relationships applies for Ampere's law at point B. The variance equations must also be defined at appropriate and consistent points in space and time. To do this we need to evaluate the variance of Faraday's and Ampere's law prior to solving for the E field terms on one side and the H field terms on the other side.

Taking the variance of (4.11) yields:

$$\sigma^2\left\{B_y^{n+1/2}(k+1/2)-B_y^{n-1/2}(k+1/2)\right\}=\frac{\Delta t^2}{\Delta z^2}\sigma^2\left\{E_x^n(k+1)-E_x^n(k)\right\} \qquad (4.16)$$

Expanding (4.16) yields the following equation:

$$\sigma^2\left\{B_y^{n+1/2}\left(k+1/2\right)\right\}+\sigma^2\left\{B_y^{n-1/2}\left(k+1/2\right)\right\}-2Cov\left(B_y^{n+1/2}\left(k+1/2\right),B_y^{n-1/2}\left(k+1/2\right)\right)$$
$$=\frac{\Delta t^2}{\Delta z^2}\left(\sigma^2\left\{E_x^n\left(k+1\right)\right\}+\sigma^2\left\{E_x^n\left(k\right)\right\}-2Cov\left(E_x^n\left(k+1\right),E_x^n\left(k\right)\right)\right) \tag{4.17}$$

This will require another identity that relates the covariance to the product of the correlation coefficient ($\rho_{X,Y}$) and the standard deviations ($\sigma\{X\}\sigma\{Y\}$) of the terms used in the covariance. Remember that the standard deviation is the square-root of the variance ($\sqrt{\sigma^2\{X\}}=\sigma\{X\}$), and the correlation coefficient $\rho_{X,Y}$ is equal to:

$$\rho_{X,Y}=\frac{Cov\{X,Y\}}{\sqrt{\sigma^2\{X\}\sigma^2\{Y\}}} \tag{4.18}$$

Therefore, the $Cov\{X,Y\}$ is equal to:

$$Cov\{X,Y\}=\rho_{X,Y}\sqrt{\sigma^2\{X\}\sigma^2\{Y\}}=\rho_{X,Y}\sigma\{X\}\sigma\{Y\} \tag{4.19}$$

Using this equation with the variance of Faraday's difference equation (4.17) gives:

$$\sigma^2\left\{B_y^{n+1/2}\left(k+1/2\right)\right\}+\sigma^2\left\{B_y^{n-1/2}\left(k+1/2\right)\right\}$$

$$-2\rho_{B_{n+1/2},B_{n-1/2}}\sigma\left\{B_y^{n+1/2}\left(k+1/2\right)\right\}\sigma\left\{B_y^{n-1/2}\left(k+1/2\right)\right\}$$

$$= \frac{\Delta t^2}{\Delta z^2}\left(\sigma^2\left\{E_x^n(k+1)\right\} + \sigma^2\left\{E_x^n(k)\right\} - 2\rho_{E_{k+1},E_k}\sigma\left\{E_x^n(k+1)\right\}\sigma\left\{E_x^n(k)\right\}\right) \tag{4.20}$$

In making this substitution for covariance, it is important to make sure that the time and spatial coordinates for all variables are consistent with the original equation. As can be seen in (4.20), the covariance terms have been modified so each has the appearance of a geometric mean of the field terms involved with a scalar weighting factor (the appropriate correlation coefficient). Each geometric mean occurs at approximately the same time and spatial coordinate as in the previous equation (4.17):

$$\mu^2\left\{\begin{array}{c}\sigma^2\left\{H_y^{n+1/2}(k+1/2)\right\} - 2\rho_{H_{n+1/2},H_{n-1/2}}\sigma\left\{H_y^{n+1/2}(k+1/2)\right\}\sigma\left\{H_y^{n-1/2}(k+1/2)\right\} \\ +\sigma^2\left\{H_y^{n-1/2}(k+1/1)\right\}\end{array}\right\}$$

$$= \frac{\Delta t^2}{\Delta z^2}\left(\sigma^2\left\{E_x^n(k+1)\right\} + \sigma^2\left\{E_x^n(k)\right\} - 2\rho_{E_{k+1},E_k}\sigma\left\{E_x^n(k+1)\right\}\sigma\left\{E_x^n(k)\right\}\right)$$

Converting from the magnetic flux density B to the magnetic field H using $B = \mu H$ where the standard symbol μ is used for the magnetic permeability gives:

$$\sigma^2\left\{H_y^{n+1/2}(k+1/2)\right\} - 2\rho_{H_{n+1/2},H_{n-1/2}}\sigma\left\{H_y^{n+1/2}(k+1/2)\right\}\sigma\left\{H_y^{n-1/2}(k+1/2)\right\}$$

$$+\sigma^2\left\{H_y^{n-1/2}(k+1/2)\right\} \tag{4.21}$$

$$= \frac{\Delta t^2}{\mu^2\Delta z^2}\left(\sigma^2\left\{E_x^n(k+1)\right\} + \sigma^2\left\{E_x^n(k)\right\} - 2\rho_{E_{k+1},E_k}\sigma\left\{E_x^n(k+1)\right\}\sigma\left\{E_x^n(k)\right\}\right)$$

We next need to complete the square for (4.21) on both sides. This is necessary to maintain the phase of the waveform so that the wave propagates and self-limits, meaning that the equation does not blowup but reaches a steady state.

Completing the square can be achieved by adding and subtracting terms on both sides of the equation. In (4.22), the term $\rho_{B,B}^2\sigma^2\left\{H_y^{n-1/2}\left(k+1/2\right)\right\}$ has been added and then subtracted from the left side of the equation. A similar process was done on the right hand side of the equation, but with the $\rho_{E,E}^2\sigma^2\left\{E_x^n\left(k\right)\right\}$ to yield:

$$\begin{aligned}
&{}^2\left\{H_y^{n+1/2}\left(k+1/2\right)\right\}-2\rho_{H_{n+1/2},H_{n-1/2}}\sigma\left\{H_y^{n+1/2}\left(k+1/2\right)\right\}\sigma\left\{H_y^{n-1/2}\left(k+1/2\right)\right\}\\
&+\rho_{H_{n+1/2},H_{n-1/2}}^2\sigma^2\left\{H_y^{n-1/2}\left(k+1/2\right)\right\}-\rho_{H_{n+1/2},H_{n-1/2}}^2\sigma^2\left\{H_y^{n-1/2}\left(k+1/2\right)\right\}\\
&+\sigma^2\left\{H_y^{n-1/2}\left(k+1/2\right)\right\}\\
=\frac{\Delta t^2}{\mu^2\Delta z^2}&\left(\begin{array}{c}\sigma^2\left\{E_x^n\left(k+1\right)\right\}-2\rho_{E_{k+1},E_k}\sigma\left\{E_x^n\left(k+1\right)\right\}\sigma\left\{E_x^n\left(k\right)\right\}+\rho_{E_{k+1},E_k}^2\sigma\left\{E_x^n\left(k\right)\right\}\\ -\rho_{E_{k+1},E_k}^2\sigma^2\left\{E_x^n\left(k\right)\right\}+\sigma^2\left\{E_x^n\left(k\right)\right\}\end{array}\right)
\end{aligned} \tag{4.22}$$

This completes the square:

$$\begin{aligned}
&\left(\sigma\left\{H_y^{n+1/2}\left(k+1/2\right)\right\}-\rho_{H_{n+1/2},H_{n-1/2}}\sigma\left\{H_y^{n-1/2}\left(k+1/2\right)\right\}\right)^2\\
&+\left(1-\rho_{H_{n+1/2},H_{n-1/2}}^2\right)\sigma^2\left\{H_y^{n-1/2}\left(k+1/2\right)\right\}
\end{aligned}$$

$$= \frac{\Delta t^2}{\mu^2 \Delta z^2}\left(\left(\sigma\left\{E_x^n(k+1)\right\} - \rho_{E_{k+1},E_k}\sigma\left\{E_x^n(k)\right\}\right)^2 + \left(1-\rho_{E_{k+1},E_k}^2\right)\sigma^2\left\{E_x^n(k)\right\}\right)$$

(4.23)

Taking the square-root of both sides of equation (4.23) yields:

$$\sqrt{\left(\sigma\left\{H_y^{n+1/2}(k+1/2)\right\} - \rho_{H_{n+1/2},H_{n-1/2}}\sigma\left\{H_y^{n-1/2}(k+1/2)\right\}\right)^2 + \left(1-\rho_{H_{n+1/2},H_{n-1/2}}^2\right)\sigma^2\left\{H_y^{n-1/2}(k+1/2)\right\}}$$

$$= \sqrt{\frac{\Delta t^2}{\mu^2 \Delta z^2}\left(\left(\sigma\left\{E_x^n(k+1)\right\} - \rho_{E_{k+1},E_k}\sigma\left\{E_x^n(k)\right\}\right)^2 + \left(1-\rho_{E_{k+1},E_k}^2\right)\sigma^2\left\{E_x^n(k)\right\}\right)}$$

(4.24)

Factoring out the squared term on both sides of the equation gives:

$$\left(\sigma\left\{H_y^{n+1/2}(k+1/2)\right\} - \rho_{H_{n+1/2},H_{n-1/2}}\sigma\left\{H_y^{n-1/2}(k+1/2)\right\}\right)$$

$$\sqrt{1+\frac{\left(1-\rho_{H_{n+1/2},H_{n-1/2}}^2\right)\sigma^2\left\{H_y^{n-1/2}(k+1/2)\right\}}{\left(\sigma\left\{H_y^{n+1/2}(k+1/2)\right\} - \rho_{H_{n+1/2},H_{n-1/2}}\sigma\left\{H_y^{n-1/2}(k+1/2)\right\}\right)^2}}$$

$$= \frac{\Delta t}{\mu \Delta z}\left(\sigma\left\{E_x^n(k+1)\right\} - \rho_{E_{k+1},E_k}\sigma\left\{E_x^n(k)\right\}\right)\sqrt{1+\frac{\left(1-\rho_{E_{k+1},E_k}^2\right)\sigma^2\left\{E_x^n(k)\right\}}{\left(\sigma\left\{E_x^n(k+1)\right\} - \rho_{E_{k+1},E_k}\sigma\left\{E_x^n(k)\right\}\right)^2}}$$

(4.25)

Remembering that $\sqrt{1 \pm x} \approx 1 \pm x/2$ for small x, gives:

$$\left(\sigma\left\{H_y^{n+1/2}\left(k+1/2\right)\right\}-\rho_{H_{n+1/2},H_{n-1/2}}\sigma\left\{H_y^{n-1/2}\left(k+1/2\right)\right\}\right)$$

$$\left(1+\frac{\left(1-\rho_{H_{n+1/2},H_{n-1/2}}^2\right)\sigma^2\left\{H_y^{n-1/2}\left(k+1/2\right)\right\}}{2\left(\sigma\left\{H_y^{n+1/2}\left(k+1/2\right)\right\}-\rho_{H_{n+1/2},H_{n-1/2}}\sigma\left\{H_y^{n-1/2}\left(k+1/2\right)\right\}\right)^2}\right)$$

$$\approx\frac{\Delta t}{\mu\Delta z}\left(\sigma\left\{E_x^n\left(k+1\right)\right\}-\rho_{E_{k+1},E_k}\sigma\left\{E_x^n\left(k\right)\right\}\right)\left(1+\frac{\left(1-\rho_{E_{k+1},E_k}^2\right)\sigma^2\left\{E_x^n\left(k\right)\right\}}{2\left(\sigma\left\{E_x^n\left(k+1\right)\right\}-\rho_{E_{k+1},E_k}\sigma\left\{E_x^n\left(k\right)\right\}\right)^2}\right) \tag{4.26}$$

Multiplying through by the first term, we obtain the following simplification:

$$\sigma\left\{H_y^{n+1/2}\left(k+1/2\right)\right\}-\rho_{H_{n+1/2},H_{n-1/2}}\sigma\left\{H_y^{n-1/2}\left(k+1/2\right)\right\}$$

$$+\frac{\left(1-\rho_{H_{n+1/2},H_{n-1/2}}^2\right)\sigma^2\left\{H_y^{n-1/2}\left(k+1/2\right)\right\}}{2\left(\sigma\left\{H_y^{n+1/2}\left(k+1/2\right)\right\}-\rho_{H_{n+1/2},H_{n-1/2}}\sigma\left\{H_y^{n-1/2}\left(k+1/2\right)\right\}\right)}$$

$$\approx\frac{\Delta t}{\mu\Delta z}\left(\sigma\left\{E_x^n\left(k+1\right)\right\}-\rho_{E_{k+1},E_k}\sigma\left\{E_x^n\left(k\right)\right\}+\frac{\left(1-\rho_{E_{k+1},E_k}^2\right)\sigma^2\left\{E_x^n\left(k\right)\right\}}{2\left(\sigma\left\{E_x^n\left(k+1\right)\right\}-\rho_{E_{k+1},E_k}\sigma\left\{E_x^n\left(k\right)\right\}\right)}\right) \tag{4.27}$$

At this point, only two major approximations have been made – the conversion from the derivative to difference form of Maxwell's equations and the truncation of the Taylor series. The next approximation will be for the correlation coefficients that arise from the covariance terms. Correlation = 1.0 means that the two are directly correlated (linearly dependent). Correlation of -1.0 means they are anticorrelated. Correlation of 0

means there is no correlation. These values could be used to bound the correlation. Alternatively, the correlation terms may be calculated from the properties of the surrounding materials. For this case, we will evaluate the effect of maximum correlation when the correlation coefficients = 1. Future approximations for improved accuracy will be left for future research.

Using the information gleaned from Section 3.3, we can approximate the time and spatial correlation coefficients as $\rho_{H_{n+1/2},H_{n-1/2}} = \rho_{E_{k+1},E_k} = 1.0$, yielding the following equation:

$$\sigma\left\{H_y^{n+1/2}\left(k+1/2\right)\right\} - \sigma\left\{H_y^{n-1/2}\left(k+1/2\right)\right\} \approx \frac{\Delta t}{\mu \Delta z}\left(\sigma\left\{E_x^n\left(k+1\right)\right\} - \sigma\left\{E_x^n\left(k\right)\right\}\right) \tag{4.28}$$

Solving equation (4.28) for $\sigma\left\{H_y^{n+1/2}\left(k+1/2\right)\right\}$ yields the variance equation for Faraday's Law:

$$\sigma\left\{H_y^{n+1/2}\left(k+1/2\right)\right\} \approx \sigma\left\{H_y^{n-1/2}\left(k+1/2\right)\right\} + \frac{\Delta t}{\mu \Delta z}\left(\sigma\left\{E_x^n\left(k+1\right)\right\} - \sigma\left\{E_x^n\left(k\right)\right\}\right) \tag{4.29}$$

This is effectively a wave equation for the variance of the magnetic field. In effect, this wave propagates along with the magnetic field, controlled by the standard deviations of all of the surrounding fields. This is the equation that will be programmed in the S-FDTD formulation for the variance of the magnetic field.

4.3 Ampere's Law

The time domain difference form of Ampere's Law (2.9) is:

$$E_x^{n+1}(k)-\frac{\frac{\varepsilon_r\varepsilon_o}{\Delta t}-\frac{\underline{\underline{\sigma}}}{2}}{\frac{\varepsilon_r\varepsilon_o}{\Delta t}+\frac{\underline{\underline{\sigma}}}{2}}E_x^n(k)=\frac{-1}{\left(\frac{\varepsilon_r\varepsilon_o}{\Delta t}+\frac{\underline{\underline{\sigma}}}{2}\right)\Delta z}\left(H_y^{n+1/2}(k)-H_y^{n+1/2}(k-1)\right) \qquad (4.30)$$

In this section, we will derive its mean and variance in the same manner as the previous section, again making use of the Delta method described in Section 4.1.2.

4.3.1 Mean Approximation

Taking the mean of both sides of (4.30) yields:

$$\underset{\sim}{E}\left\{E_x^{n+1}(k)-\frac{\frac{\varepsilon_r\varepsilon_o}{\Delta t}-\frac{\underline{\underline{\sigma}}}{2}}{\frac{\varepsilon_r\varepsilon_o}{\Delta t}+\frac{\underline{\underline{\sigma}}}{2}}E_x^n(k)\right\}=\underset{\sim}{E}\left\{\frac{-1}{\left(\frac{\varepsilon_r\varepsilon_o}{\Delta t}+\frac{\underline{\underline{\sigma}}}{2}\right)\Delta z}\left(H_y^{n+1/2}(k)-H_y^{n+1/2}(k-1)\right)\right\} \qquad (4.31)$$

By recalling the linearity of the mean operator, we can open the brackets to get:

$$\underset{\sim}{E}\left\{E_x^{n+1}(k)\right\}-\underset{\sim}{E}\left\{\frac{\frac{\varepsilon_r\varepsilon_o}{\Delta t}-\frac{\underline{\underline{\sigma}}}{2}}{\frac{\varepsilon_r\varepsilon_o}{\Delta t}+\frac{\underline{\underline{\sigma}}}{2}}E_x^n(k)\right\}=\underset{\sim}{E}\left\{\frac{1}{\left(\frac{\varepsilon_r\varepsilon_o}{\Delta t}+\frac{\underline{\underline{\sigma}}}{2}\right)\Delta z}\left(H_y^{n+1/2}(k-1)-H_y^{n+1/2}(k)\right)\right\} \qquad (4.32)$$

Solving for $E_x^{n+1}(k)$ gives:

$$\underset{\sim}{E}\left\{E_x^{n+1}(k)\right\} = \underset{\sim}{E}\left\{\frac{\frac{\varepsilon_r\varepsilon_o}{\Delta t} - \frac{\underline{\sigma}}{2}}{\frac{\varepsilon_r\varepsilon_o}{\Delta t} + \frac{\underline{\sigma}}{2}} E_x^n(k)\right\} + \underset{\sim}{E}\left\{\frac{1}{\left(\frac{\varepsilon_r\varepsilon_o}{\Delta t} + \frac{\underline{\sigma}}{2}\right)\Delta z}\left(H_y^{n+1/2}(k-1) - H_y^{n+1/2}(k)\right)\right\} \tag{4.33}$$

The right hand side of (4.33) shows a number of different functions of correlated, i.e. not independent, random variables that cannot be separated easily. We will again use the approximation determined in Section 4.1.1 for the mean which is repeated here:

$$\underset{\sim}{E}\left\{g(x_1, x_2, x_3, ..., x_n)\right\} \approx g\left(\mu_{x_1}, \mu_{x_2}, \mu_{x_3}, ..., \mu_{x_n}\right) \tag{4.34}$$

This gives the expression for the mean of the electric field derived from Ampere's Law:

$$\underset{\sim}{E}\left\{E_x^{n+1}(k)\right\} = \frac{\frac{\mu_{\varepsilon_r}\varepsilon_o}{\Delta t} - \frac{\mu_{\underline{\sigma}}}{2}}{\frac{\mu_{\varepsilon_r}\varepsilon_o}{\Delta t} + \frac{\mu_{\underline{\sigma}}}{2}} \underset{\sim}{E}\left\{E_x^n(k)\right\} + \frac{\left(\underset{\sim}{E}\left\{H_y^{n+1/2}(k-1)\right\} - \underset{\sim}{E}\left\{H_y^{n+1/2}(k)\right\}\right)}{\left(\frac{\mu_{\varepsilon_r}\varepsilon_o}{\Delta t} + \frac{\mu_{\underline{\sigma}}}{2}\right)\Delta z} \tag{4.35}$$

This equation is identical to the traditional FDTD equation for Ampere's Law and will be used in the S-FDTD formulation.

4.3.2 Variance Approximation

Taking the variance of Ampere's Law (4.30):

$$\sigma^2\left\{E_x^{n+1}(k)-\frac{\frac{\varepsilon_r\varepsilon_o}{\Delta t}-\frac{\sigma}{2}}{\frac{\varepsilon_r\varepsilon_o}{\Delta t}+\frac{\sigma}{2}}E_x^n(k)\right\}=\sigma^2\left\{\frac{-1}{\left(\frac{\varepsilon_r\varepsilon_o}{\Delta t}+\frac{\sigma}{2}\right)\Delta z}\left(H_y^{n+1/2}(k)-H_y^{n+1/2}(k-1)\right)\right\} \tag{4.36}$$

and again expanding the left-hand side of (4.36) using the same identities previously used for the variance, i.e. $\sigma^2\{aX\pm bY\}=a^2\sigma^2\{X\}+b^2\sigma^2\{Y\}\pm abCov\{X,Y\}$, gives:

$$\sigma^2\left\{E_x^{n+1}(k)-\frac{\frac{\varepsilon_r\varepsilon_o}{\Delta t}-\frac{\sigma}{2}}{\frac{\varepsilon_r\varepsilon_o}{\Delta t}+\frac{\sigma}{2}}E_x^n(k)\right\}=\sigma^2\left\{E_x^{n+1}(k)\right\}+\sigma^2\left\{\frac{\frac{\varepsilon_r\varepsilon_o}{\Delta t}-\frac{\sigma}{2}}{\frac{\varepsilon_r\varepsilon_o}{\Delta t}+\frac{\sigma}{2}}E_x^n(k)\right\}$$

$$-Cov\left\{E_x^{n+1}(k),\frac{\frac{\varepsilon_r\varepsilon_o}{\Delta t}-\frac{\sigma}{2}}{\frac{\varepsilon_r\varepsilon_o}{\Delta t}+\frac{\sigma}{2}}E_x^n(k)\right\} \tag{4.37}$$

Using the identity $Cov(X,Y)=\rho_{X,Y}\sqrt{\sigma^2\{X\}\sigma^2\{Y\}}=\rho_{X,Y}\sigma\{X\}\sigma\{Y\}$ yields:

$$\sigma^2\left\{E_x^{n+1}(k)-\frac{\frac{\varepsilon_r\varepsilon_o}{\Delta t}-\frac{\sigma}{2}}{\frac{\varepsilon_r\varepsilon_o}{\Delta t}+\frac{\sigma}{2}}E_x^n(k)\right\}=\sigma^2\left\{E_x^{n+1}(k)\right\}+\sigma^2\left\{\frac{\frac{\varepsilon_r\varepsilon_o}{\Delta t}-\frac{\sigma}{2}}{\frac{\varepsilon_r\varepsilon_o}{\Delta t}+\frac{\sigma}{2}}E_x^n(k)\right\}$$

$$-\rho_{EE}\sigma\left\{E_x^{n+1}(k)\right\}\sigma\left\{\frac{\frac{\varepsilon_r\varepsilon_o}{\Delta t}-\frac{\sigma}{2}}{\frac{\varepsilon_r\varepsilon_o}{\Delta t}+\frac{\sigma}{2}}E_x^n(k)\right\} \tag{4.38}$$

We will next complete the square of (4.38). This step of completing the square is very important, because it preserves the phases of the variables. This allows a wave-like function to exist, which in turn allows the use of typical FDTD boundary conditions at the model boundaries. Completing the square of (4.33) gives:

$$\sigma^2\left\{E_x^{n+1}(k)-\frac{\frac{\varepsilon_r\varepsilon_o}{\Delta t}-\frac{\sigma}{2}}{\frac{\varepsilon_r\varepsilon_o}{\Delta t}+\frac{\sigma}{2}}E_x^n(k)\right\}=\sigma^2\left\{E_x^{n+1}(k)\right\}-\rho_{EE}\sigma\left\{E_x^{n+1}(k)\right\}\sigma\left\{\frac{\frac{\varepsilon_r\varepsilon_o}{\Delta t}-\frac{\sigma}{2}}{\frac{\varepsilon_r\varepsilon_o}{\Delta t}+\frac{\sigma}{2}}E_x^n(k)\right\}$$

$$+\rho_{EE}^2\sigma^2\left\{\frac{\frac{\varepsilon_r\varepsilon_o}{\Delta t}-\frac{\sigma}{2}}{\frac{\varepsilon_r\varepsilon_o}{\Delta t}+\frac{\sigma}{2}}E_x^n(k)\right\}-\rho_{EE}^2\sigma^2\left\{\frac{\frac{\varepsilon_r\varepsilon_o}{\Delta t}-\frac{\sigma}{2}}{\frac{\varepsilon_r\varepsilon_o}{\Delta t}+\frac{\sigma}{2}}E_x^n(k)\right\}+\sigma^2\left\{\frac{\frac{\varepsilon_r\varepsilon_o}{\Delta t}-\frac{\sigma}{2}}{\frac{\varepsilon_r\varepsilon_o}{\Delta t}+\frac{\sigma}{2}}E_x^n(k)\right\} \tag{4.39}$$

Combining terms and simplifying yields:

$$\sigma^2\left\{E_x^{n+1}(k)-\frac{\frac{\varepsilon_r\varepsilon_o}{\Delta t}-\frac{\sigma}{2}}{\frac{\varepsilon_r\varepsilon_o}{\Delta t}+\frac{\sigma}{2}}E_x^n(k)\right\}=\left(\sigma\left\{E_x^{n+1}(k)\right\}-\rho_{EE}\sigma\left\{\frac{\frac{\varepsilon_r\varepsilon_o}{\Delta t}-\frac{\sigma}{2}}{\frac{\varepsilon_r\varepsilon_o}{\Delta t}+\frac{\sigma}{2}}E_x^n(k)\right\}\right)^2$$

$$+\left(1-\rho_{EE}^{2}\right)\sigma^{2}\left\{\frac{\frac{\varepsilon_r\varepsilon_o}{\Delta t}-\frac{\sigma}{2}}{\frac{\varepsilon_r\varepsilon_o}{\Delta t}+\frac{\sigma}{2}}E_x^n(k)\right\} \tag{4.40}$$

which can also be rearranged as :

$$\sigma^{2}\left\{E_x^{n+1}(k)-\frac{\frac{\varepsilon_r\varepsilon_o}{\Delta t}-\frac{\sigma}{2}}{\frac{\varepsilon_r\varepsilon_o}{\Delta t}+\frac{\sigma}{2}}E_x^n(k)\right\}=\left(\sigma\left\{E_x^{n+1}(k)\right\}-\rho_{EE}\sigma\left\{\frac{\frac{\varepsilon_r\varepsilon_o}{\Delta t}-\frac{\sigma}{2}}{\frac{\varepsilon_r\varepsilon_o}{\Delta t}+\frac{\sigma}{2}}E_x^n(k)\right\}\right)^{2}$$
$$\left\{1+\frac{\left(1-\rho_{EE}^{2}\right)\sigma^{2}\left\{\frac{\frac{\varepsilon_r\varepsilon_o}{\Delta t}-\frac{\sigma}{2}}{\frac{\varepsilon_r\varepsilon_o}{\Delta t}+\frac{\sigma}{2}}E_x^n(k)\right\}}{\left(\sigma\left\{E_x^{n+1}(k)\right\}-\rho_{EE}\sigma\left\{\frac{\frac{\varepsilon_r\varepsilon_o}{\Delta t}-\frac{\sigma}{2}}{\frac{\varepsilon_r\varepsilon_o}{\Delta t}+\frac{\sigma}{2}}E_x^n(k)\right\}\right)^{2}}\right\} \tag{4.41}$$

Equating (4.40) with the right-hand side of (4.36) we have:

$$\left(\sigma\left\{E_x^{n+1}(k)\right\}-\rho_{EE}\sigma\left\{\frac{\frac{\varepsilon_r\varepsilon_o}{\Delta t}-\frac{\sigma}{2}}{\frac{\varepsilon_r\varepsilon_o}{\Delta t}+\frac{\sigma}{2}}E_x^n(k)\right\}\right)^{2}$$

$$\left\{1+\frac{\left(1-\rho_{EE}^{2}\right)\sigma^{2}\left\{\dfrac{\dfrac{\varepsilon_r\varepsilon_o}{\Delta t}-\dfrac{\sigma}{2}}{\dfrac{\varepsilon_r\varepsilon_o}{\Delta t}+\dfrac{\sigma}{2}}E_x^n(k)\right\}}{\left(\sigma\left\{E_x^{n+1}(k)\right\}-\rho_{EE}\sigma\left\{\dfrac{\dfrac{\varepsilon_r\varepsilon_o}{\Delta t}-\dfrac{\sigma}{2}}{\dfrac{\varepsilon_r\varepsilon_o}{\Delta t}+\dfrac{\sigma}{2}}E_x^n(k)\right\}\right)^{2}}\right\}$$

$$=\sigma^{2}\left\{\frac{-1}{\left(\dfrac{\varepsilon_r\varepsilon_o}{\Delta t}+\dfrac{\sigma}{2}\right)\Delta z}\left(H_y^{n+1/2}(k)-H_y^{n+1/2}(k-1)\right)\right\} \tag{4.42}$$

$$\left\{1+\frac{\left(1-\rho_{EE}^{2}\right)\sigma^{2}\left\{\dfrac{\dfrac{\varepsilon_r\varepsilon_o}{\Delta t}-\dfrac{\sigma}{2}}{\dfrac{\varepsilon_r\varepsilon_o}{\Delta t}+\dfrac{\sigma}{2}}E_x^n(k)\right\}}{\left(\sigma\left\{E_x^{n+1}(k)\right\}-\rho_{EE}\sigma\left\{\dfrac{\dfrac{\varepsilon_r\varepsilon_o}{\Delta t}-\dfrac{\sigma}{2}}{\dfrac{\varepsilon_r\varepsilon_o}{\Delta t}+\dfrac{\sigma}{2}}E_x^n(k)\right\}\right)^{2}}\right\}$$

$$=\sigma^{2}\left\{\frac{-1}{\left(\dfrac{\varepsilon_r\varepsilon_o}{\Delta t}+\dfrac{\sigma}{2}\right)\Delta z}\left(H_y^{n+1/2}(k)-H_y^{n+1/2}(k-1)\right)\right\} \tag{4.43}$$

Taking the square-root of both sides of (4.43) yields:

$$\left(\sigma\left\{E_x^{n+1}(k)\right\}-\rho_{EE}\sigma\left\{\frac{\frac{\varepsilon_r\varepsilon_o}{\Delta t}-\frac{\sigma}{2}}{\frac{\varepsilon_r\varepsilon_o}{\Delta t}+\frac{\sigma}{2}}E_x^n(k)\right\}\right)$$

$$\sqrt{\left\{1+\frac{\left(1-\rho_{EE}^2\right)\sigma^2\left\{\frac{\frac{\varepsilon_r\varepsilon_o}{\Delta t}-\frac{\sigma}{2}}{\frac{\varepsilon_r\varepsilon_o}{\Delta t}+\frac{\sigma}{2}}E_x^n(k)\right\}}{\left(\sigma\left\{E_x^{n+1}(k)\right\}-\rho_{EE}\sigma\left\{\frac{\frac{\varepsilon_r\varepsilon_o}{\Delta t}-\frac{\sigma}{2}}{\frac{\varepsilon_r\varepsilon_o}{\Delta t}+\frac{\sigma}{2}}E_x^n(k)\right\}\right)^2}\right\}}$$

$$\approx\sigma\left\{\frac{-1}{\left(\frac{\varepsilon_r\varepsilon_o}{\Delta t}+\frac{\sigma}{2}\right)\Delta z}\left(H_y^{n+1/2}(k)-H_y^{n+1/2}(k-1)\right)\right\} \tag{4.44}$$

Using an approximation of the square-root, namely $\sqrt{1\pm x}\approx 1\pm x/2$, yields:

$$\sigma\left\{E_x^{n+1}(k)\right\}-\rho_{EE}\sigma\left\{\frac{\frac{\varepsilon_r\varepsilon_o}{\Delta t}-\frac{\sigma}{2}}{\frac{\varepsilon_r\varepsilon_o}{\Delta t}+\frac{\sigma}{2}}E_x^n(k)\right\}+\frac{\left(1-\rho_{EE}^2\right)\sigma^2\left\{\frac{\frac{\varepsilon_r\varepsilon_o}{\Delta t}-\frac{\sigma}{2}}{\frac{\varepsilon_r\varepsilon_o}{\Delta t}+\frac{\sigma}{2}}E_x^n(k)\right\}}{2\left(\sigma\left\{E_x^{n+1}(k)\right\}-\rho_{EE}\sigma\left\{\frac{\frac{\varepsilon_r\varepsilon_o}{\Delta t}-\frac{\sigma}{2}}{\frac{\varepsilon_r\varepsilon_o}{\Delta t}+\frac{\sigma}{2}}E_x^n(k)\right\}\right)}$$

$$\approx\sigma\left\{\frac{-1}{\left(\frac{\varepsilon_r\varepsilon_o}{\Delta t}+\frac{\sigma}{2}\right)\Delta z}\left(H_y^{n+1/2}(k)-H_y^{n+1/2}(k-1)\right)\right\}$$

(4.45)

Attempting to solve for the future E_x^{n+1} field term, we recall that the $Cov\left(E_x^{n+1}, \frac{\frac{\varepsilon_r\varepsilon_o}{\Delta t} - \frac{\sigma}{2}}{\frac{\varepsilon_r\varepsilon_o}{\Delta t} + \frac{\sigma}{2}} E_x^n \right)$ is approximately equal to $\sigma\left\{E_x^{n+1}\right\}\sigma\left\{\frac{\frac{\varepsilon_r\varepsilon_o}{\Delta t} - \frac{\sigma}{2}}{\frac{\varepsilon_r\varepsilon_o}{\Delta t} + \frac{\sigma}{2}} E_x^n\right\}$, as seen in Section 3.3. This leads us to believe ρ_{EE} (the time related correlation coefficient) is approximately equal to1, leading to the simplified version of (4.39):

$$\sigma\left\{E_x^{n+1}(k)\right\} - \sigma\left\{\frac{\frac{\varepsilon_r\varepsilon_o}{\Delta t} - \frac{\sigma}{2}}{\frac{\varepsilon_r\varepsilon_o}{\Delta t} + \frac{\sigma}{2}} E_x^n(k)\right\} \approx \sigma\left\{\frac{-1}{\left(\frac{\varepsilon_r\varepsilon_o}{\Delta t} + \frac{\sigma}{2}\right)\Delta z}\left(H_y^{n+1/2}(k) - H_y^{n+1/2}(k-1)\right)\right\} \quad (4.46)$$

The remainder term on the left-hand side of (4.45) approaches zero as the correlation coefficient approaches one. We can now solve for $\sigma\left\{E_x^{n+1}(k)\right\}$, yielding:

$$\sigma\left\{E_x^{n+1}(k)\right\} \approx \sigma\left\{\frac{\frac{\varepsilon_r\varepsilon_o}{\Delta t} - \frac{\sigma}{2}}{\frac{\varepsilon_r\varepsilon_o}{\Delta t} + \frac{\sigma}{2}} E_x^n(k)\right\} + \sigma\left\{\frac{-1}{\left(\frac{\varepsilon_r\varepsilon_o}{\Delta t} + \frac{\sigma}{2}\right)\Delta z}\left(H_y^{n+1/2}(k) - H_y^{n+1/2}(k-1)\right)\right\} \quad (4.47)$$

We are left now with finding the variance of the terms that are not easily separated, i.e. the $E_x^n(k)$ and $H_y^{n+1/2}(k)$ terms. We will use the approximations determined in Section 4.1.2, repeated below for clarity:

$$\sigma^2\left\{g\left(x_1,x_2,x_3,...,x_n\right)\right\}\approx\sum_{i=1}^{n}\sum_{j=1}^{n}\frac{\partial g}{\partial x_i}\frac{\partial g}{\partial x_j}\bigg|_{\mu_{x_1},\mu_{x_2},...,\mu_{x_n}}Cov\left\{x_i,x_j\right\} \tag{4.48}$$

This equation tells us that we need to sum up the covariance terms of the random multivariable function, taking two random variables at a time. Each covariance term is multiplied by the partial derivatives of the random function referenced to the variable in the covariance term. The stochastic function derivatives are then evaluated at the mean of each random variable contained in the random function. We will first look at the $E_x^n\left(k\right)$ term which will demonstrate how this is to be performed and then proceed with the H_y field terms.

4.3.2.1 Variance of the electric field. The variance of the E field is correlated with the electric permittivity and conductivity as seen in this term of (4.41):

$$\sigma^2\left\{\frac{\frac{\varepsilon_r\varepsilon_o}{\Delta t}-\frac{\underline{\sigma}}{2}}{\frac{\varepsilon_r\varepsilon_o}{\Delta t}+\frac{\underline{\sigma}}{2}}E_x^n\left(k\right)\right\} \tag{4.49}$$

Applying (4.48), we determine each of the factors of the approximation and then sum these factors for the final approximation of (4.49):

The $Cov\left\{\varepsilon_r,\varepsilon_r\right\}$ term (variance of ε_r, $\sigma^2\left\{\varepsilon_r\right\}$) is:

$$\left(\frac{\partial}{\partial\varepsilon_r}\left\{\frac{\frac{\varepsilon_r\varepsilon_o}{\Delta t}-\frac{\underline{\sigma}}{2}}{\frac{\varepsilon_r\varepsilon_o}{\Delta t}+\frac{\underline{\sigma}}{2}}E_x^n\left(k\right)\right\}\right)^2=\frac{16\Delta t^2\varepsilon_o^2\underline{\sigma}^2E_x^n\left(k\right)^2}{\left(2\varepsilon_o\varepsilon_r+\Delta t\underline{\sigma}\right)^4} \tag{4.50}$$

This is next evaluated at the mean of each of the stochastic variables and multiplied by the variance of ε_r:

$$\frac{16\Delta t^2 \varepsilon_o^2 \mu_{\underline{\sigma}}^2 E_x^n(k)^2}{(2\varepsilon_o \mu_{\varepsilon_r} + \Delta t \mu_{\underline{\sigma}})^4} \sigma^2\{\varepsilon_r\} \tag{4.51}$$

We have left the E field term in equation (4.51) as is, remembering that it is the mean value of $E_x^n(k)$.

We will now repeat this process for all the random variables in (4.49).

The $Cov\{\underline{\sigma},\underline{\sigma}\}$ term (variance of $\underline{\sigma}$, $\sigma^2\{\underline{\sigma}\}$) is:

$$\left(\frac{\partial}{\partial \underline{\sigma}}\left\{\frac{\frac{\varepsilon_r \varepsilon_o}{\Delta t} - \frac{\underline{\sigma}}{2}}{\frac{\varepsilon_r \varepsilon_o}{\Delta t} + \frac{\underline{\sigma}}{2}} E_x^n(k)\right\}\right)^2 = \frac{16\Delta t^2 \varepsilon_o^2 \varepsilon_r^2 E_x^n(k)^2}{(2\varepsilon_o \varepsilon_r + \Delta t \underline{\sigma})^4} \tag{4.52}$$

This is next evaluated at the mean of each of the stochastic variables and multiplied by the variance of $\underline{\sigma}$, $\sigma^2\{\underline{\sigma}\}$:

$$\frac{16\Delta t^2 \varepsilon_o^2 \mu_{\varepsilon_r}^2 E_x^n(k)^2}{(2\varepsilon_o \mu_{\varepsilon_r} + \Delta t \mu_{\underline{\sigma}})^4} \sigma^2\{\underline{\sigma}\} \tag{4.53}$$

The $Cov\{E_x^n(k), E_x^n(k)\}$ term (variance of $E_x^n(k)$, $\sigma^2\{E_x^n(k)\}$) is:

$$\left(\frac{\partial}{\partial E_x^n(k)} \left\{ \frac{\frac{\varepsilon_r \varepsilon_o}{\Delta t} - \frac{\underline{\sigma}}{2}}{\frac{\varepsilon_r \varepsilon_o}{\Delta t} + \frac{\underline{\sigma}}{2}} E_x^n(k) \right\} \right)^2 = \frac{(2\varepsilon_o \varepsilon_r - \Delta t \underline{\sigma})^2}{(2\varepsilon_o \varepsilon_r + \Delta t \underline{\sigma})^2} \tag{4.54}$$

This is next evaluated at the mean of each of the stochastic variables and multiplied by the variance of $E_x^n(k)$:

$$\frac{(2\varepsilon_o \mu_{\varepsilon_r} - \Delta t \mu_{\underline{\sigma}})^2}{(2\varepsilon_o \mu_{\varepsilon_r} + \Delta t \mu_{\underline{\sigma}})^2} \sigma^2 \left\{ E_x^n(k) \right\} \tag{4.55}$$

The $Cov\{\varepsilon_r, \underline{\sigma}\}$ term is given by:

$$2 \left(\frac{\partial}{\partial \varepsilon_r} \left\{ \frac{\frac{\varepsilon_r \varepsilon_o}{\Delta t} - \frac{\underline{\sigma}}{2}}{\frac{\varepsilon_r \varepsilon_o}{\Delta t} + \frac{\underline{\sigma}}{2}} E_x^n(k) \right\} \right) \left(\frac{\partial}{\partial \underline{\sigma}} \left\{ \frac{\frac{\varepsilon_r \varepsilon_o}{\Delta t} - \frac{\underline{\sigma}}{2}}{\frac{\varepsilon_r \varepsilon_o}{\Delta t} + \frac{\underline{\sigma}}{2}} E_x^n(k) \right\} \right) = - \frac{32 \Delta t^2 \varepsilon_o^2 \varepsilon_r \underline{\sigma} \, \mathrm{E}_x^n(k)^2}{(2\varepsilon_o \varepsilon_r + \Delta t \underline{\sigma})^4} \tag{4.56}$$

The first factor of 2 appears due to the $Cov\{\varepsilon_r, \underline{\sigma}\}$ term occurring twice in the summation approximation. This is next evaluated at the mean of each of the stochastic variables and multiplied by the covariance term, remembering that $Cov\{\varepsilon_r, \underline{\sigma}\}$ is equal to $\rho_{\varepsilon,\sigma} \sigma\{\varepsilon_r\} \sigma\{\underline{\sigma}\}$. We get the following:

$$-\frac{32\Delta t^2\varepsilon_o^2\mu_{\varepsilon_r}\mu_{\underline{\sigma}}\,\mathrm{E}_x(k)^2}{(2\varepsilon_o\mu_{\varepsilon_r}+\Delta t\mu_{\underline{\sigma}})^4}\rho_{\varepsilon,\sigma}\sigma\{\varepsilon_r\}\sigma\{\underline{\sigma}\} \tag{4.57}$$

Now the $Cov\{\varepsilon_r, E_x^n(k)\}$ term is given by:

$$2\left(\frac{\partial}{\partial\varepsilon_r}\left\{\frac{\frac{\varepsilon_r\varepsilon_o}{\Delta t}-\frac{\underline{\sigma}}{2}}{\frac{\varepsilon_r\varepsilon_o}{\Delta t}+\frac{\underline{\sigma}}{2}}E_x^n(k)\right\}\right)\left(\frac{\partial}{\partial E_x^n(k)}\left\{\frac{\frac{\varepsilon_r\varepsilon_o}{\Delta t}-\frac{\underline{\sigma}}{2}}{\frac{\varepsilon_r\varepsilon_o}{\Delta t}+\frac{\underline{\sigma}}{2}}E_x^n(k)\right\}\right)= \tag{4.58}$$

$$-\frac{8\Delta t\varepsilon_o\underline{\sigma}(-2\varepsilon_o\varepsilon_r+\Delta t\underline{\sigma})E_x^n(k)}{(2\varepsilon_o\varepsilon_r+\Delta t\underline{\sigma})^3}$$

This is next evaluated at the mean of each of the stochastic variables and multiplied by the covariance terms:

$$-\frac{8\Delta t\varepsilon_o\mu_{\underline{\sigma}}(-2\varepsilon_o\mu_{\varepsilon_r}+\Delta t\mu_{\underline{\sigma}})E_x^n(k)}{(2\varepsilon_o\mu_{\varepsilon_r}+\Delta t\mu_{\underline{\sigma}})^3}\rho_{\varepsilon_r,E}\sigma\{\varepsilon_r\}\sigma\{E_x^n(k)\} \tag{4.59}$$

The $Cov\{\underline{\sigma}, E_x^n(k)\}$ term is now written as:

$$2\left(\frac{\partial}{\partial\underline{\sigma}}\left\{\frac{\frac{\varepsilon_r\varepsilon_o}{\Delta t}-\frac{\underline{\sigma}}{2}}{\frac{\varepsilon_r\varepsilon_o}{\Delta t}+\frac{\underline{\sigma}}{2}}E_x^n(k)\right\}\right)\left(\frac{\partial}{\partial E_x^n(k)}\left\{\frac{\frac{\varepsilon_r\varepsilon_o}{\Delta t}-\frac{\underline{\sigma}}{2}}{\frac{\varepsilon_r\varepsilon_o}{\Delta t}+\frac{\underline{\sigma}}{2}}E_x^n(k)\right\}\right)= \tag{4.60}$$

$$\frac{8\Delta t\varepsilon_o\varepsilon_r(-2\varepsilon_o\varepsilon_r+\Delta t\underline{\sigma})E_x^n(k)}{(2\varepsilon_o\varepsilon_r+\Delta t\underline{\sigma})^3}$$

This is next evaluated at the mean of each of the stochastic variables and multiplied by the covariance terms:

$$\frac{8\Delta t\varepsilon_o\mu_{\underline{\sigma}}(-2\varepsilon_o\mu_{\varepsilon_r}+\Delta t\mu_{\underline{\sigma}})E_x^n(k)}{(2\varepsilon_o\mu_{\varepsilon_r}+\Delta t\mu_{\underline{\sigma}})^3}\rho_{\underline{\sigma},E}\sigma\{\underline{\sigma}\}\sigma\left\{E_x^n(k)\right\} \tag{4.61}$$

This completes the terms needed to find an approximation for $\sigma^2\left\{\frac{\frac{\varepsilon_r\varepsilon_o}{\Delta t}-\frac{\underline{\sigma}}{2}}{\frac{\varepsilon_r\varepsilon_o}{\Delta t}+\frac{\underline{\sigma}}{2}}E_x^n(k)\right\}$. Adding equations (4.51), (4.53), (4.55), (4.57), (4.59), and (4.61), equation (4.49) becomes:

$$\sigma^2\left\{\frac{\frac{\varepsilon_r\varepsilon_o}{\Delta t}-\frac{\underline{\sigma}}{2}}{\frac{\varepsilon_r\varepsilon_o}{\Delta t}+\frac{\underline{\sigma}}{2}}E_x^n(k)\right\}\approx$$

$$\frac{16\Delta t^2\varepsilon_o^2\mu_{\underline{\sigma}}^2}{(2\varepsilon_o\mu_{\varepsilon_r}+\Delta t\mu_{\underline{\sigma}})^4}E_x^n(k)^2\sigma^2\{\varepsilon_r\}+\frac{16\Delta t^2\varepsilon_o^2\mu_{\varepsilon_r}^2}{(2\varepsilon_o\mu_{\varepsilon_r}+\Delta t\mu_{\underline{\sigma}})^4}E_x^n(k)^2\sigma^2\{\underline{\sigma}\}$$

$$+\frac{(2\varepsilon_o\mu_{\varepsilon_r}-\Delta t\mu_{\underline{\sigma}})^2}{(2\varepsilon_o\mu_{\varepsilon_r}+\Delta t\mu_{\underline{\sigma}})^2}\sigma^2\left\{E_x^n(k)\right\}-\frac{32\Delta t^2\varepsilon_o^2\mu_{\varepsilon_r}\mu_{\underline{\sigma}}}{(2\varepsilon_o\mu_{\varepsilon_r}+\Delta t\mu_{\underline{\sigma}})^4}\rho_{\varepsilon,\sigma}E_x^n(k)^2\sigma\{\varepsilon_r\}\sigma\{\underline{\sigma}\}$$

$$-\frac{8\Delta t\varepsilon_o\mu_{\underline{\sigma}}(-2\varepsilon_o\mu_{\varepsilon_r}+\Delta t\mu_{\underline{\sigma}})}{(2\varepsilon_o\mu_{\varepsilon_r}+\Delta t\mu_{\underline{\sigma}})^3}\rho_{\varepsilon_r,E}E_x^n(k)\sigma\{\varepsilon_r\}\sigma\left\{E_x^n(k)\right\}$$

$$+\frac{8\Delta t\varepsilon_o\mu_{\underline{\sigma}}(-2\varepsilon_o\mu_{\varepsilon_r}+\Delta t\mu_{\underline{\sigma}})}{(2\varepsilon_o\mu_{\varepsilon_r}+\Delta t\mu_{\underline{\sigma}})^3}\rho_{\underline{\sigma},E}E_x^n(k)\sigma\{\underline{\sigma}\}\sigma\left\{E_x^n(k)\right\} \tag{4.62}$$

Combining and rearranging terms yields:

$$\sigma^2\left\{\frac{\frac{\varepsilon_r\varepsilon_o}{\Delta t}-\frac{\underline{\sigma}}{2}}{\frac{\varepsilon_r\varepsilon_o}{\Delta t}+\frac{\underline{\sigma}}{2}}E_x^n(k)\right\}\approx$$

$$\frac{(2\varepsilon_o\mu_{\varepsilon_r}-\Delta t\mu_{\underline{\sigma}})^2}{(2\epsilon_o\mu_{\epsilon_r}+\Delta t\mu_{\underline{\sigma}})^2}\sigma^2\left\{E_x^n(k)\right\}$$

$$-\frac{8\Delta t\varepsilon_o\left(-2\varepsilon_o\mu_{\varepsilon_r}+\Delta t\mu_{\underline{\sigma}}\right)\left(\mu_{\underline{\sigma}}\rho_{\varepsilon_r,E}\sigma\{\varepsilon_r\}-\mu_{\varepsilon_r}\rho_{\underline{\sigma},E}\sigma\{\underline{\sigma}\}\right)}{\left(2\varepsilon_o\mu_{\varepsilon_r}+\Delta t\mu_{\underline{\sigma}}\right)^3}\sigma\left\{E_x^n(k)\right\}E_x^n(k)$$

$$+\frac{16\Delta t^2\varepsilon_o^2\left(-2\mu_{\varepsilon_r}\mu_{\underline{\sigma}}\rho_{\underline{\sigma},\varepsilon_r}\sigma\{\varepsilon_r\}\sigma\{\underline{\sigma}\}+\mu_{\underline{\sigma}}^2\sigma\{\varepsilon_r\}^2+\mu_{\varepsilon_r}^2\sigma\{\underline{\sigma}\}^2\right)}{\left(2\varepsilon_o\mu_{\varepsilon_r}+\Delta t\mu_{\underline{\sigma}}\right)^4}E_x^n(k)^2 \tag{4.63}$$

This equation can now be rearranged in order to complete the square. It is desirable to put it into this form and simplify it by taking the square-root. Again this preserves the phase of the fields and variance terms. To complete the square of the second term of (4.63), we would need to have a factor $2\varepsilon_o\mu_{\varepsilon_r}-\Delta t\mu_{\underline{\sigma}}$ and combine with the last term in the equation. We would also need $\left(\mu_{\underline{\sigma}}\rho_{\varepsilon_r,E}\sigma\{\varepsilon_r\}-\mu_{\varepsilon_r}\rho_{\underline{\sigma},E}\sigma\{\underline{\sigma}\}\right)^2$. To take the square root of the middle term, we need to remove a -1 from the $-2\varepsilon_o\mu_{\varepsilon_r}+\Delta t\mu_{\underline{\sigma}}$ and change the sign of the second term. To get the third term, we need to add $\left(\mu_{\underline{\sigma}}\rho_{\varepsilon_r,E}\sigma\{\varepsilon_r\}-\mu_{\varepsilon_r}\rho_{\underline{\sigma},E}\sigma\{\underline{\sigma}\}\right)^2$ and subtract the same from both sides of the equation. This is shown below:

$$\frac{(2\varepsilon_o\mu_{\varepsilon_r}-\Delta t\mu_{\underline{\sigma}})^2}{(2\epsilon_o\mu_{\epsilon_r}+\Delta t\mu_{\underline{\sigma}})^2}\sigma^2\left\{E_x^n(k)\right\}$$

$$+\frac{8\Delta t\varepsilon_o\left(2\varepsilon_o\mu_{\varepsilon_r}-\Delta t\mu_{\underline{\sigma}}\right)\left(\mu_{\underline{\sigma}}\rho_{\varepsilon_r,E}\sigma\{\varepsilon_r\}-\mu_{\varepsilon_r}\rho_{\underline{\sigma},E}\sigma\{\underline{\sigma}\}\right)}{\left(2\varepsilon_o\mu_{\varepsilon_r}+\Delta t\mu_{\underline{\sigma}}\right)^3}\sigma\left\{E_x^n(k)\right\}E_x^n(k)$$

$$+\frac{16\Delta t^2\varepsilon_o^2\left(\mu_{\underline{\sigma}}\rho_{\varepsilon_r,E}\sigma\{\varepsilon_r\}-\mu_{\varepsilon_r}\rho_{\underline{\sigma},E}\sigma\{\underline{\sigma}\}\right)^2}{\left(2\varepsilon_o\mu_{\varepsilon_r}+\Delta t\mu_{\underline{\sigma}}\right)^4}E_x^n(k)^2$$

$$+\frac{16\Delta t^2\varepsilon_o^2\left(-2\mu_{\varepsilon_r}\mu_{\underline{\sigma}}\rho_{\underline{\sigma},\varepsilon_r}\sigma\{\varepsilon_r\}\sigma\{\underline{\sigma}\}+\mu_{\underline{\sigma}}^2\sigma\{\varepsilon_r\}^2+\mu_{\varepsilon_r}^2\sigma\{\underline{\sigma}\}^2\right)}{\left(2\varepsilon_o\mu_{\varepsilon_r}+\Delta t\mu_{\underline{\sigma}}\right)^4}E_x^n(k)^2$$

$$-\frac{16\Delta t^2\varepsilon_o^2\left(\mu_{\underline{\sigma}}\rho_{\varepsilon_r,E}\sigma\{\varepsilon_r\}-\mu_{\varepsilon_r}\rho_{\underline{\sigma},E}\sigma\{\underline{\sigma}\}\right)^2}{\left(2\varepsilon_o\mu_{\varepsilon_r}+\Delta t\mu_{\underline{\sigma}}\right)^4}E_x^n(k)^2 \tag{4.64}$$

This then reduces to:

$$\left\{\frac{2\varepsilon_o\mu_{\varepsilon_r}-\Delta t\mu_{\underline{\sigma}}}{2\epsilon_o\mu_{\epsilon_r}+\Delta t\mu_{\underline{\sigma}}}\sigma\left\{E_x^n(k)\right\}+\frac{4\Delta t\varepsilon_o\left(\mu_{\underline{\sigma}}\rho_{\varepsilon_r,E}\sigma\{\varepsilon_r\}-\mu_{\varepsilon_r}\rho_{\underline{\sigma},E}\sigma\{\underline{\sigma}\}\right)}{\left(2\varepsilon_o\mu_{\varepsilon_r}+\Delta t\mu_{\underline{\sigma}}\right)^2}E_x^n(k)\right\}^2 \tag{4.65}$$

$$+\frac{16\Delta t^2\varepsilon_o^2}{\left(2\varepsilon_o\mu_{\varepsilon_r}+\Delta t\mu_{\underline{\sigma}}\right)^4}E_x^n(k)^2\left(\begin{array}{l}\left(\begin{array}{r}\mu_{\underline{\sigma}}^2\sigma\{\varepsilon_r\}^2-2\mu_{\varepsilon_r}\mu_{\underline{\sigma}}\rho_{\underline{\sigma},\varepsilon_r}\sigma\{\varepsilon_r\}\sigma\{\underline{\sigma}\}\\ +\mu_{\varepsilon_r}^2\sigma\{\underline{\sigma}\}^2\end{array}\right)\\ -\left(\mu_{\underline{\sigma}}\rho_{\varepsilon_r,E}\sigma\{\varepsilon_r\}-\mu_{\varepsilon_r}\rho_{\underline{\sigma},E}\sigma\{\underline{\sigma}\}\right)^2\end{array}\right)$$

Putting it into a simpler form yields:

$$\left\{\frac{2\varepsilon_o\mu_{\varepsilon_r}-\Delta t\mu_{\underline{\sigma}}}{2\epsilon_o\mu_{\epsilon_r}+\Delta t\mu_{\underline{\sigma}}}\sigma\left\{E_x^n(k)\right\}+\frac{4\Delta t\varepsilon_o\left(\mu_{\underline{\sigma}}\rho_{\varepsilon_r,E}\sigma\{\varepsilon_r\}-\mu_{\varepsilon_r}\rho_{\underline{\sigma},E}\sigma\{\underline{\sigma}\}\right)}{\left(2\varepsilon_o\mu_{\varepsilon_r}+\Delta t\mu_{\underline{\sigma}}\right)^2}E_x^n(k)\right\}^2$$

$$+\frac{16\Delta t^2\varepsilon_o^2}{\left(2\varepsilon_o\mu_{\varepsilon_r}+\Delta t\mu_{\underline{\sigma}}\right)^4}E_x^n(k)^2\left(\begin{array}{l}\mu_{\underline{\sigma}}^2\left(1-\rho_{\underline{\sigma},\varepsilon_r}^2\right)\sigma\{\varepsilon_r\}^2\\-2\mu_{\varepsilon_r}\mu_{\underline{\sigma}}\left(\rho_{\underline{\sigma},\varepsilon_r}-\rho_{\varepsilon_r,E}\rho_{\underline{\sigma},E}\right)\sigma\{\varepsilon_r\}\sigma\{\underline{\sigma}\}\\+\mu_{\varepsilon_r}^2\left(1-\rho_{\underline{\sigma},E}^2\right)\sigma\{\underline{\sigma}\}^2\end{array}\right) \quad (4.66)$$

We can now factor out the completed square term and then take the square-root of the equation. But first let us set up some new variable that will allow a better view of what we are trying to accomplish. Let us set the completed square term equal to a^2 and the last term equal to b :

$$a^2=\left\{\frac{2\varepsilon_o\mu_{\varepsilon_r}-\Delta t\mu_{\underline{\sigma}}}{2\epsilon_o\mu_{\epsilon_r}+\Delta t\mu_{\underline{\sigma}}}\sigma\left\{E_x^n(k)\right\}+\frac{4\Delta t\varepsilon_o\left(\mu_{\underline{\sigma}}\rho_{\varepsilon_r,E}\sigma\{\varepsilon_r\}-\mu_{\varepsilon_r}\rho_{\underline{\sigma},E}\sigma\{\underline{\sigma}\}\right)}{\left(2\varepsilon_o\mu_{\varepsilon_r}+\Delta t\mu_{\underline{\sigma}}\right)^2}E_x^n(k)\right\}^2$$

$$b=\frac{16\Delta t^2\varepsilon_o^2}{\left(2\varepsilon_o\mu_{\varepsilon_r}+\Delta t\mu_{\underline{\sigma}}\right)^4}E_x^n(k)^2\left(\begin{array}{l}\mu_{\underline{\sigma}}^2\left(1-\rho_{\varepsilon_r,E}^2\right)\sigma\{\varepsilon_r\}^2\\-2\mu_{\varepsilon_r}\mu_{\underline{\sigma}}\left(\rho_{\underline{\sigma},\varepsilon_r}-\rho_{\varepsilon_r,E}\rho_{\underline{\sigma},E}\right)\sigma\{\varepsilon_r\}\sigma\{\underline{\sigma}\}\\+\mu_{\varepsilon_r}^2\left(1-\rho_{\underline{\sigma},E}^2\right)\sigma\{\underline{\sigma}\}^2\end{array}\right)$$

This yields a clearer equation:

$$a^2+b \quad (4.67)$$

Factoring out the a^2 term yields:

$$a^2\left(1+\frac{b}{a^2}\right) \tag{4.68}$$

and then taking the square-root we get:

$$a\sqrt{1+\frac{b}{a^2}} \tag{4.69}$$

Using an approximation of the above square-root ($\sqrt{1+x} \approx 1+\frac{x}{2}$), we obtain:

$$\begin{gathered} a\left(1+\frac{b}{2a^2}\right) \\ a+\frac{b}{2a} \end{gathered} \tag{4.70}$$

With $b/2a$ as a remainder term R, we obtain the following equations:

$$a=\frac{2\varepsilon_o\mu_{\varepsilon_r}-\Delta t\mu_{\underline{\sigma}}}{2\epsilon_o\mu_{\epsilon_r}+\Delta t\mu_{\underline{\sigma}}}\sigma\left\{E_x^n(k)\right\}+\frac{4\Delta t\varepsilon_o\left(\mu_{\underline{\sigma}}\rho_{\varepsilon_r,E}\sigma\{\varepsilon_r\}-\mu_{\varepsilon_r}\rho_{\underline{\sigma},E}\sigma\{\underline{\sigma}\}\right)}{\left(2\varepsilon_o\mu_{\varepsilon_r}+\Delta t\mu_{\underline{\sigma}}\right)^2}E_x^n(k) \tag{4.71}$$

$$b/2a = \frac{\dfrac{16\Delta t^2 \varepsilon_o^2}{\left(2\varepsilon_o \mu_{\varepsilon_r} + \Delta t \mu_{\underline{\sigma}}\right)^4} E_x^n(k)^2 \left(\begin{array}{l} \mu_{\underline{\sigma}}^2 \left(1-\rho_{\varepsilon_r,E}^2\right)\sigma\{\varepsilon_r\}^2 \\ -2\mu_{\varepsilon_r}\mu_{\underline{\sigma}}\left(\rho_{\underline{\sigma},\varepsilon_r} - \rho_{\varepsilon_r,E}\rho_{\underline{\sigma},E}\right)\sigma\{\varepsilon_r\}\sigma\{\underline{\sigma}\} \\ +\mu_{\varepsilon_r}^2\left(1-\rho_{\underline{\sigma},E}^2\right)\sigma\{\underline{\sigma}\}^2 \end{array} \right)}{2\left(\dfrac{2\varepsilon_o\mu_{\varepsilon_r} - \Delta t\mu_{\underline{\sigma}}}{2\epsilon_o\mu_{\epsilon_r} + \Delta t\mu_{\underline{\sigma}}}\sigma\left\{E_x^n(k)\right\} + \dfrac{4\Delta t\varepsilon_o\left(\mu_{\underline{\sigma}}\rho_{\varepsilon_r,E}\sigma\{\varepsilon_r\} - \mu_{\varepsilon_r}\rho_{\underline{\sigma},E}\sigma\{\underline{\sigma}\}\right)}{\left(2\varepsilon_o\mu_{\varepsilon_r} + \Delta t\mu_{\underline{\sigma}}\right)^2} E_x^n(k) \right)} \tag{4.72}$$

Neglecting the remainder term, we are left with:

$$\sigma\left\{ \frac{\dfrac{\varepsilon_r\varepsilon_o}{\Delta t} - \dfrac{\underline{\sigma}}{2}}{\dfrac{\varepsilon_r\varepsilon_o}{\Delta t} + \dfrac{\underline{\sigma}}{2}} E_x^n(k) \right\} \approx$$

$$\frac{2\varepsilon_o\mu_{\varepsilon_r} - \Delta t\mu_{\underline{\sigma}}}{2\epsilon_o\mu_{\epsilon_r} + \Delta t\mu_{\underline{\sigma}}}\sigma\left\{E_x^n(k)\right\} + \frac{4\Delta t\varepsilon_o\left(\mu_{\underline{\sigma}}\rho_{\varepsilon_r,E}\sigma\{\varepsilon_r\} - \mu_{\varepsilon_r}\rho_{\underline{\sigma},E}\sigma\{\underline{\sigma}\}\right)}{\left(2\varepsilon_o\mu_{\varepsilon_r} + \Delta t\mu_{\underline{\sigma}}\right)^2} E_x^n(k) \tag{4.73}$$

We have determined an approximation to the left hand side of equation (4.36) with the addition of equation (4.73). Next, we focus on the variance H field terms.

4.3.2.2 Variance of the H field. Recall that the variance of Ampere's Law (4.36) is:

$$\sigma^2\left\{ E_x^{n+1}(k) - \frac{\dfrac{\varepsilon_r\varepsilon_o}{\Delta t} - \dfrac{\underline{\sigma}}{2}}{\dfrac{\varepsilon_r\varepsilon_o}{\Delta t} + \dfrac{\underline{\sigma}}{2}} E_x^n(k) \right\} = \sigma^2\left\{ \frac{-1}{\left(\dfrac{\varepsilon_r\varepsilon_o}{\Delta t} + \dfrac{\underline{\sigma}}{2}\right)\Delta z}\left(H_y^{n+1/2}(k) - H_y^{n+1/2}(k-1)\right) \right\} \tag{4.74}$$

We have determined the left-hand side (in (4.74) above), and now we look toward the right-hand side of (4.74) which is:

$$\sigma^2\left\{\frac{-1}{\left(\frac{\varepsilon_r\varepsilon_o}{\Delta t}+\frac{\underline{\sigma}}{2}\right)\Delta z}\left(H_y^{n+1/2}(k)-H_y^{n+1/2}(k-1)\right)\right\} \tag{4.75}$$

We will follow the same procedure used in the preceding section; by finding each covariance term and then adding them for the completed variance equation we will derive an approximations of (4.75). The terms that follow are the variance terms. We are looking at $Cov\{X,X\}$ which is equal to the $\sigma^2\{X\}$. We have a variance term for each of the stochastic variables $\varepsilon_r, \underline{\sigma}, H_y^{n+1/2}(k+1/2), H_y^{n+1/2}(k-1/2)$.

The $Cov\{\varepsilon_r,\varepsilon_r\}$ term (variance of ε_r, $\sigma^2\{\varepsilon_r\}$) can be expressed as:

$$\left\{\frac{\partial}{\partial\varepsilon_r}\left\{\frac{\left(H_y^{n+1/2}(k+1/2)-H_y^{n+1/2}(k-1/2)\right)}{\Delta x(\frac{\varepsilon_r\varepsilon_o}{\Delta t}+\frac{\underline{\sigma}}{2})}\right\}\right\}^2\Bigg|_{\mu_r,\mu_{\underline{\sigma}},\mu_H}\sigma^2\{\varepsilon_r\}=$$

$$\frac{16\Delta t^2\varepsilon_o^2\left(H_y^{n+1/2}(k-1/2)-H_y^{n+1/2}(k+1/2)\right)^2}{\Delta x^2(2\varepsilon_o\mu_{\varepsilon_r}+\Delta t\mu_{\underline{\sigma}})^4}\sigma^2\{\varepsilon_r\} \tag{4.76}$$

Equation (4.76) is evaluated at the mean of each of the stochastic variables. We next multiply by the variance of ε_r, $\sigma^2\{\varepsilon_r\}$. The H field terms are the mean values,

similar to the E field terms in the previous section.

The $Cov\{\underline{\sigma},\underline{\sigma}\}$ term (variance of $\underline{\sigma}$, $\sigma^2\{\underline{\sigma}\}$) is given by:

$$\left\{\frac{\partial}{\partial\underline{\sigma}}\left\{\frac{\left(H_y^{n+1/2}(k+1/2)-H_y^{n+1/2}(k-1/2)\right)}{\Delta x(\frac{\varepsilon_r\varepsilon_o}{\Delta t}+\frac{\underline{\sigma}}{2})}\right\}\right\}^2\Bigg|_{\mu_r,\mu_{\underline{\sigma}},\mu_H}\sigma^2\{\underline{\sigma}\}$$

$$=\frac{4\Delta t^4\left(H_y^{n+1/2}(k-1/2)-H_y^{n+1/2}(k+1/2)\right)^2}{\Delta x^2(2\varepsilon_o\mu_{\varepsilon_r}+\Delta t\mu_{\underline{\sigma}})^4}\sigma^2\{\underline{\sigma}\} \qquad (4.77)$$

We next find the $Cov\left\{H_y^{n+1/2}(k-1/2),H_y^{n+1/2}(k-1/2)\right\}$ which is the variance of $H_y^{n+1/2}(k-1/2)$; that is, $\sigma^2\left\{H_y^{n+1/2}(k-1/2)\right\}$). Again we take the partial derivative of:

$$\left\{\frac{\left(H_y^{n+1/2}(k+1/2)-H_y^{n+1/2}(k-1/2)\right)}{\Delta x(\frac{\varepsilon_r\varepsilon_o}{\Delta t}+\frac{\underline{\sigma}}{2})}\right\}$$

with respect to $H_y^{n+1/2}(k-1/2)$ and square it:

$$\left\{\frac{\partial}{\partial H_y^{n+1/2}(k-1/2)}\left\{\frac{\left(H_y^{n+1/2}(k+1/2)-H_y^{n+1/2}(k-1/2)\right)}{\Delta x(\frac{\varepsilon_r\varepsilon_o}{\Delta t}+\frac{\underline{\sigma}}{2})}\right\}\right\}^2\Bigg|_{\mu_r,\mu_{\underline{\sigma}},\mu_H}\sigma^2\left\{H_y^{n+1/2}(k-1/2)\right\}$$

$$= \frac{4\Delta t^2}{\Delta x^2 (2\varepsilon_o \mu_{\varepsilon_r} + \Delta t \mu_{\underline{\sigma}})^2} \sigma^2 \left\{ H_y^{n+1/2}(k-1/2) \right\} \tag{4.78}$$

The $Cov\left\{ H_y^{n+1/2}(k+1/2), H_y^{n+1/2}(k+1/2) \right\}$ term (variance of $H_y^{n+1/2}(k+1/2)$), or $\sigma^2 \left\{ H_y^{n+1/2}(k+1/2) \right\}$) is given by:

$$\left\{ \frac{\partial}{\partial H_y^{n+1/2}(k+1/2)} \left\{ \frac{\left(H_y^{n+1/2}(k+1/2) - H_y^{n+1/2}(k-1/2) \right)}{\Delta x (\frac{\varepsilon_r \varepsilon_o}{\Delta t} + \frac{\underline{\sigma}}{2})} \right\} \right\}^2 \Bigg|_{\mu_r, \mu_{\underline{\sigma}}, \mu_H} \sigma^2 \left\{ H_y^{n+1/2}(k+1/2) \right\}$$

$$= \frac{4\Delta t^2}{\Delta x^2 (2\varepsilon_o \mu_{\varepsilon_r} + \Delta t \mu_{\underline{\sigma}})^2} \sigma^2 \left\{ H_y^{n+1/2}(k+1/2) \right\} \tag{4.79}$$

Next, the covariance terms follow, taking each variable two at a time for the same stochastic variable as before, i.e. $\varepsilon_r, \underline{\sigma}, H_y^{n+1/2}(k+1/2), H_y^{n+1/2}(k-1/2)$. The factor 2 comes into play because we have $Cov\{X,Y\}$ and $Cov\{Y,X\}$ which are equivalent and add up.

First we write the $Cov\{\varepsilon_r, \underline{\sigma}\}$ term as the following:

$$2 \left[\frac{\partial}{\partial \varepsilon_r} \left\{ \frac{\left(H_y^{n+1/2}(k+1/2) - H_y^{n+1/2}(k-1/2) \right)}{\Delta x \left(\frac{\varepsilon_r \varepsilon_o}{\Delta t} + \frac{\underline{\sigma}}{2} \right)} \right\} \right. \cdot$$

$$\frac{\partial}{\partial \underline{\sigma}}\left\{\frac{\left(H_y^{n+1/2}(k+1/2)-H_y^{n+1/2}(k-1/2)\right)}{\Delta x\left(\frac{\varepsilon_r\varepsilon_o}{\Delta t}+\frac{\underline{\sigma}}{2}\right)}\right\}\Bigg|_{\mu_r,\mu_{\underline{\sigma}},\mu_H}\rho_{\underline{\sigma},\varepsilon_r}\sigma\{\varepsilon_r\}\sigma\{\underline{\sigma}\}\Bigg]$$

$$=\frac{16\Delta t^3\varepsilon_o\left(H_y^{n+1/2}(k-1/2)-H_y^{n+1/2}(k+1/2)\right)^2}{\Delta x^2(2\varepsilon_o\mu_{\varepsilon_r}+\Delta t\mu_{\underline{\sigma}})^4}\rho_{\underline{\sigma},\varepsilon_r}\sigma\{\varepsilon_r\}\sigma\{\underline{\sigma}\} \tag{4.80}$$

We next find the $Cov\left\{\underline{\sigma},H_y^{n+1/2}(k-1/2)\right\}$ term:

$$2\Bigg[\frac{\partial}{\partial \underline{\sigma}}\left\{\frac{\left(H_y^{n+1/2}(k+1/2)-H_y^{n+1/2}(k-1/2)\right)}{\Delta x\left(\frac{\varepsilon_r\varepsilon_o}{\Delta t}+\frac{\underline{\sigma}}{2}\right)}\right\}\frac{\partial}{\partial H_y^{n+1/2}(k-1/2)}$$

$$\left\{\frac{\left(H_y^{n+1/2}(k+1/2)-H_y^{n+1/2}(k-1/2)\right)}{\Delta x\left(\frac{\varepsilon_r\varepsilon_o}{\Delta t}+\frac{\underline{\sigma}}{2}\right)}\right\}\Bigg|_{\mu_r,\mu_{\underline{\sigma}},\mu_H}\rho_{\underline{\sigma},H_y^{n+1/2}(k-1/2)}\sigma\{\underline{\sigma}\}\sigma\left\{H_y^{n+1/2}(k-1/2)\right\}$$

$$=-\frac{8\Delta t^3\left(H_y^{n+1/2}(k-1/2)-H_y^{n+1/2}(k+1/2)\right)}{\Delta x^2(2\varepsilon_o\mu_{\varepsilon_r}+\Delta t\mu_{\underline{\sigma}})^3}\rho_{\underline{\sigma},H_y^{n+1/2}(k-1/2)}\sigma\{\underline{\sigma}\}\sigma\left\{H_y^{n+1/2}(k-1/2)\right\} \tag{4.81}$$

Then, the $Cov\left\{\underline{\sigma},H_y^{n+1/2}(k+1/2)\right\}$ term is:

$$2\left[\frac{\partial}{\partial \underline{\sigma}}\left\{\frac{\left(H_y^{n+1/2}(k+1/2)-H_y^{n+1/2}(k-1/2)\right)}{\Delta x\left(\frac{\varepsilon_r\varepsilon_o}{\Delta t}+\frac{\underline{\sigma}}{2}\right)}\right\}\right.\frac{\partial}{\partial H_y^{n+1/2}(k+1/2)}$$

$$\left.\left\{\frac{\left(H_y^{n+1/2}(k+1/2)-H_y^{n+1/2}(k-1/2)\right)}{\Delta x\left(\frac{\varepsilon_r\varepsilon_o}{\Delta t}+\frac{\underline{\sigma}}{2}\right)}\right\}\right|_{\mu_r,\mu_{\underline{\sigma}},\mu_H}\rho_{\underline{\sigma},H_y^{n+1/2}(k+1/2)}\sigma\{\underline{\sigma}\}\sigma\left\{H_y^{n+1/2}(k+1/2)\right\}$$

$$=\frac{8\Delta t^3\left(H_y^{n+1/2}(k-1/2)-H_y^{n+1/2}(k+1/2)\right)}{\Delta x^2(2\varepsilon_o\mu_{\varepsilon_r}+\Delta t\mu_{\underline{\sigma}})^3}\rho_{\underline{\sigma},H_y^{n+1/2}(k-1/2)}\sigma\{\underline{\sigma}\}\sigma\left\{H_y^{n+1/2}(k+1/2)\right\}$$

(4.82)

Next, we determine the $Cov\left\{\varepsilon_r, H_y^{n+1/2}(k-1/2)\right\}$ term:

$$2\left[\frac{\partial}{\partial \varepsilon_r}\left\{\frac{\left(H_y^{n+1/2}(k+1/2)-H_y^{n+1/2}(k-1/2)\right)}{\Delta x\left(\frac{\varepsilon_r\varepsilon_o}{\Delta t}+\frac{\underline{\sigma}}{2}\right)}\right\}\right.\frac{\partial}{\partial H_y^{n+1/2}(k-1/2)}$$

$$\left.\left\{\frac{\left(H_y^{n+1/2}(k+1/2)-H_y^{n+1/2}(k-1/2)\right)}{\Delta x\left(\frac{\varepsilon_r\varepsilon_o}{\Delta t}+\frac{\underline{\sigma}}{2}\right)}\right\}\right|_{\mu_r,\mu_{\underline{\sigma}},\mu_H}\rho_{\varepsilon_r,H_y^{n+1/2}(k-1/2)}\sigma\{\varepsilon_r\}\sigma\left\{H_y^{n+1/2}(k-1/2)\right\}$$

$$=-\frac{16\Delta t^2\varepsilon_o\left(H_y^{n+1/2}(k-1/2)-H_y^{n+1/2}(k+1/2)\right)}{\Delta x^2(2\varepsilon_o\mu_{\varepsilon_r}+\Delta t\mu_{\underline{\sigma}})^3}\rho_{\varepsilon_r,H_y^{n+1/2}(k-1/2)}\sigma\{\varepsilon_r\}\sigma\left\{H_y^{n+1/2}(k-1/2)\right\}$$

(4.83)

The $Cov\left\{\varepsilon_r, H_y^{n+1/2}\left(k+1/2\right)\right\}$ term is:

$$2\left[\frac{\partial}{\partial\varepsilon_r}\left\{\frac{\left(H_y^{n+1/2}\left(k+1/2\right)-H_y^{n+1/2}\left(k-1/2\right)\right)}{\Delta x\left(\frac{\varepsilon_r\varepsilon_o}{\Delta t}+\frac{\underline{\underline{\sigma}}}{2}\right)}\right\}\ \frac{\partial}{\partial H_y^{n+1/2}\left(k+1/2\right)}\right.$$

$$\left.\left\{\frac{\left(H_y^{n+1/2}\left(k+1/2\right)-H_y^{n+1/2}\left(k-1/2\right)\right)}{\Delta x\left(\frac{\varepsilon_r\varepsilon_o}{\Delta t}+\frac{\underline{\underline{\sigma}}}{2}\right)}\right\}\right|_{\mu_r,\mu_{\underline{\underline{\sigma}}},\mu_H}\rho_{\varepsilon_r,H_y^{n+1/2}(k+1/2)}\sigma\left\{\varepsilon_r\right\}\sigma\left\{H_y^{n+1/2}\left(k+1/2\right)\right\}\Bigg]$$

$$=\frac{16\Delta t^2\varepsilon_o\left(H_y^{n+1/2}\left(k-1/2\right)-H_y^{n+1/2}\left(k+1/2\right)\right)}{\Delta x^2(2\varepsilon_o\mu_{\varepsilon_r}+\Delta t\mu_{\underline{\underline{\sigma}}})^3}\rho_{\varepsilon_r,H_y^{n+1/2}(k+1/2)}\sigma\left\{\varepsilon_r\right\}\sigma\left\{H_y^{n+1/2}\left(k+1/2\right)\right\}$$

(4.84)

The last covariance term is $Cov\left\{H_y^{n+1/2}\left(k+1/2\right), H_y^{n+1/2}\left(k-1/2\right)\right\}$:

$$2\left[\frac{\partial}{\partial H_y^{n+1/2}\left(k+1/2\right)}\left\{\frac{\left(H_y^{n+1/2}\left(k+1/2\right)-H_y^{n+1/2}\left(k-1/2\right)\right)}{\Delta x\left(\frac{\varepsilon_r\varepsilon_o}{\Delta t}+\frac{\underline{\underline{\sigma}}}{2}\right)}\right\}\right.$$

$$\left.\frac{\partial}{\partial H_y^{n+1/2}\left(k-1/2\right)}\left\{\frac{\left(H_y^{n+1/2}\left(k+1/2\right)-H_y^{n+1/2}\left(k-1/2\right)\right)}{\Delta x\left(\frac{\varepsilon_r\varepsilon_o}{\Delta t}+\frac{\underline{\underline{\sigma}}}{2}\right)}\right\}\right|_{\mu_r,\mu_{\underline{\underline{\sigma}}},\mu_H}.$$

$$\rho_{H_{k+1/2},H_{k-1/2}}\sigma\left\{\partial H_y^{n+1/2}\left(k+1/2\right)\right\}\sigma\left\{H_y^{n+1/2}\left(k-1/2\right)\right\}\Big]$$

$$=-\ \frac{8\Delta t^2}{\Delta x^2(2\varepsilon_o\mu_{\varepsilon_r}+\Delta t\mu_{\underline{\sigma}})^2}\rho_{H_{k+1/2},H_{k-1/2}}\sigma\left\{\partial H_y^{n+1/2}\left(k+1/2\right)\right\}\sigma\left\{H_y^{n+1/2}\left(k-1/2\right)\right\} \tag{4.85}$$

Combining all of the covariance terms (equations (4.76) through (4.85)) yields:

$$\frac{16\Delta t^2\varepsilon_o^2\left(H_y^{n+1/2}\left(k-1/2\right)-H_y^{n+1/2}\left(k+1/2\right)\right)^2}{\Delta x^2(2\varepsilon_o\mu_{\varepsilon_r}+\Delta t\mu_{\underline{\sigma}})^4}\sigma^2\left\{\varepsilon_r\right\}$$

$$+\frac{4\Delta t^2}{\Delta x^2(2\varepsilon_o\mu_{\varepsilon_r}+\Delta t\mu_{\underline{\sigma}})^2}\sigma^2\left\{H_y^{n+1/2}\left(k-1/2\right)\right\}$$

$$+\frac{4\Delta t^2}{\Delta x^2(2\varepsilon_o\mu_{\varepsilon_r}+\Delta t\mu_{\underline{\sigma}})^2}\sigma^2\left\{H_y^{n+1/2}\left(k+1/2\right)\right\}$$

$$+\frac{16\Delta t^3\varepsilon_o\left(H_y^{n+1/2}\left(k-1/2\right)-H_y^{n+1/2}\left(k+1/2\right)\right)^2}{\Delta x^2(2\varepsilon_o\mu_{\varepsilon_r}+\Delta t\mu_{\underline{\sigma}})^4}\rho_{\underline{\sigma},\varepsilon_r}\sigma\left\{\varepsilon_r\right\}\sigma\left\{\underline{\sigma}\right\}$$

$$-\frac{16\Delta t^2\varepsilon_o\left(H_y^{n+1/2}\left(k-1/2\right)-H_y^{n+1/2}\left(k+1/2\right)\right)}{\Delta x^2(2\varepsilon_o\mu_{\varepsilon_r}+\Delta t\mu_{\underline{\sigma}})^3}\rho_{\varepsilon_r,H_y^{n+1/2}(k-1/2)}\sigma\left\{\varepsilon_r\right\}\sigma\left\{H_y^{n+1/2}\left(k-1/2\right)\right\}$$

$$+\frac{16\Delta t^2\varepsilon_o\left(H_y^{n+1/2}\left(k-1/2\right)-H_y^{n+1/2}\left(k+1/2\right)\right)}{\Delta x^2(2\varepsilon_o\mu_{\varepsilon_r}+\Delta t\mu_{\underline{\sigma}})^3}\rho_{\varepsilon_r,H_y^{n+1/2}(k+1/2)}\sigma\left\{\varepsilon_r\right\}\sigma\left\{H_y^{n+1/2}\left(k+1/2\right)\right\}$$

$$-\frac{8\Delta t^3\left(H_y^{n+1/2}\left(k-1/2\right)-H_y^{n+1/2}\left(k+1/2\right)\right)}{\Delta x^2(2\varepsilon_o\mu_{\varepsilon_r}+\Delta t\mu_{\underline{\sigma}})^3}\rho_{\underline{\sigma},H_y^{n+1/2}(k-1/2)}\sigma\left\{\underline{\sigma}\right\}\sigma\left\{H_y^{n+1/2}\left(k-1/2\right)\right\}$$

$$+\frac{8\Delta t^3\left(H_y^{n+1/2}(k-1/2)-H_y^{n+1/2}(k+1/2)\right)}{\Delta x^2(2\varepsilon_o\mu_{\varepsilon_r}+\Delta t\mu_{\underline{\sigma}})^3}\rho_{\underline{\sigma},H_y^{n+1/2}(k-1/2)}\sigma\{\underline{\sigma}\}\sigma\left\{H_y^{n+1/2}(k+1/2)\right\}$$

$$-\frac{8\Delta t^2}{\Delta x^2(2\varepsilon_o\mu_{\varepsilon_r}+\Delta t\mu_{\underline{\sigma}})^2}\rho_{H_{k+1/2},H_{k-1/2}}\sigma\left\{H_y^{n+1/2}(k+1/2)\right\}\sigma\left\{H_y^{n+1/2}(k-1/2)\right\} \tag{4.86}$$

Reducing the previous equation yields the following equation in a form that will allow us to prepare it for completing the square:

$$\frac{4\Delta t^2}{\Delta x^2(2\varepsilon_o\mu_{\varepsilon_r}+\Delta t\mu_{\underline{\sigma}})^2}\cdot$$

$$\left(\begin{array}{l}\sigma^2\left\{H_y^{n+1/2}(k+1/2)\right\}-2\rho_{H_{k+1/2},H_{k-1/2}}\sigma\left\{H_y^{n+1/2}(k+1/2)\right\}\sigma\left\{H_y^{n+1/2}(k-1/2)\right\}\\ +\sigma^2\left\{H_y^{n+1/2}(k-1/2)\right\}\end{array}\right)$$

$$-\frac{2\left(H_y^{n+1/2}(k-1/2)-H_y^{n+1/2}(k+1/2)\right)}{(2\varepsilon_o\mu_{\varepsilon_r}+\Delta t\mu_{\underline{\sigma}})}\cdot$$

$$\left(\begin{array}{l}2\varepsilon_o\sigma\{\varepsilon_r\}\left(\rho_{\varepsilon_r,H_y^{n+1/2}(k-1/2)}\sigma\left\{H_y^{n+1/2}(k-1/2)\right\}-\rho_{\varepsilon_r,H_y^{n+1/2}(k+1/2)}\sigma\left\{H_y^{n+1/2}(k+1/2)\right\}\right)\\ +\Delta t\sigma\{\underline{\sigma}\}\left(\rho_{\underline{\sigma},H_y^{n+1/2}(k-1/2)}\sigma\left\{H_y^{n+1/2}(k-1/2)\right\}-\rho_{\underline{\sigma},H_y^{n+1/2}(k+1/2)}\sigma\left\{H_y^{n+1/2}(k+1/2)\right\}\right)\end{array}\right)$$

$$+\frac{\left(4\Delta t\varepsilon_o\rho_{\underline{\sigma},\varepsilon_r}\sigma\{\varepsilon_r\}\sigma\{\underline{\sigma}\}+4\varepsilon_o^2\sigma^2\{\varepsilon_r\}+\Delta t^2\sigma^2\{\underline{\sigma}\}\right)\left(H_y^{n+1/2}(k-1/2)-H_y^{n+1/2}(k+1/2)\right)^2}{\left(2\varepsilon_o\mu_{\varepsilon_r}+\Delta t\mu_{\underline{\sigma}}\right)^2}\Bigg) \tag{4.87}$$

From (4.87), there are a number of simplifying approximations that can be made. The Monte Carlo analysis (Chapter 3) was used to determine approximate values or to check approximations listed below:

1) $\rho_{H_{k+1/2},H_{k-1/2}} = 1$

2) $\rho_{\varepsilon_r,H_y^{n+1/2}(k+1/2)} \approx \rho_{\varepsilon_r,H_y^{n+1/2}(k-1/2)}$

3) $\rho_{\underline{\sigma},H_y^{n+1/2}(k+1/2)} \approx \rho_{\underline{\sigma},H_y^{n+1/2}(k-1/2)}$

Making these substitutions yields the following:

$$\frac{4\Delta t^2}{\Delta x^2(2\varepsilon_o\mu_{\varepsilon_r}+\Delta t\mu_{\underline{\sigma}})^2} \cdot$$

$$\left(\left(\sigma^2\left\{H_y^{n+1/2}(k+1/2)\right\}-2\sigma\left\{H_y^{n+1/2}(k+1/2)\right\}\sigma\left\{H_y^{n+1/2}(k-1/2)\right\}+\sigma^2\left\{H_y^{n+1/2}(k-1/2)\right\}\right)\right.$$

$$-\frac{2\left(H_y^{n+1/2}(k-1/2)-H_y^{n+1/2}(k+1/2)\right)}{(2\varepsilon_o\mu_{\varepsilon_r}+\Delta t\mu_{\underline{\sigma}})} \cdot$$

$$\left(2\varepsilon_o\sigma\{\varepsilon_r\}\rho_{\varepsilon_r,H_y^{n+1/2}}+\Delta t\sigma\{\underline{\sigma}\}\rho_{\underline{\sigma},H_y^{n+1/2}}\right)\left(\sigma\left\{H_y^{n+1/2}(k-1/2)\right\}-\sigma\left\{H_y^{n+1/2}(k+1/2)\right\}\right)$$

$$\left.+\frac{\left(4\Delta t\varepsilon_o\rho_{\underline{\sigma},\varepsilon_r}\sigma\{\varepsilon_r\}\sigma\{\underline{\sigma}\}+4\varepsilon_o^2\sigma^2\{\varepsilon_r\}+\Delta t^2\sigma^2\{\underline{\sigma}\}\right)\left(H_y^{n+1/2}(k-1/2)-H_y^{n+1/2}(k+1/2)\right)^2}{\left(2\varepsilon_o\mu_{\varepsilon_r}+\Delta t\mu_{\underline{\sigma}}\right)^2}\right) \tag{4.88}$$

We next complete the square of the first part of (4.88) to obtain:

$$\frac{4\Delta t^2}{\Delta x^2 (2\varepsilon_o \mu_{\varepsilon_r} + \Delta t \mu_{\underline{\sigma}})^2} \cdot$$

$$\left(\left(\sigma\left\{ H_y^{n+1/2}(k+1/2) \right\} - \sigma\left\{ H_y^{n+1/2}(k-1/2) \right\} \right)^2 - \frac{2\left(H_y^{n+1/2}(k-1/2) - H_y^{n+1/2}(k+1/2) \right)}{(2\varepsilon_o \mu_{\varepsilon_r} + \Delta t \mu_{\underline{\sigma}})} \right.$$

$$\left(2\varepsilon_o \sigma\{\varepsilon_r\} \rho_{\varepsilon_r, H_y^{n+1/2}} + \Delta t \sigma\{\underline{\sigma}\} \rho_{\underline{\sigma}, H_y^{n+1/2}} \right) \left(\sigma\left\{ H_y^{n+1/2}(k-1/2) \right\} - \sigma\left\{ H_y^{n+1/2}(k+1/2) \right\} \right)$$

$$\left. + \frac{\left(4\Delta t \varepsilon_o \rho_{\underline{\sigma}, \varepsilon_r} \sigma\{\varepsilon_r\} \sigma\{\underline{\sigma}\} + 4\varepsilon_o^2 \sigma^2\{\varepsilon_r\} + \Delta t^2 \sigma^2\{\underline{\sigma}\} \right) \left(H_y^{n+1/2}(k-1/2) - H_y^{n+1/2}(k+1/2) \right)^2}{\left(2\varepsilon_o \mu_{\varepsilon_r} + \Delta t \mu_{\underline{\sigma}} \right)^2} \right) \tag{4.89}$$

Completing the square of (4.89) preserves the phase of the various terms. We find the following changes to the equation to be helpful. We first notice that the variance terms $\left(\text{i.e. } \sigma\left\{ H_y^{n+1/2}(\bullet) \right\}\right)$ appear in the first term of the equation, and the field terms $\left(\text{i.e. } H_y^{n+1/2}(\bullet)\right)$ appear in the last term of the equation. The middle term contains both of these terms, keeping the proper sign convention as the terms are reordered to preserve the factors. We also have to add and subtract terms to complete the square:

$$\frac{4\Delta t^2}{\Delta x^2 (2\varepsilon_o \mu_{\varepsilon_r} + \Delta t \mu_{\underline{\sigma}})^2} \cdot$$

$$\left(\left(\sigma\left\{ H_y^{n+1/2}(k+1/2) \right\} - \sigma\left\{ H_y^{n+1/2}(k-1/2) \right\} \right)^2 - \frac{2\left(H_y^{n+1/2}(k-1/2) - H_y^{n+1/2}(k+1/2) \right)}{(2\varepsilon_o \mu_{\varepsilon_r} + \Delta t \mu_{\underline{\sigma}})} \right.$$

$$\left(2\varepsilon_o\sigma\{\varepsilon_r\}\rho_{\varepsilon_r,H_y^{n+1/2}}+\Delta t\sigma\{\underline{\sigma}\}\rho_{\underline{\sigma},H_y^{n+1/2}}\right)\left(\sigma\left\{H_y^{n+1/2}(k+1/2)\right\}-\sigma\left\{H_y^{n+1/2}(k-1/2)\right\}\right)$$

$$+\frac{\left(2\varepsilon_o\sigma\{\varepsilon_r\}\rho_{\varepsilon_r,H_y^{n+1/2}}+\Delta t\sigma\{\underline{\sigma}\}\rho_{\underline{\sigma},H_y^{n+1/2}}\right)^2\left(H_y^{n+1/2}(k-1/2)-H_y^{n+1/2}(k+1/2)\right)^2}{\left(2\varepsilon_o\mu_{\varepsilon_r}+\Delta t\mu_{\underline{\sigma}}\right)^2}$$

$$-\frac{\left(2\varepsilon_o\sigma\{\varepsilon_r\}\rho_{\varepsilon_r,H_y^{n+1/2}}+\Delta t\sigma\{\underline{\sigma}\}\rho_{\underline{\sigma},H_y^{n+1/2}}\right)^2\left(H_y^{n+1/2}(k-1/2)-H_y^{n+1/2}(k+1/2)\right)^2}{\left(2\varepsilon_o\mu_{\varepsilon_r}+\Delta t\mu_{\underline{\sigma}}\right)^2}$$

$$+\frac{\left(4\Delta t\varepsilon_o\rho_{\underline{\sigma},\varepsilon_r}\sigma\{\varepsilon_r\}\sigma\{\underline{\sigma}\}+4\varepsilon_o^2\sigma^2\{\varepsilon_r\}+\Delta t^2\sigma^2\{\underline{\sigma}\}\right)\left(H_y^{n+1/2}(k-1/2)-H_y^{n+1/2}(k+1/2)\right)^2}{\left(2\varepsilon_o\mu_{\varepsilon_r}+\Delta t\mu_{\underline{\sigma}}\right)^2}\Bigg)$$

(4.90)

We finish by completing the square and combining like terms to get the following expression:

$$\frac{4\Delta t^2}{\Delta x^2(2\varepsilon_o\mu_{\varepsilon_r}+\Delta t\mu_{\underline{\sigma}})^2}\cdot$$

$$\left(\left(\sigma\left\{H_y^{n+1/2}(k+1/2)\right\}-\sigma\left\{H_y^{n+1/2}(k-1/2)\right\}\right.\right.$$
$$\left.\left.-\frac{\left(2\varepsilon_o\sigma\{\varepsilon_r\}\rho_{\varepsilon_r,H_y^{n+1/2}}+\Delta t\sigma\{\underline{\sigma}\}\rho_{\underline{\sigma},H_y^{n+1/2}}\right)}{\left(2\varepsilon_o\mu_{\varepsilon_r}+\Delta t\mu_{\underline{\sigma}}\right)}\left(H_y^{n+1/2}(k-1/2)-H_y^{n+1/2}(k+1/2)\right)\right)^2$$

$$+\left(\begin{array}{l}4\Delta t\varepsilon_o\sigma\{\varepsilon_r\}\sigma\{\underline{\sigma}\}\left(\rho_{\underline{\sigma},\varepsilon_r}-\rho_{\varepsilon_r,H_y^{n+1/2}}\rho_{\underline{\sigma},H_y^{n+1/2}}\right)\\+4\varepsilon_o^2\sigma^2\{\varepsilon_r\}\left(1-\rho^2_{\varepsilon_r,H_y^{n+1/2}}\right)+\Delta t^2\sigma^2\{\underline{\sigma}\}\left(1-\rho^2_{\underline{\sigma},H_y^{n+1/2}}\right)\end{array}\right)\frac{\left(H_y^{n+1/2}(k-1/2)-H_y^{n+1/2}(k+1/2)\right)^2}{\left(2\varepsilon_o\mu_{\varepsilon_r}+\Delta t\mu_{\underline{\sigma}}\right)^2}\Bigg)$$

(4.91)

As was previously done, we take the square root of this equation. To make this traceable, let us split out terms so we can see what is happing. Set the term (4.92) equal to *a*:

$$\sigma\left\{H_y^{n+1/2}\left(k+1/2\right)\right\}-\sigma\left\{H_y^{n+1/2}\left(k-1/2\right)\right\}$$

$$-\frac{\left(2\varepsilon_o\sigma\left\{\varepsilon_r\right\}\rho_{\varepsilon_r,H_y^{n+1/2}}+\Delta t\sigma\left\{\underline{\sigma}\right\}\rho_{\underline{\sigma},H_y^{n+1/2}}\right)}{\left(2\varepsilon_o\mu_{\varepsilon_r}+\Delta t\mu_{\underline{\sigma}}\right)}\left(H_y^{n+1/2}\left(k-1/2\right)-H_y^{n+1/2}\left(k+1/2\right)\right) \tag{4.92}$$

Next set (4.93) equal to *b:*

$$\left(\begin{array}{l}4\Delta t\varepsilon_o\sigma\left\{\varepsilon_r\right\}\sigma\left\{\underline{\sigma}\right\}\left(\rho_{\underline{\sigma},\varepsilon_r}-\rho_{\varepsilon_r,H_y^{n+1/2}}\rho_{\underline{\sigma},H_y^{n+1/2}}\right)\\ \\ +4\varepsilon_o^2\sigma^2\left\{\varepsilon_r\right\}\left(1-\rho^2_{\varepsilon_r,H_y^{n+1/2}}\right)+\Delta t^2\sigma^2\left\{\underline{\sigma}\right\}\left(1-\rho^2_{\underline{\sigma},H_y^{n+1/2}}\right)\end{array}\right)\frac{\left(H_y^{n+1/2}\left(k-1/2\right)-H_y^{n+1/2}\left(k+1/2\right)\right)^2}{\left(2\varepsilon_o\mu_{\varepsilon_r}+\Delta t\mu_{\underline{\sigma}}\right)^2} \tag{4.93}$$

Equation (4.91) is reduced to:

$$\frac{4\Delta t^2}{\Delta x^2(2\varepsilon_o\mu_{\varepsilon_r}+\Delta t\mu_{\underline{\sigma}})^2}\left(a^2+b\right) \tag{4.94}$$

Now, taking the square root we find:

$$\frac{2\Delta t}{\Delta x(2\varepsilon_o\mu_{\varepsilon_r}+\Delta t\mu_{\underline{\sigma}})}a\sqrt{1+\frac{b}{2a^2}} \tag{4.95}$$

For $\left|b/a^2\right|<1$, $\sqrt{1\pm x}\approx 1\pm x/2$, equation (4.95) reduces to:

$$\frac{2\Delta t}{\Delta x(2\varepsilon_o\mu_{\varepsilon_r}+\Delta t\mu_{\underline{\sigma}})}\left(a+\frac{b}{2a}\right) \tag{4.96}$$

$$\frac{2\Delta t}{\Delta x(2\varepsilon_o\mu_{\varepsilon_r}+\Delta t\mu_{\underline{\sigma}})}\left(\begin{array}{l}\sigma\left\{H_y^{n+1/2}\left(k+1/2\right)\right\}-\sigma\left\{H_y^{n+1/2}\left(k-1/2\right)\right\}\\ -\ \dfrac{\left(2\varepsilon_o\sigma\{\varepsilon_r\}\rho_{\varepsilon_r,H_y^{n+1/2}}+\Delta t\sigma\{\underline{\sigma}\}\rho_{\underline{\sigma},H_y^{n+1/2}}\right)}{\left(2\varepsilon_o\mu_{\varepsilon_r}+\Delta t\mu_{\underline{\sigma}}\right)}\\ \bullet\ \left(H_y^{n+1/2}\left(k-1/2\right)-H_y^{n+1/2}\left(k+1/2\right)\right)\end{array}\right) \tag{4.97}$$

$$\frac{b}{2a}=\frac{\left\{\begin{array}{l}\left(\begin{array}{c}4\Delta t\varepsilon_o\sigma\{\varepsilon_r\}\sigma\{\underline{\sigma}\}\left(\rho_{\underline{\sigma},\varepsilon_r}-\rho_{\varepsilon_r,H_y^{n+1/2}}\rho_{\underline{\sigma},H_y^{n+1/2}}\right)+4\varepsilon_o^2\sigma^2\{\varepsilon_r\}\left(1-\rho^2_{\varepsilon_r,H_y^{n+1/2}}\right)\\ +\Delta t^2\sigma^2\{\underline{\sigma}\}\left(1-\rho^2_{\underline{\sigma},H_y^{n+1/2}}\right)\end{array}\right)\bullet\\ \dfrac{\left(H_y^{n+1/2}\left(k-1/2\right)-H_y^{n+1/2}\left(k+1/2\right)\right)^2}{\left(2\varepsilon_o\mu_{\varepsilon_r}+\Delta t\mu_{\underline{\sigma}}\right)^2}\end{array}\right\}}{2\left(\begin{array}{c}\sigma\left\{H_y^{n+1/2}\left(k+1/2\right)\right\}-\sigma\left\{H_y^{n+1/2}\left(k-1/2\right)\right\}\\ +\dfrac{\left(2\varepsilon_o\sigma\{\varepsilon_r\}\rho_{\varepsilon_r,H_y^{n+1/2}}+\Delta t\sigma\{\underline{\sigma}\}\rho_{\underline{\sigma},H_y^{n+1/2}}\right)}{\left(2\varepsilon_o\mu_{\varepsilon_r}+\Delta t\mu_{\underline{\sigma}}\right)}\left(H_y^{n+1/2}\left(k-1/2\right)-H_y^{n+1/2}\left(k+1/2\right)\right)\end{array}\right)} \tag{4.98}$$

We can call $b/2a$ the remainder term. Neglecting this remainder term, we are left with the following equation:

$$\sigma\left\{\frac{-1}{\left(\frac{\varepsilon_r\varepsilon_o}{\Delta t}+\frac{\underline{\sigma}}{2}\right)\Delta z}\left(H_y^{n+1/2}(k)-H_y^{n+1/2}(k-1)\right)\right\}\approx$$

$$\frac{2\Delta t}{\Delta x(2\varepsilon_o\mu_{\varepsilon_r}+\Delta t\mu_{\underline{\sigma}})}\left(\begin{array}{l}\sigma\left\{H_y^{n+1/2}(k+1/2)\right\}-\sigma\left\{H_y^{n+1/2}(k-1/2)\right\}\\ -\ \dfrac{\left(2\varepsilon_o\sigma\{\varepsilon_r\}\rho_{\varepsilon_r,H_y^{n+1/2}}+\Delta t\sigma\{\underline{\sigma}\}\rho_{\underline{\sigma},H_y^{n+1/2}}\right)}{\left(2\varepsilon_o\mu_{\varepsilon_r}+\Delta t\mu_{\underline{\sigma}}\right)}\\ \bullet\ \left(H_y^{n+1/2}(k-1/2)-H_y^{n+1/2}(k+1/2)\right)\end{array}\right) \tag{4.99}$$

We have derived an approximation (4.99) to the standard deviation of the H field terms which are shown in their variance form in (4.74). We next need to combine the results of the approximations in (4.47), (4.73), and (4.99), which will be done in the next section.

4.3.2.3 Combining the E field and H field terms. We now bring the results from (4.47), (4.73), and (4.99) in the previous section, combining both the E and H variance terms. Recalling (4.47), repeated here:

$$\sigma\left\{E_x^{n+1}(k)\right\} \approx \sigma\left\{\frac{\frac{\varepsilon_r\varepsilon_o}{\Delta t} - \frac{\underline{\sigma}}{2}}{\frac{\varepsilon_r\varepsilon_o}{\Delta t} + \frac{\underline{\sigma}}{2}} E_x^n(k)\right\} + \sigma\left\{\frac{-1}{\left(\frac{\varepsilon_r\varepsilon_o}{\Delta t} + \frac{\underline{\sigma}}{2}\right)\Delta z}\left(H_y^{n+1/2}(k) - H_y^{n+1/2}(k-1)\right)\right\} \quad (4.47)$$

The E field terms have been derived in Section 4.3.2.2 and is the term (4.73), repeated here:

$$\sigma\left\{\frac{\frac{\varepsilon_r\varepsilon_o}{\Delta t} - \frac{\underline{\sigma}}{2}}{\frac{\varepsilon_r\varepsilon_o}{\Delta t} + \frac{\underline{\sigma}}{2}} E_x^n(k)\right\} \approx$$

$$\frac{2\varepsilon_o\mu_{\varepsilon_r} - \Delta t\mu_{\underline{\sigma}}}{2\epsilon_o\mu_{\epsilon_r} + \Delta t\mu_{\underline{\sigma}}}\sigma\left\{E_x^n(k)\right\} + \frac{4\Delta t\varepsilon_o\left(\mu_{\underline{\sigma}}\rho_{\varepsilon_r,E}\sigma\{\varepsilon_r\} - \mu_{\varepsilon_r}\rho_{\underline{\sigma},E}\sigma\{\underline{\sigma}\}\right)}{\left(2\varepsilon_o\mu_{\varepsilon_r} + \Delta t\mu_{\underline{\sigma}}\right)^2} E_x^n(k) \quad (4.73)$$

The H field terms are given in (4.99), and are repeated here:

$$\sigma\left\{\frac{-1}{\left(\frac{\varepsilon_r\varepsilon_o}{\Delta t} + \frac{\underline{\sigma}}{2}\right)\Delta z}\left(H_y^{n+1/2}(k) - H_y^{n+1/2}(k-1)\right)\right\} \approx$$

$$\frac{2\Delta t}{\Delta x(2\varepsilon_o\mu_{\varepsilon_r} + \Delta t\mu_{\underline{\sigma}})}\left(\begin{array}{l}\sigma\left\{H_y^{n+1/2}(k+1/2)\right\} - \sigma\left\{H_y^{n+1/2}(k-1/2)\right\} \\ - \frac{\left(2\varepsilon_o\sigma\{\varepsilon_r\}\rho_{\varepsilon_r,H_y^{n+1/2}} + \Delta t\sigma\{\underline{\sigma}\}\rho_{\underline{\sigma},H_y^{n+1/2}}\right)}{\left(2\varepsilon_o\mu_{\varepsilon_r} + \Delta t\mu_{\underline{\sigma}}\right)} \\ \quad \bullet \left(H_y^{n+1/2}(k-1/2) - H_y^{n+1/2}(k+1/2)\right)\end{array}\right) \quad (4.100)$$

Substituting (4.73) and (4.100) into (4.47) yields:

$$\sigma\left\{E_x^{n+1}(k)\right\} \approx \frac{2\varepsilon_o\mu_{\varepsilon_r} - \Delta t\mu_{\underline{\sigma}}}{2\epsilon_o\mu_{\epsilon_r} + \Delta t\mu_{\underline{\sigma}}}\sigma\left\{E_x^n(k)\right\} + \frac{4\Delta t\varepsilon_o\left(\mu_{\underline{\sigma}}\rho_{\varepsilon_r,E}\sigma\{\varepsilon_r\} - \mu_{\varepsilon_r}\rho_{\underline{\sigma},E}\sigma\{\underline{\sigma}\}\right)}{\left(2\varepsilon_o\mu_{\varepsilon_r} + \Delta t\mu_{\underline{\sigma}}\right)^2}E_x^n(k)$$

$$+\frac{2\Delta t}{\Delta x(2\varepsilon_o\mu_{\varepsilon_r} + \Delta t\mu_{\underline{\sigma}})}\left(\begin{array}{l}\sigma\left\{H_y^{n+1/2}(k+1/2)\right\} - \sigma\left\{H_y^{n+1/2}(k-1/2)\right\} \\ - \dfrac{\left(2\varepsilon_o\sigma\{\varepsilon_r\}\rho_{\varepsilon_r,H_y^{n+1/2}} + \Delta t\sigma\{\underline{\sigma}\}\rho_{\underline{\sigma},H_y^{n+1/2}}\right)}{\left(2\varepsilon_o\mu_{\varepsilon_r} + \Delta t\mu_{\underline{\sigma}}\right)} \\ \bullet\ \left(H_y^{n+1/2}(k-1/2) - H_y^{n+1/2}(k+1/2)\right)\end{array}\right) \tag{4.101}$$

We can rearrange the above equation with standard deviation occurring prior to the field portions of the equation:

$$\sigma\left\{E_x^{n+1}(k)\right\} \approx \frac{2\varepsilon_o\mu_{\varepsilon_r} - \Delta t\mu_{\underline{\sigma}}}{2\epsilon_o\mu_{\epsilon_r} + \Delta t\mu_{\underline{\sigma}}}\sigma\left\{E_x^n(k)\right\} + \frac{2\Delta t}{\Delta x(2\varepsilon_o\mu_{\varepsilon_r} + \Delta t\mu_{\underline{\sigma}})}\left(\sigma\left\{H_y^{n+1/2}(k+1/2)\right\}\right.$$

$$\left.-\sigma\left\{H_y^{n+1/2}(k-1/2)\right\}\right) + \frac{4\Delta t\varepsilon_o\left(\mu_{\underline{\sigma}}\rho_{\varepsilon_r,E}\sigma\{\varepsilon_r\} - \mu_{\varepsilon_r}\rho_{\underline{\sigma},E}\sigma\{\underline{\sigma}\}\right)}{\left(2\varepsilon_o\mu_{\varepsilon_r} + \Delta t\mu_{\underline{\sigma}}\right)^2}E_x^n(k) - \frac{2\Delta t}{\Delta x(2\varepsilon_o\mu_{\varepsilon_r} + \Delta t\mu_{\underline{\sigma}})} \bullet$$

$$\left(\frac{\left(2\varepsilon_o\sigma\{\varepsilon_r\}\rho_{\varepsilon_r,H_y^{n+1/2}} + \Delta t\sigma\{\underline{\sigma}\}\rho_{\underline{\sigma},H_y^{n+1/2}}\right)}{\left(2\varepsilon_o\mu_{\varepsilon_r} + \Delta t\mu_{\underline{\sigma}}\right)}\left(H_y^{n+1/2}(k-1/2) - H_y^{n+1/2}(k+1/2)\right)\right) \tag{4.102}$$

This equation is now an approximation of the variance wave for Ampere's Law.

We notice in (4.102) that we have standard deviation terms and the fields terms of both the E and H fields.

4.4 S-FDTD Equations Summarized

The S-FDTD equations have all been derived in Chapter 4, and at this point, it would be appropriate to bring them all together in one place as a summary of the results. These equations are more of modified standard deviations rather than the variances themselves. If the standard deviations 'wave' is squared, you have the variance, which is what is evaluated and plotted in Chapter 5. The following four equations will be programmed in S-FDTD:

Faraday's mean equation (4.14):

$$\underset{\sim}{E}\left\{B_y^{n+1/2}\left(k+1/2\right)\right\}=\underset{\sim}{E}\left\{B_y^{n-1/2}\left(k+1/2\right)\right\} - \frac{\Delta t}{\Delta z}\left[\underset{\sim}{E}\left\{E_x^n\left(k+1\right)\right\}-\underset{\sim}{E}\left\{E_x^n\left(k\right)\right\}\right]$$

Faraday's variance equation (4.29):

$$\sigma\left\{H_y^{n+1/2}\left(k+1/2\right)\right\}\approx\sigma\left\{H_y^{n-1/2}\left(k+1/2\right)\right\}+\frac{\Delta t}{\mu\Delta z}\left(\sigma\left\{E_x^n\left(k+1\right)\right\}-\sigma\left\{E_x^n\left(k\right)\right\}\right)$$

Ampere's mean equation (4.35):

$$\underset{\sim}{E}\left\{E_x^{n+1}\left(k\right)\right\}=\frac{\frac{\mu_{\varepsilon_r}\varepsilon_o}{\Delta t}-\frac{\mu_{\underline{\sigma}}}{2}}{\frac{\mu_{\varepsilon_r}\varepsilon_o}{\Delta t}+\frac{\mu_{\underline{\sigma}}}{2}}\underset{\sim}{E}\left\{E_x^n\left(k\right)\right\}+\frac{\left(\underset{\sim}{E}\left\{H_y^{n+1/2}\left(k-1\right)\right\}-\underset{\sim}{E}\left\{H_y^{n+1/2}\left(k\right)\right\}\right)}{\left(\frac{\mu_{\varepsilon_r}\varepsilon_o}{\Delta t}+\frac{\mu_{\underline{\sigma}}}{2}\right)\Delta z}$$

Ampere's variance equation (4.102):

$$\sigma\left\{E_x^{n+1}(k)\right\} \approx \frac{2\varepsilon_o\mu_{\varepsilon_r} - \Delta t\mu_{\underline{\sigma}}}{2\epsilon_o\mu_{\epsilon_r} + \Delta t\mu_{\underline{\sigma}}}\sigma\left\{E_x^{n}(k)\right\}$$

$$+\frac{2\Delta t}{\Delta x(2\varepsilon_o\mu_{\varepsilon_r} + \Delta t\mu_{\underline{\sigma}})}\left(\sigma\left\{H_y^{n+1/2}(k+1/2)\right\} - \sigma\left\{H_y^{n+1/2}(k-1/2)\right\}\right)$$

$$+\frac{4\Delta t\varepsilon_o\left(\mu_{\underline{\sigma}}\rho_{\varepsilon_r,E}\sigma\{\varepsilon_r\} - \mu_{\varepsilon_r}\rho_{\underline{\sigma},E}\sigma\{\underline{\sigma}\}\right)}{\left(2\varepsilon_o\mu_{\varepsilon_r} + \Delta t\mu_{\underline{\sigma}}\right)^2}E_x^n(k) \; - \; \frac{2\Delta t}{\Delta x(2\varepsilon_o\mu_{\varepsilon_r} + \Delta t\mu_{\underline{\sigma}})} \; \cdot$$

$$\left(\frac{\left(2\varepsilon_o\sigma\{\varepsilon_r\}\rho_{\varepsilon_r,H_y^{n+1/2}} + \Delta t\sigma\{\underline{\sigma}\}\rho_{\underline{\sigma},H_y^{n+1/2}}\right)}{\left(2\varepsilon_o\mu_{\varepsilon_r} + \Delta t\mu_{\underline{\sigma}}\right)}\left(H_y^{n+1/2}(k-1/2) - H_y^{n+1/2}(k+1/2)\right)\right)$$

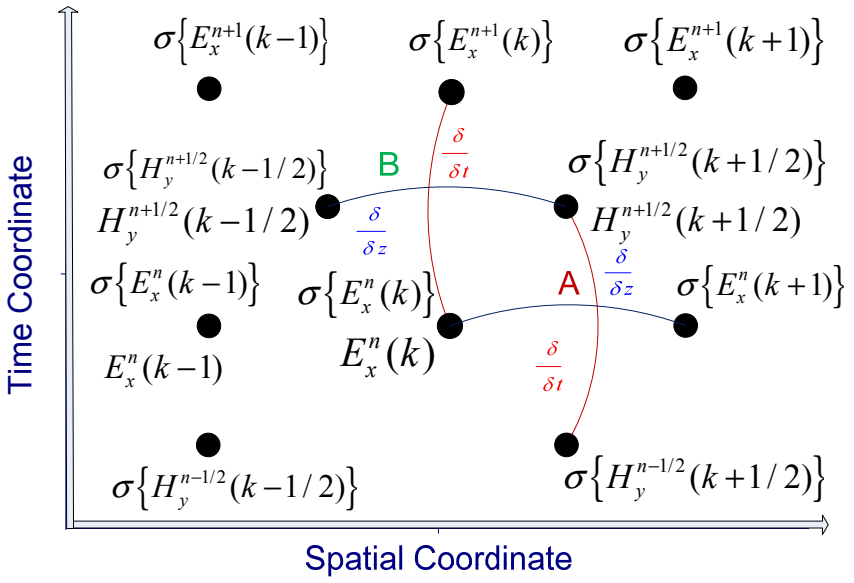

Figure 4-2 Timing and spatial diagram of 1D S-FDTD equations

The timing and the spatial coordinates are preserved as can be seen in the following diagram, Figure 4-2. Point A is time and space location of the Faraday's standard deviation equation and point B is time and space location of Ampere's standard deviation equation.

Figure 4-2 shows the time and space locations of the standard deviation variables and the field variables E and H. Lines are drawn in different colors between the difference points indicating where a central time derivative or spatial derivative was performed. This is the time and space location of the equation that uses those derivatives.

4.5 S-FDTD Algorithm Flowchart

The flow chart of S-FDTD method is shown in Figure 4-3. This is essentially the same as the traditional FDTD method with the calculation of variance immediately following its FDTD equation.

This chapter has provided the derivations of the S-FDTD equations that can be used to determine the mean of the fields (which is the same as the traditional FDTD simulation) and the variance of the fields (the stochastic addition to the code). Additional information is often required for bioelectromagnetic simulations to determine the amount of power absorbed in the model. The variation of this power is discussed in the next section. The derivation of the stochastic equation for Specific Absorption Rate (SAR) will be derived by using two different methods, verifying the derivation results.

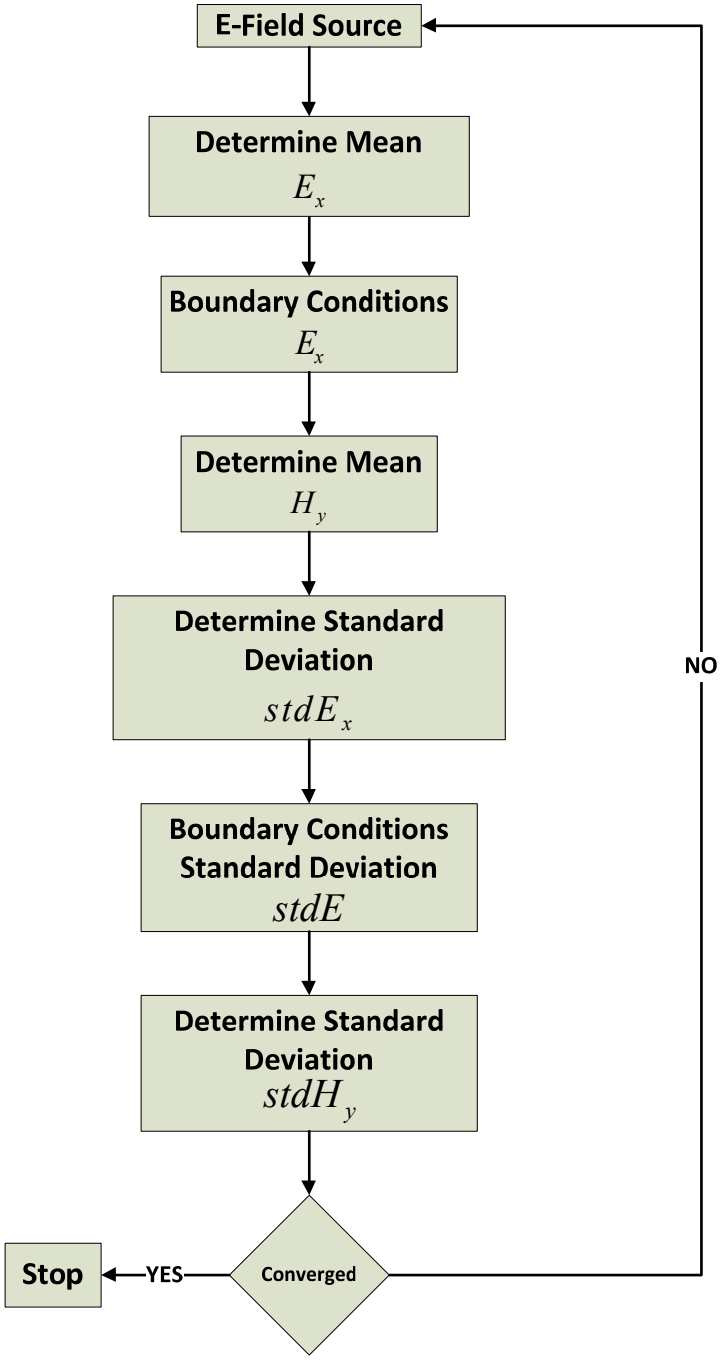

Figure 4-3 S-FDTD flow chart

4.6 Specific Absorption Rate (SAR)

The Specific Absorption Rate (SAR) is defined as [34]:

$$SAR = \frac{\underline{\sigma} E_p^{\ 2}}{2\rho_{density}} \tag{4.103}$$

and is given in W/kg. The FCC SAR guideline [1] requires that devices deposit no more than 1.6 W/kg in any 1 cm^3 of tissue. This 1-gram averaged SAR could be calculated

several ways, complicated by the fact that the peak SAR in complex models such as the head is found in highly irregular regions such as the ear, where there is no cm-cube of tissue. To calculate 1-gram SAR, we use a 1 cm^3 region, average the SAR in this region (the SAR in air is zero), and normalize by the total weight of the tissues in the region. Regions with less than 0.5 grams of tissue are ignored. We will report the localized SAR values and the peak 1-gram SAR values for a given model. The localized SAR values depend on the size of the cells used in the model, but they are instructive for observing the general patterns of the SAR in the head.

The mean values for localized SAR are calculated from (4.103) after the S-FDTD simulation is complete. The peak value of E is calculated from the time domain E fields using the 2-equations 2-unknowns [29] method. The conductivity of the tissue in that localized cell is used in (4.103) to obtain SAR.

4.6.1 Variance of SAR

The variance of the SAR can be calculated using the Delta method:

$$\sigma^2\{SAR\} = \sigma^2\left\{\frac{\underline{\sigma}E_p^{\,2}}{2\rho_{density}}\right\} \tag{4.104}$$

Constants can be brought out of the variance operator using $\sigma^2\{aX\} = a^2\,\sigma^2\{X\}$ yielding:

$$\sigma^2\{SAR\} = \frac{1}{4\rho_{density}^2}\sigma^2\left\{\underline{\sigma}E_p^{\,2}\right\} \tag{4.105}$$

The $\sigma^2\left\{\underline{\sigma}E_p^{\,2}\right\}$ portion of (4.105) is difficult to separate, but using the (4.10) Delta method, we can arrive at a good approximation. We have four terms that need to be determined, i.e. the two variance terms, the maximum field term $\sigma^2\{E_p\}$, the conductivity term $\sigma^2\{\underline{\sigma}\}$, and finally the covariance term $Cov\left\{\underline{\sigma}, E_p^{\,2}\right\}$. The complete equation is shown next:

$$\sigma^2\{SAR\} = \frac{1}{4\rho_{density}^2}\bullet$$

$$\left\{\left(\frac{\partial\left\{\underline{\sigma}E_p^2\right\}}{\partial\underline{\sigma}}\right)^2\sigma^2\{\underline{\sigma}\} + \left(\frac{\partial\left\{\underline{\sigma}E_p^2\right\}}{\partial E_p}\right)^2\sigma^2\{E_p\} + 2\left(\frac{\partial\left\{\underline{\sigma}E_p^2\right\}}{\partial E_p}\right)\left(\frac{\partial\left\{\underline{\sigma}E_p^2\right\}}{\partial\underline{\sigma}}\right)Cov\left\{\underline{\sigma}, E_p\right\}\right\}$$

The $\sigma^2\{\underline{\sigma}\}$ term:

$$\sigma^2\{\underline{\sigma}\}\left(\frac{\partial\{\underline{\sigma}E_p^2\}}{\partial\underline{\sigma}}\right)^2 = E_p^4\sigma^2\{\underline{\sigma}\} \tag{4.106}$$

The $\sigma^2\{E_p\}$ term is:

$$\sigma^2\{E_p\}\left(\frac{\partial\{\underline{\sigma}E_p^2\}}{\partial E_p}\right)^2 = 4E_p^2\underline{\sigma}^2\sigma^2\{E_p\} \tag{4.107}$$

The $Cov\{\underline{\sigma},E_p\}$ term is:

$$2Cov\{\underline{\sigma},E_p\}\left(\frac{\partial\{\underline{\sigma}E_p^2\}}{\partial E_p}\right)\left(\frac{\partial\{\underline{\sigma}E_p^2\}}{\partial\underline{\sigma}}\right) = 4Cov\{\underline{\sigma},E_p\}\underline{\sigma}E_p^3 \tag{4.108}$$

Recalling that the covariance is equal to the correlation coefficient times the standard deviations of the terms involved, we obtain:

$$Cov\{X,Y\} = \rho_{X,Y}\sigma\{X\}\sigma\{Y\}$$

Equation (4.108) can then be written as:

$$4Cov\{\underline{\sigma},E_p\}\underline{\sigma}E_p^3 = 4\underline{\sigma}E_p^3\rho_{\underline{\sigma},\mathrm{E}_p}\sigma\{\underline{\sigma}\}\sigma\{E_p\} \tag{4.109}$$

Summing equations (4.106), (4.107) and equation (4.109) and dividing by $4\rho^2$ gives the variance of the SAR:

$$\sigma^2\{SAR\} = \frac{E_p^2\left(4\underline{\sigma}E_p\rho_{\underline{\sigma},E_p}\sigma\{\underline{\sigma}\}\sigma\{E_p\} + E_p^2\sigma^2\{\underline{\sigma}\} + 4\underline{\sigma}^2\sigma^2\{E_p\}\right)}{4\rho_{density}^2} \tag{4.110}$$

In the next section, we will derive the same equation assuming all of the variables are uncorrelated normally distributed.

4.6.2 Another SAR Variance Derivation

We start off with the assumption that we have two independent random variables - the conductivity and the peak amplitude of the E field:

$$\sigma^2\{SAR\} = \sigma^2\left\{\frac{\underline{\sigma}E_p^{\ 2}}{2\rho_{density}}\right\} \tag{4.111}$$

The independence of these two variables allows certain simplifications:

$$\sigma^2\{xy\} = \underset{\sim}{E}\left\{(xy)^2\right\} - \underset{\sim}{E}\{xy\}^2 \tag{4.112}$$

With independence between x and y, the various parts can be separated [22]:

$$\underset{\sim}{E}\left\{x^2y^2\right\} = \underset{\sim}{E}\left\{x^2\right\}\underset{\sim}{E}\left\{y^2\right\}$$

$$\underset{\sim}{E}\{xy\} = \underset{\sim}{E}\{x\}\,\underset{\sim}{E}\{y\} \tag{4.113}$$

Substituting these equations into (4.112) yields:

$$\sigma^2\{xy\} = \underset{\sim}{E}\left\{x^2\right\}\underset{\sim}{E}\left\{y^2\right\} - \underset{\sim}{E}\{x\}^2\,\underset{\sim}{E}\{y\}^2 \tag{4.114}$$

Remembering that $\sigma^2\{x\} = \underset{\sim}{E}\left\{x^2\right\} - \underset{\sim}{E}\{x\}^2$, (4.114) can be manipulated to show that $\underset{\sim}{E}\left\{x^2\right\} = \sigma^2\{x\} + \underset{\sim}{E}\{x\}^2$. This result is substituted in (4.114) with the result:

$$\sigma^2\{xy\} = \left(\sigma^2\{x\} + \underset{\sim}{E}\{x\}^2\right)\left(\sigma^2\{y\} + \underset{\sim}{E}\{y\}^2\right) - \underset{\sim}{E}\{x\}^2\,\underset{\sim}{E}\{y\}^2 \tag{4.115}$$

Expanding the terms and simplifying yields:

$$\sigma^2\{xy\} = \underset{\sim}{E}\{x\}^2\,\underset{\sim}{E}\{y\}^2 + \underset{\sim}{E}\{y\}^2\,\sigma^2\{x\} + \underset{\sim}{E}\{x\}^2\,\sigma^2\{y\} + \sigma^2\{x\}\sigma^2\{y\} - \underset{\sim}{E}\{x\}^2\,\underset{\sim}{E}\{y\}^2$$

Subtracting like terms yields:

$$\sigma^2\{xy\} = \underset{\sim}{E}\{y\}^2\,\sigma^2\{x\} + \underset{\sim}{E}\{x\}^2\,\sigma^2\{y\} + \sigma^2\{x\}\sigma^2\{y\} \tag{4.116}$$

We have the following equation:

$$\sigma^2\{SAR\} = \sigma^2\left\{\frac{\underline{\sigma}E_p^{\,2}}{2\rho_{density}}\right\}$$

$$\sigma^2\{SAR\} = \frac{1}{4\rho_{density}^2}\sigma^2\left\{\underline{\sigma}E_p^{\,2}\right\} \tag{4.117}$$

Using (4.116) with (4.117) yields:

$$\frac{1}{4\rho_{density}^2}\sigma^2\left\{\underline{\sigma}E_p^{\,2}\right\} =$$

$$\frac{1}{4\rho_{density}^2}\left(\underset{\sim}{E}\left\{E_p^{\,2}\right\}^2\sigma^2\{\underline{\sigma}\} + \underset{\sim}{E}\{\underline{\sigma}\}^2\sigma^2\left\{E_p^{\,2}\right\} + \sigma^2\{\underline{\sigma}\}\sigma^2\left\{E_p^{\,2}\right\}\right) \tag{4.118}$$

Equation (4.118) has a number of terms that can be determined if we assume a normal distribution for both random variables.

The normal distribution is:

$$f(x) = \frac{1}{\sigma\sqrt{2\pi}}Exp\left(-\frac{(x-\mu)^2}{2\sigma^2}\right) \tag{4.119}$$

Using the probability distribution, we can determine $\underset{\sim}{E}\{x^2\}$ and $\sigma^2\{x^2\}$ and use the resulting equations to simplify (4.118). Solving for $\underset{\sim}{E}\{x^2\}$ using (4.119) yields:

$$\underset{\sim}{E}\{x^2\} = \underset{\sim}{E}\{x\}^2 + \sigma^2\{x\} \tag{4.120}$$

and the $\sigma^2\{x^2\}$ is:

$$\sigma^2\{x^2\} = 2\left(2\underset{\sim}{E}\{x\}^2\sigma^2\{x\} + \sigma^4\{x\}\right) \tag{4.121}$$

Substituting (4.120) and (4.121) into (4.118) yields:

$$\frac{1}{4\rho_{density}^2}\sigma^2\left\{\underline{\sigma}E_p{}^2\right\} =$$

$$\frac{\mu_{E_p}^4\sigma^2\{\underline{\sigma}\} + 4\mu_{\underline{\sigma}}^2\mu_{E_p}^2\sigma^2\{E_p\} + 6\mu_{E_p}^2\sigma^2\{\hat{\sigma}\}\sigma^2\{E_p\}}{4\rho_{density}^2} \tag{4.122}$$

Looking at (4.122), the term $6\mu_{E_p}^2\sigma^2\{\hat{\sigma}\}\sigma^2\{E_p\}$ approaches zero, yielding a final approximation:

$$\frac{1}{4\rho_{density}^2}\sigma^2\left\{\underline{\sigma}E_p{}^2\right\} \approx \frac{E_p^4\sigma^2\{\underline{\sigma}\} + 4\underline{\sigma}^2E_p^2\sigma^2\{E_p\}}{4\rho_{density}^2} \tag{4.123}$$

Comparing this expression with (4.110):

$$\sigma^2\{SAR\} = \frac{E_p^2\left(4\underline{\sigma}E_p\rho_{\underline{\sigma},E_p}\sigma\{\underline{\sigma}\}\sigma\{E_p\} + E_p^2\sigma^2\{\underline{\sigma}\} + 4\underline{\sigma}^2\sigma^2\{E_p\}\right)}{4\rho_{density}^2}$$

And setting the correlation coefficient to zero yields:

$$\sigma^2\{SAR\} = \frac{E_p^2\left(E_p^2\sigma^2\{\underline{\sigma}\} + 4\underline{\sigma}^2\sigma^2\{E_p\}\right)}{4\rho_{density}^2} = \frac{E_p^4\sigma^2\{\underline{\sigma}\} + 4\underline{\sigma}^2E_p^2\sigma^2\{E_p\}}{4\rho_{density}^2} \tag{4.124}$$

Equation (4.123) is equivalent to equation (4.124) if we assume that the variables are independent, showing that the Delta method has produced a reasonable approximation to the variance of the Specific Absorption Rate (SAR).

In Chapter 5, we will use the material from Chapter 3 in which the biological material properties were used in Monte Carlo simulations (1D), producing data for a stochastic analysis of the variable material properties. This information will be used to determine the effectiveness of the S-FDTD analysis.

CHAPTER 5

VALIDATION OF THE S-FDTD METHOD

In this dissertation, we have been discussing what we call the Stochastic FDTD (S-FDTD) method. This method computes the mean of the field equations in the same way as the traditional FDTD analysis (using the mean material properties). This was derived in Chapter 4 using a first order approximation to the Taylor's series for the mean values. The variance of the fields is calculated along with the mean values. It appears as a wave that follows the field values. This allows the stochastic analysis to proceed at the same time the normal FDTD analysis is being performed with only a slight increase in computational time over a simulation that does not compute the variance.

Currently, Monte Carlo analysis is the method of choice for statistical FDTD analysis. Monte Carlo analysis or M-FDTD (Section 2.4.1) requires the input of randomly generated stochastic variables at the start of each simulation, repeating these simulations many times with many different values for the variables, collecting all the data from each simulation, and performing statistical analysis on those data. Monte Carlo analysis requires significant resources in both computational time and memory and is rarely used in practice. Instead, the FDTD analysis is usually just made with the average material properties, and the variance is ignored.

Stochastic FDTD analysis requires the normal memory storage for each of the

fields. This is over written at each time step. The variance wave is also stored as a function of time for the electric and magnetic fields. This is also over written at each time step. So the storing of a vector represents each wave. A total of four vectors are now needed for a 1D analysis, rather than the two originally required for FDTD. Monte Carlo analysis stores each test in its thousands of runs, and its memory requirement can soar.

In this chapter, we will compare the results of Monte Carlo analysis with the results of S-FDTD analysis. We will compare data from both methods using 1D FDTD analysis of a model with skin, muscle, and fat layers. We will then provide some indication of possible future work, particularly methods for improving the approximations of the correlation coefficients in a more advanced way than described in this initial model.

For validation, we will use single- and three-layer 1D models. Monte Carlo analyses have been performed on these models to obtain the mean and standard deviation of the fields as a function of time and location in the model. These values have also been calculated with the S–FDTD analyses. These values will be compared. The Monte Carlo (M-FDTD) is assumed to be the 'gold standard' so will be assumed to be the accurate value to which the more approximate S-FDTD method is compared.

5.1 Single-layer Validation

Normally, when a traditional FDTD simulation is run, the mean values of σ (conductivity) and ε_r (permittivity) are used, and it is assumed that this will give accurate values for the mean fields. This was tested against a Monte Carlo analysis run

of 10,000 tests using a single-layer (skin, assumed to be infinitely thick) 1D model. The following table first appears in Section 3.1 and is repeated here for reference.

A single-layer analysis was performed with the model space shown in Figure 5-1. The analysis took about 2.8 hours to run 10,000 tests for each of two frequencies (915MHz and 2GHz) on an Intel(R) Core(TM)2 CPU 6400 @ 2.13GHz, 2.00GB RAM desktop computer. Dielectric layers are defined using the properties found in Table 5-1. The thicknesses were held constant, and the electrical parameters of the biological materials were chosen as independent Gaussian variables, although in practice, they may be correlated. For the Monte Carlo simulation, these material properties were selected randomly at the start of each run of the FDTD simulation. The S-FDTD analysis takes twice the time of a single FDTD.

5.1.1 Stochastic Analysis

5.1.1.1 Evaluation of mean values. In Figure 5-2, we have plotted the peak E field magnitude at each spatial step dx for the whole model space. The peak value is different from the time domain value that is originally calculated in FDTD and is shown in other plots. The peak value is determined from the time domain value using the 2 equations 2 unknowns method [29] of an assumed sinusoidal waveform. This process allows us to solve for the peak value of the wave given two closely spaced time samples of the E field as inputs. This process removes all phase information from the data and returns the peak of the wave only.

To obtain the mean from a Monte Carlo analysis, we average the total number of the stored waves. This M-FDTD mean is compared to the mean found from the S-FDTD in Figure 5-2 . The two plots are indistinguishable. There is less than 0.1% difference

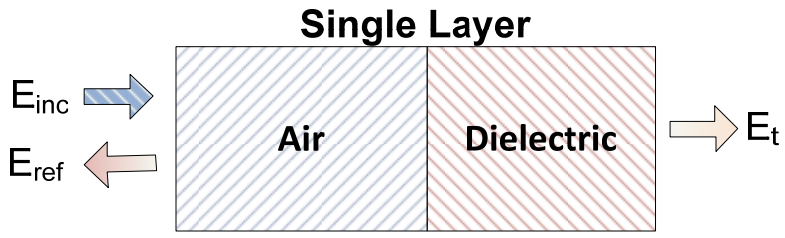

Figure 5-1 Single-layer model used for Monte Carlo analysis. Absorbing boundaries on either side effectively simulate an infinitely thick dielectric layer.

Table 5-1 Nominal dielectric constants and conductivities for human tissue [8]

Dielectric	ε_r Mean	ε_r [SD]	$\underline{\sigma}$ Mean (S/m)	$\underline{\sigma}$ [SD]	Thickness (mm) d_i
Muscle	55.0	4.6	0.87	0.10	42
Fat (infiltrated)	16.2	2.7	0.214	0.06	54
Skin	39.0	3.4	0.43	0.10	5.4

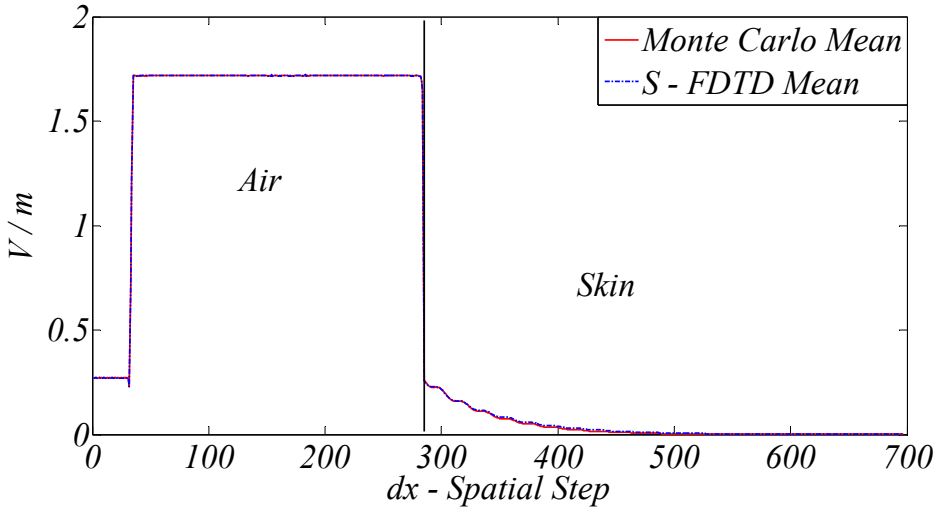

Figure 5-2 915 MHz E field mean comparison for the single-layer model: S-FDTD vs. M-FDTD

between the two means.

At the higher frequency of 2 GHz, we see slightly more discrepancy in the two methods of analysis, as shown in Figure 5-3 (a plot of the peak magnitude of the mean of the M-FDTD and that from the S-FDTD analyses). The M-FDTD shows slightly lower mean values (0.016 V/m) as the E field propagates within the dielectric material than that in the S-FDTD simulation (0.048V/m). The correlation coefficients used in the S-FDTD simulation are all equal to one. We would expect the S-FDTD results to encompass the Monte Carlo results, which they do.

5.1.1.2 Evaluation of variance. The variance of the fields is also calculated using both the S-FDTD and M-FDTD methods and compared in this section. Just as the waves propagate through the model space, the 'variance wave' also propagates through the material. The propagation of this 'wave' is seen in Figure 5-4, which shows the variance at four different times, 25 time steps apart. The wave-like structure of the variance is readily seen in Figure 5-4.

The variance of the fields at 915MHz is plotted in Figure 5-5, again comparing the M-FDTD variance with the S-FDTD variance. A wave-like appearance is shown due to the diagram being a snapshot in time at the conclusion of the $10{,}000^{th}$ time step. The figure shows good agreement with the S-FDTD method given that the correlation coefficients are set equal to one. As expected, the S-FDTD curve (dashed line) bounds the M-FDTD curve (solid line).

Figure 5-6 shows the comparison at 2 GHz of the variance determined by M-FDTD and S-FDTD analysis. This figure shows a snapshot in time at the $10{,}000^{th}$ time step. Again the S-FDTD analysis, with the correlation coefficients set equal to one,

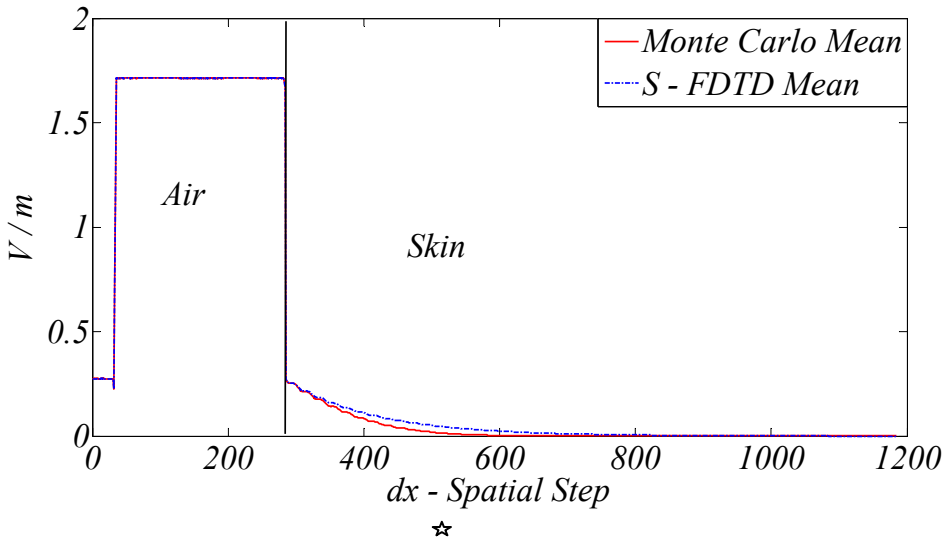

Figure 5-3 2GHz E field mean comparison for the single layer model: S-FDTD vs. Monte Carlo analysis

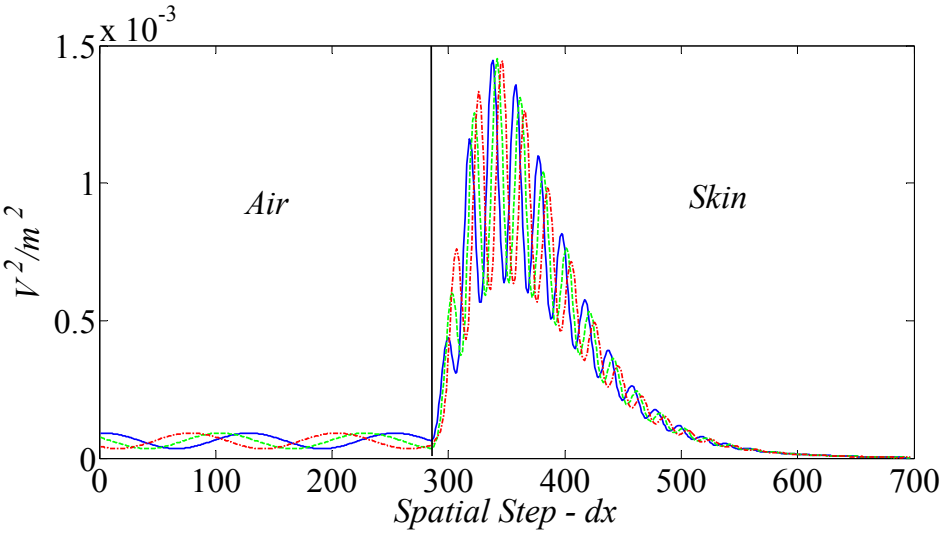

Figure 5-4 Monte Carlo simulation - propagation of the variance wave at 915MHz

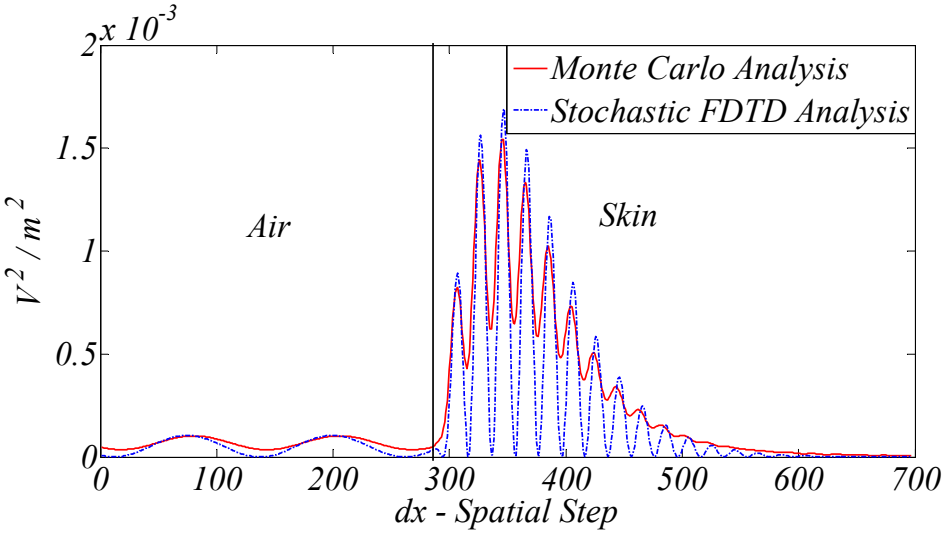

Figure 5-5 915MHz variance of E field: S-FDTD vs. M-FDTD

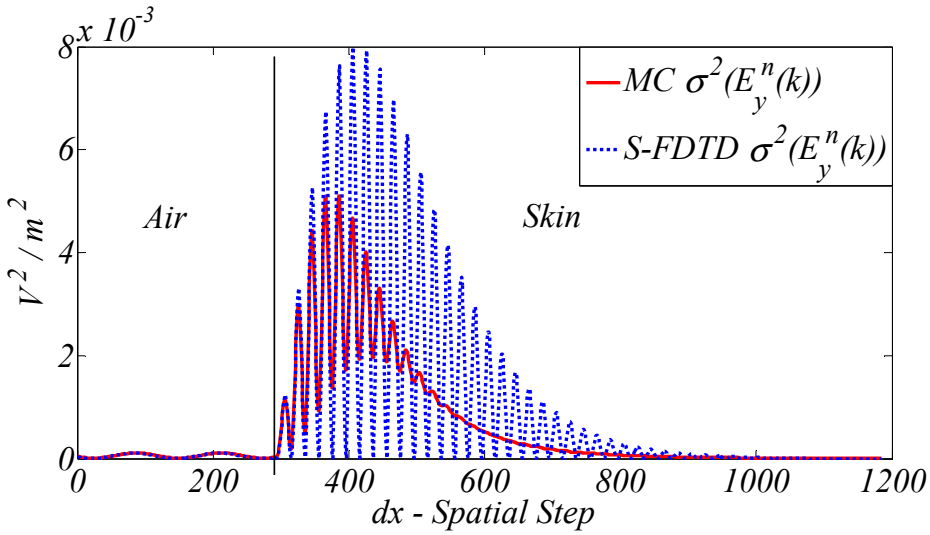

Figure 5-6 2 GHz variance of E field: S-FDTD vs. Monte Carlo analysis

bounds the Monte Carlo variance. The difference in magnitude of the two is $\sim 3x10^{-3}\, V^2/m^2$. The S-FDTD variances are 1.6 times greater than those calculated with the M-FDTD method. The attenuation is also slower as the variance propagates into the model. The comparisons at both 915MHz and 2GHz show that the S-FDTD (with correlation coefficients =1) gives a good approximation to those obtained using the M-FDTD method, and that the S-FDTD method bounds the M-FDTD values.

The length of time to perform the stochastic FDTD simulation was less than a minute, and that of the Monte Carlo simulation was over two hours on the Intel(R) Core(TM)2 CPU 6400 @ 2.13GHz 2.13 GHz, 2.00GB of RAM computer.

5.2 Three-layer Validation

We continue with our comparison of the M-FDTD analysis and the S-FDTD analysis with a three-layer model space at 915 MHz and 2 GHz. This model space is composed of three finite-thickness dielectric layers preceded and followed by air, as shown in Figure 5-7. This model will have multiple reflections within each dielectric layer. Initially, the model space is defined to be normal human tissue, i.e. 1= skin, 2=fat, and 3=muscle, with the thicknesses of each layer set at the nominal thickness. Later models in this section will mix up the ordering of these tissues to explore the impact of the configuration of the model.

The Monte Carlo analyses took more than 4 hours to run 10,000 simulations on an AMDTurion™64 x2 1.90GHz 4.00GB RAM HP Laptop. The S-FDTD took less than one minute.

As with the one-layer model, dielectric layers are defined using the properties

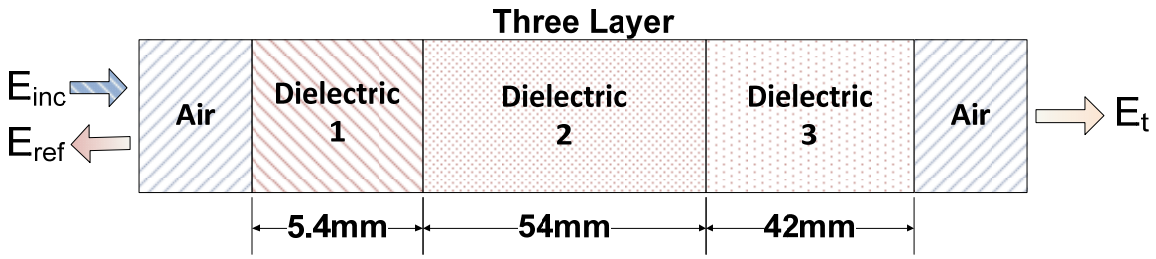

Figure 5-7 Three-layer structure used for S-FDTD and M-FDTD analysis

found in Table 3-1. The thicknesses were held constant, and the electrical parameters of the biological materials were chosen as independent Gaussian variables. For the Monte Carlo simulation, these material properties were selected randomly at the start of each run of the FDTD simulation.

These Gaussian variables were independently selected layer by layer, i.e. the conductance σ and the relative dielectric constant ε_r were assumed to be independent, although in practice, they may be correlated.

5.2.1 Stochastic Analysis

5.2.1.1 Mean at 915MHz. In Figure 5-8, we have plotted the peak amplitude for the average E field, discarding the phase information in the time domain at the 10,000th time step. The two different types of analyses show approximately the same mean for the model space previously defined, i.e. skin, fat, and muscle.

The comparison of the means shows close agreement between the two methods of analysis at 915MHz. From Figure 5-8, we see that the maximum deviation of the S-FDTD from the M-FDTD plots occurs at the interface between dielectric layers 2 and 3. The S-FDTD analysis shows the E field peak magnitude close to the interface to be approximately equal to 0.249V/m, and the M-FDTD analysis shows it to be approximately equal to 0.241V/m, about a 3.3% error between the two. The rest of the

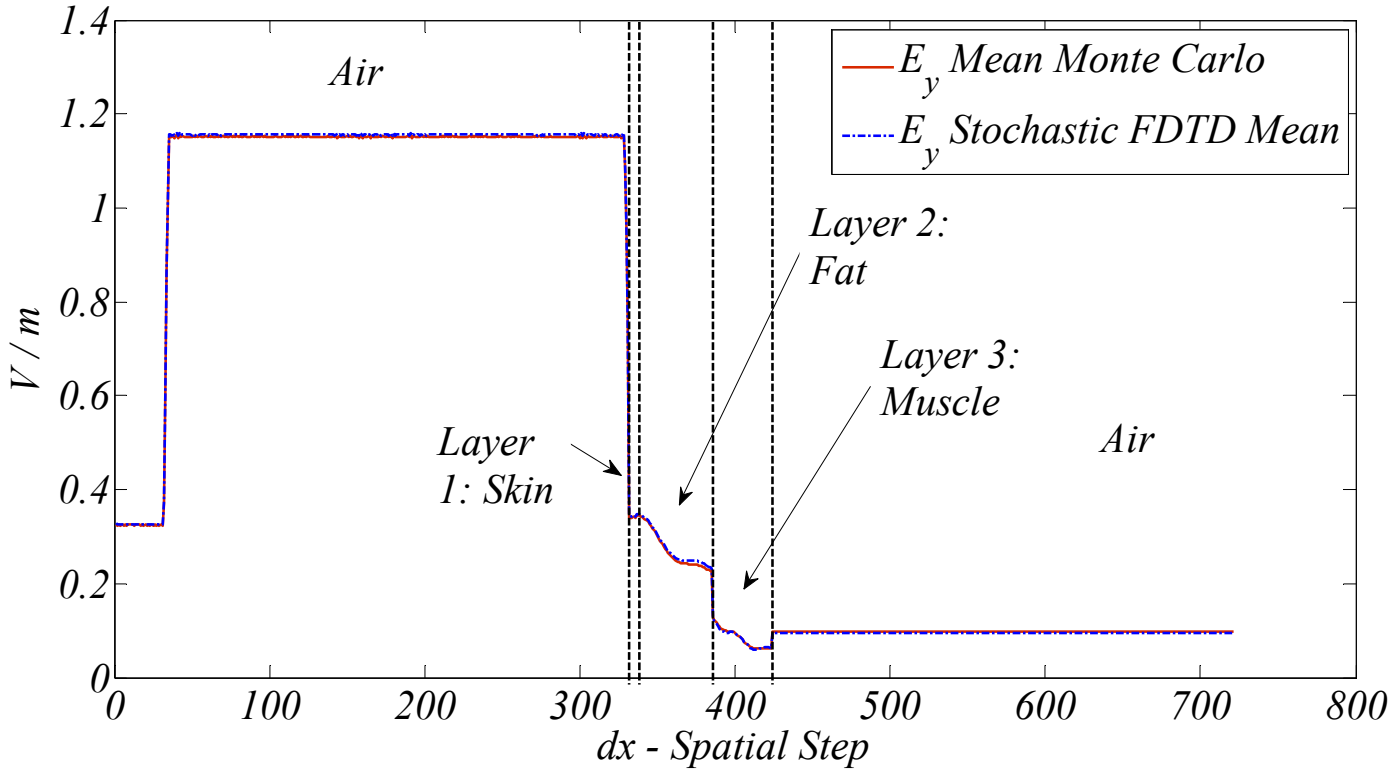

Figure 5-8 915 MHz (three-layer) E field mean comparison:
S-FDTD vs. M-FDTD analysis

plot comparison shows close agreement. Even at the boundaries between dielectrics, we have close agreement.

5.2.1.2 Variance at 915MHz. Figure 5-9 shows a time domain plot of the variance comparison between S-FDTD and M-FDTD analyses. This snapshot was at the termination of the 10,000th time step for each analysis. In Figure 5-9, in keeping with what was previously demonstrated, the correlation coefficients used in the S-FDTD simulation have been kept equal to 1.0. We see some variation in the variance as it goes across boundaries. The maximum difference between the plots is on the order of a factor of three. The accuracy of this approximation depends on the accuracy of the correlation coefficients. The value of 1.0 maximizes the variance approximation.

Continuing with the comparison of the two analysis methods, we repeat the above analysis at 2GHz. It is at this frequency that we see the greatest differences in both the mean and the variance.

5.2.1.3 Mean at 2GHz. Figure 5-10 shows the mean value of the electric fields for the three-layer region in Figure 5-7 at 2GHz calculated using the S-FDTD and M_FDTD methods. The largest difference occurs in layer two at the interface between layers two and three. The M-FDTD E field is approximately 0.14V/m and that of the S-FDTD is 0.17V/m, a difference of approximately 21%.

5.2.1.4 Variance at 2GHz. Figure 5-11 shows a snapshot at the 10,000th time step of the variance of the electric field. The variance wave proceeds through the three layers and closely follows the phase of the M-FDTD analysis. Again, using a correlation coefficient of 1.0 maximizes the approximation for the variance, thus bounding the M-FDTD variance. The S-FDTD variance is within a factor of 3.0 of the M-FDTD

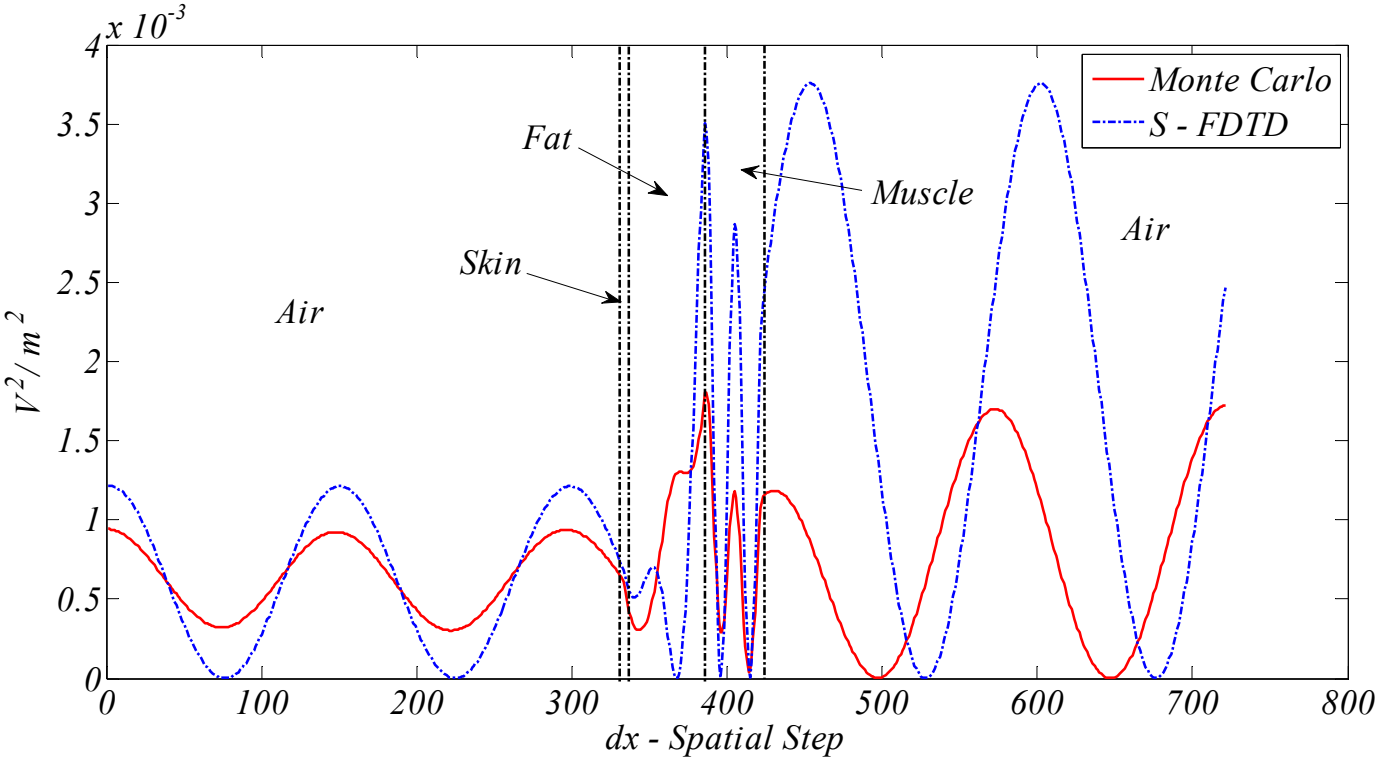

Figure 5-9 Three-layer 915 MHz E field variance comparison:
(Skin, Fat, Muscle) S-FDTD vs. Monte Carlo analysis for the fields at the 10,000th time step.

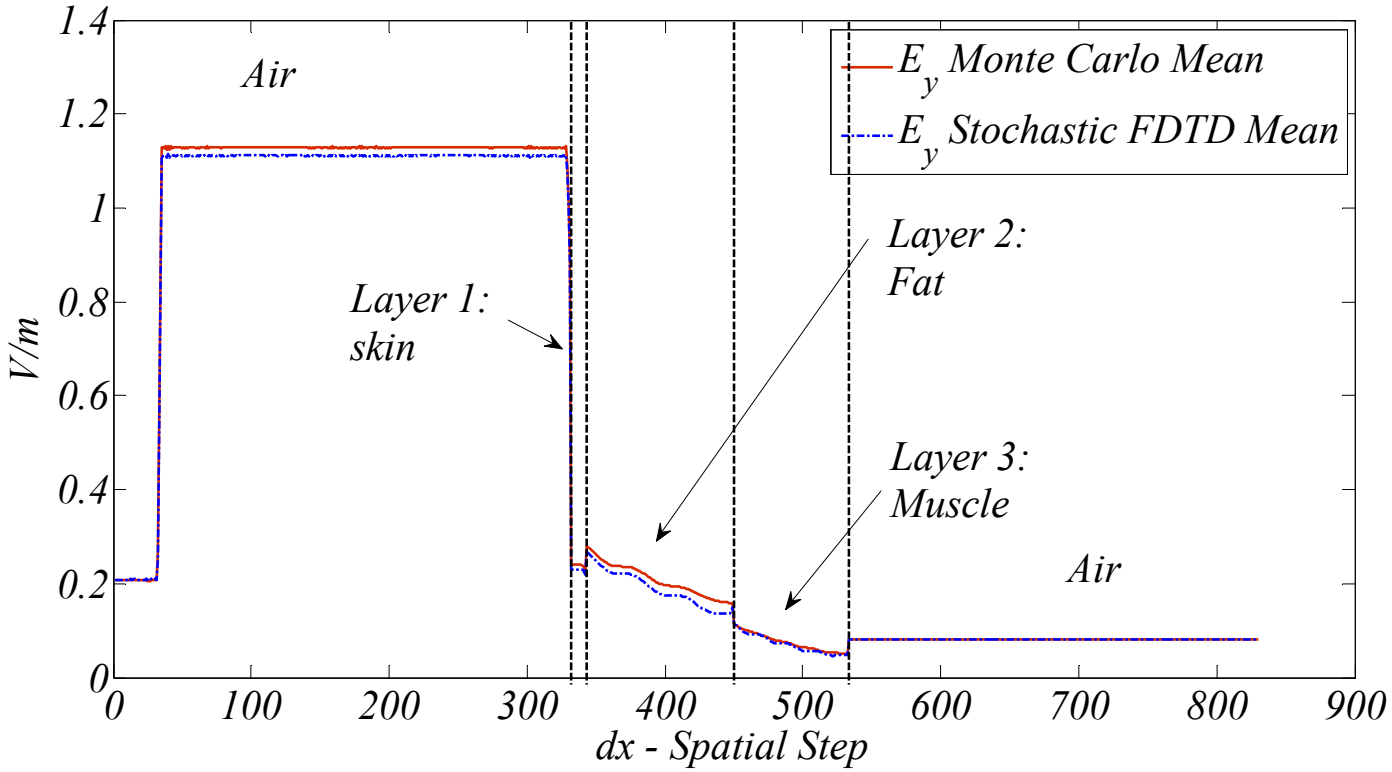

Figure 5-10 2GHz E field mean comparison: S-FDTD vs. Monte Carlo analysis for three-layer model at 2 GHz

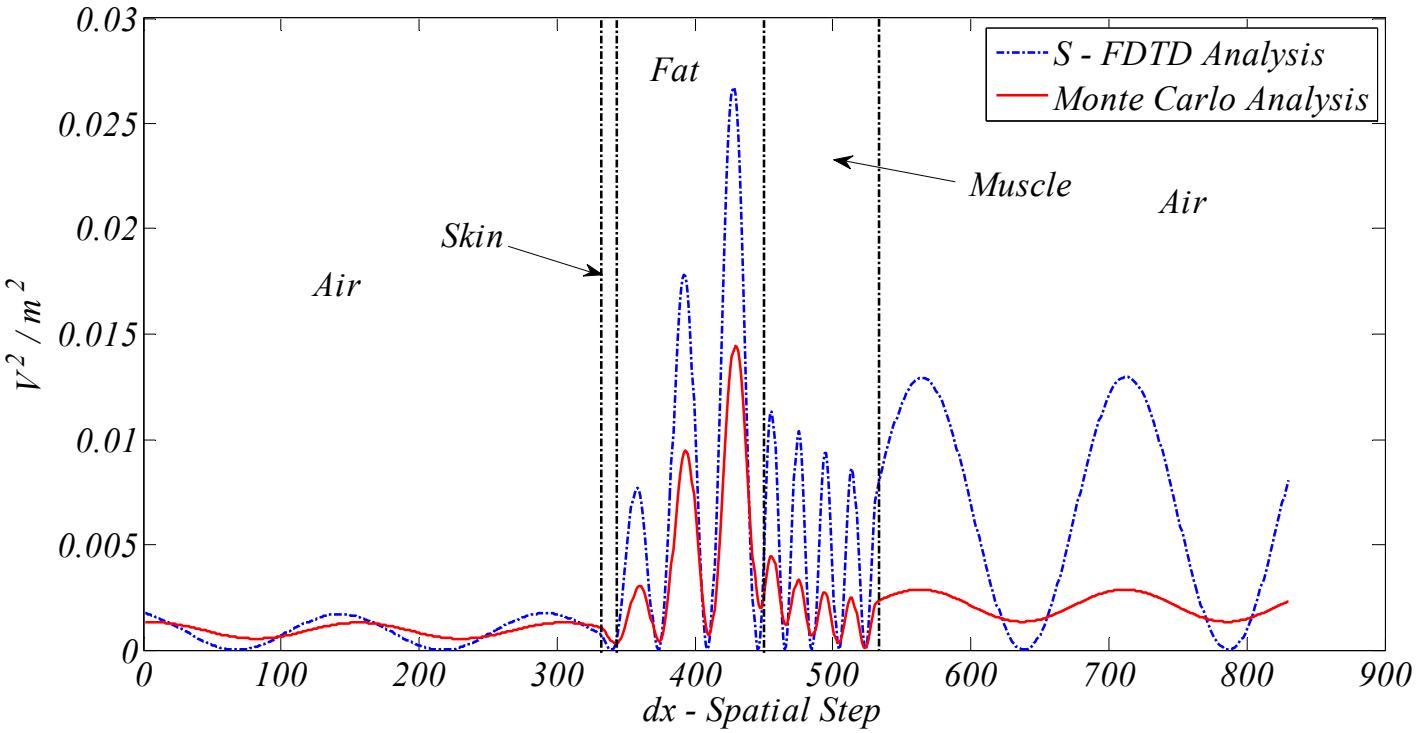

Figure 5-11 Three-layer 2 GHz E field variance comparison:
(Skin, Fat, Muscle) S-FDTD vs. Monte Carlo analysis at the 10,000th time step

variance. Further improvements to the accuracy of the correlation coefficients can bring the approximation closer.

5.2.2 Impact of Model Configuration.

The previous sections examined the effect of tissue variance on the mean and variance of the electric field. The S-FDTD method and M-FDTD methods provided excellent approximations for the mean of the field and were within a factor of 3 for its instantaneous variance. The S-FDTD method overestimates the variance because of the use of 1.0 for the correlation coefficient. In this section, we examine the effect of changing the physical configuration of the model – first by making the layers thicker and then by rearranging them. Three different models were evaluated (fat-skin-muscle, muscle-skin-fat, and muscle-fat-skin). The thickness of each tissue was the same as in the previous 3-layer model, so only the order of the layers was changed. All simulations were performed at 2 GHz.

Figure 5-12 shows three plots comparing the peak magnitude of M-FDTD and S-FDTD analyses. It can be seen that order does affect the error of the approximation of the S-FDTD analysis. The largest error is for the first model, but the calculation of the mean electric field is very good for all models.

5.2.2.1 Variance For the variance portion of the S-FDTD analysis, the correlation coefficients ρ were set equal to 1.0 as before (S-FDTD_1). An additional analysis was performed setting the correlation coefficients ρ equal to the static reflection ($\Gamma = (\eta_{n+1} - \eta_n)/(\eta_{n+1} + \eta_n)$) coefficients (S-FDTD_G) at the dielectric interfaces with this coefficient used throughout the succeeding dielectric layer. This was done to see how the change in the correlation coefficients ρ changed the approximation of the S-

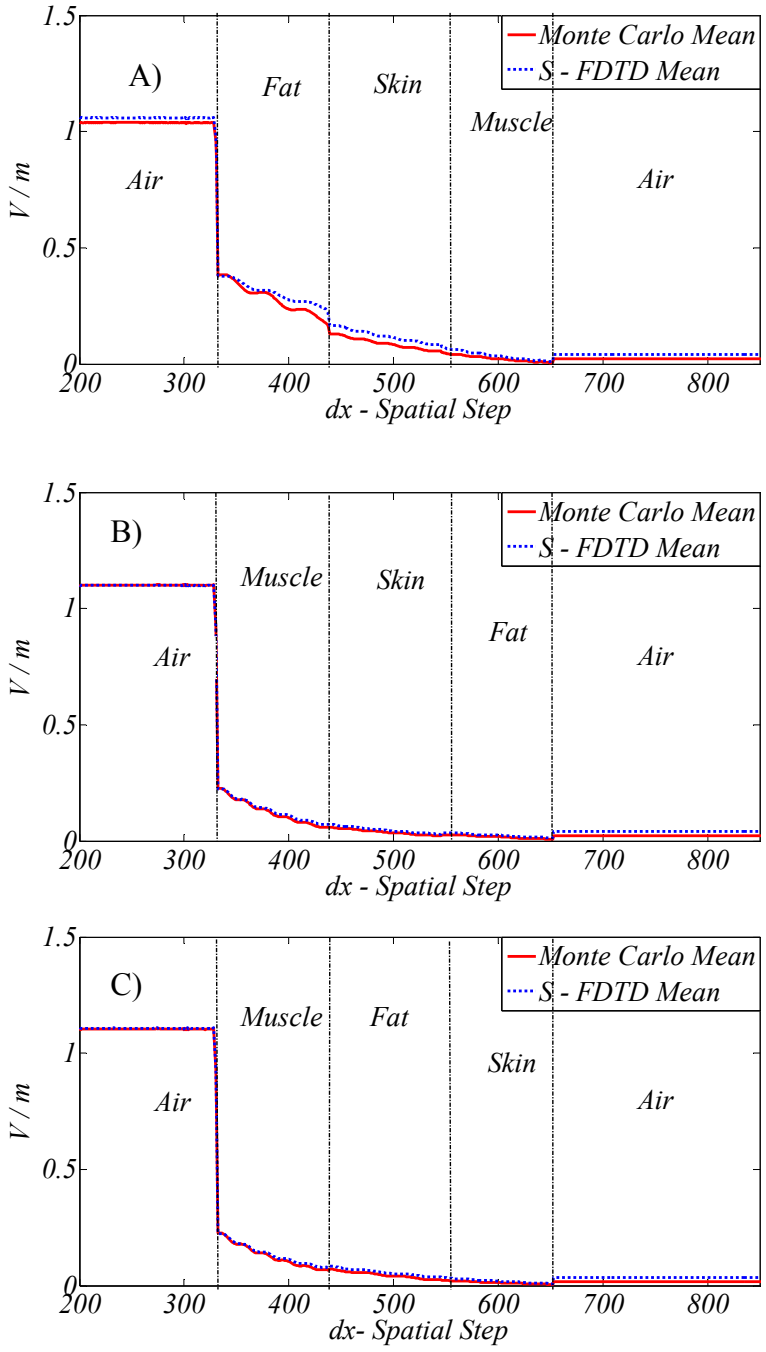

Figure 5-12 Three-layer 2 GHz E field mean comparison: S-FDTD vs. Monte Carlo analysis

FDTD variance.

Referring to Figure 5-13, it is seen that the S-FDTD_1 bounds the other two plots as expected. The S-FDTD_G plot is the smallest in magnitude, so using the reflection coefficients appears to be a better estimate (underestimate) of the variance. In the following plots, it appears that the S-FDTD_G analysis is closest to the M-FDTD analysis, thus indicating that using the reflection coefficients from an initial analysis of the model space yields better approximations to the correlation coefficients than leaving them equal to one, which acts as an upper bound. The S-FDTD_G method may underestimate the variance in some models. This also shows that additional work may be justified in finding methods to improve the approximation of the correlation coefficients. The impact of the order of the layers was considered. These models are not meant to be physical (i.e. skin is never inside of fat or muscle!), but are simply used to evaluate the effect of the configuration of the model. Figure 5-12 and Figure 5-13 shows that the changing of the order of the dielectric layers impacts the mean as well as the variance of the fields.

5.3 SAR Variance Validation

The validation of the variance of the SAR will be dealt with in this section, any discrepancies will be pointed out, and explanations proffered. These explanations may offer possible starting points for future work to be performed.

Figure 5-14 shows a comparison of S-FDTD analyses with various approximations to the correlation coefficient, compared to the Monte Carlo M-FDTD analysis. With the correlation coefficient set equal to 0.5, we see a closer agreement of the S-FDTD analysis with that of the Monte Carlo analysis. These various analyses will

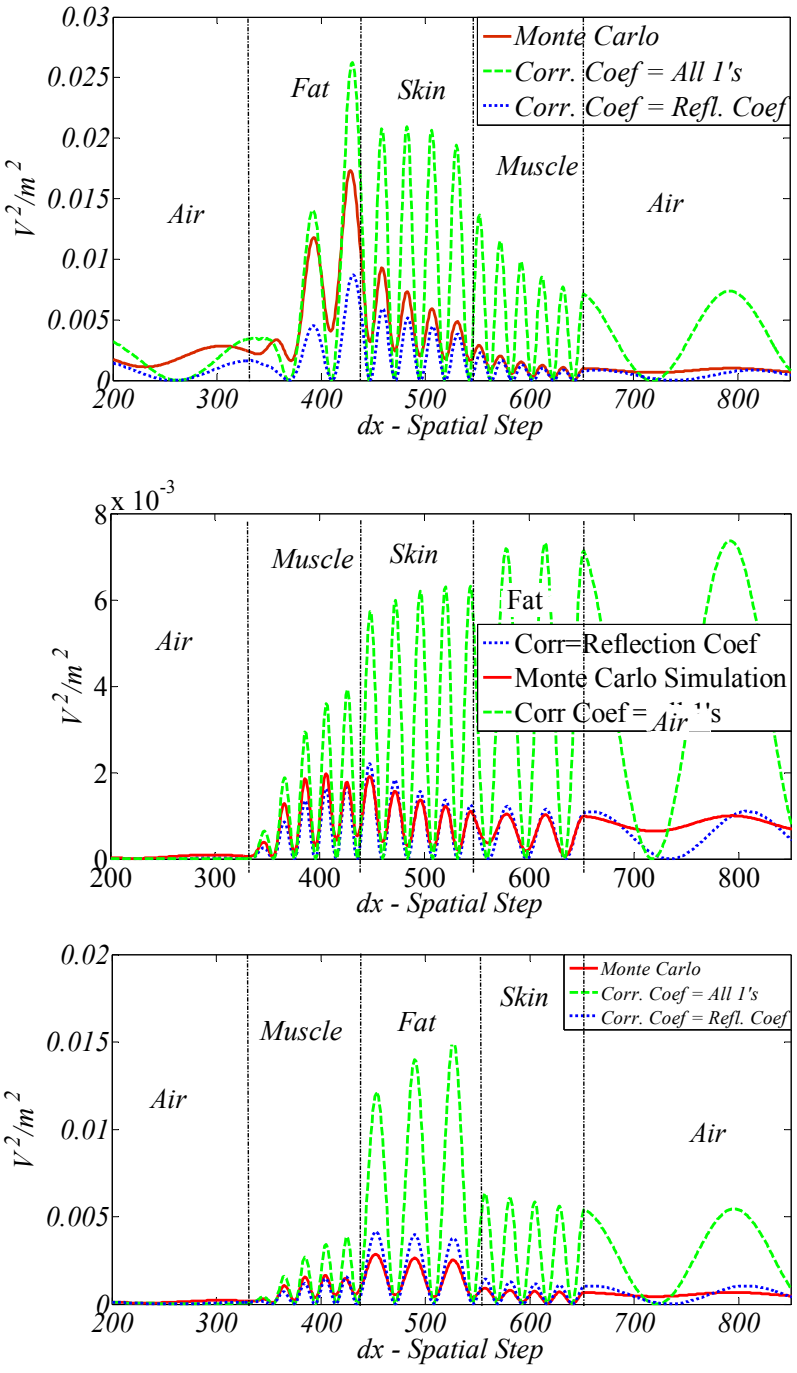

Figure 5-13 Three-layer 2GHz E field variance comparison:
S-FDTD vs. Monte Carlo analysis. Time samples taken at the 10,000th time step.

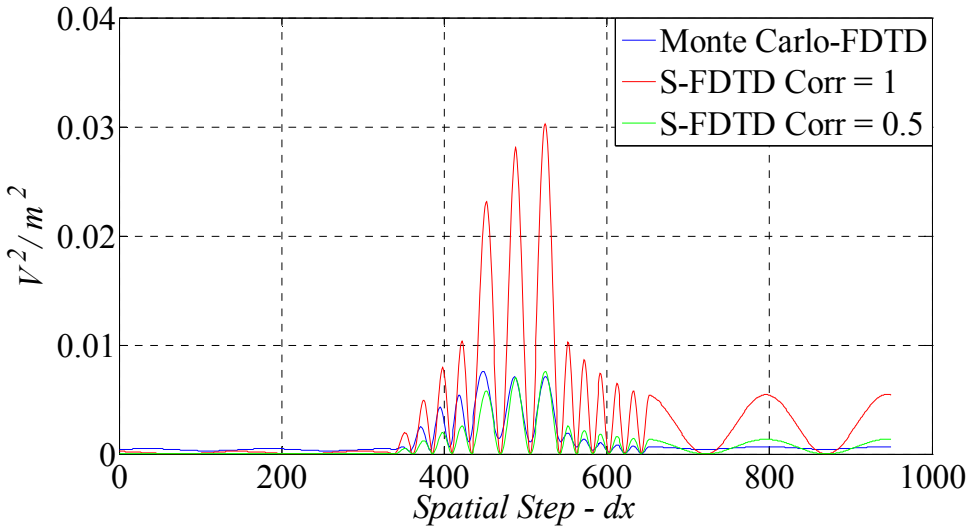

Figure 5-14 Comparison of E-field variances with different correlation coefficients used for S-FDTD Analysis

be used in discussing the variance of the SAR. In Monte Carlo analysis, as discussed in Section 3.2.3, as it relates to SAR is computed at the end of each simulation and stored away in memory for later statistical analysis. This process destroys the phase variation, leaving only the amplitude variation. This was shown in a comparison in Figure 3-24 showing the differences in E_p and E variances, which showed a difference in magnitude on the order of 7. E_p is used in determining the SAR within conductive materials such as human tissue. Figure 5-15 shows variance of the SAR for the Monte Carlo analysis performed in 1D at 2GHz, with the following parameter shown in Table 5-2. Order of the tissue was Skin, Fat, and Muscle. The variance was taken of the accumulated SAR data from the Monte Carlo analysis which took over 2 hrs to perform.

Figure 5-15 shows the SAR variance for S-FDTD with correlation coefficients set equal to 1 or 0.5. The S-SAR from S-FDTD analysis is higher than that found from the Monte Carlo analysis. Still the plots are close in form and the magnitude is off in the

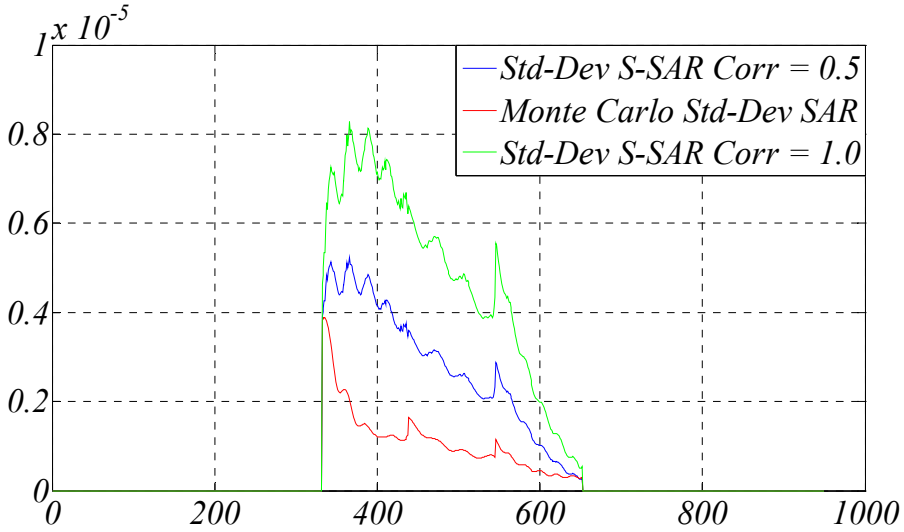

Figure 5-15 Comparison of the standard deviation of the SAR from three different analyses. S-SAR is using the S-FDTD analysis. The correlation coefficient for the S-SAR was set equal to 1.

Table 5-2 Nominal dielectric constants and conductivities and their standard deviations [SD] for human tissue[8] with specific gravity[12]

Dielectric	Spec. Gravity $10^3 kg/m^3$	ε_r Mean	ε_r [SD]	$\underline{\sigma}$ Mean (S/m)	$\underline{\sigma}$ [SD]	Nominal (mm) thickness
Muscle	1.04	55.0	4.6	0.87	0.10	42
Fat (infiltrated)	0.92	16.2	2.7	0.214	0.06	54
Skin	1.10	39.0	3.4	0.43	0.10	5.4

maximum by a factor of 5 in the $\rho = 0.5$ (Correlation Coefficient) case. But let us recall that the variance of the E fields is shown to be closer than this in Figure 5-14, so why the difference in SAR? The explanation is in the way the analyses are performed. In the S-FDTD analysis, the result is the variance of the E field taking into account all the variation of the amplitude and the phase, whereas the Monte Carlo analysis discards the phase variation to determine the SAR in the first place. This will have to be studied in greater detail in following research.

5.4 Summary

An approximate method for determining the statistical properties of an FDTD analysis has been derived, allowing the determination of the mean and the variance of the field terms of the FDTD simulation from a single run. The stochastic simulator, S-FDTD, progresses in the same fashion as an FDTD simulation but with added variables for the standard deviation of both the E and the H field at each cell in the model. The 'variance wave' (in reality the square root of the variance of the field equations derived from Maxwell's equations) propagates and reflects in much the same way as the E and H waves propagate and reflect.

Using S-FDTD, computer overhead is reduced substantially, and the first moment and the first central moment can be obtained without lengthy time-consuming simulation. Model space analysis and its effect on S-FDTD analysis is an additional topic needed for further research - required to improve the approximation of the S-FDTD analysis. With S-FDTD analysis, the variation in the SAR is overestimated.

With S-FDTD analysis, we are able to perform statistical analyses in large 3D model spaces with minor increases in simulation time and memory. Currently, this type

of analysis on large 3D model spaces is not practical due to the large computer resources required.

CHAPTER 6

VARIANCE OF FIELDS IN THE HUMAN HEAD FROM CELL PHONE USAGE

This chapter evaluates the variance of the fields and Specific Absorption Rate (SAR) in the human head while using a cell phone. Variance in the measured properties of the tissues was integrated into a 3D FDTD code using the Delta method (a truncated Taylor series approximation). This Stochastic FDTD (S-FDTD) analysis was used to approximate the mean and variance of fields and SAR in and around the head caused by variance in the tissue properties.

6.1 Introduction

Electromagnetic fields induced in the head from a cellular telephone are routinely calculated in order to determine if the phone meets RF safety guidelines [1, 2]. The allowable power absorbed, normally calculated as the Specific Absorption Rate (SAR), has a strong impact on the design of the phone and its antennas. The precise calculation of SAR depends on many factors in addition to the design of the phone. The tilt of the phone relative to the head [35-37], the size of the head (adults vs. children), the shape of the head [6, 7], the thickness of the ear [3-5], and variation in tissue properties (from

person to person or just because of uncertainty in the measurements). This variance has generally been demonstrated on a very limited case-by-case basis. Statistical evaluation of electromagnetic fields in the body has been very limited. This has been done previously with Monte Carlo [8]; however, this method requires so many computer simulations that it is too computer intensive to be used broadly on the detailed 3D simulations required for cell phone and human head analysis.

A new stochastic FDTD (S-FDTD) method was introduced in [38]. This method applies the Delta method [11] to develop additional time-dependent difference equations for variance of the fields. These can then be combined with the traditional FDTD equations to obtain both the mean and variance of the fields in a model as a function of time. The S-FDTD method provides a good approximation to the expected variance in a fraction of the computer time required for the Monte Carlo method. This paper extends the S-FDTD method to evaluate the variance of Specific Absorption Rate (SAR) and applies the method to determine the variation in fields and SAR expected in a model of a cell phone near a human head at 835MHz and 1900MHz, previously evaluated using a traditional FDTD approach in [3].

6.2 The Stochastic Finite-Difference Time-Domain (S-FDTD) Method

The Finite-Difference Time-Domain (FDTD) method has been used extensively for analysis of cell phones and the human head [16-20]. All bioelectromagnetic FDTD simulations that we are aware of use average electrical properties of the tissues [32] in a variety of models and configurations. The inevitable variability in these tissues is not normally considered. One exception is [8] that evaluated the detuning effect of the body, including variability of the tissues, on implantable antennas. By using the average

properties of the tissues, the FDTD simulation returns the average field or SAR values but does not return its expected variance. This section briefly describes a new stochastic FDTD (S-FDTD) method that integrates the expected variance in the tissue properties with the FDTD method using the Delta method. The S-FDTD derivations are described in more detail in [38]. They are summarized here and extended to analysis of SAR.

6.2.1 The Delta Method

The Delta method [11] that is used to investigate the variance of the tissue properties with the FDTD equations is a form of perturbation theory. This method assumes that the solution has a Taylor series expansion that can be truncated to the first few terms. This truncated series is substituted back into the original equation, and the equation is simplified to a point where it can be programmed as a time-domain equation along with the traditional FDTD equations which provide the mean fields. The Delta method has previously been applied to derive the stochastic properties of mechanical systems using Finite Element Method (FEM) simulations [24].

FDTD equations are Faraday's and Ampere's time-domain differential equations in finite-difference time-domain form. The E and H fields for the stochastic FDTD (S-FDTD) method are the same as the traditional equations using the mean material parameters, such as the conductivity $\underline{\sigma}$ and the permittivity ε. In 3D there are 6 FDTD equations, three for the E fields and three for the H fields. Two of these 3D FDTD equations are given below. From Faraday's Law, we get equation (6.1) and from Ampere's Law, we get equation (6.2). More details on the full 3D FDTD equations are found in [33] .

$$H_x^{n+1}\left(i-1/2,j+1,k+1\right)=\frac{2\mu_\mu-\Delta t\mu_{\sigma^*}}{2\mu_\mu+\Delta t\mu_{\sigma^*}}H_x^n\left(i-1/2,j+1,k+1\right)$$

$$+\frac{2\Delta t}{(2\mu_\mu+\Delta t\mu_{\sigma^*})}\left(\left(\begin{array}{l}\dfrac{E_y^{n+1/2}\left(i-1/2,j+1,k+3/2\right)-E_y^{n+1/2}\left(i-1/2,j+1,k+1/2\right)}{\Delta z}\\ \\ -\quad\dfrac{E_z^{n+1/2}\left(i-1/2,j+3/2,k+1\right)-E_z^{n+1/2}\left(i-1/2,j+1/2,k+1\right)}{\Delta y}\end{array}\right)\right) \tag{6.1}$$

$$E_x^{n+1/2}\left(i,j+1/2,k+1/2\right)=\frac{2\mu_\varepsilon-\Delta t\mu_\sigma}{2\mu_\varepsilon+\Delta t\mu_\sigma}E_x^{n-1/2}\left(i,j+1/2,k+1/2\right)$$

$$+\frac{2\Delta t}{(2\mu_\varepsilon+\Delta t\mu_\sigma)}\left(\left(\begin{array}{l}\dfrac{H_z^n\left(i,j+1,k+1/2\right)-H_z^n\left(i,j,k+1/2\right)}{\Delta y}\\ \\ -\quad\dfrac{H_y^n\left(i,j+1/2,k+1\right)-H_y^n\left(i,j+1/2,k\right)}{\Delta z}\end{array}\right)\right) \tag{6.2}$$

To perform a statistical analysis with FDTD, we need to find the mean and the variance of the E and H fields. The equations for the mean, it turns out, are the same as the traditional FDTD equations. The variance of the fields is much more difficult to determine due to cross correlation terms between the field components and the various material properties that influence them. The fields are correlated to the material properties and none of these terms are independent or separable.

In order to derive the variance of the FDTD equations for the E and H fields, they are described as stochastic functions of the random tissue properties, for example

$E(\varepsilon_R, \underline{\sigma})$ and $H(\varepsilon_R, \underline{\sigma})$. These field equations are expanded in a Taylor series and truncated about the mean of the two tissue property random variables ε_R (permittivity) and $\underline{\sigma}$ (conductance). We need to take note that the symbol for conductivity has been changed to ($\underline{\sigma}$) to allow the variance to be represented by its normal mathematical symbol (σ^2). The resultant expansions are evaluated about the means of the various tissue property random variables, $\mu_{\varepsilon_R}, \mu_{\underline{\sigma}}$. The expectation is taken of each equation to give the mean values.

To keep the derivation general, we will refer to a generic function of the random variables (tissue properties and fields) as $g(\bullet)$. The equation for the variance $\sigma^2\{g(\varepsilon_R, \underline{\sigma})\}$ is equal to $\underset{\sim}{E}\{g(\varepsilon_R, \underline{\sigma})^2\} - \underset{\sim}{E}\{g(\varepsilon_R, \underline{\sigma})\}^2$ [22]. These equations are expanded using the Taylor series, and higher order terms are discarded. This method is called the Delta method [11]. Its application to the FDTD equations is described below.

We start with the Taylor's series expansion of a generic function $(g(x_1, x_2, x_3, \ldots, x_n))$ with generic random variables $x_1, x_2, x_3, \ldots, x_n$. The six vector components of the E and H fields are represented by the $g(\bullet)$ functions. The variables x_i represent the average material properties such as the conductivity and the permittivity. The function can be expanded about the means of the random variables which are represented by the Greek letter μ with a subscript representing the random variable it represents:

$$g(x_1, x_2, x_3, ..., x_n) =$$

$$g\left(\mu_{x_1},\mu_{x_2},\mu_{x_3},...,\mu_{x_n}\right)+\sum_{i=1}^{n}\left.\frac{\partial g}{\partial x_i}\right|_{\mu_{x1},\mu_{x2},...,\mu_{xn}}(x_i-\mu_{x_i})$$
$$+\frac{1}{2!}\sum_{i=1}^{n}\sum_{j=1}^{n}\left.\frac{\partial^2 g}{\partial x_i\partial x_j}\right|_{\mu_{x1},\mu_{x2},...,\mu_{xn}}(x_i-\mu_{x_i})(x_j-\mu_{x_j})\ +...$$

(6.3)

The expectation of (6.3) is expanded about the mean of the parameters x_i indicated by μ_{x_i}:

$$\underset{\sim}{E}\left\{g\left(x_1,x_2,x_3,...,x_n\right)\right\}=$$
$$\underset{\sim}{E}\left\{\begin{array}{l} g\left(\mu_{x_1},\mu_{x_2},\mu_{x_3},...,\mu_{x_n}\right)+\sum_{i=1}^{n}\left.\frac{\partial g}{\partial x_i}\right|_{\mu_{x1},\mu_{x2},...,\mu_{xn}}(x_i-\mu_{x_i}) \\ +\frac{1}{2!}\sum_{i=1}^{n}\sum_{j=1}^{n}\left.\frac{\partial^2 g}{\partial x_i\partial x_j}\right|_{\mu_{x1},\mu_{x2},...,\mu_{xn}}(x_i-\mu_{x_i})(x_j-\mu_{x_j})+... \end{array}\right\} \quad (6.4)$$

Because the expectation is a linear operator, we can open the brackets of equation (6.4) and apply the expectation operator to each term, yielding the following equation:

$$\underset{\sim}{E}\left\{g\left(x_1,x_2,x_3,...,x_n\right)\right\}=\underset{\sim}{E}\left\{g\left(\mu_{x_1},\mu_{x_2},\mu_{x_3},...,\mu_{x_n}\right)\right\}$$
$$+\underset{\sim}{E}\left\{\sum_{i=1}^{n}\left.\frac{\partial g}{\partial x_i}\right|_{\mu_{x1},\mu_{x2},...,\mu_{xn}}(x_i-\mu_{x_i})\right\}+\underset{\sim}{E}\left\{\frac{1}{2!}\sum_{i=1}^{n}\sum_{j=1}^{n}\left.\frac{\partial^2 g}{\partial x_i\partial x_j}\right|_{\mu_{x1},\mu_{x2},...,\mu_{xn}}(x_i-\mu_{x_i})(x_j-\mu_{x_j})\right\}+... \quad (6.5)$$

The terms containing $\underset{\sim}{E}\left\{x_i-\mu_{x_i}\right\}$ go to zero. This is because the expectation operator is linear, so these brackets can be opened, yielding $\underset{\sim}{E}\{x\}-\mu_x$, and the

expectation of $\underset{\sim}{E}\{x_i\} = \mu_{x_i}$. We can further simplify the equation using $\underset{\sim}{E}\{aX\} = a\underset{\sim}{E}\{X\}$:

$$\underset{\sim}{E}\{g(x_1, x_2, x_3, ..., x_n)\} = g(\mu_{x_1}, \mu_{x_2}, \mu_{x_3}, ..., \mu_{x_n}) + \overbrace{\sum_{i=1}^{n} \frac{\partial g}{\partial x_i}\bigg|_{\mu_{x_1}, \mu_{x_2}, ..., \mu_{x_n}} \underset{\sim}{E}\{x_i - \mu_{x_i}\}}^{0} + \frac{1}{2!}\sum_{i=1}^{n}\sum_{j=1}^{n} \frac{\partial^2 g}{\partial x_i \partial x_j}\bigg|_{\mu_{x_1}, \mu_{x_2}, ..., \mu_{x_n}} \underset{\sim}{E}\{(x_i - \mu_{x_i})(x_j - \mu_{x_j})\} + ... \tag{6.6}$$

Neglecting high order terms reduces the equation even further

$$\underset{\sim}{E}\{g(x_1, x_2, x_3, ..., x_n)\} \approx g(\mu_{x_1}, \mu_{x_2}, \mu_{x_3}, ..., \mu_{x_n}) \tag{6.7}$$

This shows why the mean fields $\underset{\sim}{E}\{g(x_1, x_2, x_3, ..., x_n)\}$ will be approximately the fields $g(\mu_{x_1}, \mu_{x_2}, \mu_{x_3}, ..., \mu_{x_n})$ obtained using the average properties μ_{x_i}.

The variance can also be calculated using the Delta method [11]. The variance is defined as [22]:

$$\sigma^2\{g(x_1, x_2, x_3, ..., x_n)\} = \underset{\sim}{E}\{g(x_1, x_2, x_3, ..., x_n)^2\} - \underset{\sim}{E}\{g(x_1, x_2, x_3, ..., x_n)\}^2 \tag{6.8}$$

We expand the above equation in a Taylor's series expansion about the mean of

each of the stochastic variables:

$$\sigma^2\left\{g\left(x_1,x_2,x_3,...,x_n\right)\right\}= \sum_{i=1}^{n}\sum_{j=1}^{n}\frac{\partial g}{\partial x_i}\frac{\partial g}{\partial x_j}\bigg|_{\mu_{x_1},\mu_{x_2},...,\mu_{x_n}} \underset{\sim}{E}\left\{(x_i-\mu_{x_i})(x_j-\mu_{x_j})\right\}+..... \tag{6.9}$$

Removing higher order terms, the variance of the function g (the E and H fields) is:

$$\sigma^2\left\{g\left(x_1,x_2,x_3,...,x_n\right)\right\}\approx \sum_{i=1}^{n}\sum_{j=1}^{n}\frac{\partial g}{\partial x_i}\frac{\partial g}{\partial x_j}\bigg|_{\mu_{x_1},\mu_{x_2},...,\mu_{x_n}} \underset{\sim}{E}\left\{(x_i-\mu_{x_i})(x_j-\mu_{x_j})\right\} \tag{6.10}$$

Equation (6.10) provides an approximation of the variance of a function of random variables. In the next section, we will use these results to approximate the mean and the variance of Faraday's and Ampere's Laws.

6.2.2 The Stochastic-FDTD Method

The Stochastic FDTD (S-FDTD) method described in this section is a new extension of the FDTD approach that carries the variance of the fields along with their mean when the model includes stochastic variation in the tissue properties. S-FDTD uses the traditional FDTD equations to find the mean of the fields ((6.1) and (6.2)). Deriving the variance of the fields is somewhat more complex due to correlation of the various parameters of the fields and material properties. We will use the following statistical identity for the variance of a function of random variables X and Y [22]:

$$\sigma^2\left[aX \pm bY\right] = a^2\sigma_X^2 + b^2\sigma_Y^2 \pm 2abCov(X,Y)$$
$$\sigma^2\left\{aX\right\} = a^2\sigma^2\left\{X\right\} \qquad (6.11)$$
$$a \text{ is constant}$$

and the covariance identity where ρ_{XY} is the correlation coefficient:

$$Cov(X,Y) = \rho_{XY}\sigma\left\{X\right\}\sigma\left\{Y\right\} \qquad (6.12)$$

Faraday's equation for H_x (6.1) becomes:

$$\sigma\left\{H_x^{n+1}\left(i-1/2, j+1, k+1\right)\right\} =$$

$$\frac{2\mu_\mu - \Delta t\mu_{\sigma^*}}{2\mu_\mu + \Delta t\mu_{\sigma^*}}\sigma\left\{H_x^n\left(i-1/2, j+1, k+1\right)\right\}$$

$$+\frac{4\Delta t\left(\mu_{\sigma^*}\rho_{\mu,H}\sigma\left\{\mu\right\} - \mu_m\rho_{\sigma^*,H}\sigma\left\{\sigma^*\right\}\right)}{\left(2\mu_\mu + \Delta t\mu_{\sigma^*}\right)^2}H_x^n\left(i-1/2, j+1, k+1\right) +$$

$$\frac{2\Delta t}{(2\mu_\mu + \Delta t\mu_{\sigma^*})} \bullet$$

$$\left(\left(\frac{\sigma\left\{E_y^{n+1/2}\left(i-1/2, j+1, k+3/2\right)\right\} - \sigma\left\{E_y^{n+1/2}\left(i-1/2, j+1, k+1/2\right)\right\}}{\Delta z}\right.\right.$$

$$\left.\left. - \frac{\sigma\left\{E_z^{n+1/2}\left(i-1/2, j+3/2, k+1\right)\right\} - \sigma\left\{E_z^{n+1/2}\left(i-1/2, j+1/2, k+1\right)\right\}}{\Delta y}\right)\right)$$

$$- \frac{2\rho_{\mu,\mathrm{E}}\sigma\left\{\mu\right\} + \Delta t\rho_{\sigma^*,\mathrm{E}}\sigma\left\{\sigma^*\right\}}{2\mu_\mu + \Delta t\mu_{\sigma^*}} \bullet$$

$$\left(\frac{E_y^{n+1/2}\left((i-1/2, j+1, k+3/2)\right) - E_y^{n+1/2}\left\{(i-1/2, j+1, k+1/2)\right\}}{\Delta z} \right.$$

$$\left. - \frac{E_z^{n+1/2}(i-1/2, j+3/2, k+1) - E_z^{n+1/2}(1-1/2, j+1/2, k+1)}{\Delta y} \right) \tag{6.13}$$

Ampere's equation for E_x (6.2) becomes:

$$\sigma\left\{E_x^{n+1/2}(i, j+1/2, k+1/2)\right\} =$$

$$\frac{2\mu_\varepsilon - \Delta t\mu_\sigma}{2\mu_\varepsilon + \Delta t\mu_\sigma}\sigma\left\{E_x^{n-1/2}(i, j+1/2, k+1/2)\right\}$$

$$+\frac{4\Delta t\left(\mu_\sigma\rho_{\varepsilon,E}\sigma\{\varepsilon\} - \mu_\varepsilon\rho_{\sigma,E}\sigma\{\sigma\}\right)}{\left(2\mu_\varepsilon + \Delta t\mu_\sigma\right)^2}E_x^{n-1/2}(i, j+1/2, k+1/2) +$$

$$\frac{2\Delta t}{(2\mu_\varepsilon + \Delta t\mu_\sigma)} \bullet$$

$$\left(\left(\frac{\sigma\left\{H_z^n(i, j+1, k+1/2)\right\} - \sigma\left\{H_z^n(i, j, k+1/2)\right\}}{\Delta y} \right.\right.$$

$$\left.\left. - \frac{\sigma\left\{H_y^n(i, j+1/2, k+1)\right\} - \sigma\left\{H_y^n(i, j+1/2, k)\right\}}{\Delta z} \right) \right.$$

$$\left. - \frac{2\rho_{\varepsilon,H}\sigma\{\varepsilon\} + \Delta t\rho_{\sigma,H}\sigma\{\sigma\}}{2\mu_\varepsilon + \Delta t\mu_\sigma} \right) \bullet$$

$$\left(\frac{H_z^n\left((i, j+1, k+1/2)\right) - H_z^n\left\{(i, j, k+1/2)\right\}}{\Delta y} \right.$$
$$\left. - \frac{H_y^n\left(i, j+1/2, k+1\right) - H_y^n\left(i, j+1/2, k\right)}{\Delta z} \right) \tag{6.14}$$

The timing and spatial diagram in Figure 6-1 shows how the field terms are related to the standard deviation terms for the 1D case. These relationships are extended to 3D using the standard Yee cell shown in [33]. The full derivation of these equations is quite complex and is given in [33]. The only approximations that are made are limiting the Taylor series approximations for the time and spatial derivations to the first and second order terms.

In order to apply these equations, an additional approximation must be made for the correlation coefficients. These approximations turn out to be quite important for the accuracy of the variance. In this paper, we will use 1.0 and 0.5 as correlation coefficients.

In the next section, we bring in Specific Absorption Rate (SAR), a quantity that is used to determine the amount of power absorbed in human tissue. The mean and variance of the SAR are derived in the following section based on the mean and variance of the fields given in this section.

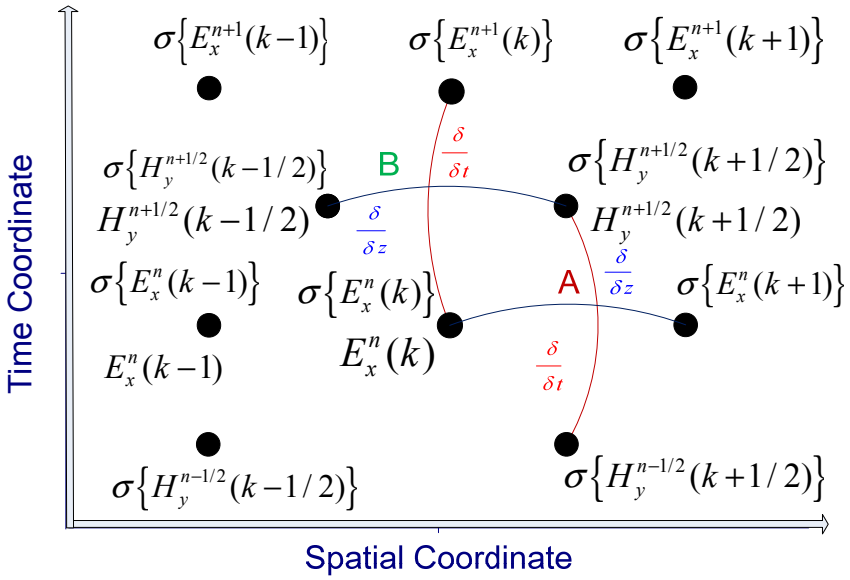

Figure 6-1 Distribution of the fields and variances in space (z or k) and time (n). The full 3D version (shown here in 1D for simplicity) is based on the standard Yee cell.

6.3 Specific Absorption Rate (SAR)

The Specific Absorption Rate (SAR) is defined as [34]:

$$SAR = \frac{\sigma E_p^{\ 2}}{2\rho_{density}} \tag{6.15}$$

The SAR is given in W/kg. The FCC SAR guideline [1] requires that devices deposit no more than 1.6 W/kg in any 1 cm^3 of tissue. This 1-gram averaged SAR could be calculated several ways, complicated by the fact that the peak SAR in the head is found in the highly irregular ear region, where there is no cm-cube of tissue. We will use the method of calculating 1-gram SAR where we use a 1 cm^3 region, average the SAR in this region (the SAR in air is zero), and normalize by the total weight of the tissues in the region. Regions with less than 0.5 grams of tissue are ignored. We will report the

localized SAR values and the peak 1-gram SAR values for a given model. The localized SAR values depend on the size of the cells used in the model, but they are instructive for observing the general patterns of the SAR in the head.

The mean values for localized SAR are calculated from (6.15) after the S-FDTD simulation is complete. The peak value of E is calculated from the time domain E fields using the 2-equations 2-unknowns [29] method. The conductivity of the tissue in that localized cell is used in (6.15) to obtain SAR.

6.3.1 SAR and the Delta Method

The variance of the SAR calculated using the Delta method:

$$\sigma^2\{SAR\} = \sigma^2\left\{\frac{\underline{\sigma}E_p{}^2}{2\rho_{density}}\right\} \tag{6.16}$$

Constants can be brought out of the variance operator using $\sigma^2\{aX\} = a^2\sigma^2\{X\}$ yielding:

$$\sigma^2\{SAR\} = \frac{1}{4\rho_{density}^2}\sigma^2\left\{\underline{\sigma}E_p{}^2\right\} \tag{6.17}$$

the $\sigma^2\left\{\underline{\sigma}E_p{}^2\right\}$ portion of (6.17) is difficult to separate, but using the Delta method, we can arrive at a good approximation. Particularly, we use equation (4.10) to derive this. We have four terms that will need to be determined, i.e. the two variance terms, the maximum field term $\sigma^2\{E_p\}$, the conductivity term $\sigma^2\{\underline{\sigma}\}$ and finally the covariance

term $Cov\left\{\underline{\sigma}, {E_p}^2\right\}$. The complete equation is shown next:

$$\sigma^2\{SAR\} = \frac{1}{4\rho_{density}^2} \bullet$$

$$\left\{\left(\frac{\partial\left\{\underline{\sigma}E_p^2\right\}}{\partial\underline{\sigma}}\right)^2 \sigma^2\{\underline{\sigma}\} + \left(\frac{\partial\left\{\underline{\sigma}E_p^2\right\}}{\partial E_p}\right)^2 \sigma^2\{E_p\} + 2\left(\frac{\partial\left\{\underline{\sigma}E_p^2\right\}}{\partial E_p}\right)\left(\frac{\partial\left\{\underline{\sigma}E_p^2\right\}}{\partial\underline{\sigma}}\right) Cov\left\{\underline{\sigma}, E_p\right\}\right\}$$

The $\sigma^2\{\underline{\sigma}\}$ term is shown as:

$$\sigma^2\{\underline{\sigma}\}\left(\frac{\partial\left\{\underline{\sigma}E_p^2\right\}}{\partial\underline{\sigma}}\right)^2 = E_p^4\sigma^2\{\underline{\sigma}\} \tag{6.18}$$

The $\sigma^2\{E_p\}$ term is:

$$\sigma^2\{E_p\}\left(\frac{\partial\left\{\underline{\sigma}E_p^2\right\}}{\partial E_p}\right)^2 = 4E_p^2\underline{\sigma}^2\sigma^2\{E_p\} \tag{6.19}$$

The $Cov\left\{\underline{\sigma}, E_p\right\}$ term is:

$$2Cov\left\{\underline{\sigma}, E_p\right\}\left(\frac{\partial\left\{\underline{\sigma}E_p^2\right\}}{\partial E_p}\right)\left(\frac{\partial\left\{\underline{\sigma}E_p^2\right\}}{\partial\underline{\sigma}}\right) = 4Cov\left\{\underline{\sigma}, E_p\right\}\underline{\sigma}E_p^3 \tag{6.20}$$

Recalling that the covariance is equal to the correlation coefficient times the standard deviations of the terms involved, this equation is shown next:

$$Cov\{X,Y\} = \rho_{X,Y}\sigma\{X\}\sigma\{Y\}$$

Equation (6.20) can then be written as:

$$4Cov\left\{\underline{\sigma}, E_p\right\}\underline{\sigma}E_p^3 = 4\underline{\sigma}E_p^3\rho_{\underline{\sigma},\mathrm{E}_p}\sigma\{\underline{\sigma}\}\sigma\left\{E_p\right\} \tag{6.21}$$

Summing equations (6.18), (6.19), and equation (6.21) yields the following equation and dividing by $4\rho^2$ gives the variance of the SAR - $\sigma^2\{SAR\}$:

$$\sigma^2\{SAR\} = \frac{E_p^2\left(4\underline{\sigma}E_p\rho_{\underline{\sigma},E_p}\sigma\{\underline{\sigma}\}\sigma\left\{E_p\right\} + E_p^2\sigma^2\{\underline{\sigma}\} + 4\underline{\sigma}^2\sigma^2\left\{E_p\right\}\right)}{4\rho_{density}^2} \tag{6.22}$$

In the next section, we shall derive the same equation but in a different manner using the assumptions of Normal random variables and these variables being uncorrelated to each other.

6.3.2 Another SAR Variance Derivation

We start off with an assumption of independence of the two random variables found in the SAR equation, namely the conductivity and the peak amplitude of the E field. The variance equation is again repeated here:

$$\sigma^2\{SAR\} = \sigma^2\left\{\frac{\underset{\sim}{\sigma} E_p^{\ 2}}{2\rho_{density}}\right\} \tag{6.23}$$

The independence of these two variables allows certain operations in simplifying equation (6.23). Let us start with a simplified equation and derive the necessary equations that will help us in this derivation:

$$\sigma^2\{xy\} = \underset{\sim}{E}\left\{(xy)^2\right\} - \underset{\sim}{E}\{xy\}^2 \tag{6.24}$$

With independence between x and y, the various parts can be separated [22]:

$$\begin{aligned} \underset{\sim}{E}\left\{x^2y^2\right\} &= \underset{\sim}{E}\left\{x^2\right\}\underset{\sim}{E}\left\{y^2\right\} \\ \underset{\sim}{E}\{xy\} &= \underset{\sim}{E}\{x\}\underset{\sim}{E}\{y\} \end{aligned} \tag{6.25}$$

Substituting these equations into (6.24) yields:

$$\sigma^2\{xy\} = \underset{\sim}{E}\left\{x^2\right\}\underset{\sim}{E}\left\{y^2\right\} - \underset{\sim}{E}\{x\}^2\,\underset{\sim}{E}\{y\}^2 \tag{6.26}$$

Remembering that $\sigma^2\{x\} = \underset{\sim}{E}\left\{x^2\right\} - \underset{\sim}{E}\{x\}^2$ and with some manipulation this shows $\underset{\sim}{E}\left\{x^2\right\} = \sigma^2\{x\} + \underset{\sim}{E}\{x\}^2$, this result is again substituted into equation (6.26) with this result:

$$\sigma^2\{xy\} = \left(\sigma^2\{x\} + \underset{\sim}{E}\{x\}^2\right)\left(\sigma^2\{y\} + \underset{\sim}{E}\{y\}^2\right) - \underset{\sim}{E}\{x\}^2\,\underset{\sim}{E}\{y\}^2 \tag{6.27}$$

Expanding the terms:

$$\sigma^2\{xy\} = \underset{\sim}{E}\{x\}^2\,\underset{\sim}{E}\{y\}^2 + \underset{\sim}{E}\{y\}^2\,\sigma^2\{x\} + \underset{\sim}{E}\{x\}^2\,\sigma^2\{y\} + \sigma^2\{x\}\sigma^2\{y\} - \underset{\sim}{E}\{x\}^2\,\underset{\sim}{E}\{y\}^2$$

Subtracting like terms yields:

$$\sigma^2\{xy\} = \underset{\sim}{E}\{y\}^2\,\sigma^2\{x\} + \underset{\sim}{E}\{x\}^2\,\sigma^2\{y\} + \sigma^2\{x\}\sigma^2\{y\} \tag{6.28}$$

We now have the following equation:

$$\sigma^2\{SAR\} = \sigma^2\left\{\frac{\underline{\sigma}E_p{}^2}{2\rho_{density}}\right\}$$

$$\sigma^2\{SAR\} = \frac{1}{4\rho_{density}^2}\sigma^2\left\{\underline{\sigma}E_p{}^2\right\} \tag{6.29}$$

Using equation (6.28) with equation (6.29) yields:

$$\frac{1}{4\rho_{density}^2}\sigma^2\left\{\underline{\sigma}E_p{}^2\right\} =$$

$$\frac{1}{4\rho_{density}^2}\left(\underset{\sim}{E}\left\{E_p{}^2\right\}^2\sigma^2\{\underline{\sigma}\} + \underset{\sim}{E}\{\underline{\sigma}\}^2\sigma^2\left\{E_p{}^2\right\} + \sigma^2\{\underline{\sigma}\}\sigma^2\left\{E_p{}^2\right\}\right) \tag{6.30}$$

The equation (6.30) has a number of terms that can be determined if we assume a Normal distribution for both random variables.

Let us recall the Normal distribution:

$$f(x) = \frac{1}{\sigma\sqrt{2\pi}} Exp\left(-\frac{(x-\mu)^2}{2\sigma^2}\right) \tag{6.31}$$

Using the probability distribution, we can determine $\underset{\sim}{E}\{x^2\}$ and $\sigma^2\{x^2\}$ and use the resulting equations to simplify equation (6.30). Solving for $\underset{\sim}{E}\{x^2\}$ using (6.31) yields:

$$\underset{\sim}{E}\{x^2\} = \underset{\sim}{E}\{x\}^2 + \sigma^2\{x\} \tag{6.32}$$

and $\sigma^2\{x^2\}$ is:

$$\sigma^2\{x^2\} = 2\left(2\underset{\sim}{E}\{x\}^2 \sigma^2\{x\} + \sigma^4\{x\}\right) \tag{6.33}$$

Substituting equations (6.32) and (6.33) into (6.30) yields:

$$\frac{1}{4\rho_{density}^2}\sigma^2\left\{\underline{\sigma}E_p{}^2\right\} = \frac{\mu_{E_p}^4\sigma^2\{\underline{\sigma}\} + 4\mu_{\underline{\sigma}}^2\mu_{E_p}^2\sigma^2\{E_p\} + 6\mu_{E_p}^2\sigma^2\{\hat{\sigma}\}\sigma^2\{E_p\}}{4\rho_{density}^2} \tag{6.34}$$

Looking at expression (6.34), the term $6\mu_{E_p}^2\sigma^2\{\hat{\sigma}\}\sigma^2\{E_p\}$ approaches zero, yielding a final approximating expression:

$$\frac{1}{4\rho_{density}^2}\sigma^2\{\underline{\sigma}E_p{}^2\} \approx \frac{E_p^4\sigma^2\{\underline{\sigma}\}+4\underline{\sigma}^2E_p^2\sigma^2\{E_p\}}{4\rho_{density}^2} \tag{6.35}$$

Compare this expression with equation (6.22), repeated below:

$$\sigma^2\{SAR\} = \frac{E_p^2\left(4\underline{\sigma}E_p\rho_{\underline{\sigma},E_p}\sigma\{\underline{\sigma}\}\sigma\{E_p\}+E_p^2\sigma^2\{\underline{\sigma}\}+4\underline{\sigma}^2\sigma^2\{E_p\}\right)}{4\rho_{density}^2}$$

Setting the correlation coefficient $\rho_{\underline{\sigma},E_p}$ equal to zero yields:

$$\begin{aligned}\sigma^2\{SAR\} &= \frac{E_p^2\left(E_p^2\sigma^2\{\underline{\sigma}\}+4\underline{\sigma}^2\sigma^2\{E_p\}\right)}{4\rho_{density}^2} \\ &= \frac{E_p^4\sigma^2\{\underline{\sigma}\}+4\underline{\sigma}^2E_p^2\sigma^2\{E_p\}}{4\rho_{density}^2}\end{aligned} \tag{6.36}$$

Equation (6.35) is equivalent to equation (6.36), showing that the Delta method has produced a reasonable approximation to the Variance of the Specific Absorption Rate (SAR) seeing that two different methods produced results close to each other.

In the 1D simulation, the SAR from the S-FDTD analyses where compared with Monte Carlo analysis. The comparison showed that the S-FDTD analysis coupled with the variance of SAR is higher for the S-FDTD analysis.

6.3.3 Validation

The S-FDTD method has been evaluated and validated in detail in [38], but a brief validation will be included here as well. The Monte Carlo method is used as the gold standard to compute the mean and variance of the fields and SAR in a 1D model. The tissues are assumed to have a Gaussian (normal) distribution with the properties given in Table 6-1. These are modeled in the Monte Carlo FDTD (M-FDTD) approach using 10,000 individual runs with different normally-distributed tissue properties and postprocessed to obtain the means and standard deviations of the fields and SAR in the model. The S-FDTD method was validated by comparing it with the M- FDTD method using a 1D tissue model shown in Figure 6-2 using 1D simplifications of equations (6.1) and (6.2) for the mean of the fields and equations (6.13) and (6.14) for their variance. The mean of the SAR is calculated from (6.15), and its variance from (6.22). Order of the tissue was Skin, Fat, and Muscle.

The mean of the fields and SAR is virtually identical to the traditional FDTD approach with the mean SAR shown in Figure 6-3, and less than 5.3% difference is seen between the S-FDTD approach and the M-FDTD method.

The accuracy of the S-FDTD calculation of variance, on the other hand, depends strongly on the approximations used for the correlation coefficients, as shown in Figure 6-4. Using a correlation coefficient of 1.0 provides a maximum estimate (upper bound) for the variance. A correlation coefficient of 0.5 provides more accurate results. Another possibility is to use the nearby reflection coefficients or other aspects of the model to improve the approximation of the correlation coefficients, but this requires additional analysis that is left for future work.

The variance of the SAR provides additional problems and is less accurate as a

Table 6-1 Nominal dielectric constants and conductivities and their standard deviations [SD] for human tissue[8] with specific gravity [12]

Dielectric	Spec. Gravity $10^3 kg/m^3$	ε_r Mean	ε_r [SD]	$\underline{\sigma}$ Mean (S/m)	$\underline{\sigma}$ [SD]	Nominal (mm) thickness
Muscle	1.04	55.0	4.6	0.87	0.10	42
Fat (infiltrated)	0.92	16.2	2.7	0.214	0.06	54
Skin	1.10	39.0	3.4	0.43	0.10	5.4

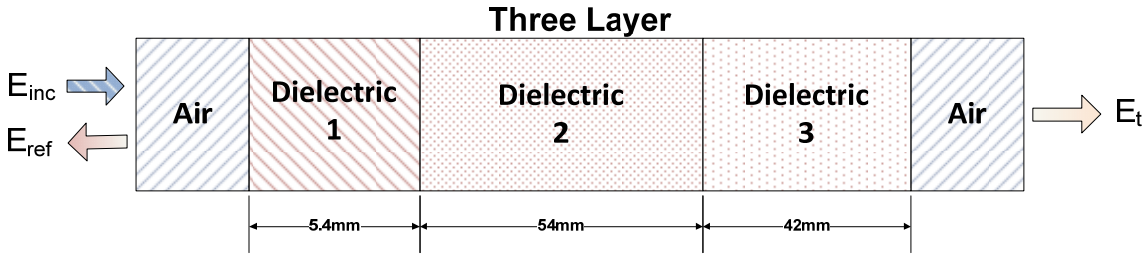

Figure 6-2 Three layer structure used for S-FDTD and M-FDTD analysis

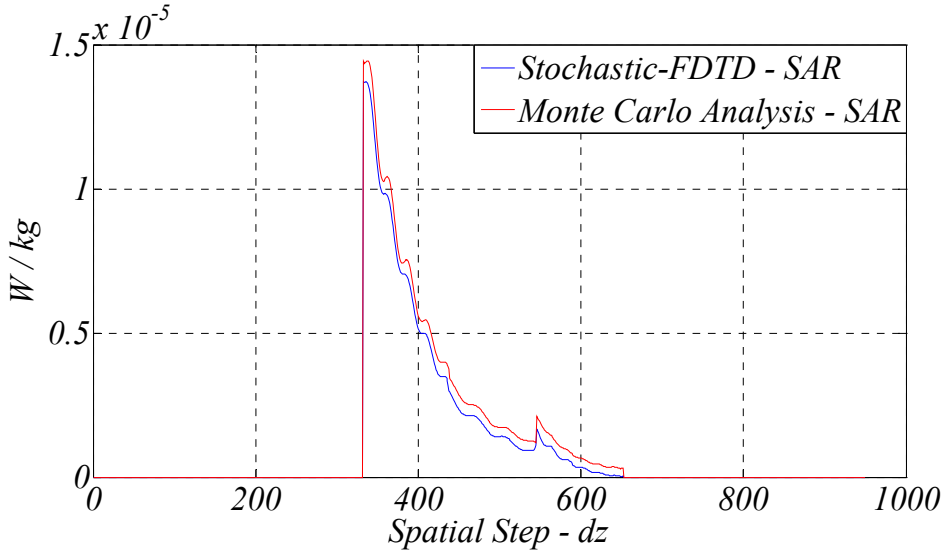

Figure 6-3 Comparison of the M-FDTD and S-FDTD mean SAR

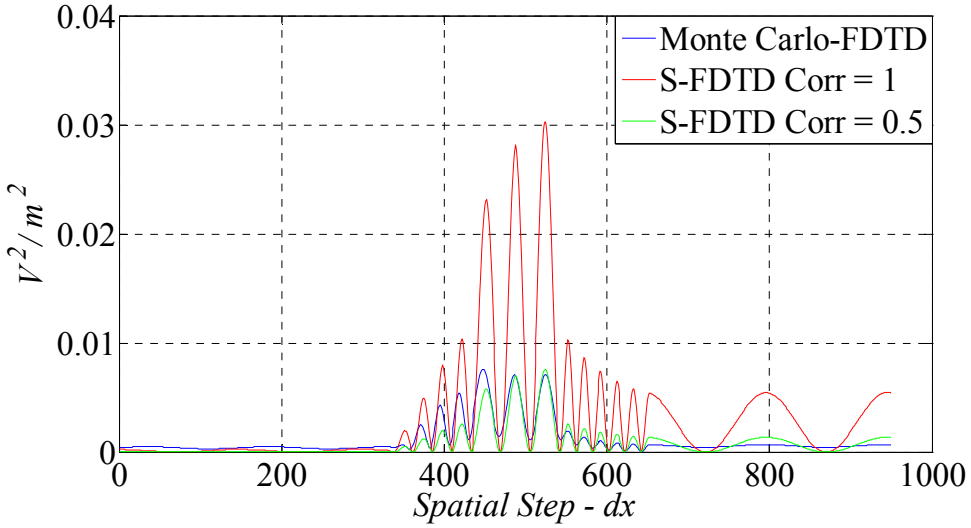

Figure 6-4 Comparison of E-field variances with different correlation coefficients used for S-FDTD analysis of the 1D model

result. In Monte Carlo analysis, discussed in Section 3.2.3, it relates to how the SAR (Specific Absorption Rate) is computed at the end of each simulation and stored away in memory for later statistical analysis. This process destroys the phase variation leaving only the amplitude variation. This is shown in Figure 6-5 showing the difference in E_p and E variances, which shows a difference in magnitude on the order of 7. E_p is used in determining the SAR within conductive materials such as human tissue.

We next show the variance of the SAR for the Monte Carlo analysis performed for the 1D model in Figure 6-6 at 2GHz using the tissue properties shown in Table 6-1. The M-FDTD variance was taken of the accumulated SAR data from the Monte Carlo analysis, which took over 2 hrs to perform on an Intel(R) Core(TM)2 CPU 6400 @ 2.13GHz 2.13 GHz, 2.00GB of RAM computer. The S-FDTD variance was computed using equation (6.22) and took ~8 seconds to calculate. The S-FDTD was calculated with correlation coefficients of 1.0 (upper bound in green) and 0.5 (more accurate for the

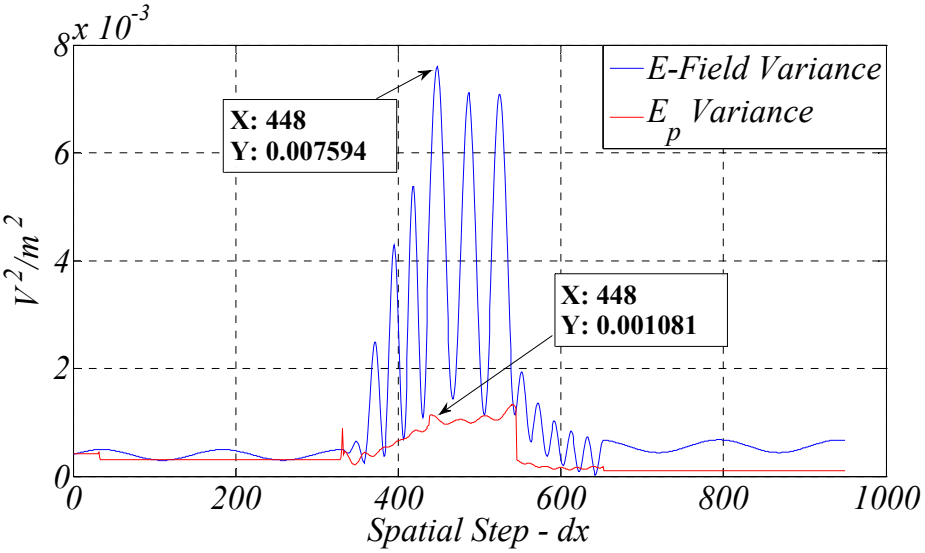

Figure 6-5 Comparison of the M-FDTD variation of the peak E field and the E field variance

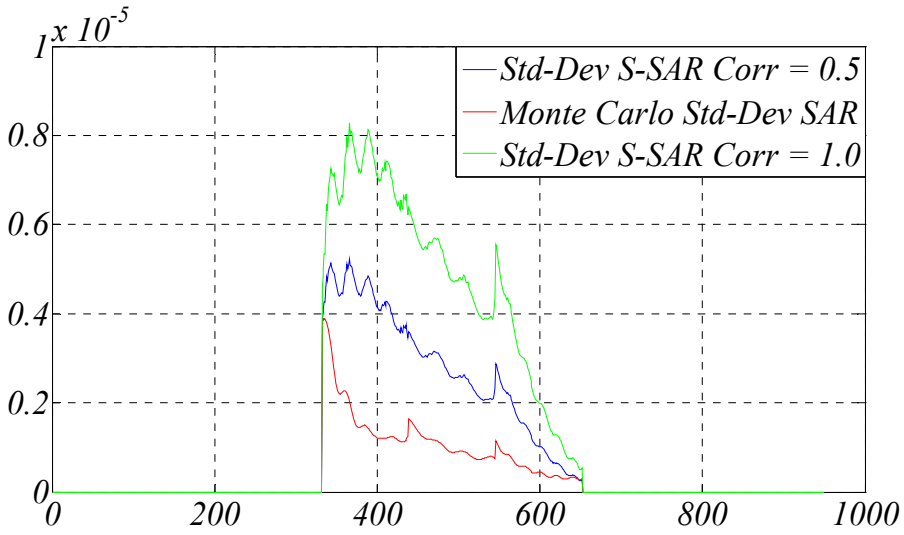

Figure 6-6 Comparison of the standard deviation of the SAR from three different analyses. S-SAR is using the S-FDTD analysis. The correlation coefficient for the S-SAR was set equal to 1.0 and 0.5

fields in blue).

6.4 3D S-FDTD Analysis of Cell Phone Near Human Head

The S-FDTD method described in Section 6.2 and 6.3 allows us to estimate the variance of the electromagnetic fields and power absorption in a model where the electrical properties are variable, such as for biological tissues. This method is much faster than the Monte Carlo method. It requires approximately twice as much time and memory as the traditional FDTD analysis, whereas the Monte Carlo method requires orders of magnitude more computer time. We validated the variances obtained using the S-FDTD method in Section 6.3.3 using a correlation coefficient of 1.0 to find an upper bound or 0.5 to provide a more accurate value. The mean values are approximately equal to those obtained using the Monte Carlo method and are not dependent on the choice of correlation coefficient.

Now we will use the S-FDTD method in 3D to estimate the variance of the SAR in the human head from a cellular telephone assuming the variation in biological tissues given in Table 6-2. We will use the same 3D head and neck model originally used in [3] for the same mobile telephone at 835MHz and 1900MHz. In [3], standard FDTD analysis was used, and no variance was calculated. The S-FDTD method will now allow us to calculate the variance in this model. The original Fortran code from [3] was updated with the S-FDTD equations, the original (untilted) Utah head model (cell size 1.974 x 1.974 x 33mm) was updated with the stochastic tissue properties, the same hand model (a block of 2/3 muscle tissue surrounding the phone on 3 sides, also assumed to vary stochastically) was used, and the original (1995 model, now outdated) cell phone

Table 6-2 835MHz - Dielectric properties from [12]. Standard deviations are from [39]

Tissue	**Specific Gravity**[1] $10^3 kg/m^3$ ρ_{densiy}	**Relative**[1] **Permittivity** ε_r	**Standard Deviation** $\sigma\{\varepsilon_r\}$	**Conductivity**[1] $\underline{\sigma}$ (S/m)	**Standard Deviation** $\sigma\{\underline{\sigma}\}$
muscle	1.04	51.76	4.33[2]	1.11	0.1[2]
fat	0.92	9.99	1.7[2]	0.17	0.06
bone	1.81	17.4	6.0	0.25	0.15
cartilage	1.10	40.69	6.69[3]	0.82	0.35[3]
Skin	1.01	35.40	4.6	0.63	0.15[3]
nerve	1.04	33.4	4.5	0.60	0.13
blood	1.06	55.5	3.2	1.86	0.10[3]
parotid gland	1.05	45.26	3.86	0.92	0.1
CSF	1.01	78.1	2.3	1.97	0.07[3]
eye humour	1.01	67.90	3.14[3]	1.68	0.08[3]
sclera	1.17	54.9	2.01	1.17	0.09
lens	1.10	36.59	2.8	0.51	0.32
pineal gland	1.05	45.26	3.32	0.92	0.10
pituitary gland	1.07	45.26	3.32	0.92	0.10
brain	1.04	45.26	3.23	0.92	0.14[3]

1) Mean values from Gandhi, Lazzi, and Furse[3, 39].
2) Scaled from Jeff Johnson's Master's Thesis (Table 3.2) [8, 39]
3) Personal Communication from Dr. Camelia Gabriel [39]

was used as in [3]. The phone is modeled as a $2.76\ x\ 5.53\ x\ 15.3\ cm$ ($14\delta_x\ x\ 28\delta_y\ x\ 51\delta_z$) plastic-coated metal box with a 3/8 wavelength whip antenna. The reason for using all of these original values rather than newer, updated phone models, for instance, is that [3] has served as the basis for numerous comparisons with other models, other codes, other phones, etc., and returning to this original model allows us to put the S-FDTD values in the context of those other comparisons, as well. Table 6-2 lists the constitutive parameters for the human tissue at 835MHz.

Figure 6-7 shows the SAR distribution for 835MHz with a $3\lambda/8$ monopole antenna. The transmit power is 600mW. The power absorbed was 318mW (53% of the power transmitted). The 1-gram SAR was averaged by summing the localized SAR values over a space of 5x5x3cells and dividing by the total weight of the tissue in those cells. This is the standard method described in [3] to compute 1-gram average from a noncubical anatomical region such as the ear.

Antenna impedance = (500 +j 472) ohms

Incident power = 600mW

Percent power absorbed = 53 %

Peak 1-gram average SAR = 1.69 W/kg

S-FDTD analysis (using a correlation coefficient of 1.0) was used to obtain the standard deviation for the SAR shown in Figure 6-8. The standard deviation for the peak 1-gram SAR was 0.76mW or about 45% of the peak 1-gram SAR. Using 1.0 for the correlation coefficient provides an upper bound on the standard deviation.

If we use a correlation coefficient of 0.5 instead of 1.0, we get the SAR variance shown in Figure 6-9. This is assumed to be a more accurate value for the variance, based

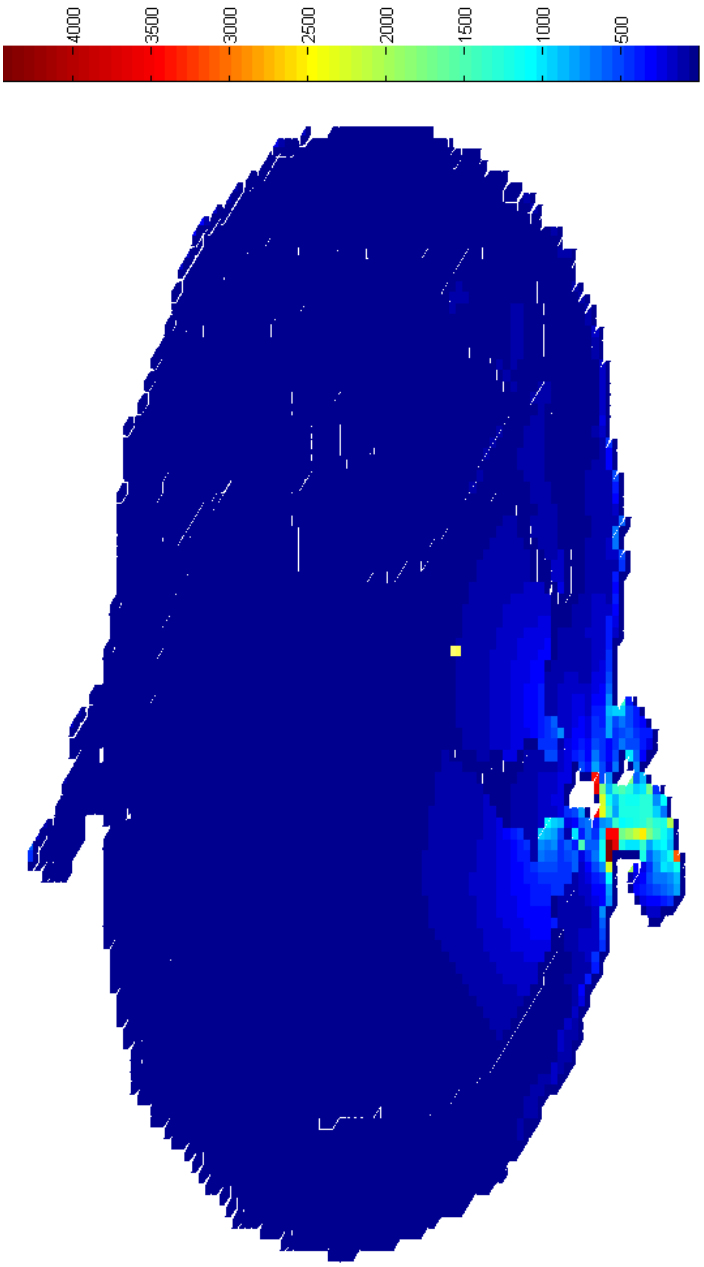

Figure 6-7 Localized SAR (mW/kg) for a radiated power = 600mW

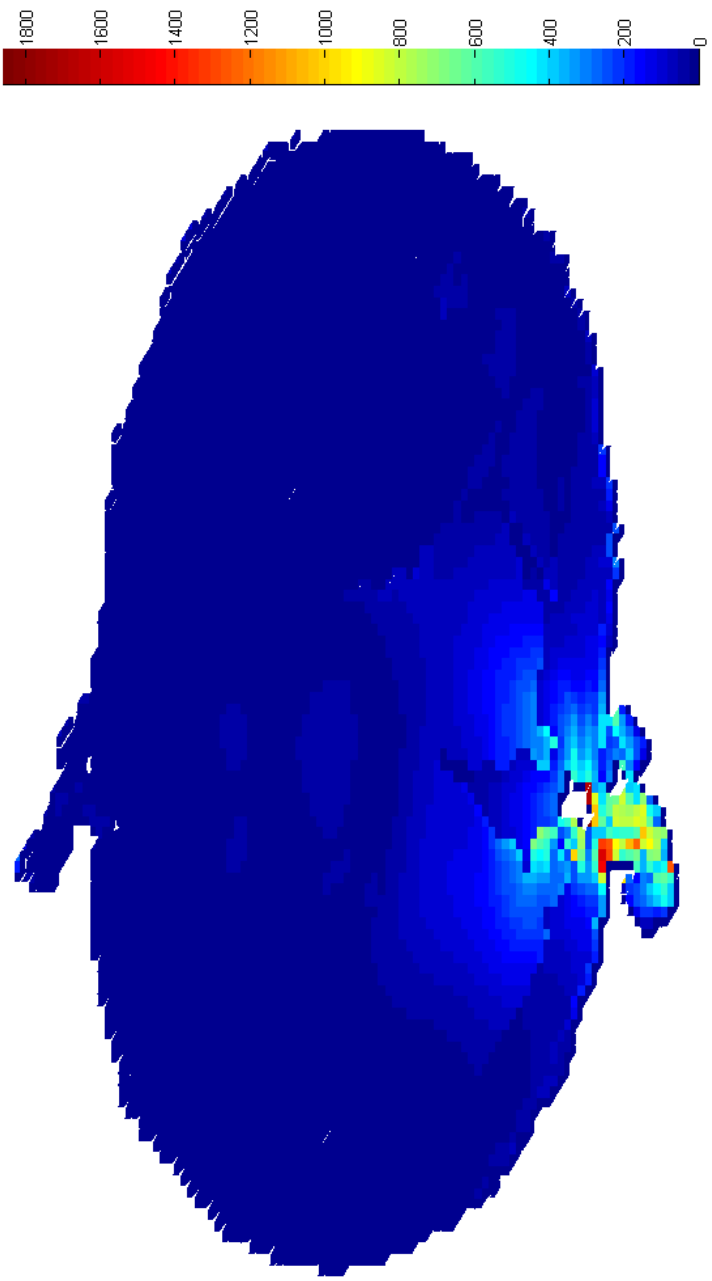

Figure 6-8 SAR (mW/kg) standard deviation using correlation coefficient = 1.0 radiated power = 600mW

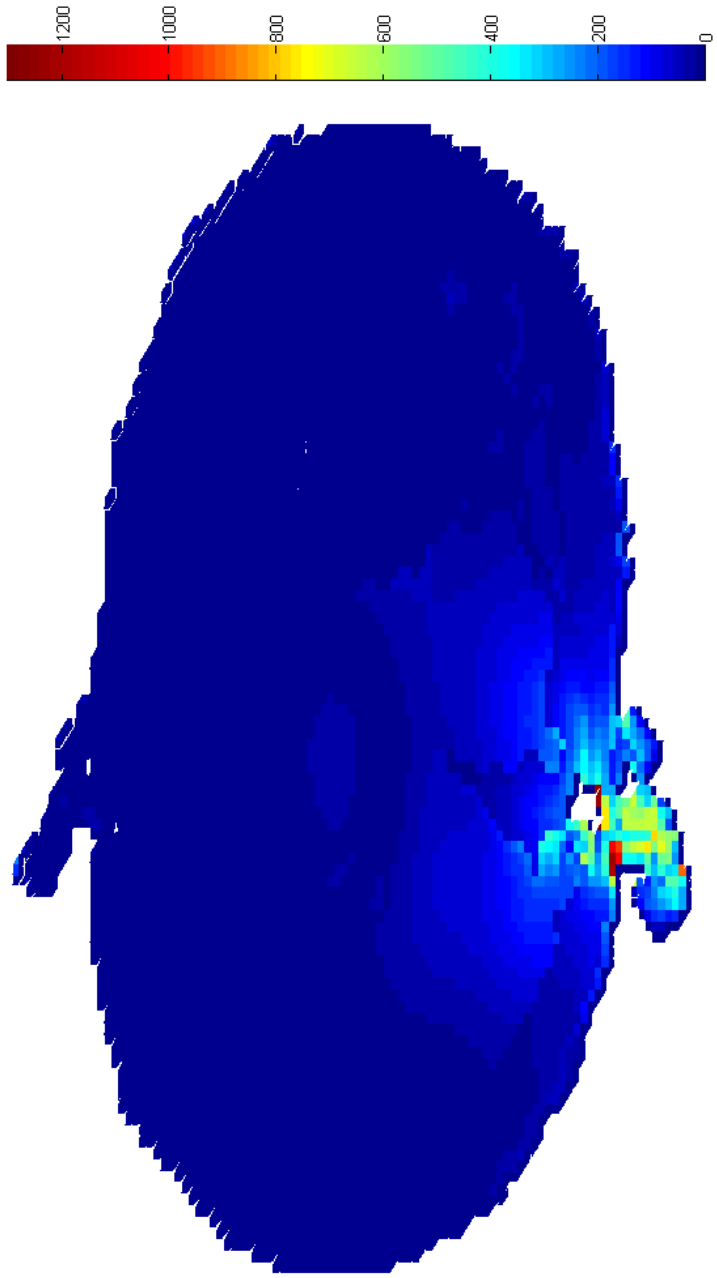

Figure 6-9 SAR (mW/kg) standard deviation using a correlation coefficient = 0.5

on the 1D validation. For this case, the standard deviation of the 1g SAR value is 0.60 W/kg compared to the value of 0.765 W/kg for the upper bound correlation coefficient of 1.0. The percent of the peak 1-gram SAR is 35.5%.

6.5 Summary

Traditional bioelectromagnetic simulations normally use the average electrical properties of tissues to obtain the average electric fields and related properties such as power absorption (defined by Specific Absorption Rate – SAR). Tissue properties are known to have statistical variation because of differences between individuals, differences within an organ, and/or measurement uncertainty, but this variation is rarely if ever reflected in the simulations. This is because the most feasible method – Monte Carlo analysis – requires significant additional computational time, orders of magnitude more than a traditional FDTD simulation, for instance. A new stochastic FDTD (S-FDTD) method has been developed to estimate the variance of the fields and SAR with minimal additional computational burden (about double that of a traditional FDTD simulation). This new S-FDTD method is used to estimate the standard deviation in a 3D model of a cell phone and adult male human head originally published in [3]. The localized SAR and peak 1-gram SAR values are evaluated using an upper bound correlation coefficient of 1.0 and a correlation coefficient of 0.5 which should give a more accurate value for the standard deviation of the SAR. Table 6-3 summarizes the results obtained for the peak 1-gram SAR in the model.

Table 6-3 Standard Deviation comparison for correlation coefficients equal to 1.0 and 0.5

Antenna	Peak 1-g SAR(W/kg) [3]	Peak 1-g SAR(W/kg)	Std Dev Corr Coef = 1.0	Std Dev Corr Coef = 0.5
3/8 Wave	1.6	1.69	0.77	0.60

6.6 Conclusions

This paper describes a new statistical FDTD (S-FDTD) method and its application to 3D analysis of cell phone and human head models with statistically varying electrical properties. S-FDTD provides a method of estimating the statistical properties of the fields and SAR in FDTD simulations in a timely way. This method shows promise for enabling routine inclusion of the statistical variability of tissues in bioelectromagnetic simulations. For simple models of block telephones with whip antennas, the standard deviation of the SAR was found to be approximately 36-45% of the peak 1-gram average.

The highest value is an upper bound, and the lower value is a more realistic approximation, probably also higher than actual values, based on validations performed in 1D. These simulations show that the variation in the fields and SAR is likely to be significant enough that it should not be ignored in many applications. For instance, when designing antennas for implantation in the body, it has already been shown that the variation of the tissues should be considered to ensure the final design will not be detuned by unanticipated changes in the body [8]. This new S-FDTD analysis also shows that this consideration may be important in cell phone evaluation. The analysis in this paper is highly preliminary. The values provided are for cellular telephones that are very different from today's models, so the SAR values are also expected to be very different. The values given are approximations – an upper bound and a rough estimate. Further work is warranted to provide closer approximations to the variation by determining more accurate

correlation coefficients to be used in the S-FDTD analysis.

The S-FDTD method is the first of its kind – a way to estimate the variability in fields, power, etc. in a complex model as a function of time and space. It may also be applied in other applications with statistically varying electrical properties such as soils and agricultural applications, sea ice, plasma, etc. It is hoped that this paper provides a starting point for further research in how statistics can be included in time domain simulations in a natural and direct way, thus opening up opportunities to further understand the impact of uncertainty in our world.

6.7 Acknowledgment

The authors gratefully acknowledge Camelia Gabriel for providing the statistical properties for the tissues.

CHAPTER 7

SUMMARY

The analysis of radio wave absorption is a continuing concern for the cell phone industry due to health effects (and associated regulations) for the person using the cell phone [1, 2]. The amount of allowable power absorbed has a strong impact on the design of the phone (antenna, electromagnetic interference, shielding, etc.). Cost and size are typically also conflicting tradeoffs. The analysis of these designs prior to the building of prototypes and the actual testing of the radio is critical to contain cost and design cycle time, so numerical simulations are routinely used in this industry. One of the unanswered questions with these simulations is how variation between individuals or uncertainty in measured tissue properties may impact the absorbed power. Studies of adults and children have shown that size of the head and thickness of the ear have a significant effect on absorbed power [3-5]. Other studies [6, 7] have shown the nonnegligible effect of head shape. Variability in tissue properties (from person to person or just because of uncertainty in the measurements) has also been shown to have a significant effect on absorbed power [8].

An approximate method for determining the statistical properties of a Finite-Difference Time-Domain (FDTD) analysis has been derived in this dissertation, allowing the determination of the mean and the variance of the field terms of the FDTD simulation

from a single run. This is much more efficient than the alternative, the Monte Carlo method. The stochastic simulator, S-FDTD, progresses in the same fashion as an FDTD simulation but with added variables for the standard deviation of both the E and the H field in each cell in the model. The 'variance wave' (in reality the square root of the variance of the field equations derived from Maxwell's equations) propagates and reflects in much the same way as the E and H waves propagate and reflect.

The method substantially speeds up stochastic analysis providing a good approximation or bound for the mean and variance of the FDTD analysis for statistically varying electrical properties with only a minor increase in computer simulation time and memory.

Chapter 3 provided information that was used in the verification of the S-FDTD analysis by providing Monte Carlo results used for comparison with the results from S-FDTD analysis. Approximations for the correlation coefficients were explored to help derive the S-FDTD equations. It was found that using a correlation coefficient of 1.0 provided an upper bound, overestimating the variance. A coefficient of 0.5 provided a closer approximation, and correlation coefficients based on the reflection coefficients in the model also provided improved approximations but at the cost of complexity of the simulation.

Chapter 4 showed that using a Taylor's series expansion of the stochastic FDTD equations, we could determine an approximation to the mean of a function with numerous random variables and then perform the same operation to approximate the variance in the Stochastic FDTD (S-FDTD) equations. The Delta method was derived and used to approximate stochastic functions of multirandom variables. For dependent random

variables, these functions would be hard to separate into simple standalone functions. This Delta method was used throughout the remainder of the dissertation in developing the S-FDTD equations, as discussed in Chapter 4. The S-FDTD equations for the fields were derived in this chapter, as well as stochastic SAR equations.

In Chapter 5, we compared Monte Carlo analysis for 1D biological models with S-FDTD analysis. The accuracy of the S-FDTD method for predicting the mean of the field and SAR values was excellent for all cases. Its accuracy for predicting the variance of the fields or SAR depended on the correlation coefficients used. Using a correlation coefficient of 1.0, the S-FDTD analysis bounded the Monte Carlo analysis, overestimating it by 800%. Using the reflection coefficient determined from the interface of each dielectric provided an even closer approximation to the Monte Carlo result sometimes underestimating by 50% and sometimes overestimating the result by 200%. The results bracketed the Monte Carlo results.

With S-FDTD analysis, we were now able to perform statistical analyses in large 3D model spaces with only minor increases in simulation time and memory. Using Monte Carlo, this type of analysis on large 3D model spaces is not practical due to the large computer resources required.

In Chapter 6, we described a 3D analysis using S-FDTD and stochastic SAR for cell phone and human head models with statistically varying electrical properties. S-FDTD provided a method for estimating the statistical properties of the fields and SAR in FDTD simulations in a timely way. A sample of the results for the analysis found in 0 for a 3/8 wave antenna with the mean 1gSAR was determined to be 1.69W/kg. The standard deviation with a correlation coefficient of 1.0 was determined to be 0.77W/kg

and with the coefficient set to 0.5, the standard deviation was found to be 0.60W/kg. The method shows promise for enabling routine inclusion of the statistical variability of tissues in bioelectromagnetic simulations. This 3D simulation showed in 0 that the variation in the fields and SAR is likely to be significant enough that it should not be ignored in many applications. This S-FDTD analysis shown in the work is highly preliminary. Further work is warranted to provide closer approximations to the variation by determining more accurate correlation coefficients to be used in the S-FDTD analysis.

The major contribution of this dissertation is the development and implementation of a stochastic FDTD method, the first of its kind. This is the first method we are aware of that efficiently enables analysis of large heterogeneous structures with statistically varying electrical properties. This provides a way to estimate the variability in fields, power, etc. in a complex model as a function of time and space. It may also be applied in other applications with statistically varying electrical properties such as soils and agricultural applications, sea ice, plasma, etc. This research provides a starting point for further research in how statistics can be included in time domain simulations in a natural and direct way, thus opening up opportunities to further understand the impact of uncertainty in our world.

APPENDIX A

THREE-DIMENSIONAL FDTD EQUATIONS

This appendix was put together to derive the 3D S-FDTD equations; the same technique for deriving the 1D equations was used; see Chapter 4. The mean field equations are just the same equations as the standard equations used for FDTD analysis as determined in Chapter 4. The input parameters are the mean values of the electrical properties of the materials used as input parameters for the simulation.

A.1 Mean

A.1.1 Faraday's Law

Maxwell's equations are the starting point for the derivation with Faraday's equation shown below which can be converted to its finite difference form:

$$\frac{\partial \mathbf{B}}{\partial t} = -\nabla x \mathbf{E} - \mathbf{M} \tag{A.1}$$

using the same notation and form of the FDTD equations found in reference [33]. With simplifying assumptions, the following approximations are arrived at, giving the mean FDTD equations. Again recall the mean is arrived at by using the mean of each of the stochastic variables within the normal FDTD equation. These equations are listed below.

$$H_x^{n+1}\left(i-1/2,j+1,k+1\right)=\frac{1-\dfrac{\mu_{\sigma^*}\Delta t}{2\mu_\mu}}{1+\dfrac{\mu_{\sigma^*}\Delta t}{2\mu_\mu}}H_x^n\left(i-1/2,j+1,k+1\right)$$

$$+\frac{\dfrac{\Delta t}{\mu_\mu}}{1+\dfrac{\mu_{\sigma^*}\Delta t}{2\mu_\mu}}\left(\begin{array}{l}\left(\dfrac{E_y^{n+1/2}\left(i-1/2,j+1,k+3/2\right)-E_y^{n+1/2}\left(i-1/2,j+1,k+1/2\right)}{\Delta z}\right)\\ -\left(\dfrac{E_z^{n+1/2}\left(i-1/2,j+3/2,k+1\right)-E_z^{n}\left(i-1/2,j+1/2,k+1\right)}{\Delta y}\right)\end{array}\right) \tag{A.2}$$

$$H_y^{n+1}\left(i,j+1/2,k+1\right)=\frac{1-\dfrac{\mu_{\sigma^*}\Delta t}{2\mu_\mu}}{1+\dfrac{\mu_{\sigma^*}\Delta t}{2\mu_\mu}}H_y^n\left(i,j+1/2,k+1\right)$$

$$+\frac{\dfrac{\Delta t}{\mu_\mu}}{1+\dfrac{\mu_{\sigma^*}\Delta t}{2\mu_\mu}}\left(\begin{array}{l}\left(\dfrac{E_z^{n+1/2}\left(i+1/2,j+1/2,k+1\right)-E_z^{n+1/2}\left(i-1/2,j+1/2,k+1\right)}{\Delta x}\right)\\ -\left(\dfrac{E_x^{n+1/2}\left(i,j+1/2,k+3/2\right)-E_x^{n}\left(i,j+1/2,k+1/2\right)}{\Delta z}\right)\end{array}\right) \tag{A.3}$$

$$H_z^{n+1}\left(i,j+1/2,k+1/2\right)=\frac{1-\frac{\mu_{\sigma^*}\Delta t}{2\mu_\mu}}{1+\frac{\mu_{\sigma^*}\Delta t}{2\mu_\mu}}H_z^n\left(i,j+1,k+1/2\right)$$

$$+\frac{\frac{\Delta t}{\mu_\mu}}{1+\frac{\mu_{\sigma^*}\Delta t}{2\mu_\mu}}\left(\begin{array}{l}\left(\frac{E_x^{n+1/2}\left(i,j+3/2,k+1/2\right)-E_x^{n+1/2}\left(i,j+1/2,k+1/2\right)}{\Delta y}\right)\\ -\left(\frac{E_y^{n+1/2}\left(i+1/2,j+1,k+1/2\right)-E_y^{n}\left(i-1/2,j+1,k+1/2\right)}{\Delta x}\right)\end{array}\right) \tag{A.4}$$

A.1.2 Ampere's Law Mean

$$E_x^{n+1/2}\left(i,j+1/2,k+1/2\right)-\frac{1-\frac{\mu_\sigma\Delta t}{2\mu_\varepsilon}}{1+\frac{\mu_\sigma\Delta t}{2\mu_\varepsilon}}E_x^{n-1/2}\left(i,j+1/2,k+1/2\right)=$$

$$\frac{\frac{\Delta t}{\mu_\varepsilon}}{1+\frac{\mu_\sigma\Delta t}{2\mu_\varepsilon}}\left(\frac{\left(H_z^n\left(j+1\right)-H_z^n\left(j\right)\right)}{\Delta y}-\frac{H_y^n\left(k+1\right)-H_y^n\left(k\right)}{\Delta z}\right)$$

$$E_y^{n+1/2}\left(i-1/2,j+1,k+1/2\right)-\frac{1-\frac{\mu_\sigma\Delta t}{2\mu_\varepsilon}}{1+\frac{\mu_\sigma\Delta t}{2\mu_\varepsilon}}E_y^{n-1/2}\left(i-1/2,j+1,k+1/2\right)=$$

$$\frac{\frac{\Delta t}{\mu_\varepsilon}}{1+\frac{\mu_\sigma\Delta t}{2\mu_\varepsilon}}\left(\frac{\left(H_x^n\left(k+1\right)-H_x^n\left(k\right)\right)}{\Delta z}-\frac{H_z^n\left(i\right)-H_z^n\left(i-1\right)}{\Delta x}\right)$$

$$E_z^{n+1/2}\left(i-1/2,j+1/2,k+1\right)-\frac{1-\frac{\mu_\sigma\Delta t}{2\mu_\varepsilon}}{1+\frac{\mu_\sigma\Delta t}{2\mu_\varepsilon}}E_z^{n-1/2}\left(i-1/2,j+1/2,k+1\right)=$$

$$\frac{\frac{\Delta t}{\mu_\varepsilon}}{1+\frac{\mu_\sigma\Delta t}{2\mu_\varepsilon}}\left(\frac{\left(H_y^n\left(i\right)-H_z^n\left(i-1\right)\right)}{\Delta x}-\frac{H_x^n\left(j+1\right)-H_x^n\left(j\right)}{\Delta y}\right)$$

A.2 Variance

We next look to the variance of Maxwell's equations.

A.2.1 Faraday's Law

Starting with equation (A.5), take the variance of both sides of the equation. Doing this maintains the time and spatial grids in their proper form:

$$\sigma^2\left\{H_x^{n+1}\left(i-1/2,j+1,k+1\right)-\frac{1-\frac{\sigma^*\Delta t}{2\mu}}{1+\frac{\sigma^*\Delta t}{2\mu}}H_x^n\left(i-1/2,j+1,k+1\right)\right\}=$$

$$\sigma^2\left\{\frac{\frac{\Delta t}{\mu}}{1+\frac{\sigma^*\Delta t}{2\mu}}\left(\begin{array}{c}\frac{\left(E_y^{n+1/2}\left(k+3/2\right)-E_y^{n+1/2}\left(k+1/2\right)\right)}{\Delta z}\\ -\frac{E_z^{n+1/2}\left(j+3/2\right)-E_z^{n+1/2}\left(j+1/2\right)}{\Delta y}\end{array}\right)\right\} \tag{A.5}$$

Using the following identities:

$$\sigma^2\{X \pm Y\} = \sigma^2\{X\} + \sigma^2\{Y\} \pm Cov\{X,Y\}$$

$$\sigma^2\{aX\} = a^2\sigma^2\{X\}$$

Focus for now on the left side of the stochastic field equation:

$$\sigma^2\left\{H_x^{n+1}(i-1/2,j+1,k+1) - \frac{1-\frac{\sigma^*\Delta t}{2\mu}}{1+\frac{\sigma^*\Delta t}{2\mu}} H_x^n(i-1/2,j+1,k+1)\right\} \tag{A.6}$$

Expanding this equation we arrive at the following equation:

$$\sigma^2\left\{H_x^{n+1}(i-1/2,j+1,k+1)\right\} + \sigma^2\left\{\frac{1-\frac{\Delta t\sigma^*}{2\mu}}{1+\frac{\Delta t\sigma^*}{2\mu}} H_x^{n+1}(i-1/2,j+1,k+1)\right\}$$

$$-2Cov\left\{H_x^{n+1}(i-1/2,j+1,k+1), \frac{1-\frac{\Delta t\sigma^*}{2\mu}}{1+\frac{\Delta t\sigma^*}{2\mu}} H_x^{n+1}(i-1/2,j+1,k+1)\right\} \tag{A.7}$$

Using this next identity:

$$Cov\{X,Y\} = \rho_{X,Y}\sigma\{X\}\sigma\{Y\}$$

We change the equation to the following:

$$\sigma^2\left\{H_x^{n+1}\left(i-1/2,j+1,k+1\right)\right\}-$$

$$2\rho_{H_x^{n+1}(i-1/2,j+1,k+1),\frac{1-\frac{\Delta t\sigma^*}{2\mu}}{1+\frac{\Delta t\sigma^*}{2\mu}}H_x^n(i-1/2,j+1,k+1)}$$

$$\sigma\left\{\frac{1-\frac{\Delta t\sigma^*}{2\mu}}{1+\frac{\Delta t\sigma^*}{2\mu}}H_x^n\left(i-1/2,j+1,k+1\right)\right\}\sigma[H_x^{n+1}\left(i-1/2,j+1,k+1\right)]+$$

$$\sigma^2\left\{\frac{1-\frac{\Delta t\sigma^*}{2\mu}}{1+\frac{\Delta t\sigma^*}{2\mu}}H_x^n\left(i-1/2,j+1,k+1\right)\right\} \tag{A.8}$$

It can be shown that the correlation coefficient in the above equation is approximately equal to one. So the form changes to the following equation:

$$\sigma^2\left\{H_x^{n+1}\left(i-1/2,j+1,k+1\right)\right\}-$$

$$\sigma\left\{\frac{1-\frac{\Delta t\sigma^*}{2\mu}}{1+\frac{\Delta t\sigma^*}{2\mu}}H_x^n\left(i-1/2,j+1,k+1\right)\right\}\sigma\left\{H_x^{n+1}\left(i-1/2,j+1,k+1\right)\right\}+ \tag{A.9}$$

$$\sigma^2\left\{\frac{1-\frac{\Delta t\sigma^*}{2\mu}}{1+\frac{\Delta t\sigma^*}{2\mu}}H_x^n\left(i-1/2,j+1,k+1\right)\right\}$$

This equation is a perfect square so we change the form to:

$$\left(\sigma\left\{ H_x^{n+1}\left(i-1/2, j+1, k+1\right)\right\} - \sigma\left\{ \frac{1-\frac{\Delta t\sigma^*}{2\mu}}{1+\frac{\Delta t\sigma^*}{2\mu}} H_x^n\left(i-1/2, j+1, k+1\right)\right\} \right)^2 \quad \text{(A.10)}$$

The second variance term is a function of three stochastic variables. Using the Delta method developed in Section 4.1 we find the second variance term in the above equation. The approximate equation is repeated below next:

$$\sum_{i=1}^{n}\sum_{j=1}^{n} \frac{\partial g}{\partial x_i}\frac{\partial g}{\partial x_j}\bigg|_{\mu_{x_1},\mu_{x_2},\ldots,\mu_{x_n}} E\left\{(x_i-\mu_{x_i})(x_j-\mu_{x_j})\right\}$$

Performing all the operations in the above equation on equation (A.11):

$$\sigma^2\left\{ \frac{1-\frac{\Delta t\sigma^*}{2\mu}}{1+\frac{\Delta t\sigma^*}{2\mu}} H_x^n\left(i-1/2, j+1, k+1\right)\right\} \quad \text{(A.11)}$$

1) Magnetic conductivity variance term:

$$\left\{ \frac{\delta}{\delta\sigma^*}\left\{ \frac{1-\frac{\Delta t\sigma^*}{2\mu}}{1+\frac{\Delta t\sigma^*}{2\mu}} H_x^n\left(i-1/2, j+1, k+1\right)\right\}\right\}^2 \sigma^2\left\{\sigma^*\right\}\bigg|_{\mu_\mu,\mu_{\sigma^*},\mu_H}$$

equals:

$$\frac{16\Delta t^2 \mu_\mu^2 H_x^n \left(i-1/2, j+1, k+1\right)^2}{\left(2\mu_\mu + \Delta t \mu_{\sigma^*}\right)^4} \sigma^2 \left\{\sigma^*\right\}$$

2) Permeability variance term:

$$\left\{ \frac{\delta}{\delta \mu} \left\{ \frac{1-\dfrac{\Delta t \sigma^*}{2\mu}}{1+\dfrac{\Delta t \sigma^*}{2\mu}} H_x^n \left(i-1/2, j+1, k+1\right) \right\} \right\}^2 \sigma^2 \left\{\mu\right\} \Bigg|_{\mu_\mu, \mu_{\sigma^*}, \mu_H}$$

equals:

$$\frac{16\Delta t^2 \mu_{\sigma^*}^2 H_x^n \left(i-1/2, j+1, k+1\right)^2}{\left(2\mu_\mu + \Delta t \mu_{\sigma^*}\right)^4} \sigma^2 \left\{\mu\right\}$$

3) The H field variance term:

$$\left\{ \frac{\delta}{\delta H} \left\{ \frac{1-\dfrac{\Delta t \sigma^*}{2\mu}}{1+\dfrac{\Delta t \sigma^*}{2\mu}} H_x^n \left(i-1/2, j+1, k+1\right) \right\} \right\}^2 \sigma^2 \left\{H_x^n \left(i-1/2, j+1, k+1\right)\right\} \Bigg|_{\mu_\mu, \mu_{\sigma^*}, \mu_H}$$

equals:

$$\frac{\left(2\mu_{\mu}-\Delta t\mu_{\sigma^*}\right)^2}{\left(2\mu_{\mu}+\Delta t\mu_{\sigma^*}\right)^2}\sigma^2\left\{H_x^n\left(i-1/2,j+1,k+1\right)\right\}$$

We next perform the covariance terms:

4) The $Cov\{\sigma^*,\mu\}$:

$$2\left\{\begin{array}{l}\dfrac{\delta}{\delta\sigma^*}\left\{\dfrac{1-\dfrac{\Delta t\sigma^*}{2\mu}}{1+\dfrac{\Delta t\sigma^*}{2\mu}}H_x^n\left(i-1/2,j+1,k+1\right)\right\} \\ \qquad\qquad \dfrac{\delta}{\delta\mu}\left\{\dfrac{1-\dfrac{\Delta t\sigma^*}{2\mu}}{1+\dfrac{\Delta t\sigma^*}{2\mu}}H_x^n\left(i-1/2,j+1,k+1\right)\right\}\end{array}\right\}Cov\{\sigma^*,\mu\}\Bigg|_{\mu_{\mu},\mu_{\sigma^*},\mu_H}$$

equals:

$$-\frac{32\Delta t^2\mu_{\mu}\mu_{\sigma^*}H_x^n\left(i-1/2,j+1,k+1\right)^2}{\left(2\mu_{\mu}+\Delta t\mu_{\sigma^*}\right)^4}\rho_{\sigma^*,\mu}\sigma\{\mu\}\sigma\{\sigma^*\}$$

5) The $Cov\{\sigma^*,H_x^n\left(i-1/2,j+1,k+1\right)\}$:

$$2\left\{\begin{array}{l}\dfrac{\delta}{\delta\sigma^*}\left\{\dfrac{1-\dfrac{\Delta t\sigma^*}{2\mu}}{1+\dfrac{\Delta t\sigma^*}{2\mu}}H_x^n\left(i-1/2,j+1,k+1\right)\right\} \\ \dfrac{\delta}{\delta H}\left\{\dfrac{1-\dfrac{\Delta t\sigma^*}{2\mu}}{1+\dfrac{\Delta t\sigma^*}{2\mu}}H_x^n\left(i-1/2,j+1,k+1\right)\right\}\end{array}\right\} Cov\left\{\sigma^*, H_x^n\left(i-1/2,j+1,k+1\right)\right\}\Big|_{\mu_\mu,\mu_{\sigma^*},\mu_H}$$

equals:

$$-\frac{8\Delta t\mu_\mu\left(2\mu_\mu-\Delta t\mu_{\sigma^*}\right)}{\left(2\mu_\mu+\Delta t\mu_{\sigma^*}\right)^3}\rho_{\sigma^*,H}\sigma\left\{\sigma^*\right\}$$

$$\sigma\left\{H_x^n\left(i-1/2,j+1,k+1\right)\right\}H_x^n\left(i-1/2,j+1,k+1\right)$$

6) The $Cov\left\{\mu, H_x^n\left(i-1/2,j+1,k+1\right)\right\}$:

$$2\left\{\begin{array}{l}\dfrac{\delta}{\delta\mu}\left\{\dfrac{1-\dfrac{\Delta t\sigma^*}{2\mu}}{1+\dfrac{\Delta t\sigma^*}{2\mu}}H_x^n\left(i-1/2,j+1,k+1\right)\right\} \\ \dfrac{\delta}{\delta H}\left\{\dfrac{1-\dfrac{\Delta t\sigma^*}{2\mu}}{1+\dfrac{\Delta t\sigma^*}{2\mu}}H_x^n\left(i-1/2,j+1,k+1\right)\right\}\end{array}\right\} Cov\left\{\sigma^*, H_x^n\left(i-1/2,j+1,k+1\right)\right\}\Big|_{\mu_\mu,\mu_{\sigma^*},\mu_H}$$

equals:

$$8\Delta t\mu_{\sigma^*}\frac{(2\mu_\mu-\Delta t\mu_{\sigma^*})}{(2\mu_\mu+\Delta t\mu_{\sigma^*})^3}\rho_{\mu,H}\sigma\{\mu\}\sigma\left\{H_x^n(i-1/2,j+1,k+1)\right\}$$
$$H_x^n(i-1/2,j+1,k+1)$$

Adding all the above terms together yields the following equation:

$$\frac{\left(2\mu_\mu-\Delta t\mu_{\sigma^*}\right)^2}{\left(2\mu_\mu+\Delta t\mu_{\sigma^*}\right)^2}\sigma^2\left\{H_x^n(i-1/2,j+1,k+1)\right\}$$

$$+8\Delta t\mu_{\sigma^*}\frac{2\mu_\mu-\Delta t\mu_{\sigma^*}}{\left(2\mu_\mu+\Delta t\mu_{\sigma^*}\right)^3}\rho_{\mu,H}\sigma\{\mu\}\sigma\left\{H_x^n(i-1/2,j+1,k+1)\right\}H_x^n(i-1/2,j+1,k+1)$$

$$-8\Delta t\mu_\mu\frac{2\mu_\mu-\Delta t\mu_{\sigma^*}}{\left(2\mu_\mu+\Delta t\mu_{\sigma^*}\right)^3}\rho_{\sigma^*,H}\sigma\{\sigma^*\}\sigma\left\{H_x^n(i-1/2,j+1,k+1)\right\}H_x^n(i-1/2,j+1,k+1)$$

$$-\frac{32\Delta t^2\mu_\mu\mu_{\sigma^*}}{\left(2\mu_\mu+\Delta t\mu_{\sigma^*}\right)^4}\rho_{\sigma^*,\mu}\sigma\{\mu\}\sigma\{\sigma^*\}H_x^n(i-1/2,j+1,k+1)^2$$

$$+\frac{16\Delta t^2\mu_{\sigma^*}^2}{\left(2\mu_\mu+\Delta t\mu_{\sigma^*}\right)^4}\sigma^2\{\mu\}H_x^n(i-1/2,j+1,k+1)^2$$

$$+\frac{16\Delta t^2\mu_\mu^2}{\left(2\mu_\mu+\Delta t\mu_{\sigma^*}\right)^4}\sigma^2\{\sigma^*\}H_x^n(i-1/2,j+1,k+1)^2$$

Combining terms and simplifying:

$$\frac{\left(2\mu_{\mu}-\Delta t\mu_{\sigma^*}\right)^2}{\left(2\mu_{\mu}+\Delta t\mu_{\sigma^*}\right)^2}\sigma^2\left\{H_x^n\left(i-1/2,j+1,k+1\right)\right\}$$

$$+\frac{8\Delta t(2\mu_{\mu}-\Delta t\mu_{\sigma^*})\left(\mu_{\sigma^*}\rho_{\mu,H}\sigma\{\mu\}-\mu_{\mu}\rho_{\sigma^*,H}\sigma\{\sigma^*\}\right)}{\left(2\mu_{\mu}+\Delta t\mu_{\sigma^*}\right)^3} \tag{A.12}$$

$$\sigma\left\{H_x^n\left(i-1/2,j+1,k+1\right)\right\}H_x^n\left(i-1/2,j+1,k+1\right)$$

$$-16\Delta t^2\frac{\left(\mu_{\sigma^*}^2\sigma^2\{\mu\}+2\mu_{\mu}\mu_{\sigma^*}\rho_{\sigma^*,\mu}\sigma\{\mu\}\sigma\{\sigma^*\}+\mu_{\mu}^2\sigma^2\{\sigma^*\}\right)}{\left(2\mu_{\mu}+\Delta t\mu_{\sigma^*}\right)^4}H_x^n\left(i-1/2,j+1,k+1\right)^2$$

We need to complete the square on equation (A.12):

$$\frac{\left(2\mu_{\mu}-\Delta t\mu_{\sigma^*}\right)^2}{\left(2\mu_{\mu}+\Delta t\mu_{\sigma^*}\right)^2}\sigma^2\left\{H_x^n\left(i-1/2,j+1,k+1\right)\right\}$$

$$+\frac{8\Delta t\left(2\mu_{\mu}-\Delta t\mu_{\sigma^*}\right)\left(\mu_{\sigma^*}\rho_{\mu,H}\sigma\{\mu\}-\mu_{\mu}\rho_{\sigma^*,H}\sigma\{\sigma^*\}\right)}{\left(2\mu_{\mu}+\Delta t\mu_{\sigma^*}\right)^3}$$

$$\sigma\left\{H_x^n\left(i-1/2,j+1,k+1\right)\right\}H_x^n\left(i-1/2,j+1,k+1\right)$$

$$+\frac{4^2\Delta t^2\left(\mu_{\sigma^*}\rho_{\mu,H}\sigma\{\mu\}-\mu_{\mu}\rho_{\sigma^*,H}\sigma\{\sigma^*\}\right)^2}{\left(2\mu_{\mu}+\Delta t\mu_{\sigma^*}\right)^4}H_x^n\left(i-1/2,j+1,k+1\right)^2$$

$$-\frac{4^2\Delta t^2\left(\mu_{\sigma^*}\rho_{\mu,H}\sigma\{\mu\}-\mu_{\mu}\rho_{\sigma^*,H}\sigma\{\sigma^*\}\right)^2}{\left(2\mu_{\mu}+\Delta t\mu_{\sigma^*}\right)^4}H_x^n\left(i-1/2,j+1,k+1\right)^2$$

$$-\frac{16\Delta t^2(\mu_{\sigma^*}^2\sigma^2\{\mu\}+2\mu_m\mu_{\sigma^*}\rho_{\sigma^*,\mu}\sigma\{\mu\}\sigma\{\sigma^*\}+\mu_m^2\sigma^2\{\sigma^*\})}{\left(2\mu_m+\Delta t\mu_{\sigma^*}\right)^4}$$

$$H_x^n\left(i-1/2,j+1,k+1\right)^2 \tag{A.13}$$

Now simplifying more:

$$\left(\begin{array}{l}\dfrac{\left(2\mu_{\mu}-\Delta t\mu_{\sigma^*}\right)}{\left(2\mu_{\mu}+\Delta t\mu_{\sigma^*}\right)}\sigma\left\{H_x^n\left(i-1/2,j+1,k+1\right)\right\} \\ \\ \quad +\dfrac{4\Delta t\left(\mu_{\sigma^*}\rho_{\mu,H}\sigma\{\mu\}-\mu_{\mu}\rho_{\sigma^*,H}\sigma\left\{\sigma^*\right\}\right)}{\left(2\mu_{\mu}+\Delta t\mu_{\sigma^*}\right)^2}H_x^n\left(i-1/2,j+1,k+1\right)\end{array}\right)^2 \tag{A.14}$$

$$-\frac{16\Delta t^2 H_x^n\left(i-1/2,j+1,k+1\right)^2}{\left(2\mu_{\mu}+\Delta t\mu_{\sigma^*}\right)^4}\left(\begin{array}{l}2\mu_m\mu_{\sigma^*}\left(\rho_{\sigma^*,\mu}-\rho_{\mu,H}\rho_{\sigma^*,H}\right)\sigma\{\mu\}\sigma\left\{\sigma^*\right\} \\ +\mu_{\sigma^*}^2\left(\rho_{\mu,H}^2\sigma\{\mu\}^2+\sigma^2\{\mu\}\right) \\ +\mu_{\mu}^2\left(\rho_{\sigma^*,H}^2\sigma\left\{\sigma^*\right\}^2+\sigma^2\left\{\sigma^*\right\}\right)\end{array}\right)$$

We are trying to find:

$$\sigma\left\{\frac{1-\dfrac{\Delta t\sigma^*}{2\mu}}{1+\dfrac{\Delta t\sigma^*}{2\mu}}H_x^n\left(i-1/2,j+1,k+1\right)\right\}$$

Which is the square-root of expression(A.14). We can use an approximation for $\sqrt{1\pm x}\approx 1\pm x/2$. Now, getting the expression(A.14) into the form of $\sqrt{1\pm x}$ yields the next:

$$\frac{\left(2\mu_{\mu}-\Delta t\mu_{\sigma^*}\right)}{\left(2\mu_{\mu}+\Delta t\mu_{\sigma^*}\right)}\sigma\left\{H_x^n\left(i-1/2,j+1,k+1\right)\right\}$$

$$+\frac{4\Delta t\left(\mu_{\sigma^*}\rho_{\mu,H}\sigma\{\mu\}-\mu_{\mu}\rho_{\sigma^*,H}\sigma\left\{\sigma^*\right\}\right)}{\left(2\mu_{\mu}+\Delta t\mu_{\sigma^*}\right)^2}H_x^n\left(i-1/2,j+1,k+1\right)$$

$$\sqrt{1-\frac{\dfrac{16\Delta t^2H_x^n\left(i-1/2,j+1,k+1\right)^2}{(2\mu_{\mu}+\Delta t\mu_{\sigma^*})^4}\left(\begin{array}{l}2\mu_{\mu}\mu_{\sigma^*}\left(\rho_{\sigma^*,\mu}-\rho_{\mu,H}\rho_{\sigma^*,H}\right)\sigma\{\mu\}\sigma\left\{\sigma^*\right\}\\+\mu_{\sigma^*}^2\left(\rho_{\mu,H}^2\sigma\{\mu\}^2+\sigma^2\{\mu\}\right)\\+\mu_{\mu}^2\left(\rho_{\sigma^*,H}^2\sigma\left\{\sigma^*\right\}^2+\sigma^2\left\{\sigma^*\right\}\right)\end{array}\right)}{\left(\begin{array}{l}\dfrac{\left(2\mu_{\mu}-\Delta t\mu_{\sigma^*}\right)}{\left(2\mu_{\mu}+\Delta t\mu_{\sigma^*}\right)}\sigma\left\{H_x^n\left(i-1/2,j+1,k+1\right)\right\}\\\\+\dfrac{4\Delta t(\mu_{\sigma^*}\rho_{\mu,H}\sigma\{\mu\}-\mu_{\mu}\rho_{\sigma^*,H}\sigma\left\{\sigma^*\right\})}{\left(2\mu_{\mu}+\Delta t\mu_{\sigma^*}\right)^2}H_x^n\left(i-1/2,j+1,k+1\right)\end{array}\right)^2}}$$

Assuming the second term under the radical is close to zero, this is seen by an analysis of the magnitude of the terms involves in the equation, the multiplier in the second term under the radical. Δt is very small and it is squared in the numerator and in the denominator; the μ_m term's magnitude is much larger than Δt and therefore, the Δt term can be neglected so as long $\Delta t^2 << 2^4\mu_{\mu}^4$:

$$\frac{16\Delta t^2}{(2\mu_{\mu}+\Delta t\mu_{\sigma^*})^4}$$

due to the factors involved in the equation, we then are left with:

$$\frac{\left(2\mu_{\mu}-\Delta t\mu_{\sigma^*}\right)}{\left(2\mu_{\mu}+\Delta t\mu_{\sigma^*}\right)}\sigma\left\{H_x^n\left(i-1/2,j+1,k+1\right)\right\} + \frac{4\Delta t\left(\mu_{\sigma^*}\rho_{\mu,H}\sigma\{\mu\}-\mu_{\mu}\rho_{\sigma^*,H}\sigma\{\sigma^*\}\right)}{\left(2\mu_{\mu}+\Delta t\mu_{\sigma^*}\right)^2}H_x^n\left(i-1/2,j+1,k+1\right) \tag{A.15}$$

Completing the approximation of the left side of Faraday's equation leaves the following equation:

$$\left(\begin{array}{c}\sigma\left\{H_x^n\left(i-1/2,j+1,k+1\right)\right\}-\frac{\left(2\mu_{\mu}-\Delta t\mu_{\sigma^*}\right)}{\left(2\mu_{\mu}+\Delta t\mu_{\sigma^*}\right)}\sigma\left\{H_x^n\left(i-1/2,j+1,k+1\right)\right\} \\ -\frac{4\Delta t\left(\mu_{\sigma^*}\rho_{\mu,H}\sigma\{\mu\}-\mu_{\mu}\rho_{\sigma^*,H}\sigma\{\sigma^*\}\right)}{\left(2\mu_{\mu}+\Delta t\mu_{\sigma^*}\right)^2}H_x^n\left(i-1/2,j+1,k+1\right)\end{array}\right)^2 \tag{A.16}$$

Now we will deal with the right-hand side of (A.5) repeated next:

$$\sigma^2\left\{\frac{\frac{\Delta t}{\mu}}{1+\frac{\sigma^*\Delta t}{2\mu}}\left(\frac{\left(E_y^{n+1/2}\left(k+3/2\right)-E_y^n\left(k+1/2\right)\right)}{\Delta z}-\frac{E_z^{n+1/2}\left(j+3/2\right)-E_z^n\left(j+1/2\right)}{\Delta y}\right)\right\}$$

We will need to apply the Delta approximation to the above equation due to the inability of separating the equation, which we perform next:

$$\sum_{i=1}^{n}\sum_{j=1}^{n}\frac{\partial g}{\partial x_i}\frac{\partial g}{\partial x_j}\bigg|_{\mu_{x_1},\mu_{x_2},\ldots,\mu_{x_n}} E\left\{(x_i-\mu_{x_i})(x_j-\mu_{x_j})\right\}$$

Combining all the terms for the right-hand side of the equation:

$$-\frac{8\Delta t^2}{\Delta z^2\left(2\mu_\mu+\Delta t\mu_{\sigma^*}\right)^2}\rho_{E_y^{n+1/2}(k+3/2),E_y^{n+1/2}(k+1/2)}\sigma\left\{E_y^{n+1/2}\left(k+1/2\right)\right\}\sigma\left\{E_y^{n+1/2}\left(k+3/2\right)\right\}$$

$$-\frac{8\Delta t^2}{\Delta y\Delta z\left(2\mu_\mu+\Delta t\mu_{\sigma^*}\right)^2}\rho_{E_y^{n+1/2}(k+1/2),E_z^{n+1/2}(j+1/2)}\sigma\left\{E_y^{n+1/2}\left(k+1/2\right)\right\}\sigma\left\{E_z^{n+1/2}\left(j+1/2\right)\right\}$$

$$+\frac{8\Delta t^2}{\Delta y\Delta z\left(2\mu_\mu+\Delta t\mu_{\sigma^*}\right)^2}\rho_{E_y^{n+1/2}(k+3/2),E_z^{n+1/2}(j+1/2)}\sigma\left\{E_y^{n+1/2}\left(k+3/2\right)\right\}\sigma\left\{E_z^{n+1/2}\left(j+1/2\right)\right\}$$

$$+\frac{8\Delta t^2}{\Delta y\Delta z\left(2\mu_\mu+\Delta t\mu_{\sigma^*}\right)^2}\rho_{E_y^{n+1/2}(k+1/2),E_z^{n+1/2}(j+3/2)}\sigma\left\{E_y^{n+1/2}\left(k+1/2\right)\right\}\sigma\left\{E_z^{n+1/2}\left(j+3/2\right)\right\}$$

$$-\frac{8\Delta t^2}{\Delta y\Delta z\left(2\mu_\mu+\Delta t\mu_{\sigma^*}\right)^2}\rho_{E_y^{n+1/2}(k+3/2),E_z^{n+1/2}(j+3/2)}\sigma\left\{E_y^{n+1/2}\left(k+3/2\right)\right\}\sigma\left\{E_z^{n+1/2}\left(j+3/2\right)\right\}$$

$$-\frac{8\Delta t^2}{\Delta y^2\left(2\mu_\mu+\Delta t\mu_{\sigma^*}\right)^2}\rho_{E_z^{n+1/2}(j+3/2),E_z^{n+1/2}(j+1/2)}\sigma\left\{E_z^{n+1/2}\left(j+1/2\right)\right\}\sigma\left\{E_z^{n+1/2}\left(j+3/2\right)\right\}$$

$$+\frac{4\Delta t^2}{\Delta z^2\left(2\mu_\mu+\Delta t\mu_{\sigma^*}\right)^2}\sigma^2\left\{E_y^{n+1/2}\left(k+1/2\right)\right\}+\frac{4\Delta t^2}{\Delta z^2\left(2\mu_\mu+\Delta t\mu_{\sigma^*}\right)^2}\sigma^2\left\{E_y^{n+1/2}\left(k+3/2\right)\right\}$$

$$+\frac{4\Delta t^2}{\Delta y^2\left(2\mu_\mu+\Delta t\mu_{\sigma^*}\right)^2}\sigma^2\left\{E_z^{n+1/2}\left(j+1/2\right)\right\}+\frac{4\Delta t^2}{\Delta y^2\left(2\mu_\mu+\Delta t\mu_{\sigma^*}\right)^2}\sigma^2\left\{E_z^{n+1/2}\left(j+3/2\right)\right\}$$

$$+16\Delta t^2\frac{-\Delta yE_y^{n+1/2}\left(k+1/2\right)+\Delta yE_y^{n+1/2}\left(k+3/2\right)+\Delta zE_z^{n+1/2}\left(j+1/2\right)-\Delta zE_z^{n+1/2}\left(j+3/2\right)}{\Delta y\Delta z^2\left(2\mu_\mu+\Delta t\mu_{\sigma^*}\right)^3}$$

$$\rho_{\mu,E_y^{n+1/2}(k+1/2)}\sigma\{\mu\}\sigma\left\{E_y^{n+1/2}\left(k+1/2\right)\right\}$$

$$+\frac{8\Delta t^3\left(\Delta yE_y^{n+1/2}\left(k+3/2\right)-\Delta yE_y^{n+1/2}\left(k+1/2\right)+\Delta zE_z^{n+1/2}\left(j+1/2\right)-\Delta zE_z^{n+1/2}\left(j+3/2\right)\right)}{\Delta y\Delta z^2\left(2\mu_\mu+\Delta t\mu_{\sigma^*}\right)^3}$$

$$\rho_{\sigma^*,E_y^{n+1/2}(k+1/2)}\sigma\left\{\sigma^*\right\}\sigma\left\{E_y^{n+1/2}\left(k+1/2\right)\right\}$$

$$+\frac{16\Delta t^2(\Delta yE_y^n\left(k+1/2\right)-\Delta yE_y^n\left(k+3/2\right)-\Delta zE_z^n\left(j+1/2\right)+\Delta zE_z^n\left(j+3/2\right))}{\Delta y\Delta z^2\left(2\mu_\mu+\Delta t\mu_{\sigma^*}\right)^3}$$

$$\rho_{\mu,E_y^n(k+3/2)}\sigma\{\mu\}\sigma\left\{E_y^n\left(k+3/2\right)\right\}$$

$$+\frac{8\Delta t^3\left(\Delta yE_y^{n+1/2}\left(k+1/2\right)-\Delta yE_y^{n+1/2}\left(k+3/2\right)-\Delta zE_z^{n+1/2}\left(j+1/2\right)+\Delta zE_z^{n+1/2}\left(j+3/2\right)\right)}{\Delta y\Delta z^2\left(2\mu_\mu+\Delta t\mu_{\sigma^*}\right)^3}$$

$$\rho_{\sigma^*,E_y^{n+1/2}(k+3/2)}\sigma\left\{\sigma^*\right\}\sigma\left\{E_y^{n+1/2}\left(k+3/2\right)\right\}$$

$$+\frac{16\Delta t^2\left(\Delta yE_y^{n+1/2}\left(k+1/2\right)-\Delta yE_y^{n+1/2}\left(k+3/2\right)-\Delta zE_z^{n+1/2}\left(j+1/2\right)+\Delta zE_z^{n+1/2}\left(j+3/2\right)\right)}{\Delta y^2\Delta z\left(2\mu_\mu+\Delta t\mu_{\sigma^*}\right)^3}$$

$$\rho_{\mu,E_z^{n+1/2}(j+1/2)}\sigma\{\mu\}\sigma\left\{E_z^{n+1/2}\left(j+1/2\right)\right\}$$

$$+(\frac{8\Delta t^3\left(\Delta yE_y^{n+1/2}\left(k+1/2\right)-\Delta yE_y^{n+1/2}\left\{k+3/2\right\}-\Delta zE_z^{n+1/2}\left(j+1/2\right)+\Delta zE_z^{n+1/2}\left(j+3/2\right)\right)}{\Delta y^2\Delta z\left(2\mu_\mu+\Delta t\mu_{\sigma^*}\right)^3}$$

$$\rho_{\sigma^*,E_z^{n+1/2}(j+1/2)}\sigma\left\{\sigma^*\right\}\sigma\left\{E_z^{n+1/2}\left(j+1/2\right)\right\}$$

$$-\frac{16\Delta t^2\left(\Delta yE_y^{n+1/2}\left(k+1/2\right)-\Delta yE_y^{n+1/2}\left(k+3/2\right)-\Delta zE_z^{n+1/2}\left(j+1/2\right)+\Delta zE_z^{n+1/2}\left(j+3/2\right)\right)}{\Delta y^2\Delta z\left(2\mu_\mu+\Delta t\mu_{\sigma^*}\right)^3}$$

$$\rho_{\mu,E_z^{n+1/2}(j+3/2)}\sigma\{\mu\}\sigma\left\{E_z^{n+1/2}\left(j+3/2\right)\right\}$$

$$-\frac{8\Delta t^3\left(\Delta yE_y^{n+1/2}\left(k+1/2\right)-\Delta yE_y^{n+1/2}\left(k+3/2\right)-\Delta zE_z^{n+1/2}\left(j+1/2\right)+\Delta zE_z^{n+1/2}\left(j+3/2\right)\right)}{\Delta y^2\Delta z\left(2\mu_\mu+\Delta t\mu_{\sigma^*}\right)^3}$$

$$\rho_{\sigma^*,E_z^{n+1/2}(j+3/2)}\sigma\left\{\sigma^*\right\}\sigma\left\{E_z^n\left(j+3/2\right)\right\}$$

$$+\frac{(16\Delta t^3\left(\Delta yE_y^{n+1/2}\left(k+1/2\right)-\Delta yE_y^{n+1/2}\left(k+3/2\right)-\Delta zE_z^{n+1/2}\left(j+1/2\right)+\Delta zE_z^{n+1/2}\left(j+3/2\right)\right)^2}{\Delta y^2\Delta z^2\left(2\mu_\mu+\Delta t\mu_{\sigma^*}\right)^4}$$

$$\rho_{\sigma^*,\mu}\sigma\{\mu\}\sigma\left\{\sigma^*\right\}$$

$$+\frac{16\Delta t^2\left(\Delta yE_y^{n+1/2}\left(k+1/2\right)-\Delta yE_y^{n+1/2}\left(k+3/2\right)-\Delta zE_z^{n+1/2}\left(j+1/2\right)+\Delta zE_z^{n+1/2}\left(j+3/2\right)\right)^2)}{\Delta y^2\Delta z^2\left(2\mu_\mu+\Delta t\mu_{\sigma^*}\right)^4}$$

$$\sigma^2\{\mu\}$$

$$+\frac{4\Delta t^4(\Delta yE_y^{n+1/2}\left(k+1/2\right)-\Delta yE_y^{n+1/2}\left(k+3/2\right)-\Delta zE_z^{n+1/2}\left(j+1/2\right)+\Delta zE_z^{n+1/2}\left(j+3/2\right)))^2}{\Delta y^2\Delta z^2\left(2\mu_\mu+\Delta t\mu_{\sigma^*}\right)^4}$$

$$\sigma^2\left\{\sigma^*\right\}$$

Using the following approximations:

$$\rho_{E_y^{n+1/2}(k+3/2),E_y^{n+1/2}(k+1/2)}\to 1$$

$$\rho_{E_y^{n+1/2}(k+1/2),E_z^{n+1/2}(j+1/2)}\to 1$$

$$\rho_{E_y^{n+1/2}(k+3/2),E_z^{n+1/2}(j+1/2)}\to 1$$

$$\rho_{E_y^{n+1/2}(k+3/2),E_z^{n+1/2}(j+3/2)}\to 1$$

$$\rho_{E_y^{n+1/2}(k+1/2),E_z^{n+1/2}(j+3/2)}\to 1$$

$$\rho_{E_z^{n+1/2}(j+3/2),E_z^{n+1/2}(j+1/2)}\to 1$$

$$\rho_{\mu,E_y^{n+1/2}(k+1/2)}, \rho_{\mu,E_z^{n+1/2}(j+1/2)} \rightarrow \rho_{\mu,E}$$

$$\rho_{\sigma^*,E_z^{n+1/2}(j+1/2)}, \rho_{\sigma^*,E_y^{n+1/2}(k+1/2)} \rightarrow \rho_{\sigma^*,E}$$

$$\rho_{\mu,E_z^{n+1/2}(j+3/2)} \rightarrow \rho_{\mu,E}$$

$$\rho_{\sigma^*,E_z^{n+1/2}(j+3/2)} \rightarrow \rho_{\sigma^*,E}$$

$$\rho_{\mu,E_y^{n+1/2}(k+3/2)} \rightarrow \rho_{\mu,E}$$

$$\rho_{\sigma^*,E_y^{n+1/2}(k+3/2)} \rightarrow \rho_{\sigma^*,E}$$

After applying these approximations, we arrive at the following expression:

$$\frac{4\Delta t^2}{(2\mu_\mu + \Delta t \mu_{\sigma^*})^2}\left(\frac{\sigma\left\{E_y^{n+1/2}(k+3/2)\right\}-\sigma\left\{E_y^{n+1/2}(k+1/2)\right\}}{\Delta z} - \frac{\sigma\left\{E_z^{n+1/2}(j+3/2)\right\}-\sigma\left\{E_z^{n+1/2}(j+1/2)\right\}}{\Delta y}\right)^2$$

$$-\frac{2\left(2\rho_{\mu,\mathrm{E}}\sigma\{\mu\}+\Delta t\rho_{\sigma^*,\mathrm{E}}\sigma\{\sigma^*\}\right)}{\left(2\mu_\mu+\Delta t\mu_{\sigma^*}\right)}$$

$$\left(\frac{\sigma\left\{E_y^{n+1/2}(k+3/2)\right\}-\sigma\left\{E_y^{n+1/2}(k+1/2)\right\}}{\Delta z} - \frac{\sigma\left\{E_z^{n+1/2}(j+3/2)\right\}-\sigma\left\{E_z^{n+1/2}(j+1/2)\right\}}{\Delta y}\right)$$

$$\left(\frac{E_y^{n+1/2}(k+3/2)-E_y^{n+1/2}(k+1/2)}{\Delta z} - \frac{E_z^{n+1/2}(j+3/2)-E_z^{n+1/2}(j+1/2)}{\Delta y}\right)$$

$$+\frac{\left(4\sigma^2\{\mu\}+4\Delta t\rho_{\sigma^*,\mu}\sigma\{\mu\}\sigma\{\sigma^*\}+\Delta t^2\sigma^2\{\sigma^*\}\right)}{\left(2\mu_\mu+\Delta t\mu_{\sigma^*}\right)^2}$$

$$\left(\frac{E_y^{n+1/2}\left(j+3/2\right)-E_y^{n+1/2}\left(j+1/2\right)}{\Delta z} - \frac{E_z^{n+1/2}\left(j+3/2\right)-E_z^{n+1/2}\left(j+1/2\right)}{\Delta y} \right)^2$$

We next complete the square and arrive at the next expression by adding and subtracting:

$$\frac{\left(2\rho_{\mu,\mathrm{E}}\sigma\{\mu\}+\Delta t\rho_{\sigma^*,\mathrm{E}}\sigma\{\sigma^*\}\right)^2}{\left(2\mu_\mu+\Delta t\mu_{\sigma^*}\right)^2} \left(\begin{array}{l} \dfrac{E_y^{n+1/2}\left(k+3/2\right)-E_y^{n+1/2}\left(k+1/2\right)}{\Delta z} \\ \qquad - \dfrac{E_z^{n+1/2}\left(j+3/2\right)-E_z^{n+1/2}\left(j+1/2\right)}{\Delta y} \end{array} \right)^2$$

Yielding the following expression:

$$\frac{4\Delta t^2}{(2\mu_\mu+\Delta t\mu_{\sigma^*})^2} \left(\begin{array}{l} \dfrac{\sigma\left\{E_y^{n+1/2}\left(k+3/2\right)\right\}-\sigma\left\{E_y^{n+1/2}\left(k+1/2\right)\right\}}{\Delta z} \\ \qquad - \dfrac{\sigma\left\{E_z^{n+1/2}\left(j+3/2\right)\right\}-\sigma\left\{E_z^{n+1/2}\left(j+1/2\right)\right\}}{\Delta y} \end{array} \right)^2$$

$$- \frac{2\left(2\rho_{\mu,\mathrm{E}}\sigma\{\mu\}+\Delta t\rho_{\sigma^*,\mathrm{E}}\sigma\{\sigma^*\}\right)}{\left(2\mu_\mu+\Delta t\mu_{\sigma^*}\right)} \left(\begin{array}{l} \dfrac{\sigma\left\{E_y^{n+1/2}\left(k+3/2\right)\right\}-\sigma\left\{E_y^{n+1/2}\left(k+1/2\right)\right\}}{\Delta z} \\ \qquad - \dfrac{\sigma\left\{E_z^{n+1/2}\left(j+3/2\right)\right\}-\sigma\left\{E_z^{n+1/2}\left(j+1/2\right)\right\}}{\Delta y} \end{array} \right)$$

$$\left(\frac{E_y^{n+1/2}\left(k+3/2\right)-E_y^{n+1/2}\left(k+1/2\right)}{\Delta z} - \frac{E_z^{n+1/2}\left(j+3/2\right)-E_z^{n+1/2}\left(j+1/2\right)}{\Delta y} \right)$$

$$+\frac{\left(2\rho_{\mu,\mathrm{E}}\sigma\{\mu\}+\Delta t\rho_{\sigma^*,\mathrm{E}}\sigma\{\sigma^*\}\right)^2}{\left(2\mu_\mu+\Delta t\mu_{\sigma^*}\right)^2}\left(\frac{E_y^{n+1/2}(k+3/2)-E_y^{n+1/2}(k+1/2)}{\Delta z}-\frac{E_z^{n+1/2}(j+3/2)-E_z^{n+1/2}(j+1/2)}{\Delta y}\right)^2$$

$$-\frac{\left(2\rho_{\mu,\mathrm{E}}\sigma\{\mu\}+\Delta t\rho_{\sigma^*,\mathrm{E}}\sigma\{\sigma^*\}\right)^2}{\left(2\mu_\mu+\Delta t\mu_{\sigma^*}\right)^2}\left(\frac{E_y^{n+1/2}(j+3/2)-E_y^{n+1/2}(j+1/2)}{\Delta z}-\frac{E_z^{n+1/2}(j+3/2)-E_z^{n+1/2}(j+1/2)}{\Delta y}\right)^2$$

$$+\frac{\left(4\sigma^2\{\mu\}+4\Delta t\rho_{\sigma^*,\mu}\sigma\{\mu\}\sigma\{\sigma^*\}+\Delta t^2\sigma^2\{\sigma^*\}\right)}{\left(2\mu_\mu+\Delta t\mu_{\sigma^*}\right)^2}\left(\frac{E_y^{n+1/2}(j+3/2)-E_y^{n+1/2}(j+1/2)}{\Delta z}-\frac{E_z^{n+1/2}(j+3/2)-E_z^{n+1/2}(j+1/2)}{\Delta y}\right)^2$$

Finishing this process, we arrive at the following:

$$\frac{4\Delta t^2}{(2\mu_\mu + \Delta t \mu_{\sigma^*})^2}\left(\left(\left(\frac{\sigma\left\{E_y^{n+1/2}\left(k+3/2\right)\right\}-\sigma\left\{E_y^{n+1/2}\left(k+1/2\right)\right\}}{\Delta z} - \frac{\sigma\left\{E_z^{n+1/2}\left(j+3/2\right)\right\}-\sigma\left\{E_z^{n+1/2}\left(j+1/2\right)\right\}}{\Delta y}\right)\right)^2 - \frac{(2\rho_{\mu,\mathrm{E}}\sigma\{\mu\}+\Delta t\rho_{\sigma^*,\mathrm{E}}\sigma\{\sigma^*\})}{\left(2\mu_\mu+\Delta t\mu_{\sigma^*}\right)}\left(\frac{E_y^{n+1/2}\left(k+3/2\right)-E_y^{n+1/2}\left(k+1/2\right)}{\Delta z} - \frac{E_z^{n+1/2}\left(j+3/2\right)-E_z^{n+1/2}\left(j+1/2\right)}{\Delta y}\right)\right) - \frac{\left(4(1+\rho_{\mu,\mathrm{E}}^2)\sigma^2\{\mu\}+4\Delta t(\rho_{\mu,\mathrm{E}}\rho_{\sigma^*,\mathrm{E}}+\rho_{\sigma^*,\mu})\sigma\{\mu\}\sigma\{\sigma^*\} + \Delta t^2(1+\rho_{\sigma^*,\mathrm{E}}^2)\sigma^2\{\sigma^*\}\right)}{\left(2\mu_\mu+\Delta t\mu_{\sigma^*}\right)^2}\left(\frac{E_y^{n+1/2}\left(k+3/2\right)-E_y^{n+1/2}\left(k+1/2\right)}{\Delta z} - \frac{E_z^{n+1/2}\left(j+3/2\right)-E_z^{n+1/2}\left(j+1/2\right)}{\Delta y}\right)^2\right) \tag{A.17}$$

This is an approximation of the right-hand side of equation (A.5); this equation can be reduced a bit more by bringing the left- and right-hand sides of Faraday's Law together:

$$\left(\begin{array}{c}\sigma\left\{H_x^{n+1}\left(i-1/2,j+1,k+1\right)\right\}-\dfrac{\left(2\mu_\mu-\Delta t\mu_{\sigma^*}\right)}{\left(2\mu_\mu+\Delta t\mu_{\sigma^*}\right)}\sigma\left\{H_x^{n}\left(i-1/2,j+1,k+1\right)\right\}\\ \\ -\dfrac{4\Delta t\left(\mu_{\sigma^*}\rho_{\mu,H}\sigma\{\mu\}-\mu_\mu\rho_{\sigma^*,H}\sigma\left\{\sigma^*\right\}\right)}{\left(2\mu_\mu+\Delta t\mu_{\sigma^*}\right)^2}H_x^n\left(i-1/2,j+1,k+1\right)\end{array}\right)^2\approx$$

$$\frac{4\Delta t^2}{(2\mu_\mu+\Delta t\mu_{\sigma^*})^2}\left(\begin{array}{c}\left(\begin{array}{c}\left(\dfrac{\sigma\left\{E_y^{n+1/2}\left(k+3/2\right)\right\}-\sigma\left\{E_y^{n+1/2}\left(k+1/2\right)\right\}}{\Delta z}\right.\\ \left.-\dfrac{\sigma\left\{E_z^{n+1/2}\left(j+3/2\right)\right\}-\sigma\left\{E_z^{n+1/2}\left(j+1/2\right)\right\}}{\Delta y}\right)\end{array}\right)^2\\ -\dfrac{(2\rho_{\mu,\mathrm{E}}\sigma\{\mu\}+\Delta t\rho_{\sigma^*,\mathrm{E}}\sigma\left\{\sigma^*\right\})}{\left(2\mu_\mu+\Delta t\mu_{\sigma^*}\right)}\\ \left(\begin{array}{c}\dfrac{E_y^{n+1/2}\left(k+3/2\right)-E_y^{n+1/2}\left(k+1/2\right)}{\Delta z}\\ -\dfrac{E_z^{n+1/2}\left(j+3/2\right)-E_z^{n+1/2}\left(j+1/2\right)}{\Delta y}\end{array}\right)\end{array}\right)-$$

$$\left(\begin{array}{c}\dfrac{\left(\begin{array}{c}4(1+\rho_{\mu,\mathrm{E}}^2)\sigma^2\left\{\mu\right\}+4\Delta t(\rho_{\mu,\mathrm{E}}\rho_{\sigma^*,\mathrm{E}}+\rho_{\sigma^*,\mu})\sigma\{\mu\}\sigma\left\{\sigma^*\right\}\\ +\Delta t^2(1+\rho_{\sigma^*,\mathrm{E}}^2)\sigma^2\left\{\sigma^*\right\}\end{array}\right)}{\left(2\mu_\mu+\Delta t\mu_{\sigma^*}\right)^2}\\ \left(\begin{array}{c}\dfrac{E_y^{n+1/2}\left(k+3/2\right)-E_y^{n+1/2}\left(k+1/2\right)}{\Delta z}\\ -\dfrac{E_z^{n+1/2}\left(j+3/2\right)-E_z^{n+1/2}\left(j+1/2\right)}{\Delta y}\end{array}\right)^2\end{array}\right)$$

We see from the previous equation that we need to take the square-root of both sides of the equation. Let us do this now:

$$\sigma\left\{H_x^{n+1}\left(i-1/2,j+1,k+1\right)\right\}-\frac{\left(2\mu_\mu-\Delta t\mu_{\sigma^*}\right)}{\left(2\mu_\mu+\Delta t\mu_{\sigma^*}\right)}\sigma\left\{H_x^{n}\left(i-1/2,j+1,k+1\right)\right\}$$

$$-\frac{4\Delta t\left(\mu_{\sigma^*}\rho_{\mu,H}\sigma\{\mu\}-\mu_\mu\rho_{\sigma^*,H}\sigma\left\{\sigma^*\right\}\right)}{\left(2\mu_\mu+\Delta t\mu_{\sigma^*}\right)^2}H_x^n\left(i-1/2,j+1,k+1\right)\approx$$

$$\frac{2\Delta t}{(2\mu_\mu+\Delta t\mu_{\sigma^*})}\left(-\frac{(2\rho_{\mu,\mathrm{E}}\sigma\{\mu\}+\Delta t\rho_{\sigma^*,\mathrm{E}}\sigma\left\{\sigma^*\right\})}{\left(2\mu_\mu+\Delta t\mu_{\sigma^*}\right)}\left(\begin{array}{l}\dfrac{E_y^{n+1/2}\left(k+3/2\right)-E_y^{n+1/2}\left(k+1/2\right)}{\Delta z}\\ \qquad -\dfrac{E_z^{n+1/2}\left(j+3/2\right)-E_z^{n+1/2}\left(j+1/2\right)}{\Delta y}\end{array}\right)\right.$$

$$\left.\left(\begin{array}{l}\dfrac{\sigma\left\{E_y^{n+1/2}\left(k+3/2\right)\right\}-\sigma\left\{E_y^{n+1/2}\left(k+1/2\right)\right\}}{\Delta z}\\ \qquad -\dfrac{\sigma\left\{E_z^{n+1/2}\left(j+3/2\right)\right\}-\sigma\left\{E_z^{n+1/2}\left(j+1/2\right)\right\}}{\Delta y}\end{array}\right)\right)$$

$$\sqrt{\begin{array}{l} 1- \\ \dfrac{\left(4(1+\rho_{\mu,\mathrm{E}}^2)\sigma^2\{\mu\}+4\Delta t(\rho_{\mu,\mathrm{E}}\rho_{\sigma^*,\mathrm{E}}+\rho_{\sigma^*,\mu})\sigma\{\mu\}\sigma\{\sigma^*\}+\Delta t^2(1+\rho_{\sigma^*,\mathrm{E}}^2)\sigma^2\{\sigma^*\}\right)}{\left(2\mu_\mu+\Delta t\mu_{\sigma^*}\right)^2} \\ \dfrac{\left(\dfrac{E_y^{n+1/2}(k+3/2)-E_y^{n+1/2}(k+1/2)}{\Delta z}-\dfrac{E_z^{n+1/2}(j+3/2)-E_z^{n+1/2}(j+1/2)}{\Delta y}\right)^2}{\left(\dfrac{\sigma\{E_y^{n+1/2}(k+3/2)\}-\sigma\{E_y^{n+1/2}(k+1/2)\}}{\Delta z}-\dfrac{\sigma\{E_z^{n+1/2}(j+3/2)\}-\sigma\{E_z^{n+1/2}(j+1/2)\}}{\Delta y}\right)^2} \\ -\dfrac{(2\rho_{\mu,\mathrm{E}}\sigma\{\mu\}+\Delta t\rho_{\sigma^*,\mathrm{E}}\sigma\{\sigma^*\})}{\left(2\mu_\mu+\Delta t\mu_{\sigma^*}\right)} \\ \left(\dfrac{E_y^{n+1/2}(k+3/2)-E_y^{n+1/2}(k+1/2)}{\Delta z}-\dfrac{E_z^{n+1/2}(j+3/2)-E_z^{n+1/2}(j+1/2)}{\Delta y}\right) \end{array}}$$

Now, let us take a look at what is under the radical sign, in particular the next term:

$$\frac{\left(\begin{array}{l} 4(1+\rho_{\mu,\mathrm{E}}^2)\sigma^2\{\mu\}+4\Delta t(\rho_{\mu,\mathrm{E}}\rho_{\sigma^*,\mathrm{E}}+\rho_{\sigma^*,\mu})\sigma\{\mu\}\sigma\{\sigma^*\} \\ \qquad\qquad +\Delta t^2(1+\rho_{\sigma^*,\mathrm{E}}^2)\sigma^2\{\sigma^*\} \end{array}\right)}{\left(2\mu_\mu+\Delta t\mu_{\sigma^*}\right)^2}$$

$$\frac{\left(\begin{array}{l} \dfrac{E_y^{n+1/2}(k+3/2)-E_y^{n+1/2}(k+1/2)}{\Delta z} \\ \qquad -\dfrac{E_z^{n+1/2}(j+3/2)-E_z^{n+1/2}(j+1/2)}{\Delta y} \end{array}\right)^2}{\left(\begin{array}{l} \left(\begin{array}{l} \dfrac{\sigma\{E_y^{n+1/2}(k+3/2)\}-\sigma\{E_y^{n+1/2}(k+1/2)\}}{\Delta z} \\ \qquad -\dfrac{\sigma\{E_z^{n+1/2}(j+3/2)\}-\sigma\{E_z^{n+1/2}(j+1/2)\}}{\Delta y} \end{array}\right)^2 \\ -\dfrac{(2\rho_{\mu,\mathrm{E}}\sigma\{\mu\}+\Delta t\rho_{\sigma^*,\mathrm{E}}\sigma\{\sigma^*\})}{\left(2\mu_\mu+\Delta t\mu_{\sigma^*}\right)} \\ \left(\begin{array}{l} \dfrac{E_y^{n+1/2}(k+3/2)-E_y^{n+1/2}(k+1/2)}{\Delta z} \\ \qquad -\dfrac{E_z^{n+1/2}(j+3/2)-E_z^{n+1/2}(j+1/2)}{\Delta y} \end{array}\right) \end{array}\right)}$$

Looking at the numerator's magnitude:

$$\frac{\left(4(1+\rho_{\mu,\mathrm{E}}^2)\sigma^2\{\mu\}+4\Delta t(\rho_{\mu,\mathrm{E}}\rho_{\sigma^*,\mathrm{E}}+\rho_{\sigma^*,\mu})\sigma\{\mu\}\sigma\{\sigma^*\}+\Delta t^2(1+\rho_{\sigma^*,\mathrm{E}}^2)\sigma^2\{\sigma^*\}\right)}{\left(2\mu_\mu+\Delta t\mu_{\sigma^*}\right)^2}$$

$$\left(\begin{array}{l} \dfrac{E_y^{n+1/2}(k+3/2)-E_y^{n+1/2}(k+1/2)}{\Delta z} \\ \qquad -\dfrac{E_z^{n+1/2}(j+3/2)-E_z^{n+1/2}(j+1/2)}{\Delta y} \end{array}\right)^2$$

Assuming maximum correlation between all parameters yields:

$$\frac{\left(8\sigma^2\{\mu\}+8\Delta t\sigma\{\mu\}\sigma\{\sigma^*\}+2\Delta t^2\sigma^2\{\sigma^*\}\right)}{\left(2\mu_\mu+\Delta t\mu_{\sigma^*}\right)^2}$$

In the denominator, $2\mu_\mu$ dominates and any factor multiplied by Δt would also be small in comparison, yielding:

$$\frac{8\sigma^2\{\mu\}}{4\mu_\mu^{\,2}}=2\frac{\sigma^2\{\mu\}}{\mu_\mu^{\,2}}$$

By and large, in materials, the mean is greater than the variance of the same parameter of the material in question, allowing as an approximation the neglecting of the second term under the radical. This now reduces the resulting equation to:

$$\sigma\left\{H_x^{n+1}(i-1/2,j+1,k+1)\right\}-\frac{\left(2\mu_\mu-\Delta t\mu_{\sigma^*}\right)}{\left(2\mu_\mu+\Delta t\mu_{\sigma^*}\right)}\sigma\left\{H_x^{n}(i-1/2,j+1,k+1)\right\}$$

$$-\frac{4\Delta t\left(\mu_{\sigma^*}\rho_{\mu,H}\sigma\{\mu\}-\mu_\mu\rho_{\sigma^*,H}\sigma\{\sigma^*\}\right)}{\left(2\mu_\mu+\Delta t\mu_{\sigma^*}\right)^2}H_x^n(i-1/2,j+1,k+1)\approx$$

$$\frac{2\Delta t}{(2\mu_{\mu}+\Delta t\mu_{\sigma^*})}\left(\begin{array}{l}\left(\begin{array}{l}\dfrac{\sigma\left\{E_y^{n+1/2}\left(k+3/2\right)\right\}-\sigma\left\{E_y^{n+1/2}\left(k+1/2\right)\right\}}{\Delta z}\\ \qquad -\dfrac{\sigma\left\{E_z^{n+1/2}\left(j+3/2\right)\right\}-\sigma\left\{E_z^{n+1/2}\left(j+1/2\right)\right\}}{\Delta y}\end{array}\right)\\ -\dfrac{(2\rho_{\mu,\mathrm{E}}\sigma\{\mu\}+\Delta t\rho_{\sigma^*,\mathrm{E}}\sigma\{\sigma^*\})}{2\mu_{\mu}+\Delta t\mu_{\sigma^*}}\\ \qquad\left(\begin{array}{l}\dfrac{E_y^{n+1/2}\left(k+3/2\right)-E_y^{n+1/2}\left(k+1/2\right)}{\Delta z}\\ \qquad -\dfrac{E_z^{n+1/2}\left(j+3/2\right)-E_z^{n+1/2}\left(j+1/2\right)}{\Delta y}\end{array}\right)\end{array}\right)$$

Solving for the future and using the symmetry, the preceding equation's form can be used to derive the other equations for 3D space. These are listed in the following pages:

Faraday's 3D Equations

$$\sigma\left\{H_x^{n+1}\left(i-1/2,j+1,k+1\right)\right\}\approx$$

$$\frac{2\mu_\mu-\Delta t\mu_{\sigma^*}}{2\mu_\mu+\Delta t\mu_{\sigma^*}}\sigma\left\{H_x^{n}\left(i-1/2,j+1,k+1\right)\right\}$$

$$+\frac{4\Delta t\left(\mu_{\sigma^*}\rho_{\mu,H}\sigma\{\mu\}-\mu_m\rho_{\sigma^*,H}\sigma\left\{\sigma^*\right\}\right)}{\left(2\mu_\mu+\Delta t\mu_{\sigma^*}\right)^2}H_x^{n}\left(i-1/2,j+1,k+1\right)+$$

$$\frac{2\Delta t}{(2\mu_\mu+\Delta t\mu_{\sigma^*})}\bullet$$

$$\left(\begin{array}{l}\left(\begin{array}{l}\dfrac{\sigma\left\{E_y^{n+1/2}\left(i-1/2,j+1,k+3/2\right)\right\}-\sigma\left\{E_y^{n+1/2}\left(i-1/2,j+1,k+1/2\right)\right\}}{\Delta z}\\ -\dfrac{\sigma\left\{E_z^{n+1/2}\left(i-1/2,j+3/2,k+1\right)\right\}-\sigma\left\{E_z^{n+1/2}\left(i-1/2,j+1/2,k+1\right)\right\}}{\Delta y}\end{array}\right)\\ -\dfrac{2\rho_{\mu,\mathrm{E}}\sigma\{\mu\}+\Delta t\rho_{\sigma^*,\mathrm{E}}\sigma\left\{\sigma^*\right\}}{2\mu_\mu+\Delta t\mu_{\sigma^*}}\\ \quad\left(\begin{array}{l}\dfrac{E_y^{n+1/2}\left(\left(i-1/2,j+1,k+3/2\right)\right)-E_y^{n+1/2}\left\{\left(i-1/2,j+1,k+1/2\right)\right\}}{\Delta z}\\ -\dfrac{E_z^{n+1/2}\left(i-1/2,j+3/2,k+1\right)-E_z^{n+1/2}\left(1-1/2,j+1/2,k+1\right)}{\Delta y}\end{array}\right)\end{array}\right)$$

$$\sigma\left\{H_y^{n+1}\left(i,j+1/2,k+1\right)\right\}\approx$$

$$\frac{2\mu_\mu-\Delta t\mu_{\sigma^*}}{2\mu_\mu+\Delta t\mu_{\sigma^*}}\sigma\left\{H_y^{n}\left(i,j+1/2,k+1\right)\right\}$$

$$+\frac{4\Delta t\left(\mu_{\sigma^*}\rho_{\mu,H}\sigma\{\mu\}-\mu_m\rho_{\sigma^*,H}\sigma\left\{\sigma^*\right\}\right)}{\left(2\mu_\mu+\Delta t\mu_{\sigma^*}\right)^2}H_y^{n}\left(i,j+1/2,k+1\right)+$$

$$\frac{2\Delta t}{(2\mu_\mu+\Delta t\mu_{\sigma^*})}$$

$$\left(\begin{array}{l}\left(\begin{array}{l}\dfrac{\sigma\left\{E_z^{n+1/2}\left(i+1/2,j+1/2,k+1\right)\right\}-\sigma\left\{E_z^{n+1/2}\left(i-1/2,j+1/2,k+1\right)\right\}}{\Delta x}\\ -\dfrac{\sigma\left\{E_x^{n+1/2}\left(i,j+1/2,k+3/2\right)\right\}-\sigma\left\{E_x^{n+1/2}\left(i,j+1/2,k+1/2\right)\right\}}{\Delta z}\end{array}\right)\\ -\dfrac{2\rho_{\mu,\mathrm{E}}\sigma\{\mu\}+\Delta t\rho_{\sigma^*,\mathrm{E}}\sigma\left\{\sigma^*\right\}}{2\mu_\mu+\Delta t\mu_{\sigma^*}}\\ \quad\left(\begin{array}{l}\dfrac{E_z^{n+1/2}\left(\left(i+1/2,j+1/2,k+1\right)\right)-E_z^{n+1/2}\left\{\left(i-1/2,j+1/2,k+1\right)\right\}}{\Delta x}\\ -\dfrac{E_x^{n+1/2}\left(i,j+1/2,k+3/2\right)-E_x^{n+1/2}\left(1,j+1/2,k+1/2\right)}{\Delta z}\end{array}\right)\end{array}\right)$$

(A.18)

$$\sigma\left\{H_z^{n+1}\left(i,j+1,k+1/2\right)\right\}\approx$$

$$\frac{2\mu_\mu-\Delta t\mu_{\sigma^*}}{2\mu_\mu+\Delta t\mu_{\sigma^*}}\sigma\left\{H_z^{n}\left(i,j+1,k+1/2\right)\right\}$$

$$+\frac{4\Delta t\left(\mu_{\sigma^*}\rho_{\mu,H}\sigma\{\mu\}-\mu_m\rho_{\sigma^*,H}\sigma\left\{\sigma^*\right\}\right)}{\left(2\mu_\mu+\Delta t\mu_{\sigma^*}\right)^2}H_z^{n}\left(i,j+1,k+1/2\right)+$$

$$\frac{2\Delta t}{(2\mu_\mu+\Delta t\mu_{\sigma^*})}$$

$$\left(\begin{array}{l}\left(\begin{array}{l}\dfrac{\sigma\left\{E_x^{n+1/2}\left(i,j+3/2,k+1/2\right)\right\}-\sigma\left\{E_x^{n+1/2}\left(i,j+1/2,k+1\right)\right\}}{\Delta y}\\[2ex] -\dfrac{\sigma\left\{E_y^{n+1/2}\left(i+1/2,j+1,k+1/2\right)\right\}-\sigma\left\{E_y^{n+1/2}\left(i-1/2,j+1,k+1/2\right)\right\}}{\Delta x}\end{array}\right)\\[2ex] -\dfrac{2\rho_{\mu,\mathrm{E}}\sigma\{\mu\}+\Delta t\rho_{\sigma^*,\mathrm{E}}\sigma\left\{\sigma^*\right\}}{2\mu_\mu+\Delta t\mu_{\sigma^*}}\\[2ex] \qquad\left(\begin{array}{l}\dfrac{E_x^{n+1/2}\left(i,j+3/2,k+1/2\right)-E_x^{n+1/2}\left(i,j+1/2,k+1\right)}{\Delta y}\\[2ex] -\dfrac{E_y^{n+1/2}\left(i+1/2,j+1,k+1/2\right)-E_y^{n+1/2}\left(i-1/2,j+1,k+1/2\right)}{\Delta y}\end{array}\right)\end{array}\right)$$

(A.19)

A.2.2 Ampere's Law

$$\frac{\partial \mathbf{D}}{\partial t} = \nabla x \mathbf{H} - \mathbf{J} \tag{A.20}$$

Because the form of Ampere's and Faraday's Law are the same, we can use the results in the previous section and write down directly the approximate equations:

$$\sigma^2 \left\{ E_x^{n+1/2}\left(i, j+1/2, k+1/2\right) - \frac{1-\frac{\sigma\Delta t}{2\varepsilon}}{1+\frac{\sigma\Delta t}{2\varepsilon}} E_x^{n-1/2}\left(i, j+1/2, k+1/2\right) \right\} =$$

$$\sigma^2 \left\{ \frac{\frac{\Delta t}{\varepsilon}}{1+\frac{\sigma\Delta t}{2\varepsilon}} \left(\frac{\left(H_z^n\left(j+1\right) - H_z^n\left(j\right)\right)}{\Delta y} - \frac{H_y^n\left(k+1\right) - H_y^n\left(k\right)}{\Delta z} \right) \right\}$$

The above equation is compared with Faraday's Law (repeated next) of the previous section. With the appropriate change of variables, we can write down the 3D equations for Ampere's Law by inspection:

$$\sigma^2 \left\{ H_x^{n+1}\left(i-1/2, j+1, k+1\right) - \frac{1-\frac{\sigma^*\Delta t}{2\mu}}{1+\frac{\sigma^*\Delta t}{2\mu}} H_x^n\left(i-1/2, j+1, k+1\right) \right\} =$$

$$\sigma^2 \left\{ \frac{\dfrac{\Delta t}{\mu}}{1+\dfrac{\sigma^* \Delta t}{2\mu}} \left(\begin{array}{l} \dfrac{(E_y^{n+1/2}(k+3/2) - E_y^{n+1/2}(k+1/2))}{\Delta z} \\ \qquad - \dfrac{E_z^{n+1/2}(j+3/2) - E_z^{n+1/2}(j+1/2)}{\Delta y} \end{array} \right) \right\}$$

Ampere's 3D Equations

$$\sigma\left\{E_x^{n+1/2}\left(i,j+1/2,k+1/2\right)\right\}=$$

$$\frac{2\mu_\varepsilon-\Delta t\mu_\sigma}{2\mu_\varepsilon+\Delta t\mu_\sigma}\sigma\left\{E_x^{n-1/2}\left(i,j+1/2,k+1/2\right)\right\}$$

$$+\frac{4\Delta t\left(\mu_\sigma\rho_{\varepsilon,E}\sigma\{\varepsilon\}-\mu_\varepsilon\rho_{\sigma,E}\sigma\{\sigma\}\right)}{\left(2\mu_\varepsilon+\Delta t\mu_\sigma\right)^2}E_x^{n-1/2}\left(i,j+1/2,k+1/2\right)+$$

$$\frac{2\Delta t}{(2\mu_\varepsilon+\Delta t\mu_\sigma)}$$

$$\left(\begin{array}{l}\left(\begin{array}{l}\dfrac{\sigma\left\{H_z^n\left(i,j+1,k+1/2\right)\right\}-\sigma\left\{H_z^n\left(i,j,k+1/2\right)\right\}}{\Delta y}\\[2ex] -\dfrac{\sigma\left\{H_y^n\left(i,j+1/2,k+1\right)\right\}-\sigma\left\{H_y^n\left(i,j+1/2,k\right)\right\}}{\Delta z}\end{array}\right)\\[2ex] -\dfrac{2\rho_{\varepsilon,H}\sigma\{\varepsilon\}+\Delta t\rho_{\sigma,H}\sigma\{\sigma\}}{2\mu_\varepsilon+\Delta t\mu_\sigma}\\[2ex] \quad\left(\begin{array}{l}\dfrac{H_z^n\left(\left(i,j+1,k+1/2\right)\right)-H_z^n\left\{\left(i,j,k+1/2\right)\right\}}{\Delta y}\\[2ex] -\dfrac{H_y^n\left(i,j+1/2,k+1\right)-H_y^n\left(i,j+1/2,k\right)}{\Delta z}\end{array}\right)\end{array}\right)$$

$$\sigma\left\{E_y^{n+1/2}\left(i-1/2,j+1,k+1/2\right)\right\}=$$

$$\frac{2\mu_\varepsilon-\Delta t\mu_\sigma}{2\mu_\varepsilon+\Delta t\mu_\sigma}\sigma\left\{E_y^{n-1/2}\left(i-1/2,j+1,k+1/2\right)\right\}$$

$$+\frac{4\Delta t\left(\mu_\sigma\rho_{\varepsilon,E}\sigma\{\varepsilon\}-\mu_\varepsilon\rho_{\sigma,E}\sigma\{\sigma\}\right)}{\left(2\mu_\varepsilon+\Delta t\mu_\sigma\right)^2}E_y^{n-1/2}\left(i-1/2,j+1,k+1/2\right)+$$

$$\frac{2\Delta t}{(2\mu_\varepsilon+\Delta t\mu_\sigma)}$$

$$\left(\begin{array}{l}\left(\begin{array}{l}\dfrac{\sigma\left\{H_x^n\left(i-1/2,j+1,k+1\right)\right\}-\sigma\left\{H_x^n\left(i-1/2,j+1,k\right)\right\}}{\Delta z}\\[2ex] -\dfrac{\sigma\left\{H_z^n\left(i,j+1,k+1/2\right)\right\}-\sigma\left\{H_z^n\left(i-1,j+1,k+1/2\right)\right\}}{\Delta x}\end{array}\right)\\[2ex] -\dfrac{2\rho_{\varepsilon,H}\sigma\{\varepsilon\}+\Delta t\rho_{\sigma,H}\sigma\{\sigma\}}{2\mu_\varepsilon+\Delta t\mu_\sigma}\\[2ex] \left(\begin{array}{l}\dfrac{H_x^n\left(i-1/2,j+1,k+1\right)-H_x^n\left\{\left(i-1/2,j+1,k\right)\right\}}{\Delta z}\\[2ex] -\dfrac{H_z^n\left(i,j+1,k+1/2\right)-H_z^n\left(i-1,j+1,k+1/2\right)}{\Delta x}\end{array}\right)\end{array}\right)$$

$$\sigma\left\{E_z^{n+1/2}\left(i-1/2,j+1/2,k+1\right)\right\}=$$

$$\frac{2\mu_\varepsilon-\Delta t\mu_\sigma}{2\mu_\varepsilon+\Delta t\mu_\sigma}\sigma\left\{E_z^{n-1/2}\left(i-1/2,j+1/2,k+1\right)\right\}$$

$$+\frac{4\Delta t\left(\mu_\sigma\rho_{\varepsilon,E}\sigma\{\varepsilon\}-\mu_\varepsilon\rho_{\sigma,E}\sigma\{\sigma\}\right)}{\left(2\mu_\varepsilon+\Delta t\mu_\sigma\right)^2}E_z^{n-1/2}\left(i-1/2,j+1/2,k+1\right)+$$

$$\frac{2\Delta t}{(2\mu_\varepsilon+\Delta t\mu_\sigma)}$$

$$\left(\begin{array}{l}\left(\begin{array}{l}\dfrac{\sigma\left\{H_y^n\left(i,j+1/2,k+1\right)\right\}-\sigma\left\{H_y^n\left(i-1,j+1/2,k+1\right)\right\}}{\Delta x}\\[2ex] -\dfrac{\sigma\left\{H_x^n\left(i-1/2,j+1,k+1\right)\right\}-\sigma\left\{H_x^n\left(i-1/2,j/2,k+1\right)\right\}}{\Delta y}\end{array}\right)\\[2ex] -\dfrac{2\rho_{\varepsilon,H}\sigma\{\varepsilon\}+\Delta t\rho_{\sigma,H}\sigma\{\sigma\}}{2\mu_\varepsilon+\Delta t\mu_\sigma}\\[2ex] \left(\begin{array}{l}\dfrac{H_y^n\left(\left(i,j+1/2,k+1\right)\right)-H_y^n\left\{\left(i-1,j+1/2,k+1\right)\right\}}{\Delta x}\\[2ex] -\dfrac{H_x^n\left(i-1/2,j+1,k+1\right)-H_x^n\left(i-1/2,j/2,k+1\right)}{\Delta y}\end{array}\right)\end{array}\right)$$

APPENDIX B

ELECTROMAGNETICS

Table 7-1 Maxwell's Equations

Differential Form	Integral Form	Significance
$\nabla x\mathbf{E} = -\frac{\partial \mathbf{B}}{\partial t}$	$\oint_C \mathbf{B} \bullet \mathbf{dl} = -\frac{d\Phi}{dt}$	Faraday's Law
$\nabla x\mathbf{H} = \mathbf{J} + \frac{\partial \mathbf{D}}{\partial t}$	$\int_C \mathbf{H} \bullet \mathbf{dl} = I + \int_S \frac{\partial \mathbf{D}}{\partial t} \bullet \mathbf{ds}$	Ampere's Circuital Law
$\nabla \bullet \mathbf{D} = \rho$	$\int_S \mathbf{D} \bullet \mathbf{ds} = Q$	Gauss's Law
$\nabla \bullet \mathbf{B} = 0$	$\int_S \mathbf{B} \bullet \mathbf{ds} = 0$	No isolated Magnetic charge

APPENDIX C

PROBABILITY RELATIONS AND PROPERTIES

This appendix gives all the probability relations needed for this dissertation; for additional information, see Ronald [22].

C.1 Estimation Properties

$$\underset{\sim}{E}[X] = \mu_X = \int_{-\infty}^{\infty} x f_X(x)\, dx \tag{C.1}$$

$$\underset{\sim}{E}\{aX + b\} = a\underset{\sim}{E}\{X\} + b \tag{C.2}$$

a and b are constant

$$\underset{\sim}{E}\{X - Y\} = \underset{\sim}{E}\{X\} - \underset{\sim}{E}\{Y\} \tag{C.3}$$

$$\underset{\sim}{E}\{XY\} = \iint xy f_{XY}(xy)\, dxdy \tag{C.4}$$

$$\textit{uncorrelated}: \quad \underset{\sim}{E}\{XY\} = \underset{\sim}{E}\{X\}\,\underset{\sim}{E}\{Y\}$$

$$\textit{Orthogonal}: \quad \underset{\sim}{E}\{XY\} = 0$$

$$\textit{Independent}: \; f_{XY}(xy) = f_X(x) f_Y(y) \tag{C.5}$$

C.2 Variance Properties

The variance of a constant random variable is zero:

$$\begin{aligned} \sigma^2\{X\} &= \underset{\sim}{E}\left\{(X-\mu_X)^2\right\} = \int_{-\infty}^{\infty}(x-\mu_X)^2 f_X(x)\,dx \\ &= \underset{\sim}{E}\left\{X^2\right\} - 2\mu_X \underset{\sim}{E}\{X\} + \mu_X^2 = \underset{\sim}{E}\left\{X^2\right\} - \mu_X \end{aligned} \tag{C.6}$$

$$\sigma^2\{aX+b\} = a^2\sigma^2\{X\} \tag{C.7}$$

$$\begin{aligned} \sigma^2\{X \pm Y\} &= \underset{\sim}{E}\left\{(X \pm Y)^2\right\} - \left\{\underset{\sim}{E}\{X\} + \underset{\sim}{E}\{Y\}\right\}^2 \\ &= \underset{\sim}{E}\left\{X^2\right\} - \left\{\underset{\sim}{E}\{X\}\right\}^2 + \underset{\sim}{E}\left\{Y^2\right\} - \left\{\underset{\sim}{E}\{Y\}\right\}^2 \\ &\qquad \pm 2\left\{\underset{\sim}{E}\{XY\} - \underset{\sim}{E}\{X\}\underset{\sim}{E}\{Y\}\right\} \\ &= \sigma_X^2 + \sigma_Y^2 \pm 2\left\{\underset{\sim}{E}\{XY\} - \underset{\sim}{E}\{X\}\underset{\sim}{E}\{Y\}\right\} \end{aligned} \tag{C.8}$$

With constants a and b:

$$\begin{aligned} \sigma^2\{aX \pm bY\} &= \underset{\sim}{E}\left\{(aX \pm bY)^2\right\} - \left\{a\underset{\sim}{E}\{X\} \pm b\underset{\sim}{E}\{Y\}\right\}^2 \\ &= \underset{\sim}{E}\left\{a^2X^2 \pm 2abXY + b^2Y^2\right\} - \left\{a^2\underset{\sim}{E}\{X\}^2 \pm 2ab\underset{\sim}{E}\{X\}E\{Y\} + b^2E\{Y\}^2\right\} \end{aligned}$$

$$= a^2 \underset{\sim}{E}\{X^2\} + b^2 \underset{\sim}{E}\{Y^2\} \pm 2ab\underset{\sim}{E}\{XY\} - a^2 \underset{\sim}{E}\{X\}^2 \pm 2ab\underset{\sim}{E}\{X\}\underset{\sim}{E}\{Y\} - b^2 \underset{\sim}{E}\{Y\}^2$$

$$= a^2 \underset{\sim}{E}\{X^2\} - a^2 \underset{\sim}{E}\{X\}^2 + b^2 \underset{\sim}{E}\{Y^2\} - b^2 \underset{\sim}{E}\{Y\}^2 \pm 2ab\left\{\underset{\sim}{E}\{XY\} - \underset{\sim}{E}\{X\}\underset{\sim}{E}\{Y\}\right\}$$

$$= a^2\sigma^2\{X\} + b^2\sigma^2\{Y\} \pm 2ab\left\{\underset{\sim}{E}\{XY\} - \underset{\sim}{E}\{X\}\underset{\sim}{E}\{Y\}\right\} \tag{C.9}$$

If the random variables are uncorrelated, the variance of the sum of random variables are as seen in (C.10):

$$\sigma^2\{X \pm Y\} = \sigma_X^2 + \sigma_Y^2 \tag{C.10}$$

$$\begin{aligned} C\,\mathrm{ov}\{X,Y\} = \sigma_{xy} &= \underset{\sim}{E}\left\{\left(X - \mu_x\right)\left(Y - \mu_y\right)\right\} \\ &= \underset{\sim}{E}\{XY\} - \mu_x\mu_y \end{aligned} \tag{C.11}$$

Correlation function:

$$\rho_{XY} = \frac{\mathrm{cov}\{X,Y\}}{\sqrt{\sigma^2\{X\}\sigma^2\{Y\}}} = \frac{\sigma_{XY}}{\sigma_X\sigma_Y} \tag{C.12}$$

C.3 Approximations

Using the correlation function, we can approximate the cross-correlation using equation (C.13) and $-1 \le \rho_{XY} \le 1$ equation(C.13) yields equation(C.14):

$$\rho_{XY} = \frac{\operatorname{cov}\{X,Y\}}{\sqrt{\sigma^2\{X\}\sigma^2\{Y\}}} = \frac{\sigma_{XY}}{\sigma_X \sigma_Y} \tag{C.13}$$

$$\sigma_{XY}{}^2 \le \sigma_X{}^2 \sigma_Y{}^2 \tag{C.14}$$

With σ_{XY} bracketed as shown in the following equation:

$$-\sigma_X \sigma_Y \le \sigma_{XY} \le \sigma_X \sigma_Y \tag{C.15}$$

From $\sigma^2\{X\} = \underset{\sim}{E}\{X^2\} - \mu_X$, we find (C.16) due to the property of the variance being a positive quantity:

$$\underset{\sim}{E}\{X\}^2 \le \underset{\sim}{E}\{X^2\} \tag{C.16}$$

REFERENCES

[1] M. H. Repacholi, M. Grandolfo, A. Ahlborn, U. Bergqvist, J. H. Bernhardt, J. P. Cesarini, L. A. Court, A. F. McKinlay, D. H. Sliney, J. A. J. Stolwijk, M. L. Swicord, L. D. Szabo, T. S. Tenforde, H. P. Jammet, and R. Matthes, "Health issus related to the use of hand-held radiotelephones and base transmitters," *Health Physics,* vol. 70, pp. 586-593, 1996.

[2] 2004-2008, C. I. Vecchia P, V.-C. F. Hietanen M, A. A. (Sweden), B. E. (Germany), D. G. F. (Netherlands), L. J. (USA), M. R. (Germany), P. A. (Philippines), S. R. U. Kingdom), S. P. (Sweden), S. B. (USA), S. A. (UK), T. M. (Japan), V. B. (France), S. S. G. Ziegelberger G, S. 2008, C. I. Vecchia P, V.-C. G. Matthes R, F. M. (Sweden), G. A. (Australia), J. K. (Finland), L. J. (USA), P. A. (Philippines), S. R. U. Kingdom), S. K. (Austria), S. P. (Sweden), S. B. (USA), S. A. (UK), V. B. (France), and S. S. G. Ziegelberger G. (2009). Exposure to high frequency electromagnetic fields, biological effects and health consequences (100 kHz-300 GHz) [Electronic].

[3] O. P. Gandhi, G. Lazzi, and C. M. Furse, "Electromagnetic absorption in the human head and neck for mobile telephones at 835 and 1900 MHz," *Microwave Theory and Techniques, IEEE Transactions on,* vol. 44, pp. 1884-1897, 1996.

[4] C. M. Furse, G. Lazzi, and O. P. Gandhi, "FDTD computation of power deposition in the head for cellular telephones," in *Antennas and Propagation Society International Symposium*, AP-S. Digest, vol. 3, pp. 1794-1797, 1996.

[5] V. Pandit, R. McDermott, G. Lazzi, C. Furse, and O. Gandhi, "Electrical energy absorption in the human head from a cellular telephone," in *Visualization '96. Proceedings.*, 1996, pp. 371-374.

[6] A. Christ and N. Kuster, "Differences in RF energy absorption in the heads of adults and children," *Bioelectromagnetics,* pp. S31-S44, 2005.

[7] B. B. Beard, W. Kainz, T. Onishi, T. Iyama, S. Watanabe, O. Fujiwara, J. Q. Wang, G. Bit-Babik, A. Faraone, J. Wiart, A. Christ, N. Kuster, A. K. Lee, H. Kroeze, M. Siegbahn, J. Keshvari, H. Abrishamkar, W. Simon, D. Manteuffel, and N. Nikoloski, "Comparisons of computed mobile phone induced SAR in the SAM phantom to that in anatomically correct models of the human head," *IEEE Transactions on Electromagnetic Compatibility*, vol. 48, pp. 397-407, May 2006.

[8] J. D. Johnson, "Statistical ananlysis of detuning effects for impantable microstrip antennas, M.S. thesis, University of Utah, Salt Lake City, 2007.

[9] H. M. Panayirci, unpublished|.

[10] M. N. O. Sadiku, *Monte Carlo Methods for Electromagnetics*. Boca Raton: CRC Press, 2009.

[11] R. L. B. George Casella, Statistical Inference, 2nd ed. Pacific Grove: Duxbury, Thompson Learning, 2002.

[12] O. P. Gandhi, G. Lazzi, and C. Furse, "Electromagnetic absorption in the human head and neck for mobile telephones at 835 and 1900 MHz," *IEEE Transactions on Microwave Therory and Techniques,* vol. 44, pp. 1884-1897, Oct. 1996 1996.

[13] Y. Kane, "Numerical solution of initial boundary value problems involving maxwell's equations in isotropic media," *Antennas and Propagation, IEEE Transactions on,* vol. 14, pp. 302-307, 1966.

[14] A. Taflove and M. E. Brodwin, "Numerical solution of steady-state electromagnetic scattering problems using the time-dependent Maxwell's equations," *Microwave Theory and Techniques, IEEE Transactions on,* vol. 23, pp. 623-630, 1975.

[15] A. Taflove, *Computational Electrodynamics*, 2nd ed. Boston, MA: Artech House, Inc, 2000.

[16] S. Aalto, C. Haarala, A. Bruck, H. Sipila, H. Hamalainen, and J. O. Rinne, "Mobile phone affects cerebral blood flow in humans," *Journal of Cerebral Blood Flow and Metabolism,* vol. 26, pp. 885-890, Jul 2006.

[17] E. Adair, Q. Balzano, H. Bassen, G. J. Beers, C. K. Chou, R. Cleveland, C. C. Davis, L. Erdreich, K. R. Foster, J. Lin, J. Moulder, R. Petersen, P. Polson, M. L. Swicord, R. Tell, M. Ziskin, and R. M. S. I. Comm, "Human exposure to radio frequency and microwave radiation from portable and mobile telephones and ether wireless communication devices - A COMAR technical information statement," *IEEE Engineering in Medicine and Biology Magazine,* vol. 20, pp. 128-131, Jan-Feb 2001.

[18] M. Bank and B. Levin, "The development of a cellular phone antenna with small irradiation of human-organism tissues," *IEEE Antennas and Propagation Magazine,* vol. 49, pp. 65-73, Aug 2007.

[19] P. Bernardi, M. Cavagnaro, S. Pisa, and E. Piuzzi, "Specific absorption rate and temperature increases in the head of a cellular-phone user," *IEEE Transactions on*

Microwave Theory and Techniques, vol. 48, pp. 1118-1126, Jul 2000.

[20] O. P. Gandhi, "Electromagnetic fields: Human safety issues," *Annual Review of Biomedical Engineering,* vol. 4, pp. 211-234, 2002.

[21] M. N. O. Sadiku, *Numerical Techniques in Electromagnetics*, 2nd ed. New York: CRC Press, 2001.

[22] R. H. M. Ronald E. Walpole, Sharon L. Myers, and Keying Ye, *Probability and Statistics for Engineers and Scientists*. Upper Saddle River: Pearson Prentice-Hall, 2007, p. 816.

[23] M. Denny, "Introduction importance sampling and rare-event simulations," *European Journal of Physics,* vol. 22, pp. 403 – 411, 2001.

[24] M. Kleiber and T. D. Hein, *The Stochastic Finite Element Method Basic Perturbation Technique and Computer Implementation*, 1st ed. New York: John Wiley & Sons, 1992.

[25] A. Nayfeh, *Perturbation Methods*, 1st ed. New York: John Wiley & Sons, 1973.

[26] E. R. Adair and R. C. Petersen, "Biological effects of radio-frequency/microwave radiation," *IEEE Transactions on Microwave Theory and Techniques,* vol. 50, pp. 953-962, Mar 2002.

[27] C. Gabriel, "Dielectric properties of biological tissue: Variation with age," *Bioelectromagnetics,* pp. S12-S18, 2005.

[28] D. M. Sullivan, O. P. Gandhi, and A. Taflove, "Use of the finite-difference time-domain method for calculating EM absorption in man models," *Biomedical Engineering, IEEE Transactions on,* vol. 35, pp. 179-186, 1988.

[29] C. Furse, "Faster than Fourier-- Ultra-efficient time-to-frequency domain conversions for FDTD simulations," *Antennas and Propagation Magazine, IEEE,* vol. 42, pp. 24-34, Dec. 2000.

[30] A. Hadjem, D. Lautru, C. Dale, W. Man Fai, V. F. Hanna, and J. Wiart, "Study of specific absorption rate (SAR) induced in two child head models and in adult heads using mobile phones," *Microwave Theory and Techniques, IEEE Transactions on,* vol. 53, pp. 4-11, 2005.

[31] A. V. S. I.I. Gikhman, *Introduction to the Theory of Random Processes*, English ed. New York: Dover Publications, Inc., 1969.

[32] C. Gabriel and A. Peyman, "Dielectric measurement: Error analysis and assessment of uncertainty," *Physics in Medicine and Biology,* vol. 51, pp. 6033-

6046, Dec 7 2006.

[33] A. Taflove and S. C. Hagness, *Computational Electrodynamics The Finite Time-Difference Domain Method*, 3rd ed. Norward, MA: Artech House, Inc., 2005.

[34] O. P. Gandhi and C. Jin-Yuan, "Electromagnetic absorption in the human head from experimental 6-GHz handheld transceivers," *Electromagnetic Compatibility, IEEE Transactions on,* vol. 37, pp. 547-558, 1995.

[35] A. K. Lee, H. D. Choi, and J. I. Choi, "Study on SARs in head models with different shapes by age using SAM model for mobile phone exposure at 835 MHz," *IEEE Transactions on Electromagnetic Compatibility,* vol. 49, pp. 302-312, May 2007.

[36] C. H. Li, E. Ofli, N. Chavannes, and N. Kuster, "Effects of hand phantom on mobile phone antenna performance," *IEEE Transactions on Antennas and Propagation,* vol. 57, pp. 2763-2770, Sep 2009.

[37] C. C. Davis and Q. Balzano, "The international intercomparison of SAR measurements on cellular telephones," *IEEE Transactions on Electromagnetic Compatibility,* vol. 51, pp. 210-216, May 2009.

[38] S. M. Smith, "Stochastic FDTD," May, 2011 ed. Salt Lake City, Utah: University of Utah, 2011.

[39] C. Gabriel, "Dr. Camelia Gabriel, personal communication."